

Copyright is owned by the Author of the thesis. Permission is given for a copy to be downloaded by an individual for the purpose of research and private study only. The thesis may not be reproduced elsewhere without the permission of the Author.

A search for biomarkers of ovine pre-partum vaginal prolapse

A thesis presented to Massey University in partial fulfilment of the requirement for the
degree of Doctor of Philosophy in Biochemistry

Stuart Brown

2019

Abstract

Ovine pre-partum vaginal prolapse (known as bearings in sheep) occurs within a few weeks prior to lambing and unless treated both ewes and unborn lambs will die. Rates of prolapse in New Zealand vary from 0.1 to 5% per annum, varying between season and farms and is a worldwide problem. Much research has been undertaken over many years to determine the cause of this condition but no clear etiology has emerged. In this study plasma samples were collected prior to prolapse occurring in order to determine physiological changes leading to prolapse. 650 ewes were ear tagged and blood sampled on one day prior to lambing, 28 of these ewes subsequently prolapsed. The date of occurrence and tag number of prolapsing ewes was recorded to enable a comparison of the plasma profile of prolapsing ewes and non-prolapsing ewes. An improved method for running sheep plasma on 2D gels was developed resulting in improved protein spot resolution along with a lower coefficient of variation for spot volume. Using this improved method samples were subjected to 2D DIGE (two dimensional differential in gel electrophoresis) to determine if there were differences between the two groups of ewes. One of the differences was in haptoglobin, a major acute phase protein in ruminants, in which some isoforms were upregulated approximately 3 fold prior to prolapse occurring. This may indicate an inflammatory response due to either infection or injury. A good correlation was found between total haptoglobin spot volume data and quantitative haptoglobin assay data from the same samples ($r^2 = 0.91$) validating the haptoglobin gel spot data. Another finding was that alpha-1B-glycoprotein was down regulated close to prolapse, however the biological significance of this is unknown. It was also found that there was a negative correlation between cortisol and days to prolapse from sampling ($r^2 = 0.36$) *i.e.* ewes closest to prolapse had higher plasma cortisol concentrations than controls. These findings in conjunction with a literature search, field observations and an argument from logic lead the author to propose that chronic stress or anxiety may raise intra-abdominal pressure and contribute to the development of prolapse.

Acknowledgements

I would like to thank my primary supervisor Associate Professor Gillian Norris for her patience, support and encouragement, especially with all the difficulties I had producing good quality gels. Also thanks to my co-supervisor Professor Kevin Stafford for his support and for organising Vet students to do the sample collection. Special thanks to Eion Poole for allowing sample collection on his farm.

Thanks to the C. Alma Baker Trust for providing funding for laboratory consumables to enable the DIGE work to be done in this project and for their patience in receiving reports on the outcomes. I want to thank the Fonterra Research and Development Centre for letting me use their laser scanner that was used for the first two DIGE experiments and to Carel Jobsis for organising this. Similarly to the Hopkirk Research Institute for allowing me the use of their large format gel equipment and to Richard Shaw and Roy Meeking for organizing this. Thanks to the Liggins Institute for the provision of a spot picker and to Eric Thorstensen for organizing this.

I want to thank the Massey University Capital Equipment committee for purchasing a Fuji 5000 fluorescent scanner and Ettan Dalt gel equipment which enabled me to do my later gel work within the Institute of Fundamental Science. I wish to thank the library staff for their support in providing what must have seemed like endless requests for interlibrary journal articles.

Special thanks to all in the X-lab, particularly to Trevor Loo for his support and encouragement through this project and especially for his help with mass spectrometry. Also thanks to staff in SFS, particularly Ann Truter, Cynthia Cresswell and Mark Patchett for their general assistance and friendly banter as well as to Anne Lawrence for help with statistics.

To my family and friends thank you, especially to my mum Joan Brown, daughters Amy and Laura, and Sarah and Ian for their support, patience and understanding as I have pursued my dream. Thanks to my brother Bill for his support and inspiration as a dedicated scientist and special thanks to Jon Bjornsson for his assistance on the farm and patience while I have been working on this.

To the sheep who contributed blood samples my thanks and apologies, it was not anticipated that blood sampling may trigger prolapse as it was assumed that only monitoring was taking place.

I offer this tribute in the words of Salomon Frank written in 1713:

“Sheep may safely graze and pasture
In a watchful Shepherd's sight.

Those who rule with wisdom guiding
Bring to hearts a peace abiding
Bless a land with joy made bright.”

Contents

Abstract	i
Acknowledgements	ii
Contents	iii
Figures	v
Tables	vii
Abbreviations	viii
Chapter 1. Introduction	1
Physical mechanisms and intra-abdominal pressure	1
Epidemiological studies	4
Nutrition	6
Experimental Research in South Otago	7
Biochemical and physiological mechanisms	8
Human pelvic organ prolapse	9
Predator stress	10
Other stressors	12
Population control in the Snowshoe hare and the evolution of chronic stress	13
Measurement of stress	14
Biomarkers	15
Proteomics	17
Depletion	17
Two-dimensional gel electrophoresis	19
Sample preparation and conditions for 2D gel electrophoresis of plasma samples	21
Extraction	22
Mixed disulfide bonding	22
Sample clean-up	23
Loading methods and running conditions	24
Other proteomic methods	26
Data analysis	27
Mass Spectrometry (MS)	29
Present study	30
Sample choice and methodology	30
Hypothesis	31
Aims	31
Chapter 2. Method development	32
Sample collection	33
Method development – albumin depletion trial	34
Initial 2D gel methodology	34
Antibody depletion and trialing of clean up methods	36
Improving 1 st dimension resolution	43
Basic sample preparation method	45
First DIGE experiment	46
Second DIGE experiment	49
Increased protein load	50
Spin clean-up experiment	52
Equilibration time	54

Nature Protocols method (also using cup loading).....	55
Improved electrical connection	58
Gel casting issues	61
Chapter 3. DIGE methodology	65
Labelling	65
IEF.....	66
Second dimension.....	68
Image acquisition, spot detection, editing and matching	69
Data comparison – DIGE A and DIGE B	74
Extracting standard data.....	74
Extracting experimental data.....	74
Normalisation.....	74
Evaluating the 2D PAGE methods	76
Chapter 4. Data analysis	79
Data extraction: obtaining standard data.....	79
Data extraction: obtaining control and bearing ewe data.....	80
Normalisation.....	80
Normalisation before or after standardisation.....	83
Evaluation of normalisation	83
Non-linear normalisation	87
Non-linear normalisation applied after standardisation	88
Non-linear normalisation applied before standardisation	90
Data distribution	94
Chapter 5. Results	101
Prolapse occurrence	101
DIGE data analysis.....	102
Data re-normalisation.....	103
False discovery; Benjamini & Hochberg FDR and q values	110
FDR testing	116
Data distribution	119
Alternate normalisation methods.....	122
Effect of albumin depletion variability.....	122
Loading control normalisation - using spots with the lowest variation	123
Normalising with all spots – with blanks filled to calculate normalisation factor	123
Correlation with days to prolapse.....	124
Spots of interest from DIGE A and matched spots in DIGE B	131
Spots of interest from DIGE B and matched spots in DIGE A	135
Spots of interest for identification by mass spectrometry	135
Preparatory gels used for spot identification	150
Mass spectrometry (MS).....	138
Combined spots results.....	147
Haptoglobin assay	150
Phosphate assay.....	155
Cortisol assay	156
Chapter 6. Discussion and conclusion.....	159
Summary of analysis and results.....	159
Alpha-1B-glycoprotein	161
Haptoglobin.....	162

Fetuin A and Serpin	165
Cortisol	165
Future directions	169
Conclusion	170
Bibliography	172
Statement of contribution to publication	188

Figures

Figure 2-1. 2D PAGE of sheep plasma sample depleted with Blue ligand column, small format.....	35
Figure 2-2. 2D PAGE of sheep plasma sample depleted with Blue ligand column, medium format.	36
Figure 2-3. 2D PAGE showing depletion with the Amersham albumin and IgG removal kit.....	38
Figure 2-4. 2D PAGE of flow through from GenWay depletion column, medium format.....	39
Figure 2-5. GenWay column bound fraction and flow through, small format 2D PAGE.	40
Figure 2-6. Chloroform/methanol precipitation, non-depleted and depleted, medium format.	41
Figure 2-7. Protein G and GenWay column bound fractions.....	42
Figure 2-8. Poor quality large format 2D PAGE gels.	43
Figure 2-9. Schematic diagram showing relative placement of IPG strip, wicks and electrodes.	44
Figure 2-10. Heating and/or SDS samples causing charge trains in 2D PAGE, large format.....	45
Figure 2-11. DIGE experiment 1, example gel.	47
Figure 2-12. Trialing voltage gradients during IEF, large format.	47
Figure 2-13. Voltage and resultant current profiles for 2 different IEF regimes.	48
Figure 2-14. Intermediate voltage gradient vs an extra long voltage gradient during IEF.	50
Figure 2-15. Aligning horizontal resolution of DIGE gel with non-DIGE gel.....	51
Figure 2-16. Alkylation protocols and spot resolution.....	52
Figure 2-17. Spin clean up and spot resolution.	53
Figure 2-18. Acetone precipitation and spot resolution, small format.	53
Figure 2-19. Equilibration time and spot resolution.....	54
Figure 2-20. 2D PAGE cup loading experiment, large format.....	55
Figure 2-21. Evaluation of Nature Protocol method, large format.....	56
Figure 2-22. Further evaluation of Nature Protocol method, large format.	57
Figure 2-23. Reduced electrode wick water and spot resolution, small format.	57
Figure 2-24. Increased carrier ampholytes, reduced wick water & spot resolution, small format. .	58
Figure 2-25. Carrier ampholytes in wick water, human plasma sample, large format.....	59
Figure 2-26. Carrier ampholytes in wick water, 150 µg depleted sheep plasma, large format.	59
Figure 2-27. Standard images from DIGE experiment B.	60
Figure 2-28. Example of an extremely wobbly top gel.	61
Figure 2-29. Uneven polymerisation.....	62
Figure 2-30. Effect of wobbly top gels on apparent protein resolution.	63
Figure 2-31. Supplementing buffer solution.....	64
Figure 2-32. Gel from DIGE experiment B with a partial casting issue.	64
Figure 3-1. Diagram showing the relative positions of the IPG strip, wicks and electrode wires. ...	68
Figure 3-2. Inconsistent spot boundaries identified in DeCyder 7.0.	70
Figure 3-3. Example of spot rejection.	71
Figure 3-4. Further example of spot rejection.	71
Figure 3-5. Example of spot inclusion.	71
Figure 3-6. 428 matched spots representing visibly discernible spots were found in DIGE B.	72

Figure 3-7. 208 matched spots representing visibly discernible spots were found in DIGE A.	73
Figure 3-8. Correlation of spot variation (CV) with spot volume of the internal standards.	78
Figure 4-1. Ratio-intensity plots to evaluate linear normalisation methods.	84
Figure 4-2. Variance ratio plots to evaluate the linear normalisation methods used.	85
Figure 4-3. Variance between gels was compared to variance within gels.	86
Figure 4-4. Box plots showing data variation before and after each normalisation method.	87
Figure 4-5. Ratio-intensity plots for the evaluation of non-linear normalisation methods.	88
Figure 4-6. Variance ration plots for the non-linear normalisation methods.	89
Figure 4-7. Ratio-intensity plots for non-linear normalisation applied before standardisation.	90
Figure 4-8. Variance ratio plots, non-linear normalisation applied before/after standardisation. ..	91
Figure 4-9. Variance ratio plots for VSN normalisation applied with missing values allowed.	92
Figure 4-10. Box plots showing data distribution after two non-linear normalisation methods.	92
Figure 4-11. Variance ratio plots for DIA and alternative normalisation methods.	93
Figure 4-12. Scatter plot of paired Bearing vs Control samples.	94
Figure 4-13. Distribution histogram for scaled spot volumes.	95
Figure 4-14. Quantile comparison plot of normalised and standardised spot volume data.	96
Figure 4-15. Quantile comparison plot of log(2) normalised & standardised volume data.	97
Figure 4-16. Quantile comparison plot of VSN normalised data.	97
Figure 4-17. Quantile comparison plot of quantile normalised log(2) data.	98
Figure 4-18. Distribution histograms for log transformations and normalisations.	98
Figure 4-19. Scatter plots for transformed paired spots, bearing vs control.	99
Figure 4-20. Scatter plots showing average spot volumes, bearing vs control.	100
Figure 5-1. Distribution of prolapse occurrence.	101
Figure 5-2. The master gel from DIGE experiment A.	107
Figure 5-3. Standard images for all gels from DIGE experiment A.	108
Figure 5-4. The master gel from DIGE experiment B.	109
Figure 5-5. Standard images for all gels from DIGE experiment B.	110
Figure 5-6. Distribution of <i>p</i> values for DIGE experiment A, from DIA analysis.	111
Figure 5-7. Distribution of <i>p</i> values for DIGE experiment B, from DIA analysis.	111
Figure 5-8. Distribution of <i>p</i> values for DIGE experiment A, linear normalised (all spots).	111
Figure 5-9. Distribution of <i>p</i> values for DIGE experiment B, linear normalized (all spots).	112
Figure 5-10. Distribution of <i>p</i> values for DIGE experiment A, VSN normalisation.	112
Figure 5-11. Distribution of <i>p</i> values for DIGE experiment B, VSN normalisation.	112
Figure 5-12. Distribution of <i>p</i> values for DIGE A, quantile normalisation of volume.	113
Figure 5-13. Distribution of <i>p</i> values for DIGE B, quantile normalisation of volume.	113
Figure 5-14. Distribution of <i>p</i> values for DIGE A, quantile normalisation of log(2) volume.	113
Figure 5-15. Distribution of <i>p</i> values for DIGE B, quantile normalisation of log(2) volume.	114
Figure 5-16. <i>P</i> value distribution using quantile normalised volume, FDR and <i>q</i> values.	117
Figure 5-17. <i>P</i> value distribution using linear normalised (all spots) data, FDR and <i>q</i> values.	118
Figure 5-18. Example FRD plots generated in the R package 'prot2D'	119
Figure 5-19. Distribution boxplots and scatter plots for FDR spots from DIGE A.	120
Figure 5-20. Distribution boxplots and scatter plots for FDR spots from DIGE B.	121
Figure 5-21. Location of albumin spots removed for depletion variability check.	123
Figure 5-22. Days to prolapse vs abundance & control boxplots for FDR spots, DIGE A.	125
Figure 5-23. Days to prolapse vs abundance & control boxplots for correlated spots, DIGE A.	125
Figure 5-24. Days to prolapse vs abundance and control boxplots where controls fit correlation.	126
Figure 5-25. Days to prolapse vs abundance and control boxplots for FDR spots, DIGE B.	127
Figure 5-26. Days to prolapse vs abundance and control boxplots for correlated spots, DIGE B.	128

Figure 5-27. Days to prolapse vs abundance and control boxplots for correlated spots, DIGE B. .	128
Figure 5-28. Days to prolapse vs abundance and control boxplots for correlated spots, DIGE B. .	129
Figure 5-29. Days to prolapse vs abundance and control boxplots for correlated spots, DIGE B. .	129
Figure 5-30. Days to prolapse vs abundance and control boxplots for matching spots.....	132
Figure 5-31. Days to prolapse vs abundance and control boxplots for matching spots.....	134
Figure 5-32. The master gel from DIGE B showing positions of the spots of interest.	136
Figure 5-33. Spots of interest in 3D view.	137
Figure 5-34. Schematic showing the location of the paper bridge, IPG strip and electrode wick..	152
Figure 5-35. Preparatory 2D PAGE gels for mass spectrometry.	152
Figure 5-36. Combined preparatory gel images.	153
Figure 5-37. Example MSMS spectrum.	141
Figure 5-38. Locations of spots extracted for mass spectrometry.	145
Figure 5-39. 2D reference map of sheep serum proteins, pH 4-7 [170].....	146
Figure 5-40. 2D reference map of sheep serum proteins, pH 3-10 [170].....	147
Figure 5-41. Spot positions and 3D views for globally quantified proteins.	148
Figure 5-42. Combined alpha-1B-glycoprotein spots, days to prolapse and control boxplot.	150
Figure 5-43. Correlation of combined haptoglobin spot volume with haptoglobin assay.	154
Figure 5-44. Haptoglobin assay, same samples as DIGE B, correlation with days and boxplots. ...	154
Figure 5-45. Haptoglobin assay, all pre-prolapse samples, correlation with days and boxplots. ..	155
Figure 5-46. Box and whisker plot of serum phosphate levels as found by Hilson <i>et al.</i> [4].....	156
Figure 5-47. Plasma phosphate, days to prolapse and boxplots.	156
Figure 5-48. Plasma cortisol boxplots, all pre-prolapse samples, 1 st 3 weeks and control.	157
Figure 5-49. Log(2) transformed plasma cortisol, 1 st 3 weeks and controls.....	158
Figure 5-50. Plasma cortisol, days to prolapse vs abundance and control boxplot.	158

Tables

Table 2-1. Source of key lab consumables.....	32
Table 2-2. Theoretical water consumption due to electrolysis during isoelectric focusing.	49
Table 3-1. Voltage profiles used for isoelectric focusing in two DIGE experiments.	67
Table 3-2. Summary table comparing spot resolution in DIGE A and DIGE B.....	77
Table 5-1. Initial data analysis for DIGE experiment A using DeCyder 7.0.	102
Table 5-2. Initial data analysis for DIGE experiment B using DeCyder 7.0.	103
Table 5-3. T-test <i>p</i> values using linear normalised log(2) transformed data, from DIGE A.	104
Table 5-4. T-test <i>p</i> values using linear normalised log(2) transformed data, DIGE B.	104
Table 5-5. T-test <i>p</i> values using non-linear (VSN) re-normalised data, DIGE A.	105
Table 5-6. T-test <i>p</i> values using non-linear (VSN) re-normalised data, DIGE B.	106
Table 5-7. Summary table of student's t-test <i>p</i> values and ratios, DIGE A.	106
Table 5-8. Summary table of student's t-test <i>p</i> values and ratios, DIGE B.	106
Table 5-9. <i>P</i> values, adjusted <i>p</i> values and <i>q</i> values for spots where <i>p</i> < 0.05.	116
Table 5-10. FDR spots using the 'prot2D' R package, DIGE A data.	118
Table 5-11. FDR spots using the 'prot2D' R package, DIGE B data.	119
Table 5-12. Summary table for alternative normalisation methods.	124
Table 5-13. Spots from DIGE experiment A that correlate with days to prolapse.	126
Table 5-14. Spots from DIGE experiment B that correlate with days to prolapse.....	131
Table 5-15. Spots of interest.	135
Table 5-16. Protein IDs for spots 1-5.	142

Table 5-17. Protein IDs for spots close to and including B 765.	143
Table 5-18. Protein IDs for spots close to and including B 1071.	144
Table 5-19. Protein IDs for protein spots B 2373, B 1588 and B 1577.	144
Table 5-20. Protein IDs for protein spot B 891.	145
Table 5-21. Haptoglobin spot changes, individual and combined results.....	148
Table 5-22. Two rows of fetuin spots and combined results (linear normalised).....	149
Table 5-23. Alpha-1B-glycoprotein spot changes, individual and combined results.	149
Table 5-24. Correlation between alpha-1B-glycoprotein and days to prolapse.	150

Abbreviations

AA	amino acid
BCA	bicinchoninic acid
BSA	bovine serum albumin
BVA	biological variation analysis (DeCyder 7.0 software module)
CHAPS	3-[(3-cholamidopropyl)dimethylammonio]-1-propanesulfonate
CI	confidence interval
CV	coefficient of variation
DAMP	damage associated molecular pattern
DCAB	dietary cation-anion balance
DIA	difference in-gel analysis (DeCyder 7.0 software module)
DIGE	difference in-gel electrophoresis
DMF	dimethylformamide
DNA	deoxyribonucleic acid
DTE	dithio-1,4-erythritol
DTT	dithiothreitol
EDTA	ethylenediaminetetraacetic acid
ELISA	enzyme-linked immunosorbent assay
ESI	electrospray ionisation
FDR	false discovery rate
HCD	higher-energy collisional dissociation
HCl	hydrochloric acid
HEC	human ethics committee
HPLC	high-performance liquid chromatography
HPA	hypothalamic pituitary adrenal (axis)
IAP	intra-abdominal pressure
ID	identification (number)
IEF	isoelectric focusing
IPG	immobilised pH gradient
IgG	Immunoglobulin G
IgY	Immunoglobulin Y
LCMS	liquid chromatography - mass spectrometry
Log	logarithm (either base 2 or base 10)
LSA	log standard abundance
M	molar
MALDI-TOF	matrix-assisted laser desorption/ionization - time of flight
MQ	Milli-Q

MS	mass spectrometry
MSMS	tandem mass spectrometry
MUAEC	Massey University animal ethics committee
MWCO	molecular weight cut-off
NA	not available
NCBI	National Center for Biotechnology Information
NL	non-linear
NMR	nuclear magnetic resonance
OR	odds ratio
PAGE	polyacrylamide gel electrophoresis
PCA	principle component analysis
PCR	polymerise chain reaction
PD	Proteome Discoverer (software)
PEP	posterior error probability
PI	isoelectric point
PMF	peptide mass fingerprint
PMT	photomultiplier tube
POP	pelvic organ prolapse (human)
PSM	peptide spectral match
RNA	ribonucleic acid
SD	standard deviation
SDS	sodium dodecyl sulphate
SNP	single nucleotide polymorphism
TBS	tris-buffered saline
TCA	trichloroacetic acid
TCEP	tris(2-carboxyethyl)phosphine
TPP	trans proteomic pipeline
Tris	tris(hydroxymethyl)aminomethane
VSN	variance stabilising normalisation
WEHI	Walter + Eliza Hall Institute of Medical Research

Chapter 1. Introduction

Ovarian pre-partum vaginal prolapse is a common condition of sheep that occurs in the days and weeks leading up to lambing. It occurs worldwide at widely varying rates ranging from less than 0.1 % up to 20% of ewes per flock per annum [1-4]. It has occurred in New Zealand since the early days of farming and been observed to be widespread since about 1890 [5]. The prolapsed organ consists of all or part of the vagina that has everted to the outside of the animal [6]. In most cases the whole vagina is pushed out including the cervix, turning the organ inside out, which then hangs out of the rear of the animal. It often contains the bladder within it [7], kinking the urethra [8] and preventing urination, which is potentially lethal in itself. Further, lambing cannot proceed unless the prolapse is repaired. Prompt repair is imperative for two reasons. Firstly the vagina needs to be put back into its normal place to enable the lamb to engage in the birth canal. Secondly, the unsupported weight of the prolapsed vagina tends to pinch off its own blood supply, and if not treated, the vagina necroses causing blood poisoning, or if close to lambing results in the cervix failing to dilate, a condition known as ringwomb [9]. Unless the prolapse is treated promptly, death of the pregnant ewe surely follows and even if the prolapse is repaired, the survival rate is at best only moderate [10]. Thus pre-partum prolapse is a serious problem.

Physical mechanisms and intra-abdominal pressure

In New Zealand during the 1950's several studies were undertaken in which the pelvic regions of sheep were examined with a view to understanding the etiology of prolapse were undertaken. Bassett and Phillips [11] compared the anatomy of ewes with a history of previous prolapse to those of normal ewes, and found that the length of vaginal tract attachments tended to be longer in ewes with a history of prolapse compared to the control animals. Furthermore, the sacro-iliac joints (which affect the size of the pelvic opening) of prolapsed ewes were more relaxed in prolapsed ewes [12]. However, this study could not determine if the prolapse caused the vaginal attachments to be lengthened or if the lengthening precipitated prolapse. It was concluded that the pelvic peritoneum is important in controlling movement of the reproductive organs.

McLean [13], looked at live, pregnant, non-prolapsed sheep to determine the degree of distensibility and lability of the normal vagina and to quantify the changes that occur as pregnancy progresses. He found that the vagina becomes increasingly enlarged and distensible as lambing approaches. His

work determined that the constrictor vestibuli muscle (the muscle at the mouth of the vagina) performs a physical role in relation to prolapse that is distinct from the vagina itself. Although unclear about the specific roles of these organs in relation to prolapse, by undertaking physical measurements he determined that the volumetric capacity of the vagina was different to the distensibility of the vulva and vestibule, suggesting that the relative flexibility of these organs have different effects on prolapse. As field observations had long suggested that fat ewes are more prone to prolapse [14], McLean looked for differences in the vagina, vulva and vestibule between fat ewes and control animals. It was found that although fat ewes looked flabby around the vulva the strength of the relevant tissues was similar [15]. He suggested that instead of differences in the relative strength of pelvic tissues being causal in prolapse, it may be a result of excessive intra-abdominal pressure.

In another study, McLean [16], reported a survey of 105 farms (112,886 ewes) looking at the effect of farm contour on prolapse rate. The survey found a statistically significant difference between the rate of prolapse on flat farms compared to hilly farms. On hilly farms there was an overall prolapse rate of 0.503% while on flat farms it was 0.165%. They concluded that the difference resulted from ewes lying down on slopes with their hindquarters lower than their forequarters, which could lead to excessive pressure on the vagina.

It should be noted at this point that the Hilson *et al.* study (described below) also looked at the effect of terrain and found that lambing on moderate to steep terrain, as opposed to lambing on a mix of flat and steep paddocks, increased the odds of prolapse (1.37x, $p < 0.1$) although this finding was not supported in a large Scottish survey [3].

McLean and Claxton [15], monitored the intra-abdominal pressure (IAP) of pasture grazed sheep by inserting an instrument into the vagina that was able to measure the pressure adjacent to the cervix. There was a small correlation of IAP with body weight and gut fill. However, when body position was controlled, IAP was largely independent of the stage of pregnancy and the number of lambs carried. It was found that there was a high level of variation between individual animals and between the various positions (*e.g.* lying or standing) of the animal when IAP was measured, standing resulted in low to negative levels of IAP, whilst lying down substantially increased it, and lying with buttocks downhill increased it even further. The authors concluded that lying down on

sloping ground “is the critical factor determining whether or not outbreaks of the disease will occur”. It was reported however, that “the only case of prolapse that occurred in the experimental ewes had [prior to the prolapse occurring], in fact, very high pressures in all positions” [*i.e.* lying or standing].

An Egyptian study measured IAP in feedlot ewes before and after feeding and found that IAP was actually higher before feeding than after feeding. It was also found that IAP was lower in ewes carrying multiple foetuses than in ewes carrying a single foetus [17].

In an unpublished study, Ayen and Noakes looked at the effect of diet on intra-abdominal pressure in pregnant ewes and found that dietary fiber content had no effect on IAP. They also observed no changes in pressure “throughout pregnancy or significant differences between ewes with single or twin lambs” (reported in [2]). Ayen and Noakes also looked at the effect of diet composition on the positional displacement of the genital tract in pregnant ewes but found no significant effect [6]. However, a later report indicated, that when grain-fed ewes had their ration split into two feeds, as opposed to getting it all at once, they had a markedly decreased rate of prolapse [18].

Premature uterine contraction may raise IAP to levels that are higher than normal. In a study looking at the effects of various hormones on uterine contraction and IAP, surgically implanted sensors were used to monitor contractions [19]. It was found that although both oxytocin and PGF2 alpha produced uterine contractions, they had no effect on IAP.

In summary, it is widely agreed that IAP is a significant precipitating factor in pre-partum prolapse. Increases in IAP can be caused by increases in total gut weight, pregnancy status (both advancing pregnancy and number of fetuses), the position of ewe viscera in relation to the pelvis (*e.g.* due to lying on a slope with buttocks downhill) and other unknown individual differences. There is however, a dearth of research looking at the biological causes of increased IAP in most species [20], although there is some interest in the measurement of IAP as a diagnostic tool in humans. This is because high IAP (sometimes called abdominal compartment syndrome in humans [21]) has very serious medical consequences for both humans and animals [22], [23]. Abdominal compartment syndrome seems to be mainly associated with recent physical trauma, particularly in those that have received blood transfusions, and is increasingly monitored in critical care patients [24]. As post-

mortem studies of prolapsed ewes show no evidence of recent injury apart from damage due to the prolapse itself [11], the etiology of this syndrome is probably not directly relevant to the present study. It is, however, interesting that human IAP is affected by the level of abdominal wall tension, and that strategies to reduce abdominal wall tension have been found to be effective in reducing human IAP [25, 26].

While it is as not yet understood what mechanisms are responsible for raising IAP in sheep, it is possible that psychological stress may be involved, especially given the effect that psychological stressors are known to have on hypertension (high blood pressure) in humans [27] as well as the conclusions of McLean and Claxton that IAP was closely involved in ovine vaginal prolapse [15]. Although research on this hasn't been reported, it does seem likely that stress hormones such as cortisol or adrenalin could raise IAP, particularly given that abdominal muscles (and other skeletal muscles) have increased basal activity when adrenalin levels are elevated [28].

Epidemiological studies

The first reported farmer survey attempting to find causes of prolapse appears to be that of a group of New Zealand veterinarians in 1936 [29] which concluded that although controlling the condition of ewes along with exercise should prevent prolapse, much more detailed information was needed. An area of possible research was to investigate the relationship between pelvic size and prolapse as ewes with a large pelvis appeared to be more susceptible (Laing 1945, cited in Edgar 1952 [1]).

In 1952 Edgar [1] reported a two year survey of 34 flocks and some associated experimental work. He concluded that unknown environmental factors lead to the occurrence of prolapse and that farmers should make sure that both repaired ewes and surviving offspring were culled.

A 1970s survey of several hundred cases of prolapse on UK farms found that there were as many suggested causes of prolapse as there were prolapse cases. No useful conclusions could be drawn so a formal report was not published, although the work was described in a letter to the Veterinary Record [30].

A 1980's survey of over 500 farmers in the Border region of Scotland found that rates of prolapse varied considerably and "appeared to be a flock problem rather than a problem of individual ewes"

[3]. However despite some high rates of occurrence (including one of over 15%) it was concluded that pre-partum prolapse is a relatively rare condition, and that research efforts should concentrate on farms that have a problem. It was noted that the rate of prolapse among hill farms was lower than on flat farms (contrary to New Zealand findings) and that it was more common in highly fecund flocks.

With the advent of routine ultrasound scanning of pregnant ewes in the 1990s, farmers became much more aware of the pregnancy status of the prolapsed ewes they were treating, leading to the observation that prolapse is largely a disease of ewes carrying twins [2]. This conclusion was reinforced by a large NZ epidemiological study of 201 farms (Hilson *et al.* [4] reported in [31]), which found that the incidence was 5.31 times higher for ewes scanned with twins compared to singles, and 11.3 times higher for ewes carrying triplets (406 ewes prolapsed out of the 36,695 ewes monitored).

As well as pregnancy status, Hilson *et al.* looked at a number of other parameters that were suspected in the etiology of prolapse. They found that shearing, either prior to mating, or in the second half of pregnancy, slightly lowered the rate of prolapse. Farmer culling of affected ewes and their offspring did not appear to reduce prolapse rate in subsequent years, suggesting that environmental factors are likely to be more important than genetics in the etiology of prolapse. They also examined several basic serum markers of pregnant ewes prior to the prolapse period. A statistically significant correlation found in these studies was a positive correlation between serum phosphate levels and subsequent prolapse, although no explanation for this could be provided.

Hilson *et al.* also looked at body condition, weight, and weight gain over gestation. There was no correlation between either body weight or condition score with prolapse, indicating that neither the size of the ewe nor its weight, is causal in prolapse. There was however, a small positive correlation between weight gain in the first two thirds of pregnancy and later prolapse. Hilson *et al.* cautiously concluded that this may be due to an effect of nutrition on the combined volume of the placenta and fetuses. The study concluded that prolapse is multi-factorial and that there is “considerable influence from other as yet unrecognized factors” because survey questions “cannot be expected to capture all the detailed information about individual farm management practices or day to day husbandry decisions outside the normal patterns” [31].

Nutrition

Two studies [32, 33] compared the serum calcium levels of normal pregnant ewes with ewes that had already prolapsed. In both studies serum calcium concentrations were lower in prolapsed ewes than in the control ewes. The authors therefore concluded that poor nutrition could be a contributing factor in prolapse. Another study looked at the overall nutritional status of prolapsed ewes and concluded that the cases of hypocalcaemia in prolapsed ewes was a consequence of prolapse, rather than a cause of it [34].

Several studies examining the effect of nutrition on both lamb birth weight and placental growth have been reported [35-39]. Fogarty *et al.* [36] looked at the effect of changes in feeding during mid-pregnancy (weeks 11-13, 20 weeks is full term) in 1220 ewes. They found that changes in feeding resulted in the low fed group being 5 kg lower in total bodyweight than the high fed group, but that diet had no significant effect on lamb birth weight. Holst *et al.* [37] looked at the effect of feeding levels during weeks, 6-15 and 15-20, of gestation. They found that the biggest difference in lamb birth weight was linked to changes in the feeding of twin bearing ewes in their last trimester (15-20 weeks) of pregnancy. Smeaton *et al.* [40] looked at the effects of feeding in early to mid-pregnancy in highly fertile ewes. They found that a loss of more than 4 kg of body weight during weeks 3-10 of pregnancy could lead to a reduction in lamb birth weight.

Hilson *et al.* found that access to salt and the feeding of swedes to ewes in the latter part of pregnancy slightly increased the risk of prolapse (odds ratios of 1.40, P=0.07 and 1.45, P=0.07 respectively). The authors concluded that this effect was probably due to salt and swedes increasing the animals water intake resulting in straining during urination. Hilson *et al.* also looked at serum levels of magnesium, calcium, phosphate, chloride and β hydroxybutyrate in samples collected before the onset of bearings. This data set was obtained from 994 blood samples, 18 of which were from ewes that subsequently prolapsed. As mentioned earlier a statistically significant association was found between serum phosphate and subsequent prolapse. They found that “ewes with higher serum phosphate were subsequently 2.6 times more likely to have a bearing than those with lower concentrations.” [41].

As mentioned above, Hilson *et al.* also noted that there was a small positive association (OR 1.29, P=0.02) between an increase in ewe body weight during the first two trimesters of pregnancy with subsequent prolapse. It was suggested this may be due to an increase in the combined size of the placenta and fetuses (conceptus).

Litherland *et al.* looked at a range of nutritional measures in the grass being offered to sheep before lambing as well as serum calcium, magnesium, phosphate and β hydroxybutyrate and urine pH, calcium and creatine in a small number of ewes. As well as these factors they also looked at the effect of adjusting pasture dietary cation-anion balance (DCAB), vitamin D and calcium supplementation on the incidence of bearings and the levels of nutrients. Although it was the authors opinion “that there is a strong ‘environmental’ component in bearings” they were not able to determine any significant factor involved, including calcium levels [41].

Experimental Research in South Otago

Very few experimental studies have been undertaken to establish the possible causes of prolapse. This is in part due to the paucity of leads from epidemiological studies. However, a study based on a large flock in South Otago, New Zealand, with a history of high rates of prolapse yielded an interesting result [42]. A 2005 survey of the South Otago flock found that varying feed conditions in the second half of pregnancy had no effect on prolapse, consistent with the Hilson *et al.* study. Anecdotal evidence that feeding levels in the first half of pregnancy may have an effect on rates of prolapse led the South Otago group to experiment with the management of feed in the first half of pregnancy.

In an experiment carried out in 2006, 1200 ewes were split into two groups during the first half of pregnancy. One group was shifted every 2 days, while the second group was moved every 4 days. Both groups were allocated the same total amount of grass. The 2 day mob got half the allocation at each move as compared to the 4 day mob, but were moved twice as often and so got the same total amount of grass. The mobs were joined back together for the second half of pregnancy and lambing. The prolapse rates were 2.99% (17/582) for the 2 day mob and 0.9% (5/579) for the 4 day mob (significance t pr = 0.009). This experiment was repeated in 2007 with a similar result. The researchers could not propose a reason for the difference, although they speculated that the different feeding regimes may have resulted in differences in placental size. It was also noted that

the 4 day mob were very settled both when shifting and after several days in the paddock, which presumably reflected lower stress levels at the time of management manipulation (the first half of pregnancy).

Biochemical and physiological mechanisms

Ayen and Noakes [43] used histological methods to look at vaginal wall collagen distribution to see if there were differences between prolapsed ewes and non-prolapsed ewes, but found none. They also experimented with supplementing oestradiol and progesterone to see if increasing the levels of these hormones would affect the physiology of the vagina and result in prolapse [44]. It was found that while oestradiol and progesterone did cause an increase in vaginal capacity, vaginal compliance was reduced. On the surface therefore, it seems unlikely that those hormones play a role in prolapse. It should be noted however, that considerable variation was found between animals.

A more recent study investigated the transcription of specific collagens in the vagina of prolapsed ewes using semiquantitative reverse transcription-PCR in order to determine if RNA expression levels for these proteins differed in prolapsed ewes. Ennen *et al.* looked at samples from 6 prolapsed sheep from 3 different breeds and found that the mRNA levels for the alpha 2 chain of collagen I was lower in prolapsed ewes than in the 4 late pregnancy control ewes examined. This was also the case for vaginal estrogen receptor alpha, where mRNA expression was reduced in prolapsed sheep. It should be noted that the mRNA levels for the genes from the small sample group was variable and that data could not be obtained from some samples. Other findings from this work were that the vaginas of affected ewes were characterised by epithelial hyperplasia or a doubling of thickness of the vaginal epithelia. There was however, no sign of inflammation. They also found that plasma progesterone concentration was higher in affected animals compared to the controls [45]. As the samples were taken after prolapse occurred it is not possible to determine if these changes were causal to, or consequential of prolapse.

The present study uses samples collected prior to the occurrence of prolapse in the hope of finding some clues to shed light on possible biochemical and physiological mechanisms in the etiology of bearings. There has been some retrospective research focused on blood samples taken from ewes that have already prolapsed. Butcher and McIntyre [46] found that serum copper levels were higher in ewes that had recently had a bearing compared to the levels in control ewes. Although the

difference was statistically significant at the 5% level, it should be noted that the sample size was small (9 in each group), and as mentioned, samples were taken after prolapse had occurred. Two other studies by Sobiraj *et al.* [33] and Stubbings [32], found that serum calcium levels were lower in affected animals than in unaffected animals. However, as mentioned earlier, it was concluded that this was probably a consequence of prolapse rather than a cause *i.e.* sub-clinical hypocalcaemia was probably induced by the trauma of prolapse [34]. This finding serves to highlight the problems associated with retrospective blood sampling.

As mentioned earlier, the Hilson *et al.* epidemiological study found a small but statistically significant correlation of serum phosphate with subsequent prolapse. While the association was not strong, (OR 2.65, CI 95%) it was reported that the correlation between serum phosphate and subsequent prolapse was still present when farm identity was treated as a random effect, demonstrating the robustness of the statistics. The connection between raised serum phosphate and subsequent prolapse is difficult to explain in the absence of more information. If a systemic (*i.e.* blood born) mechanism is involved in prolapse then systemic factors other than just phosphate (or phosphate carriers) are also likely to be involved.

Human pelvic organ prolapse

Human pelvic organ prolapse (known amongst researchers as POP) is a common condition affecting up to 25% of women [47] and is characterised by the intrusion of pelvic organs into the vagina [48]. The definition for human POP differs to that of ovine vaginal prolapse (the eversion of part or all of the vagina to the outside) in that the vagina may not be displaced out to the exterior during POP, meaning the affected individual may be unaware of their condition, in contrast to ovine vaginal prolapse which is an obvious condition. Further, ovine prolapse occurs more commonly pre-partum [31], whereas human POP is more common post-partum (and is associated with vaginal childbirth trauma) [49]. Human POP occurs much less frequently in nulliparous women than in parous women and cesarean section is protective at least for some types of POP [50]. It should be noted that humans are bipedal and so, for standing individuals, the vagina is underneath the other pelvic organs whereas sheep are quadrupeds, with the vagina being level with, or above the other pelvic organs. This means that, for humans, the pressure on the pelvic organs is almost always positive, regardless of position [21], whereas in the standing relaxed sheep, pressure on the vagina is negative [15]. The timing of occurrence and pressure differences between sheep and humans suggests that damaged

pelvic support may be more important in the etiology of POP than it is for ovine vaginal prolapse. These timing and intra-abdominal pressure differences may be reflected in POP being associated with physical childbirth trauma, whereas ovine prolapse may be associated with unusually high intra-abdominal pressure prior to delivery. The differences between the two conditions seem to suggest that there are differences in the etiology of the conditions. There is however, interest in using sheep as a model for understanding human POP, particularly in working towards improving human vaginal surgery techniques [51, 52].

Predator stress

As noted earlier, there are some indications that ovine pre-partum prolapse may be induced by abnormally high intra-abdominal pressure (IAP). Indications are that while anecdotal reports suggest that a bulky diet may occasionally produce abnormally high IAP, research evidence suggests this is not commonly the case [17] indicating other causes of increased IAP need to be considered. For sheep, it appears likely that stress contributes to an increase in IAP [15] and exposure to predators is known to be very stressful for sheep [53]. Although standing relaxed ewes have been shown to have negative internal pressure on the organ (in contrast to humans), it was reported that the one ewe being monitored that prolapsed, had high IAP in all positions. It is possible that ewes that are not able to relax have higher than normal IAP and this contributes to prolapse. Supporting evidence for this comes from an Otago study across two lambing seasons that found unsettled sheep were more prone to subsequent prolapse [42].

Predation is not just an incidental problem for life on earth. It has been a serious problem for living organisms for eons, in fact, it seems to have been one of the key driving forces in evolution since the time when only single celled organisms existed approximately 1 billion (1000 million) years ago [54, 55].

Anti-predator behavior has been studied in many species, and some of the most interesting effects are chemically mediated and quite sophisticated [56]. For instance, Kusch *et al.* [57] found that fathead minnows are able to distinguish, at distance, the difference between small pike (a predator) and large pike (who are not interested in minnows) through recognition of chemical signals.

In a US study it was found that coyote faecal matter was more effective at deterring sheep from feeding than either oil of wintergreen or fox, cougar or bear faecal matter [58].

Another study in France found that faecal matter from domestic dogs (a close relative of the coyote) is an effective sheep repellent (Poindron, 1974, cited in [59]). Arnould and Signoret [59], used dog faeces to find out if their repellent properties were temporary, and found that sheep wouldn't habituate to (*i.e.* get used to) the odor. They also combined anosmic ewes (ewes with no sense of smell, which aren't repelled by dog faeces) with normal ewes to see if the normal ewes would maintain their distance from the faeces in the presence of ewes that didn't avoid them. The purpose of this experiment was to ascertain whether social facilitation had an effect on the repellent nature of dog faeces. It was found that it did not. From this work, it appears that the predator-avoidance behaviour of sheep, at least that triggered by smell, has innate rather than acquired characteristics. Work is still underway to characterise the essential ingredients of dog odor that elicits predator stress in sheep. Indications are that a complex mixture of fatty acids and neutral compounds are involved [60, 61] and that the diet of the predator may have an effect [62].

It is understood that sheep very successfully survived the recent ice-ages. This is demonstrated in the genetic diversity of wild sheep and in the number of breeds that survive to this day. Part of this success is undoubtedly due to successful anti-predator behaviour which has a strong genetic basis [63]. It is thought that the ungulates (hoofed mammals) co-evolved with predators for millions of years. Sheep and other species of the ungulate family, along with the sub-ungulates (elephants), are characterised by a high degree of gregariousness and other related social behaviors. This is typified by herding or flocking in sheep, where sheep will run together at the slightest sign of danger. It is thought that these behaviors arose in ancestral species in Africa as "a consequence of moving from the cover of closed forests to more open habitats such as savannas, grasslands, and meadows" (p 484 [64]) and that predator management was the primary driver. The ancestor of the modern coyote followed horned sheep from Asia, across the land bridge to North America, approximately 100,000 years ago [64]. Humans have been closely associated with sheep for about the last 12,000 years [65]. Wolves (the ancestor of the modern dog) are, however, likely to have had a much more significant impact on the predator awareness of sheep than humans. This is reflected in research that shows that sheep are more adverse to the presence of a dog than to a human [53].

Although domestication may have weakened anti-predator behavior [66, 67], there is ample evidence that it still exists in farmed sheep. In fact farmers rely upon the predator-prey relationship to enable efficient stock management [68]. This is especially apparent when one considers the use of working dogs on sheep farms.

Other stressors

Baldock and Sibley [69], found that although both visual isolation and introduction to a new flock increased the heart rate of sheep moderately, an approaching man and dog had a much greater effect. Being transported in a stock trailer had a much smaller effect than being herded by a man and dog. In fact herding was found to increase sheep heart rates to very high levels *i.e.* much higher than could be accounted for by the exertion alone. It has been shown that although human presence has no significant effect on the heart rate of two breeds of lambs, human movement has a moderate effect on sheep heart rate [69, 70]. Interestingly, repetitive handling has been shown to reduce stress during later handling events, as well as reducing flight distance [71]. Simple confinement is another stress for sheep [72], and the confined isolation of one sheep from the rest of the flock has been shown to be even more stressful [73] [74]. Sheep have been shown to display a range of different responses to the same psychological stressor, and while these differences can relate to breed differences [75], individual differences within a flock are also significant [76].

Density dependent population regulation was a concept that gained traction as ecology was emerging as a science in the 1930's [77]. At that time it was thought that the density of a particular species within a given habitat regulated the population size. Debate on this issue continues [78, 79], and while it can be argued that the simplest explanations for density dependent population regulation may be related to the availability of food rather than population density [80], it is clear that other factors are also at play [81, 82].

The gregariousness of sheep, along with other closely related species, indicates that density is not necessarily a problem for them and that they may in fact prefer to be in a crowd. Boe *et al.* showed that sheep can exist in a relatively crowded barn situation without a change in behavior [83]. It has also been shown that there are positive physiological benefits to sheep when they are in a flock. A study published in Nature showed that sheep secreted more saliva when in the presence of other

sheep than compared to when they are isolated, and that saliva secretion decreased to nil in the presence of a dog [84].

Population control in the Snowshoe hare and the evolution of chronic stress

In the 1920's researchers began looking at data relating to population cycles of the Snowshoe hare. This information was gleaned from the analysis of Canadian records of snowshoe hare pelt sales over more than 200 years. This work showed a regular cycle of extreme highs and lows of numbers with a period of between 6 and 9 years [85]. Research interest in the population cycling of the snowshoe hare continued, particularly in trying to find an explanation for the lag phase – where the population fails to recover as expected when food levels are adequate and predators are low. In 1995 Hik proposed a hypothesis that snowshoe hares are able to assess the risk of predation and adjust their foraging habits to avoid predation. It was suggested that reduced body condition caused by predator avoidance behavior resulted in decreased fertility. While this hypothesis was supported by the available data [86], it did not fully account for the lag phase. Further research work found that predator induced elevation of stress hormone levels in dams was echoed in offspring leading to a greater activation of the stress hormone system (the HPA axis, see below) in their offspring. It was proposed that maternally inherited stress hormones affect the rate of reproduction in the next generation accounting for the lag phase in the recovery of the snowshoe hare population [82, 87, 88]. This research showed there is an adaptive role for chronic predator stress. Note the HPA (hypothalamic-pituitary-adrenal) axis is an endocrine system that controls reactions to stress and regulates many other processes including digestion, immunity and energy availability [89].

Chronic stress has traditionally been regarded as a maladaptive but necessary consequence of acute stress systems [90, 91]. It has been long acknowledged that stress has an inhibitory effect on reproduction [92, 93], and it is becoming recognized that stress in pregnant females may have an adaptive role in maternal programming of offspring [94, 95]. In the case of humans it has been suggested that chronic stress may have benefits for other members of the population [96]. In the case of sheep, it is known that lambs in the wild are very vulnerable to predators around the time of birth and that anti-predator behaviour peaks at this time [67, 97, 98].

Measurement of stress

When attempting to measure stress in vertebrates, distinctions are made based on the time periods involved, with stress being generally divided into either acute or chronic. Acute stress is the fight or flight response, in response to a transient threat, lasting only seconds or minutes. This involves the sympathetic nervous system and the HPA system and many hormones can be activated that restore the organism to its original state. The stress hormones that are most commonly measured are the glucocorticoids, which are produced mainly by the adrenal gland (cortisol in humans and sheep [99]). Among the biological functions that change in mammals suffering acute stress are; increased heart-rate, breathing, and energy availability, improved immunity, and reduced digestion [100]. These changes serve to protect the organism from danger. Chronic stress on the other hand is by definition, long term in its nature, and is generally regarded as maladaptive.

There have been many biological indicators proposed as markers for chronic stress. The HPA system has often been found to be more active in situations of chronic stress and so cortisol response is sometimes used as a measure of chronic stress [101]. However there are some reports that suggest the reverse is true, *i.e.* that HPA system activity can be reduced under chronic stress, notably in humans [102] and cows [103]. In fact, a seminal review published in 2000 on the role of hypocortisolism in stress related disease has, at the time of writing (from a Web of Science search on 14/8/2019) been cited over 1000 times [104], and there is much current research being done to enhance current understanding of the role of the HPA system in chronic stress [102]. A point of note is that it is now appreciated that glucocorticoids have an essential role in reproductive processes as well as a negative role in chronic stress [105].

Chronic stress is also often associated with immune system suppression [106]. This generally shows up as a reduction in lymphocytes (*e.g.* the B & T cells that are involved in cell mediated immunity) and an increase in neutrophils (cells that are involved in the inflammatory response), which can lead to an increase in disease in chronically stressed animals. The test for immune suppression is complex and not suitable for tests requiring large sample numbers [107].

In recent years there has been growing interest in animal welfare of farmed animals [108]. One of the areas of interest has been in the measurement of a set of proteins produced by the liver and secreted into the blood called acute phase proteins [109]. Proteins defined as acute phase proteins

vary between species, and in ruminants the most important are haptoglobin and serum amyloid A [110]. Blood concentrations of these proteins fluctuate by amounts that are typically more than 25% in response to pro-inflammatory cytokines. Most acute phase proteins are up regulated during inflammation, and are called positive acute phase proteins, while some are down regulated, and are known as negative acute phase proteins. Albumin is sometimes down regulated during an acute phase response, possibly because the liver is diverting resources towards the production of positive acute phase proteins [111]. Acute phase proteins are sensitive indicators of inflammation, trauma and disease [109] and there is also growing interest in their use as biomarkers for cancer [112], drug toxicity [113], cardiovascular disease [114], and rheumatic diseases [115]. They are also becoming more commonly used to identify problems in veterinary medicine [107, 109, 116].

There has also been growing interest in the use of acute phase proteins as indicators of stress [107, 117]. Pieneiro *et al.* looked at the effect of transportation on acute phase proteins in pigs [118]. They found that four acute phase proteins increased in concentration after transportation (pig-MAP, haptoglobin, serum amyloid A and C-reactive protein), and one decreased in concentration (apolipoprotein A-I). Another study looked at the effect of mulesing in merino lambs (the removal of skin around the breech area to prevent flystrike) on the level of three acute phase proteins (haptoglobin, serum amyloid A and fibrinogen) [119]. It was found that concentrations of all of these proteins significantly increased as a result of mulesing in comparison to controls.

Biomarkers

It is important to acknowledge that there are few strong clues as to the etiology of prolapse other than that it is strongly associated with carrying multiple foetuses. The current poor understanding of the mechanisms involved in causing prolapse is reflected in the fact that there has been almost no attempt to experimentally induce prolapse. Given this poor understanding a biomarker search is required.

A joint venture looking into biomarker definition led by the World Health Organisation in association with the United Nations and the International Labour Organisation defined biomarkers as “any substance, structure, or process that can be measured in the body or its products and influence or predict the incidence of outcome or disease” [120]. Often the goal in biomarker analysis is the provision of a predictor of a clinical endpoint [121], however biomarkers can also be used to predict

normal processes, such as in a pregnancy test. The US National Institutes of Health defines biomarkers as “a characteristic that is objectively measured and evaluated as an indicator of normal biological processes, pathogenic processes, or pharmacologic responses to a therapeutic intervention” [122]. While some institutions, such as the US National Cancer Institute use a narrow definition that includes only biological molecules [123] biomarkers are often not just molecular compounds (such as DNA or protein) but can include physical observations such as blood pressure (a predictor of pre-eclampsia in pregnant women) or body-mass index (used as a biomarker of a number of diseases including cardio-vascular conditions) [124].

There are a number of different kinds of disease biomarkers; antecedent (for predicting risk of a particular disease), screening (for subclinical disease), diagnostic (for determining overt disease type), stage (for disease severity) and prognostic (predicting disease course or response to therapy) [125]. Biomarkers are indicators of a particular state of an organism, and there are many thousands of biomarkers used to identify disease states and predict outcomes. Biomarkers also significantly contribute to the understanding of disease mechanisms and are widely used for research purposes. Plasma proteins can be useful biomarkers due to the ease of obtaining plasma and the fact that plasma flows through almost all parts of the body [126].

It should be noted that there is sometimes a distinction made between causality and association in biomarker definition. The term for biomarkers that are associated with a disease but not involved in the disease process is epiphenomena. An epiphenomenon may be a host response to damage such as inflammation, or a change in acute phase proteins [127]. Alternatively, acute phase proteins may be implicated in the causality of disease, either positively [128] or negatively [129], in which case the change is not an epiphenomenon. Tissue leakage proteins are a widely used indicator of disease, for example, alanine transaminase at higher than normal levels in plasma, is an indicator of liver damage [130].

Plasma represents the single most informative sample that can be collected from an individual [131]. Plasma proteins, have been categorised into eight types (1) classical secreted plasma proteins produced by liver and intestines (*e.g.* albumin), (2) immunoglobulins (antibodies), (3) circulating receptor ligands (*e.g.* insulin) (4) local receptor ligands (*e.g.* cytokines) (5) temporary passengers

(e.g. lysosomal proteins) (6) tissue damage proteins (e.g. cardiac proteins) (7) aberrant secretions (e.g. tumor proteins) (8) foreign proteins (e.g. from viruses) [132].

Proteomics

The term proteomics refers to the examination of the total set of proteins expressed in a given biological fluid, tissue, organelle, membrane or cell line. It aims to show as complete a picture as possible of all the proteins that are being expressed in, or introduced to, a biological system at any particular point in time, in a particular environment. This picture includes not only the level of expression of individual proteins but also any post-translational modifications that may alter their physical properties. Once established, the proteome of the biological system in question can be compared to biological systems under different conditions to evaluate the changes that have occurred. For example, the protein complement of diseased tissue can be compared to non-diseased tissue [133]. Proteomic models of disease in farm animals are also increasingly being used to understand disease process in humans [134, 135].

Blood is unique in being the only fluid that flows to all parts of the body and because of this it contains information about the whole organism. Plasma is the fluid component of blood *i.e.* blood less the blood cells (hematocytes). When collecting serum, blood is allowed to coagulate after collection, but when obtaining plasma, coagulation is chemically inhibited. This is usually done by collecting the blood samples into tubes that have been treated by an anti-coagulant, generally either EDTA (ethylenediaminetetraacetic acid), citrate or heparin. Blood cells are then pelleted by centrifugation, after which the plasma can be removed and stored frozen until required for analysis.

One of the difficulties in analyzing the proteins in plasma samples is the presence of a small number of proteins that are highly abundant in blood, *e.g.* albumin and immunoglobulins. These highly abundant proteins make the task of quantifying and identifying the other proteins present much more difficult.

Depletion

More than 60% of human plasma is made up of albumin and immunoglobulins [136] and these proteins are at similarly high levels in sheep plasma [137, 138]. The presence of these, and other abundant proteins can mask the presence of many less abundant other proteins and prevent their

quantitation. There have been many attempts to develop new and better methods of depleting abundant proteins[139].

One of the earliest methods for removing albumin from blood samples for proteomic analysis used dye ligand columns *e.g.* Cibacron Blue or Mimetic Blue columns [140]. While these achieved some measure of success [141], they are generally regarded as being too non-specific because not only did they remove other proteins in addition to albumin, they also did not completely remove albumin [142, 143]. This finding coincided with growing interest in plasma proteomics and led to a flurry of research into the development of new and better depletion strategies as well as the establishment of a related biotech industry [144, 145].

The main thrust of improved depletion strategies has been the use of antibody based methods. Some of the first antibody depletion methods used monoclonal IgG antibodies to ensure protein specificity [142], although it was later found that polyclonal antibodies were easier to make and were still reliable and efficient when immobilised [146]. A further development has been the use of Immunoglobulin Y (IgY) antibodies raised in chickens [147]. Chicken IgY antibodies have the advantage of being cheap and easy to obtain as they are produced in egg yolk. Furthermore, IgY antibodies are less species specific with respect to mammalian species than IgGs due to the greater evolutionary distance between birds and mammals compared to that between mammalian species. At first there were concerns that IgY depletion may bind non-target proteins but it has since been found to be very effective in terms of both non-specific binding and target depletion [148].

There are however, some issues with using depletion methods for proteomic studies. The first is the introduction of variability, as any experimental manipulation, such as depletion, can introduce technical variation to samples [149, 150]. Secondly, high abundance proteins, such as albumin can have biological variation that is related to the research question, and so depleting them can result in the loss of an important piece of information [151]. Finally, high abundance proteins, particularly albumin, can bind other proteins that may be of interest and so depletion can cause a loss of this information [152].

Two-dimensional gel electrophoresis

The classical method of two-dimensional polyacrylamide gel electrophoresis (2D PAGE) was first described by O'Farrell in 1975 [153] and with some modifications is still a core technique in proteomics today [154, 155]. The heart of 2D PAGE lies in the separation and visualisation of proteins in two different dimensions within a gel. Firstly proteins are separated according to their electrical charge in one direction (known as isoelectric focusing or IEF) and then they (after equilibration with SDS) are separated in the other direction according to molecular weight. Isoelectric focusing for 2D gels is now generally done with the use of an Immobilised pH gradient gel (IPG) which has been fixed to a plastic strip, and then dried for storage [156]. These strips just need to be rehydrated with an appropriate buffer prior to use. Proteins are loaded onto the strip using a variety of methods (see below) and focused by applying an electrical voltage to the ends of the strip. This is usually done in an either step-wise or gradient manner so the voltage applied gradually increases over the time of the isoelectric focusing. Final voltages are typically between 5,000 and 10,000 volts depending on factors such as strip length, pH range, and conductivity.

Once the proteins on the IPG strip have been focused the strip is then placed into a solution containing SDS so that the proteins can be separated in a second direction according to their mass. With appropriate staining and imaging, this results in a visual array of hundreds, if not thousands of spots. Each spot represents either a unique protein (or protein modification) or with overlapping spots, a group of unique proteins. The spots can then be quantified so that differences between groups can be analysed. Spots of interest can be excised from the gel and processed to produce free peptides which can then be analysed by mass spectrometry to identify the protein concerned (see below).

While 2D PAGE can be used to identify a large number of proteins, there are some potential problems with this method. Firstly, some proteins are present in large amounts, such as albumin in serum, while at the same time others, such as growth factors, will be present in very low amounts and so be outside of the limits of detection [157]. This problem may be partially overcome with the use of depletion methods as outlined above.

Secondly, some proteins such as hydrophobic, or very small or very large proteins often are not well represented in 2D gels. For hydrophobic proteins this is because of the difficulty in retaining these

proteins in solution – they have a tendency to precipitate, particularly during separation in the first dimension [158]. Hydrophobic proteins, however, are not known to be a large component of plasma proteins. The absence of very small or very large proteins on 2D gels can be partially overcome with the use of appropriate acrylamide concentrations in the second dimension [159]. Thirdly, poor horizontal resolution is a common problem with 2D gels. These problems are typically sample specific and optimising sample preparation and running conditions is required to overcome them [160].

One of the biggest problems with 2D PAGE is unacceptable gel to gel variation both in spot position and size. Spot position variation is commonly overcome with the use of warping technology within analysis software [161]. Differences between gels in spot size or volume may be due to differences in loading, staining or scanning sensitivity and this can be overcome with the use of normalization procedures [162]. Note that spot volume refers to the horizontal two dimensional area of a spot, multiplied by the staining intensity, which is depicted in the vertical dimension in 3D representations of spots to give a spot volume. As staining intensity is measured as emitted light (in a fluorescent scanner) arbitrary units of spot volume are almost universally reported, as is the case in this study.

Differences in individual spot volumes (*i.e* from the same sample) can be due to each IPG strip having slightly different electrochemical characteristics during IEF, not only between strips but between different parts of the same strip (*e.g.* due to slight differences in rehydration profiles [163]) resulting in individual spot volume variation. This technical variation can be partially dealt with careful rehydration technique and also by controlling individual strip current flow. Most commercially available IEF instruments can accommodate up to twelve IPG strips at once, which are all run using the same voltage and current program, regardless of any conductivity differences between strips. The development of commercial isoelectric focusing instrument capable of monitoring individual strip conductivity is underway [164].

Technical variation can also be reduced with the use of differential in-gel electrophoresis (DIGE), where two samples plus a control (made up from a pool of all samples) are labelled with dyes with different fluorescent properties. All samples are mixed, and then run on the same gel [165]. The pooled control sample is used to correct each spot for technical variation between samples on different gels. It should be noted that as with post-stained gels, DIGE gel spots need to be matched

between gels, requiring a high degree of consistency in spot appearance. Further, resolution of spots is not helped by DIGE, and in fact it may be hindered, as DIGE typically requires a three times higher protein load than non-DIGE gels. There have been suggestions that the DIGE three dye system could be reduced to a two dye system (one sample and one control per gel) enabling a 50% higher protein load. Indications are however, that using only two DIGE dyes per gel results in a higher level of technical variation [166]. The normal 3 dye DIGE system results in low levels of technical variation in comparison to normal biological variation [167].

Finally, 2D PAGE is a slow and laborious process that has proved difficult to automate. The main way of addressing this problem has been to use alternative proteomic methods, particularly liquid based chromatography such as HPLC based fractionation coupled to a MS instrument [168]. However, 2D PAGE still has plenty of useful applications for those with the patience to use it [155]. There are some technical advantages for gel based quantitation over MS based quantitation in that separation and quantitation are performed prior to proteolysis. This reduces the dependence on the resolution of the mass spectrometer for ion availability as well as facilitating the assessment of protein modification differences between groups [169]. A 2D gel map of sheep plasma proteins has been produced by an Italian group, who analysed 250 protein spots, and identified 138 of them [170].

Sample preparation and conditions for 2D gel electrophoresis of plasma samples

As plasma samples are often difficult to resolve well on 2D gels a variety of methods can be explored in order to find improved methods. Improvements in spot resolution are mostly related to improving resolution in the first dimension *i.e.* during isoelectric focusing. The cause of poor focusing can be due to a variety of reasons, for example by the formation of mixed disulfide bonds between different protein molecules or by the presence of substances in the sample that interfere with focusing. Problems with mixed disulfide bonding are not sample specific, and this is addressed with a variety of reagents (see below). Interfering substances are sample specific and include salts, lipids and nucleic acids, and as these substances vary widely between sample types and biological species, sample preparation methods are generally sample specific. The first step of sample preparation for 2D PAGE, after depletion, is extraction. Note that depletion (of highly abundant proteins) is typically done with native (folded) proteins and is not specific to any particular proteomic method, whereas the following steps, extraction, sample clean-up and dealing with mixed disulfides are specific to the proteomic method in question, in this case 2D PAGE.

Extraction

In order to be run on a 2D gel proteins are denatured so that charge groups and cysteines are exposed and any interfering substances are released. In the second dimension, the entire peptide chain making up the protein needs to be available for SDS binding. This extraction process, is typically done with the use of chaotropes, detergents and reducing agents. The chaotropes urea and thiourea are routinely used in 2D PAGE to both denature and maintain the solubility of denatured proteins [171]. Heat is generally avoided during extraction as the most commonly used chaotrope, urea, degrades when heated above room temperature and will carbamylate proteins affecting the spot pattern [172]. The detergent SDS can be used for extraction, but as it is (singly) charged, it can interfere with IEF and so either needs to be removed prior to IEF or diluted with a non-ionic detergent [173, 174]. Uncharged detergents, such as Triton X-100, or zwitterionic detergents (with balanced charges) such as CHAPS are commonly used in IEF [175].

Mixed disulfide bonding

The amino acid cysteine is able to form disulfide bonds with other cysteine residues that may be in different protein molecules. This is known as mixed disulfide bonding and generates non-biologically relevant proteins and thus confusing results. In the past researchers using 2D PAGE relied on reducing agents such as β -mercaptoethanol or dithiothreitol (DTT) to prevent mixed disulfides by keeping cysteine residues reduced [176]. However it has been found that as these reducing agents become diluted they lose their effectiveness. For example both β -mercaptoethanol and DTT are weak acids and so as negatively charged molecules they migrate away towards the anode during IEF, depleting the strip of reducing agents, resulting in smearing of proteins, particularly in the basic region [177, 178]. A variety of methods have been employed to overcome this problem such as by supplying DTT in the electrode wick [179]. Another approach is to include an oxidizing agent in excess so that all cysteines are mixed disulfides, but are consistently resolved due to being oxidized with the one reagent. Hydroxyethyl disulphide (commercially available as DeStreak) has been used for this purpose [180]. Instead of supplying reducing or oxidizing agents, cysteines can be covalently inactivated by alkylation, removing the requirement for subsequent reduction such as for second dimension electrophoresis and in preparation for MS [181]. A variety of agents are available for alkylation, such as iodoacetamide, acrylamide or one of the vinylpyridines. 4-vinylpyridine has been shown to be both highly specific and highly effective for alkylating cysteine residues [182-184].

Sample clean-up

It is often necessary to remove any non-protein substances that might interfere with isoelectric focusing, such as salts or lipids, which can either interfere with or mask the charge on proteins, affecting their migration to the isoelectric point or entry into the IPG matrix [185]. There are clean-up methods that are specifically aimed at delipidating plasma proteins. These are mostly two phase systems such as butanol/di-isopropanol ether extraction [186] or methanol/chloroform extraction [187]. Alternatively, delipidation can be simply achieved by centrifugation at 4° C [188]. There are also a variety of solvent induced precipitation methods for removing both lipids and salts in one step *e.g.* with acetone, TCA, ethanol, methanol, acetonitrile [189, 190] either separately or in mixtures [191].

Although it has long been assumed that denaturing conditions prevent metal (salt) protein binding, recent reports show that even under denaturing conditions, metal salts can co-precipitate with protein. Acidification of the sample prior to precipitation has been shown to reduce salt binding [192] most likely because protonation of the negatively charged acidic groups on proteins reduces their affinity for positively charged metal ions such as sodium. The improved clean-up by TCA/acetone precipitation compared to acetone precipitation alone [191] may be due to the same effect. Unfortunately the use of TCA often results in problematic resolubilisation of the protein pellet [193, 194], and if not completely removed, interferes with isoelectric focusing [195]. Acidification with other acids (*e.g.* citric acid) prior to precipitation has, however, been shown to be an effective clean-up step for microbial samples, particularly for the high molecular weight proteins [196].

As an alternative to solvent/precipitation based clean-up methods there are also device based clean-up techniques, such as those based on dialysis [197], spin-column exchange [198], solid phase extraction [199], and by focusing the IPG strip slowly (*i.e.* for an extended period at low voltage) to enable (charged) interfering substances to exit the IPG strip prior to focusing [179, 200]. When using membrane dependent clean-up processes, such as dialysis and spin-columns, there is a risk of substantial protein loss due to non-specific protein binding to the device itself or the membrane. The use of detergents and chaotropes in the protein solutions substantially improves protein solubility and reduces this risk [193].

A complicating problem for sample clean-up generally is that a low level of salt concentration may be necessary for maximum protein solubility [201]. While it is generally claimed that carrier ampholytes (such as in proprietary IPG buffers) provide this function [202, 203], buffers such as Tris, used after sample clean-up, can enhance spot resolution [204]. Alkaline buffers (such as Tris buffers) are required to raise the pH of sample for dye labeling in DIGE experiments, and that these are added after sample clean-up [205] and so may aid in protein solubility during IEF.

Loading methods and running conditions

There are a variety of methods of loading the protein sample onto the IPG strip. The simplest way is to mix the sample with the rehydration buffer so that it is absorbed into the IPG matrix as it rehydrates overnight prior to IEF. This is termed passive rehydration. When a small voltage (typically around 30v) is applied to the strip, with sample dissolved in the rehydration buffer, the rehydration is termed active and aids absorption of protein into the IPG strip [206].

In cup loading a small sample cup is placed over the rehydrated IPG strip during IEF so that the sample is loaded onto the strip at one point. Cup loading is often used when there are problems with sample solubility, particularly at one end of the pH range [207]. Paper bridge loading is where the sample is applied to a piece of paper at one end of the strip forming a bridge between the electrode and the IPG strip. Paper bridge loading can be useful when a high protein load is required [208]. In G electrode loading, the sample is absorbed into several paper slips, which are then placed on top of the end of an IPG strip and an electrode shaped like a “G” is placed on top of them, above the sample and the strip [209]. There are other less common protein loading methods such as slip, side, and tap loading [210]. Quantitative evaluation has shown that passive rehydration loading results in good spot number and intensity, albeit with a small increase in spot variance [206].

Several researchers have looked at new types of detergents to provide more options to improve solubility during the first dimension [211]. There was a flurry of research in the 1980’s looking to improve processes that occur within IPG strips during focusing with an emphasis on gaining an understanding of the changes that occurred in conductivity during IEF, and the relationship to protein adsorption and movement across the strip [200, 212]. While there hasn’t been much recent

research on this topic, what has been done demonstrates that there is potential to further improve understanding in this area [213, 214].

The addition of carrier ampholytes to both sample solutions and rehydration solutions for IPG strips enhances protein solubility, particularly as proteins approach their isoelectric point during IEF [215]. While the exact make up of each type of commercially available solution has only recently been determined [203], the type and concentration of carrier ampholytes is often found to be sample specific [202].

While standard focusing protocols dictate a rapid rise in voltage during the early stages of IEF some difficult to focus proteins have been shown to focus more effectively when subjected to a slow rise in voltage rather than a sudden increase regardless of the protein loading method [216]. The downside is that more time is required for focusing.

Isoelectric focusing of IPG strips gel side up (as opposed to gel side down) requires a paper wick to be placed between the electrode and the IPG strip. The wick has water applied to it to absorb contaminants (such as salt ions), to enable an electrical connection to be made and to provide a reservoir to replace water lost due to electrolysis. In 1997 Gorg *et al.* [217] reported that the addition of hydrophilic agents such as glycerol to the isoelectric focusing system improved protein resolution in the alkaline pH region by reducing water flow through the IPG strip. It was suggested that hydroxide ions (present at alkaline pH) flow towards the anode, carrying water with them, resulting in an electro-osmotic flow and smearing of protein spots. A further report published in 2009 supported the hypothesis that electro-osmotic water flow along IPG strips caused gaps in the proteome at high pH regions [218].

Occasionally issues are reported with protein carbamylation due to reaction of proteins with urea breakdown products such as cyanate that can develop in urea solutions under certain conditions, such as warm temperatures. These are, however, negligible during electrophoresis (especially with temperature control) as any cyanate ions that develop are negatively charged and drawn towards the anode as they form, reducing the availability of these ions for carbamylation, in an effect similar to the removal of partially charged reducing agents [172, 184].

Recently Bengtsson *et al.* [219] found that they could reduce the water loss that occurs during electrophoresis due to electrolysis (*i.e.* the splitting of water to hydrogen and oxygen which bubbles up at the electrodes) by using conducting polymer electrodes to make electrical contact with the gel instead of platinum wire. Observed improvements in protein electrophoresis with one dimensional SDS gels were purported to be due to either a reduction in the electrolysis that induced gel drying or a reduction in the acid/base by-products of electrolysis that interfered with protein charge. Note that these experiments did not include the use of carrier ampholytes.

Other proteomic methods

Another powerful proteomic technique is based on protein separation in liquid chromatography columns combined with mass spectrometry (LCMS). These two processes can be combined automatically to yield results relatively quickly [220]. This method also has the advantage that hydrophobic proteins may be more easily identified, as organic or partially organic solvents are often used. Another advantage can be a better dynamic range [221].

The problem of limited dynamic range in 2D gels is at least partially addressed by depletion [222] and also with the use of fluorescent dyes [223]. The issue of hydrophobic proteins can sometimes be a problem for 2D PAGE, depending on the sample type. It can be addressed by a variety of means such as using LC separation followed by one-dimensional gel electrophoresis to analyse the hydrophobic protein fractions and 2D electrophoresis for the soluble protein fractions [224]. Because problems with protein solubility are encountered in the first dimension of 2D electrophoresis this procedure can improve the dynamic range [158]. However, as mentioned earlier, it was not anticipated there will be problems with hydrophobic proteins with the use of plasma samples.

One of the issues in employing LCMS based proteomic investigations is that it is generally necessary for samples to undergo an enzymatic digestion process prior to quantitation. This methodology is known as bottom up proteomics, and is used because it can be difficult to get a large number of intact proteins from complex solutions (such as in a plasma sample) to fly adequately in a MS instrument. Digestion with enzymes such as trypsin prior to analysis facilitates the reliability and sensitivity of data acquisition methods, however digestion prior to protein quantitation can also result in the loss of information about the relative quantities of each protein isoform. One of the

characteristics of plasma is the large number of isoforms that many proteins have. Quantification of intact proteins prior to the fragmentation required for MS is known as top down proteomics. Top down proteomics facilitates protein isoform quantitation [225].

Another top down proteomic technique that has been developed is the use of protein arrays. This involves the use of a glass slide to which many different proteins or antibodies are covalently linked. A sample is then exposed to the slide and incubated to allow protein-protein interactions to develop. The slide is then analyzed to see which spots have proteins bound. Unfortunately, protein arrays are sample specific and because novel proteins cannot be identified in this way they have some limitations in proteomics [226].

Data analysis

The main application of proteomics is to quantify and identify individual proteins (or modifications of proteins) so that protein changes associated with a particular condition can be found. As mentioned above, the motivation for this work can be varied, for example to find biomarkers so that a particular disease state can be predicted, or so that the molecular mechanisms involved in a condition can be better understood for research purposes. In order to quantitatively evaluate the proteins associated with a particular condition requires controls for comparison. Further, this quantitative evaluation requires an understanding of the quantitative variation present for each protein (or protein modification) that exists for all the conditions of interest. Statistical analysis is then required to assess the variation of each protein in order to determine if there are significant differences between for the levels of each protein [227].

There are two main types of ways of analyzing data where a large number of variables have been monitored, such as in proteomics or expression analysis (microarray data). The primary statistical analysis is in the evaluation of each variable to determine if there are any outstanding variables involved in the process of interest, this is called univariate analysis, and in proteomics, produces what are termed proteins of interest. The most common statistical test used in the univariate analysis of proteomics experiments is the student's t-test. However while there is no doubt about the validity of individual results obtained using student's t-tests one needs to interpret them with caution when a large number of variables have been searched in parallel in order to find a few variables with statistical significance. This problem is termed multiple testing. If, for example a

statistical significance (p value) of 0.05 is chosen, and a student's t -test is used to find the significance of differences between groups of a variable, and the p value is found to be less than 0.05, it means that there is a 1 in 20 chance (5%) that this result is a false positive [228].

The problem of multiple testing means that if one tests, for example, 1000 variables simultaneously, and if a p value threshold of 0.05 is adopted, then assuming normal distribution, one would expect to find 50 (5%) are positive *i.e.* by chance [125]. There are a number of ways of addressing the problem of multiple testing, for example by reducing the p value that is required for significance (*e.g.* by using algorithms such as the Benjamini-Hochberg method [229]). However this widely used method (with over 26,000 citations) has been criticised by the original authors among others, as too conservative [230]. The main problem with algorithms that adjust p values is that they reduce the power of the experiment to find significant variables. Other methods to address this include raising the difference ratio threshold between groups [231], testing variables for their degree of co-variability enabling one to choose the most appropriate adjustment algorithm [232], or using false discovery rate (FDR) statistics. FDR calculations, such as q values, are being widely used in micro array data analysis [233] and are beginning to be used in proteomics [166]. External validation, which is the use of a different technique in order to quantitate a particular protein, such as with an ELISA assay, particularly with a new set of samples, is a valuable way of demonstrating that proteins of interest are indeed biomarkers [129].

The second general area of statistical interest (other than univariate analysis) is in comparing data sets as a whole, for example between diseased and non-diseased samples, which is termed multivariate analysis. Multivariate analysis methods such as principle component analysis (PCA) can be used to examine data to test if there is too much technical noise or biological noise for a true signal to be detected [234]. Multivariate analysis can also be used to find clustering among individuals or variables and can be used to improve methodology [235].

Another type of statistical analysis, that is also multivariate, is to use data mining statistics in order to identify multiple variables that can be used collectively for decision making, such as decision trees [236].

Mass Spectrometry (MS)

Proteins of interest are identified by mass spectrometry. To identify protein spots classed as interesting on analytical 2D gels, preparatory gels, with higher than normal protein loads and different staining procedures than those used for the spot quantification process, may be run [237]. Spots are cut out of gels, either manually or robotically, and subjected to enzymatic digestion, typically by trypsin, to facilitate protein removal from the gel slice and mass spectrometry processes. These tryptic digests contain the peptides that make up one protein, or several proteins if there are overlapping spots [238].

The peptides from proteolytic digests are extracted from the gel piece and are subjected to mass spectrometry. Mass spectrometers used for protein identification either have samples in solid or liquid phases for introduction of the material to the MS. In MALDI-TOF (matrix assisted laser desorption ionization – time of flight) MS the sample has been incorporated into a solid phase ionisable substance, that is subjected to a laser to vaporise and ionise the mixture. The ions are then taken up into the mass analyser and the detector which records the time of flight in order calculate the mass of the ions. Typically the data collected produces what is known as a peptide mass fingerprint (PMF) [239].

In MS instruments where the sample is introduced in a liquid form, at the front end is often some form of liquid chromatography to at least partially separate the tryptic peptides. This is then usually subjected to atmospheric electrospray ionization (ESI) where the partially separated sample is sprayed into the machine, the solvent evaporates, leaving the charged peptides to be attracted electrically into and through the instrument [240]. When using ESI, larger multiply charged ions are possible, producing ions with different mass to charge ratios. Most modern electrospray MS instruments that are used for protein identification incorporate a fragmentation process so that peptides are fragmented, enabling some sequence data to be obtained for each peptide. Fragmentation involves selected ions being allowed to enter a collision cell, and fragmented using controlled voltages in the presence of an inert gas. Specific bonds, such as the peptide bond, can be broken by collision with energized gas molecules to produce a series of y and b ions that can be used to sequence the peptide [241]. This provides additional data that comes from samples that may represent more than one protein, as fragment ions come from one parent ion rather than a mixed source.

To recap; there are two main types of data obtained from mass spectrometry, peptide mass fingerprinting and peptide fragmentation (sequence) data. A peptide mass fingerprint (PMF) consists of a series of peptide masses resulting from the protease digest of a protein, plus or minus modifications such as alkylation, phosphorylation or glycosylation. Peptide fragmentation data consists of a series of smaller protein masses resulting from the peptides produced in the protease digest being fragmented within a collision cell of the mass spectrometer. Both types of data can be used together to identify proteins by comparison to information in databases such as theoretical mass fingerprints generated from genomic sequence databases [242] or from dedicated MS databases to find a match with known or predicted proteins [243]. This has historically been a very demanding and time-consuming process, however improvements in the ease of use and accessibility of computer software to undertake this work have occurred regularly over the last few years [244, 245].

Present study

As there have been no strong leads regarding the etiology of ovine pre-partum vaginal prolapse to date [41], another broad based research approach is required in order to gain some insight as to what is causing this problem, assuming that there is a major cause. The fact that the disease has seasonal or farm outbreaks [3] does give some indication that there may be at least some unknown factors that are involved in the etiology of ovine prolapse. While large scale epidemiological studies have been able to rule out certain factors, they have not yet provided much many clues to its etiology.

Sample choice and methodology

One of the main issues in using samples in order to determine disease etiology is confidence in separating out causes of the disease from effects. Collecting samples prior to disease occurrence is one way of removing the effects of the problem from the cause of it and provides more confidence that the mechanism causing the condition is being addressed. The disadvantage of this is that it is difficult to collect vaginal tissue from sheep that will subsequently prolapse, due to the low level of numbers involved. Further, while the main tissue involved is clearly vaginal, there is very little evidence to suggest that changes in that tissue cause prolapse to occur in sheep. An alternative to vaginal tissue is to take blood samples so that plasma (or serum) can be obtained. This enables

collection to be done in large numbers, and with the sheep identified, samples can be later used from sheep that subsequently prolapse and compared to those that do not. Such a sample collection requires ethical approval.

The analytical method of choice, a molecular analysis *i.e.* proteomics, and specifically 2D DIGE was debated prior to beginning the project. There have been a variety of research methods that have been employed in order to understand what is going on with ovine pre-partum prolapse, as reviewed above, however there has been only limited attempts to use modern biochemical methods in prolapse research. Modern biochemical analysis underpins much of current biological research, especially with the advent of high throughput DNA sequencing technology, as well as related developments in technology such as protein sequencing in MS. The reasons for this research emphasis lie with the improved understanding of living processes, that all living entities have a common ancestor, and that common biochemical processes underpin the sustenance of life itself. Proteomics is a natural extension of these processes, and 2D DIGE is a high quality proteomic technique that could reasonably be applied in our laboratory.

The only non-proteomic tools employed were with the use of a plasma cortisol assay as well as a plasma phosphate test.

Hypothesis

1. That there will be quantitative differences in the plasma proteins between samples collected from ewes that subsequently prolapse and controls.
2. That stress is a contributing factor in ovarian pre-partum prolapse.

Aims

1. To identify plasma proteins that are associated with subsequent prolapse occurrence in sheep.
2. To determine if cortisol is associated with subsequent prolapse occurrence in sheep.

Chapter 2. Method development

Item	Type	Supplier	Supplier location
IgY-C12 depletion kit	spin column + buffers	Genway Biotech	San Diego, CA, USA
Protein G Sepharose	Fast flow	Sigma-Aldrich	St Louis, MO, USA
TCEP (sample prep.)	Reducing agent	Soltec	Beverly, MA, USA
TCEP (MS prep.)	Reducing agent	GoldBio	St Louis, MO, USA
Triton X-100	Neutral detergent	Sigma-Aldrich	St Louis, MO, USA
Tris (sample buffer)	Buffer, PlusOne	GE Life Sciences	Uppsula, Sweden
Urea	Chaotrope, PlusOne	GE Life Sciences	Uppsula, Sweden
4-Vinylpyridine, 95%	Alkylating agent	Sigma-Aldrich	St Louis, MO, USA
Protein quantitation	EZQ kit	Invitrogen	Eugene, OR, USA
IPG strips	Dehydrated strips	GE Life Sciences	Uppsula, Sweden
Electrode wicks	Paper	GE Life Sciences	Uppsula, Sweden
CHAPS	Zwitterionic detergent, 1 g pack	Bio-Rad	Hercules, CA, USA
Thiourea	Chaotrope, 100g pack	GE Life Sciences	Uppsula, Sweden
Carrier ampholytes	Range depending on IPG strips	GE Life Sciences	Uppsula, Sweden
Bromophenol blue	Trace dye	Sigma-Aldrich	St Louis, MO, USA
DeStreak	Hydroxyethyl disulphide, 1ml pack	GE Life Sciences	Uppsula, Sweden
Cover fluid	Mineral oil, PlusOne	GE Life Sciences	Uppsula, Sweden
Iodoacetamide	Alkylating agent, 25g pack	GE Life Sciences	Uppsula, Sweden
DTT	Reducing agent	Apollo Scientific	Manchester, UK
Agarose	Low melt, 25g pack	Bio-Rad	Hercules, CA, USA
Acrylamide	Acrylamide-bis 40% solution	Merck	Darmstadt, Germany
Ammonium persulfate	Polymerisation agent	Sigma-Aldrich	St Louis, MO, USA
TEMED	Polymerisation agent	Sigma-Aldrich	St Louis, MO, USA
SDS (strips)	Negatively charged detergent, PlusOne	GE Life Sciences	Uppsula, Sweden
SDS (tank)	Ultrapure	Affymetrix	Cleveland, OH, USA
Tris (tank)		Sigma-Aldrich	St Louis, MO, USA
Glycine	PlusOne	GE Life Sciences	Uppsula, Sweden
Coomassie blue R250	Gel stain	Sigma-Aldrich	St Louis, MO, USA
Coomassie blue G250	Colloidal Coomassie	Bio-Rad	Hercules, CA, USA
Sypro Ruby	Fluorescent gel stain	Invitrogen	Eugene, OR, USA
Cy2, Cy3 and Cy5	Minimal fluorescent labelling dyes	GE Life Sciences	Uppsula, Sweden
Dimethylformamide	<0.003% H ₂ O	Merck	Darmstadt, Germany
Trypsin	Porcine pancreas	Sigma-Aldrich	St Louis, MO, USA
Haptoglobin assay	Phase	Tridelta Development	Maynooth, Ireland

Table 2-1. Source of key lab consumables.

Sample collection

Ethical approval for blood sampling was obtained (MUAEC protocol 05/61). A farm was identified that regularly had a high percentage of ewes with bearings at lambing time. The farmer was willing to provide ewes for ear tagging, blood sample collection, and subsequent monitoring to identify prolapsed ewes. The farm is a hill country sheep and beef farm in the Tararua district, running approximately 1000 breeding ewes plus fattening cattle with a winter wet/summer moist climate and sedimentary soils.

Ewes were not bred on the farm but were mixed age ewes with Romney genetics. The farm had a practice of purchasing mixed age Romney ewes in the summer for mating with a terminal sire in the autumn for lambing the following spring. The ewes from which blood samples were taken had previously had an ultrasound pregnancy scan and all had been identified as carrying multiple foetuses. The rams were introduced to the flock on the 10th April and were due to begin lambing in early September. They were shorn in late July and sample collection took place the following week, on the 4th August 2005, 116 days after the ram was put with them.

Massey University Veterinary students ear tagged the ewes and collected 5 – 10 mLs of whole blood from each ewe into EDTA treated tubes. The tubes were labelled with the ewe tag number and placed on ice. The samples were centrifuged (1500 *g* for 10 minutes) to pellet cells, then the plasma was removed by pipette and transferred into 5 mL cryo tubes which were frozen and stored in liquid nitrogen.

Tagging/sampling started at number 1 at 9am and finished at number 698 by 3pm, with approximately 650 ewes being sampled. Ear tagging and sampling were done together and sequentially so that controls could be selected that were sampled at the same time of day as samples from ewes that later prolapsed. The farmer observed the ewes for the following 6 weeks, during which time 28 ewes prolapsed, although one sample from a prolapsed ewe could not be found (ID number 122 which prolapsed 29 days after sampling) meaning that there were 27 plasma samples from prolapsed ewes. The date of prolapse and the identification number of affected ewes was recorded, see Figure 5-1 for the distribution of prolapse occurrence.

Work then began using plasma taken from control ewes to determine what preparation methods were required to obtain reasonably well resolved 2D PAGE gels along with trialling depletion methods to remove the most abundant proteins.

Method development – albumin depletion trial

A 1 mL HiTrap Blue HP (Cibacron Blue F3G-A ligand) column (Amersham Biosciences) was obtained and tested for its ability to bind sheep albumin. The columns capacity for albumin in plasma is claimed by the manufacturer to be 20mg human albumin/ml medium. Testing was carried out according to the instructions. Briefly, 1 mL of plasma (from a control ewe) was added to 10 mL 20 mM sodium phosphate buffer, pH 7.1. The conductivity was checked and matched to that of the equilibration buffer. 2 mL of the diluted sample was loaded onto the column (0.2 mL of plasma) and 1 mL of the flow through was concentrated using a centrifugal concentrator (Vivaspin 2 mL 3 kD MWCO membrane). Bradford assays were used to determine the protein concentration, and samples from both depleted and bound fractions run on 1D SDS PAGE. As some measure of depletion was observed in the 1D gels (data not shown) it was decided to progress to 2D gels.

Initial 2D gel methodology

A thiourea rehydration buffer was made up as follows: 7 M urea, 2 M thiourea, 1% CHAPS, 1% Triton X-100, DeStreak (12 µL/mL), 0.5% IPG buffer pH 3-10 NL, and a trace of bromophenol blue. 20 µg of protein was added to rehydration buffer, mixed gently and loaded into a 7 cm strip holder strip for rehydration loading. A pH 3-10 NL IPG strip was inserted into the strip holder, covered with Drystrip cover fluid and left for overnight rehydration. The next day, the strip holder was placed into an Ettan™ IPGPhor II™ IEF instrument and run using the recommended voltage protocol as described in the GE Healthcare manual “2D Electrophoresis – Principles and Methods” (GE 2D manual) [246]. It should be noted that when using the individual strip holders the IPG strips are run face down.

After IEF, the strip was equilibrated in reducing solution for 15 minutes on a horizontal shaker in 5 mL of 75 mM Tris-HCl, pH 8.8, 6 M urea, 87% (w/w) glycerol, 2% SDS, and 65 mM DTT, with a trace of bromophenol blue. This solution was then poured off and replaced with 5 mL of an alkylating solution consisting of 75 mM Tris-HCl, pH 8.8, 6 M urea, 87% (w/w) glycerol, 2% SDS, and 135 mM iodoacetamide, with a trace of bromophenol blue for a further 15 minutes.

A small format 0.75 mm thick, 12% acrylamide gel (8 cm wide by 7 cm tall) was cast using a Bio-Rad mini-PROTEAN II gel system according to the recommended protocol with no stacking gel and no comb. The gel was poured to within 5 mm of the top of the lower glass plate and overlaid with water saturated butanol. The focused strip was placed into the top of the gel and sealed in place with agarose sealing solution (25 mM Tris base, 192 mM glycine, 0.1% SDS, 0.5% agarose and a trace of bromophenol blue. Once the agarose was set, the gel was run at a uniform voltage of 180v until the dye front was near the bottom of the gel. It was then removed from the apparatus, carefully extracted from the glass plates and placed into a staining tray with Coomassie Brilliant Blue stain (50% methanol, 10% acetic acid, 40% MQ water and 0.1% Coomassie R250 powder) for 20 minutes. It was destained with 12% methanol, 7% acetic acid for 10 minutes and is shown in Figure 2-1.

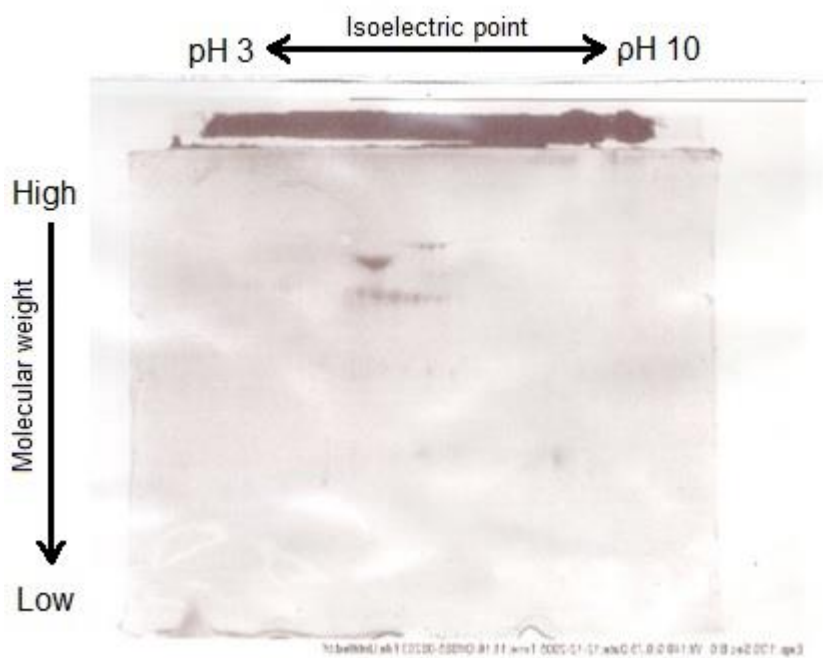


Figure 2-1. 2D PAGE of sheep plasma sample depleted with Blue ligand column, small format. 20 µg protein load, 7 cm IPG strip pH 3-10 NL, 12% acrylamide 2nd dimension. Coomassie Blue R250 stain. Note all 2D PAGE gels presented in this thesis have the same orientation as indicated in this diagram *i.e.* with the acidic (low pH) end of the IPG strips on the left and with high molecular weight proteins at the top. The stained IPG strip is shown at the top of the gel in this image.

As can be seen in Figure 2-1, the spot resolution was reasonable, although the protein abundance was low, and so the same sample was run on a larger gel with a higher protein load and a more sensitive stain. An 18 cm pH 3-10 strip was rehydration loaded (as above) with 40 µg protein, and run according to the previously used protocol, except that a 10% acrylamide mixture was used along

with a Bio-Rad Protean® II xi Cell to accommodate the 18 cm IPG strips for the second dimension. The medium format gels used in the 2nd dimension were 18.5 cm wide (the plastic backing on the IPG strips had to be trimmed to fit in the top of the gel), 18 cm long and 1 mm thick. Following 2D electrophoresis the gel was fixed in 50% methanol, 5% acetic acid and stained with silver nitrate according to the protocol of Simpson [195], except that the gel was in 0.02% sodium thiosulfate for 2 minutes instead of 1 minute, and the silver nitrate concentration was increased from 0.1% to 0.2%, to improve the consistency of staining. The gel is shown in Figure 2-2 and was stained with silver nitrate to provide more sensitivity. Note cooling was not provided when the second dimension was run.

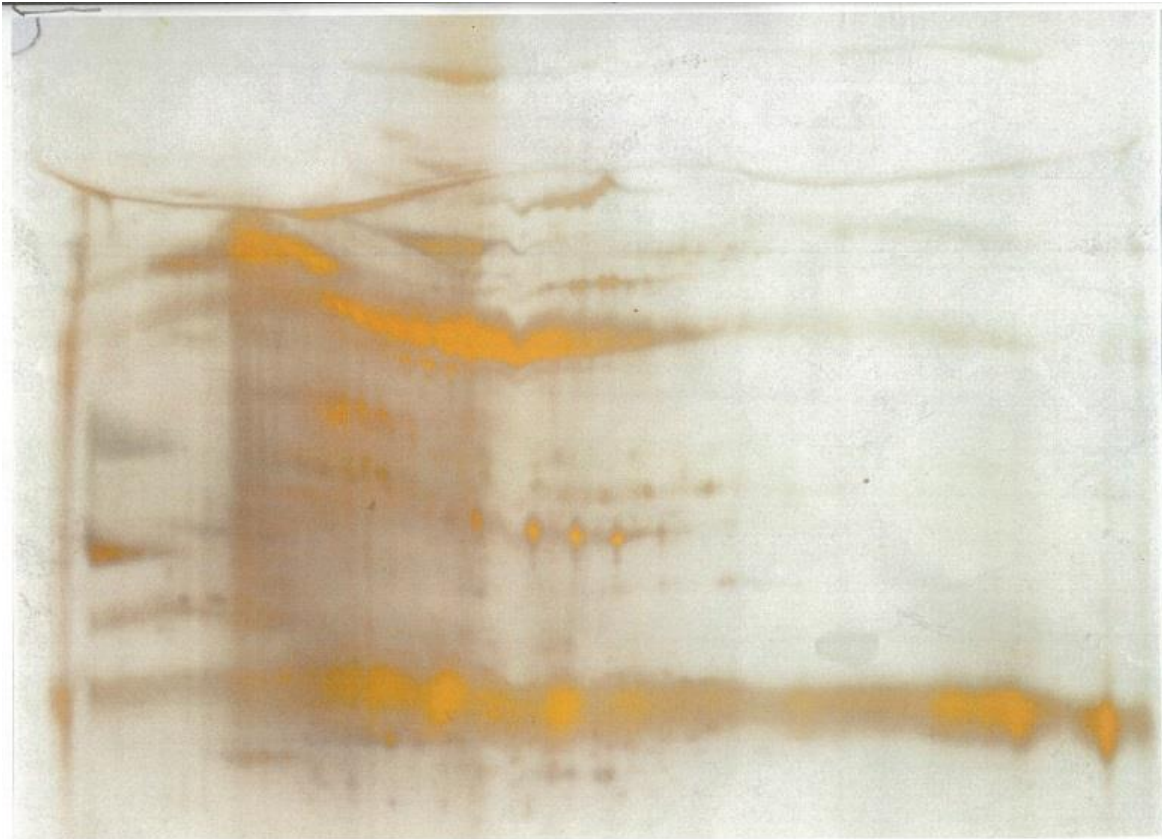


Figure 2-2. 2D PAGE of sheep plasma sample depleted with Blue ligand column, medium format. 40 µg protein load, 18 cm IPG strip pH 3-10, 10% acrylamide 2nd dimension. Silver nitrate stain.

Antibody depletion and trialing of clean up methods

As albumin depletion using the Cibacron Blue cartridge was not efficient and the resolution of medium format gels (*e.g.* as shown in Figure 2-2) was not particularly good, it was decided to experiment with alternative sample preparation methods. An albumin and Immunoglobulin G (IgG)

removal kit (Amersham Biosciences, RPN6300) was used according to the manufacturer's instructions using a 25 μ L plasma load. Next chloroform-methanol precipitation [247] was applied in order to; (a) remove salts and lipids from the sample which are known to interfere with IEF, and (b) to concentrate the sample so it can be equilibrated into the correct buffer for IEF. Methanol (0.4 mL) methanol was added to 0.1 mL of sample and the mixture vortexed then centrifuged (10 seconds at 9000 g). 0.1mL chloroform was then added, mixed by vortexing and the phases separated by centrifugation for 1 minute at 9000 g. The upper phase was discarded, 0.3 mL methanol added to the lower phase, then vortexed and centrifuged for 2 minutes at 9000 g. The supernatant was discarded, the pellet air dried, and 50 μ L of sample buffer (2 M thiourea, 7 M urea, 1% CHAPs, 1% Triton X-100) added to dissolve the protein pellet.

Protein concentration was measured using the bicinchoninic acid assay (BCA) assay (Pierce, 23227) as detergents in the resuspension buffer can interfere with the Bradford assay. 40 μ g protein was loaded onto an 18 cm pH3-10 strip using the rehydration method and run as before, to produce the separation shown in Figure 2-3.

While the spot resolution of the gel had improved it was apparent that the sample was not well depleted of abundant plasma proteins. Information was subsequently provided by the GE technical advisor that the kit contained antibodies raised in goats, which were unlikely to bind to sheep proteins.

Anti-bovine serum albumin (anti-BSA) antibodies (raised in Donkeys) were obtained and coupled to agarose beads, however this also proved to be ineffective in removing sheep albumin (data not shown). Later advice suggested that to make an effective depletion column, the required antibodies had to be affinity purified using the appropriate antigen which was not available.

A commercially produced depletion column for cattle based on purified antibodies from chicken eggs was obtained (IgY-C12 spin column from GenWay Biotech Inc, California, USA. Note that the IgY-C12 columns are no longer available but IgY anti-BSA spin columns are available from GenWay and Beckman Coulter and have been shown to deplete sheep albumin [248]). The column contained immobilised antibodies raised against BSA, plus the 12 most abundant human plasma proteins. The

manufacturers claimed this column effectively depleted bovine plasma of the most abundant proteins including albumin and IgGs.



Figure 2-3. 2D PAGE showing depletion with the Amersham albumin and IgG removal kit.

After depletion of the sheep plasma sample with the kit, chloroform-methanol precipitation was done to clean up the sample. 40 μ g protein load, 18 cm IPG strip pH 3-10, medium format 10% acrylamide 2nd dimension. Silver nitrate stain.

A sample was depleted with the IgY C12 column according to manufacturer's instructions and then after chloroform-methanol precipitation was analysed on a medium format gel, as shown in Figure 2-4.

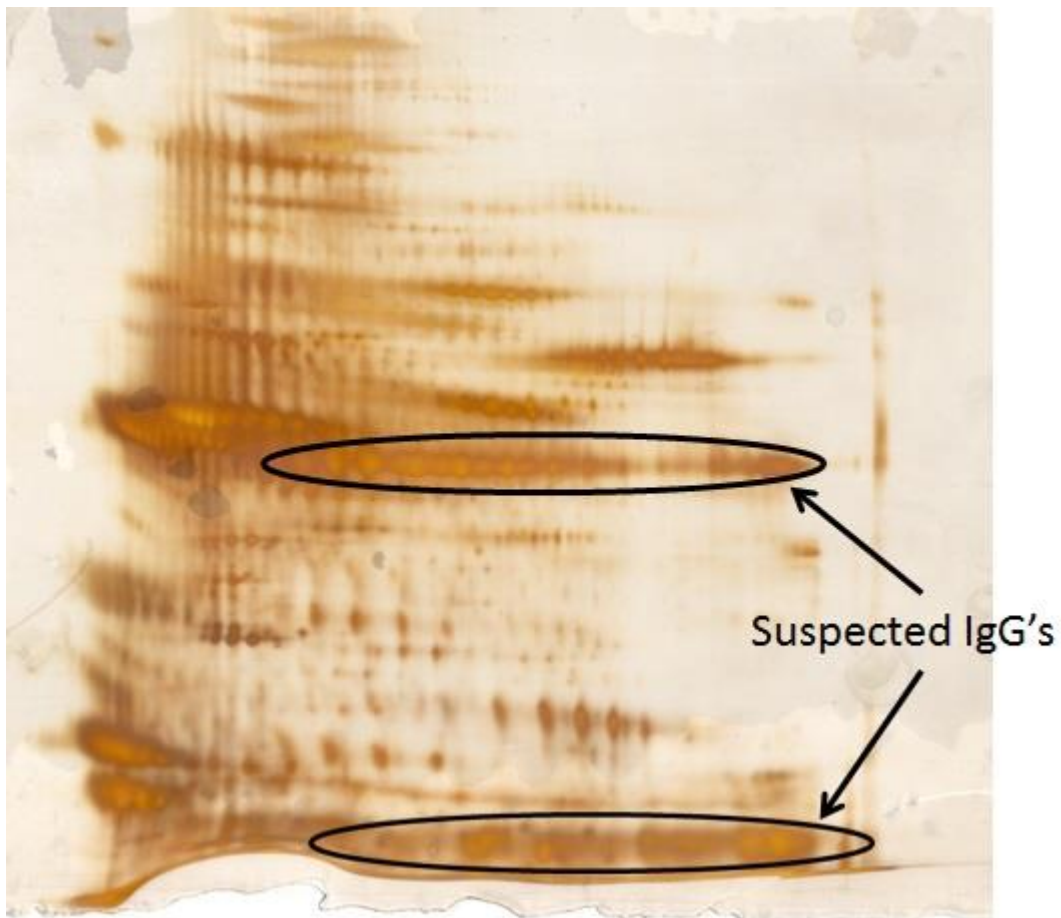


Figure 2-4. 2D PAGE of flow through from GenWay depletion column, medium format.
18 cm pH 3-10 NL IPG strip, 7-12% acrylamide 2nd dimension, Silver nitrate stain.

From the gel image (see Figure 2-4) the GenWay column appeared to be effective at removing sheep albumin however it was apparent that it was not effectively removing IgG's. The shelf life of the column initially appeared to be poor as the first depletion run removed most of the albumin, but subsequent runs did not. A modification was found to be required in the post cleaning equilibration protocol as described below, this extended the life of the column considerably.

According to the manufacturer's instructions, bound proteins were eluted from the column by an acid wash step, requiring multiple washes with 100 mM glycine-HCl (pH 2.5) followed by a

neutralization step (100 mM Tris-HCl, pH 8.0) to rapidly neutralize the acid conditions. This neutralization was necessary to restore the binding capacity of the column and to protect the antibodies from acid degradation during storage. Monitoring the pH of the column flow through showed that the recommended neutralization step was not effective in restoring the pH of the column to neutral values. It was found that the concentration of neutralization buffer had to be doubled (from 100 mM to 200 mM Tris-HCl, pH 8.0) in order to rapidly restore the pH of the column buffer flow through to neutral.

Figure 2-5 shows small format 2D gels of the bound fraction and flow through of the GenWay column. Although the resolution of the flow through was poor, it can be seen again that it still contained IgG's.

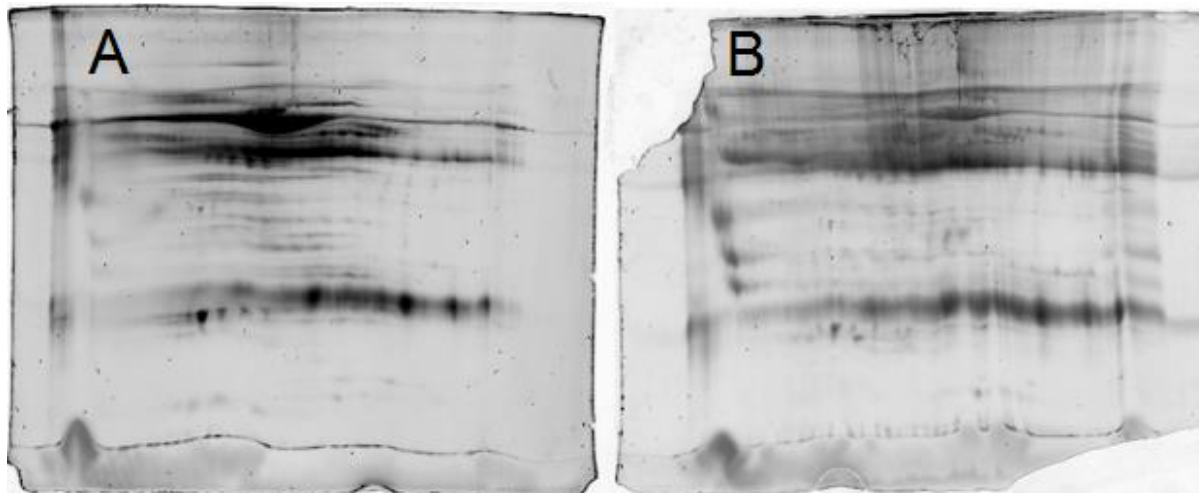


Figure 2-5. GenWay column bound fraction and flow through, small format 2D PAGE.

7 cm pH 3-10 NL IPG strips, 10% acrylamide 2nd dimension. Gel A shows GenWay column bound fraction, Gel B is flow through. The gels are stained with the fluorescent stain Sypro Ruby.

As a result of discussions with other researchers in the field it became apparent that depletion columns designed for use with human plasma rely on the high affinity of IgG for protein A, whereas ovine IgGs have only a moderate affinity for protein A. Thus protein G was then trialed on the basis that it may have higher affinity for sheep IgG.

Sheep plasma (100 μ L) was mixed with 4.9 mL of Tris-buffered saline (TBS, 10 mM Tris-HCl, 150 mM NaCl, pH 7.4). 3 mL of this was applied to a 1 mL protein G agarose column (Sigma), the last 0.5

mL of this was retained to be applied to a GenWay depletion column for albumin depletion. To remove bound proteins from the protein G column, 3 mL of 100 mM glycine (pH 2.5) was used, followed by neutralization with 1 mL of 200 mM Tris-HCl (pH 8.0) and then equilibration with TBS (pH 7.4). Using the same sample preparation and electrophoresis methods as before produced the gels shown in Figure 2-6. Bound fractions are shown in Figure 2-7.

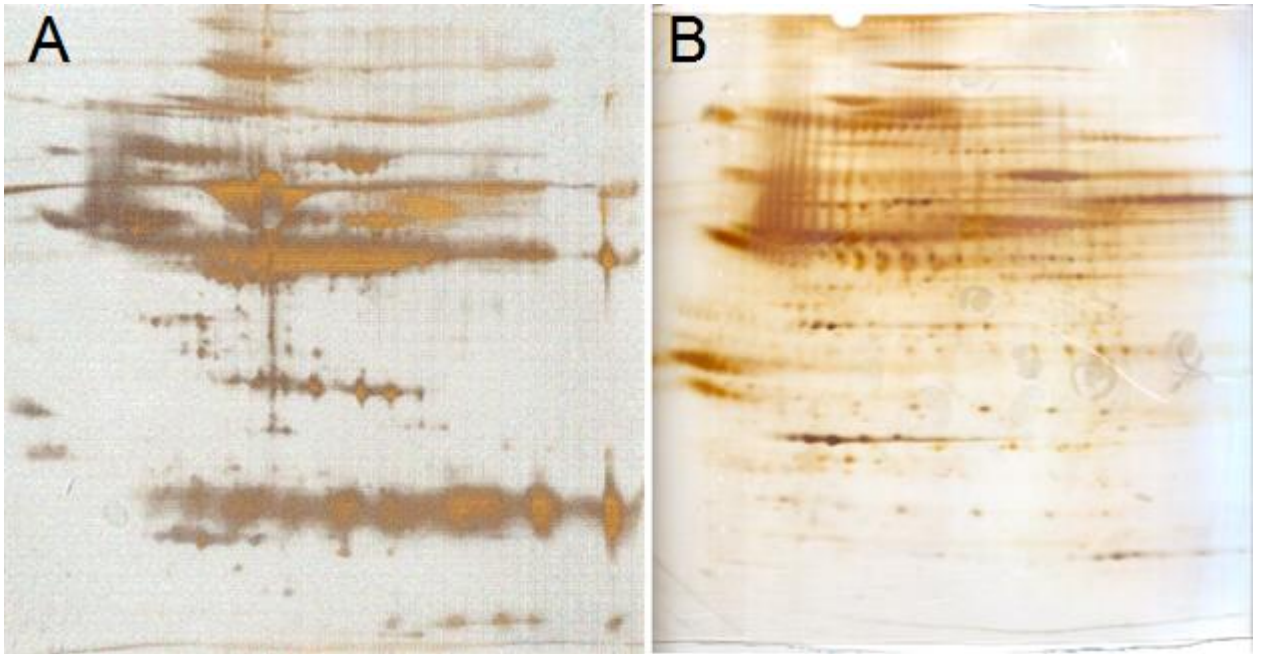


Figure 2-6. Chloroform/methanol precipitation, non-depleted and depleted, medium format.

2D PAGE gels run using 18 cm pH 3-10 NL IPG strips with samples prepared using chloroform/methanol precipitation. 10% acrylamide 2nd dimension. Gels were stained with silver nitrate. **Gel A** had a non-depleted sample. **Gel B** sample was depleted using both a protein G and GenWay columns. Note that the albumin in **A** shows some negative staining.

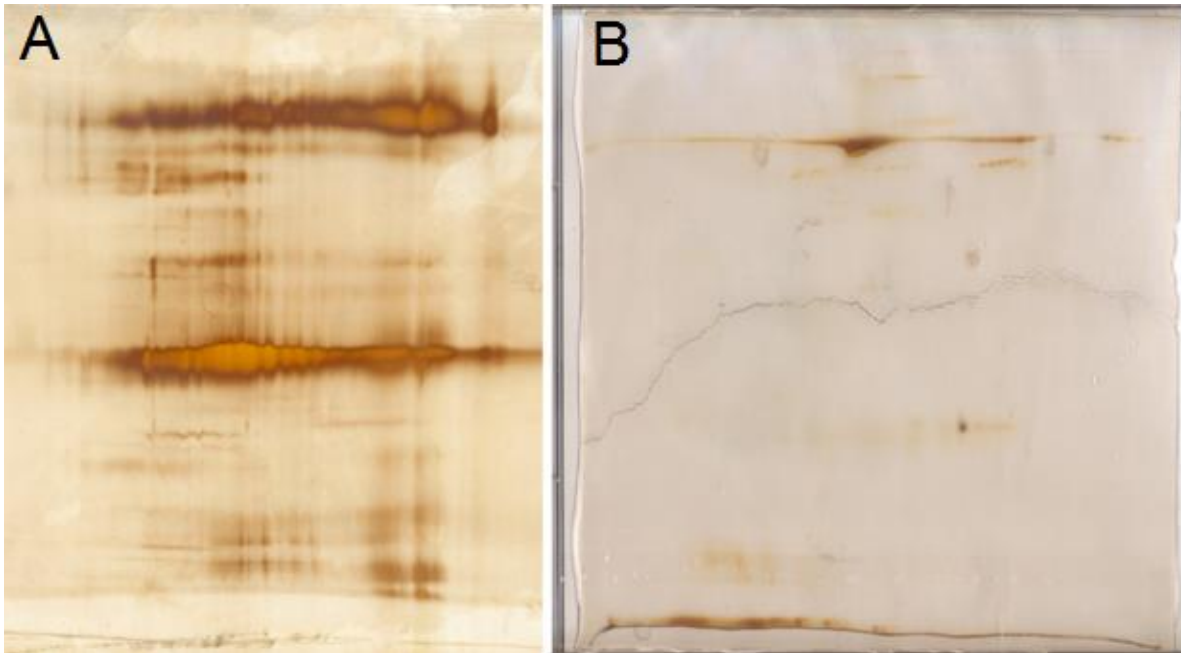


Figure 2-7. Protein G and GenWay column bound fractions.

2D PAGE where both gels had samples were prepared with chloroform/methanol precipitation. **Gel A** had an 18 cm pH 3-10 NL IPG strip loaded with the bound fraction from protein G depletion, second dimension was a gradient gel with 8-14% acrylamide, medium format. **Gel B** had a 24 cm pH 3-10 NL IPG strip loaded with the bound fraction from a GenWay column after IgG depletion, second dimension was 10% acrylamide, large format.

Despite some gels having reasonable resolution, there was considerable variation in the quality of spot resolution produced. It was therefore decided not to continue with quantitative analyses for two reasons. Firstly, it was difficult to objectively assess if a gel was acceptable for quantitation. Secondly, as it was intended to use an expensive DIGE methodology for quantitative analysis it would be wasteful to have to produce many gels in order to obtain enough of suitable quality. Examples of gels with poor resolution are shown in Figure 2-8.

Discussion with a technical advisor at GE Healthcare raised the possibility that some of the resolution problems encountered occurred in the second dimension, as can be seen when vertical resolution is poor (for examples see Figure 2-2 and Figure 2-8 A). It was suggested that this may be due to buffer warming in the Ettan DALTSix upper buffer tank, which occurred when moderately high electrical current flows were used to run the second dimension, particularly during the first part of the run. By placing an immersion thermometer in the upper buffer tank it was found that even moderate current flow resulted in an increase in temperature in the upper buffer tank. Such

an increase in temperature causes glycine ions to run faster than normal, resulting in its depletion from the upper buffer tank. An improved upper buffer tank with better heat dispersion was obtained to help minimise this problem. Programming the power supply for longer run times, particularly when the unit is fully loaded with gels also reduced upper buffer tank heating.

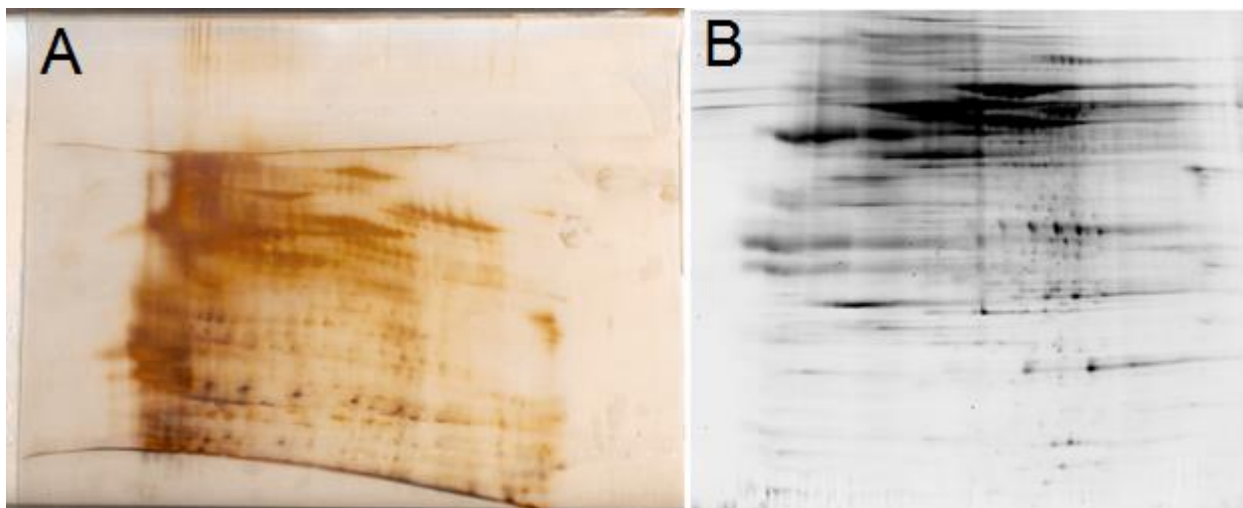


Figure 2-8. Poor quality large format 2D PAGE gels.

Examples of 2D PAGE gels using 24 cm pH 3-10 NL IPG strips loaded with depleted sheep plasma showing poor resolution. Gel A had problems with both first and second dimension resolution. Gel B mainly had poor horizontal resolution *i.e.* due to problems during IEF.

Improving 1st dimension resolution

A wide range of methods were explored in order to improve IEF, many of which involved optimization of sample preparation methods as well as experimenting with protein loading methods and IEF running conditions. The parameters evaluated included: different reagents to precipitate the protein in the sample (methanol, ethanol, phenol, acetone and TCA/acetone), adjusting the pH during precipitation, and introducing a solid phase extraction step. The solvent precipitation methods were trialed in conjunction with heat extraction and SDS extraction. Also tested were methods used for alkylation and the reagents used in this procedure. Variables for IEF included; the composition of the rehydration buffer, concentration of carrier ampholytes, the use of hydrophilic agents in the rehydration solution, the method used to load the protein into the IPG strip, the length of the strips, voltage gradients used and equilibration time.

As it had been previously observed that strips that had surplus rehydration fluid removed, (by blotting with tissue paper prior to IEF *i.e.* after overnight rehydration) generally focused with a lower current flow and had better spot resolution, rehydration volumes as well as rehydration constituents were optimised. The purchase of a manifold for the Ettan IPGPhor II meant that as well as being able to accommodate a larger range of different IPG strip lengths (*i.e.* including 24 cm IPG strips) strips could then be run with the gel surface facing up rather than down as is the case with the strip holders. 24 cm IPG strips require the use of a large format 2nd dimension gel system, the Ettan DALT six electrophoresis system, from GE, was used. The gel dimensions were 25.5 cm wide, 21 cm long and 1 mm thick for the large format system.

When using the manifold, electrode wicks (soaked in water) are used to connect the metal electrode to the gel, rather than there being direct contact between the gel and the metal electrode (see Figure 2-9).

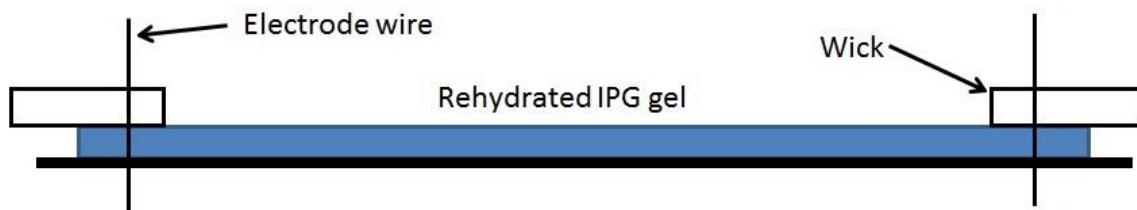


Figure 2-9. Schematic diagram showing relative placement of IPG strip, wicks and electrodes.

Initially the goal for work focused on maximizing the number of spots that appeared on gels. Towards this end, a sample was depleted as before, had SDS added to 2%, TCEP to 20mM, then heated at 60°C for 5 minutes and then the protein was precipitated by adding acetone to 90%. Pellets were resuspended in Triton X-100 and heated for 5 min at 60°C. After the protein concentration was determined, samples were diluted into rehydration buffer containing 2 M thiourea, 7 M urea, 4% CHAPS along with DeStreak and rehydration loaded onto pH3-10 NL 24 cm IPG strips. An example is shown in Figure 2-10. Although the number of detected spots increased, it was apparent that charge chains were appearing, most likely due to heating and/or SDS. As SDS is charged it can affect IEF. Subsequently neither heating or SDS were used in sample preparation and charge chains were not seen again.

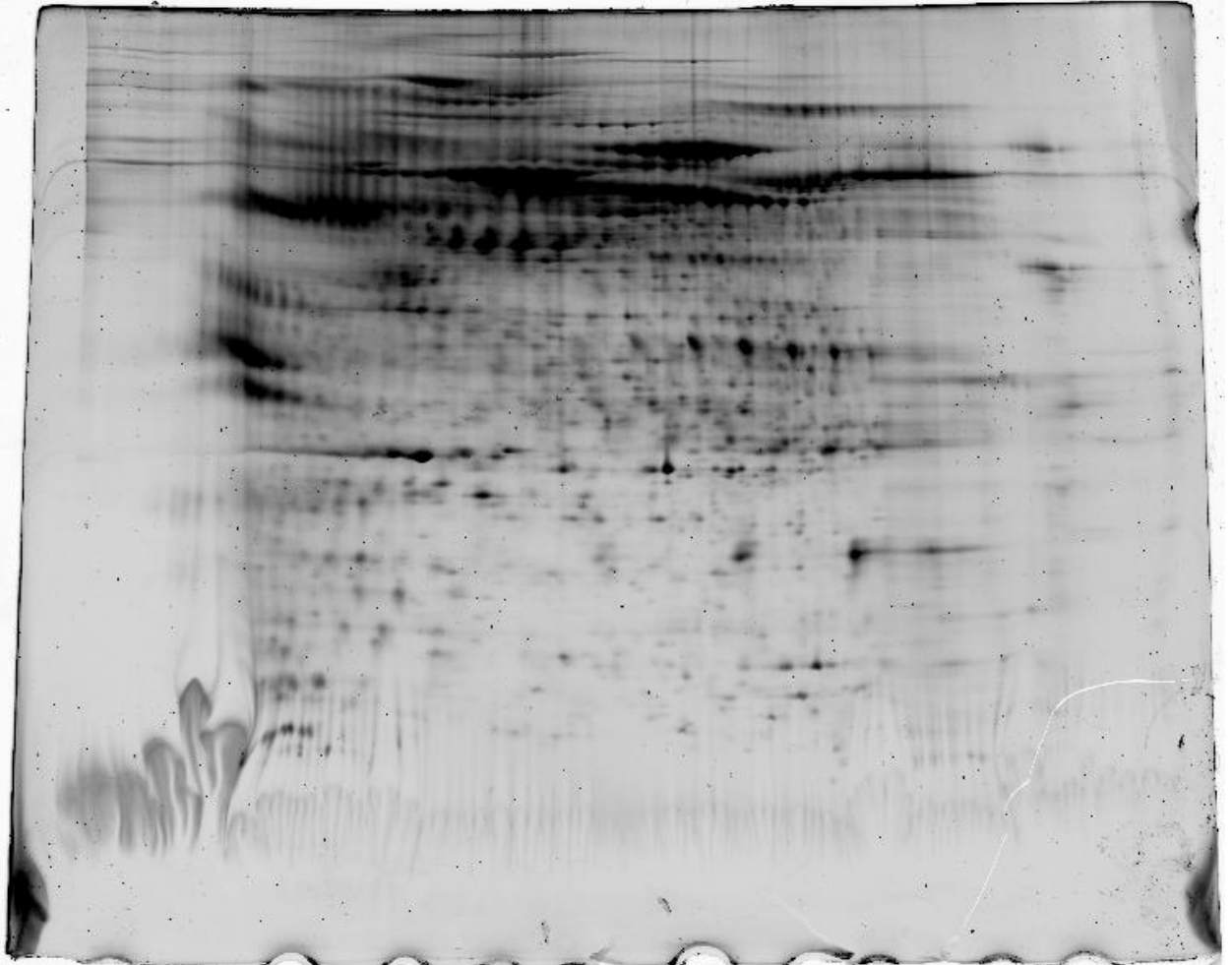


Figure 2-10. Heating and/or SDS samples causing charge trains in 2D PAGE, large format.

2D PAGE of depleted sheep serum using a 24 cm IPG strip, pH 3-10 NL with an 8-16% acrylamide gradient gel stained with Sypro Ruby. Samples were prepared by heating in SDS prior to sample clean-up.

Basic sample preparation method

The basic sample preparation used for all following experiments was (unless otherwise stated): 100 μ L of plasma was diluted to 5 mL with TBS. 2 mL of this solution was applied to a 1mL Protein G Sepharose column and eluted without additional buffer being applied. The final 0.5 mL fraction was collected and applied to a GenWay C12 IgY depletion column and mixed gently. The column was then rotated in an end over end rotator for 15 minutes at room temperature. The column was eluted by centrifugation (30 seconds at 0.3 g) to remove the unbound fraction followed by two 0.5 mL column washes with TBS which were added to the flow through to produce a total of 1.5 mL of

depleted sample. Urea was added to a final concentration of 8M, along with Tris(2-carboxyethyl)phosphine (TCEP) to 10 mM, Tris base to 65 mM, and triton-X100 to 4%.

The final pH was approximately 8.6 and the volume approximately 2.5 mL. This resulting solution was alkylated by the addition of 1/20 vol 0.4 M 4-vinylpyridine (made up in 4 M urea) for 2 hours in the dark under oxygen free nitrogen gas. The reduced and alkylated proteins were then precipitated by the addition of acetone to make a final volume of 15 mL (90% acetone). After gentle mixing the solution was left to incubate for a minimum of 4 hours at -20°C, then brought to room temperature and the precipitated proteins were pelleted by centrifugation (3000 *g* for 10 min at room temperature). The supernatant was carefully removed, 5 mL 90% acetone added and vortexed, followed by incubation at -20°C for a minimum of two hours. The precipitated proteins were pelleted by centrifugation at 4°C (3000 *g* for 10 minutes). This washing procedure was repeated two more times and the pellet washed 3 more times. The precipitated protein pellet was finally dried by lyophilisation overnight before being resuspended in 50 µL of 2D buffer (4% CHAPS, 7 M urea, 2 M thiourea).

While the resolution of spots using this method was sometimes good, variation in resolution consistency continued to be an issue. One of the concerning issues was the accuracy with which the protein load on each strip was determined. An Invitrogen EZQ protein quantitation kit (Cat No. R33200) was used to determine sample protein concentration. This kit transfers the protein to a membrane so that contaminants that might interfere with quantitation (*e.g.* detergent, reducing agents) can be washed away before quantitation takes place. Membranes were stained with the supplied fluorescent stain according to the manufacturer's protocol and scanned with a Fujifilm FLA-3000 fluorescent scanner using the blue laser. Image analysis (for quantitation) was done with Fujifilm Image Gauge 4.0, an example screen shot showing a stained membrane, standard curve and data is included in the Appendix (['34 - Protein concentration - Image Gauge 4.0 screen shot.TIF'](#)).

First DIGE experiment

A DIGE experiment was carried out that resulted in disappointingly poor resolution (Figure 2-11).

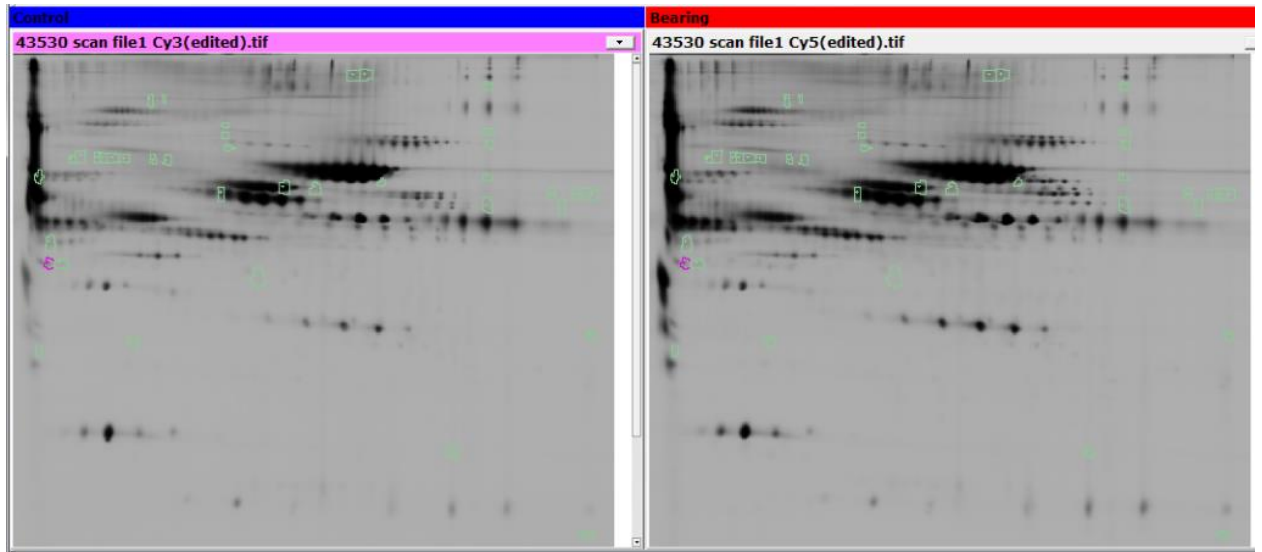


Figure 2-11. DIGE experiment 1, example gel.

24 cm pH 3-10 NL IPG strips were used with GE 12% acrylamide pre-cast gels along with the GE 2nd dimension buffer system. Resolution is poor, particularly at the acidic end (left). The two images shown are from the same gel probed with a different laser *i.e.* from different biological samples.

In an attempt to explore better methods with the aim of improving spot resolution in DIGE gels it was found that the resolution was improved in non-DIGE gels when a long voltage ramp was employed during IEF (Figure 2-12 and Figure 2-13).

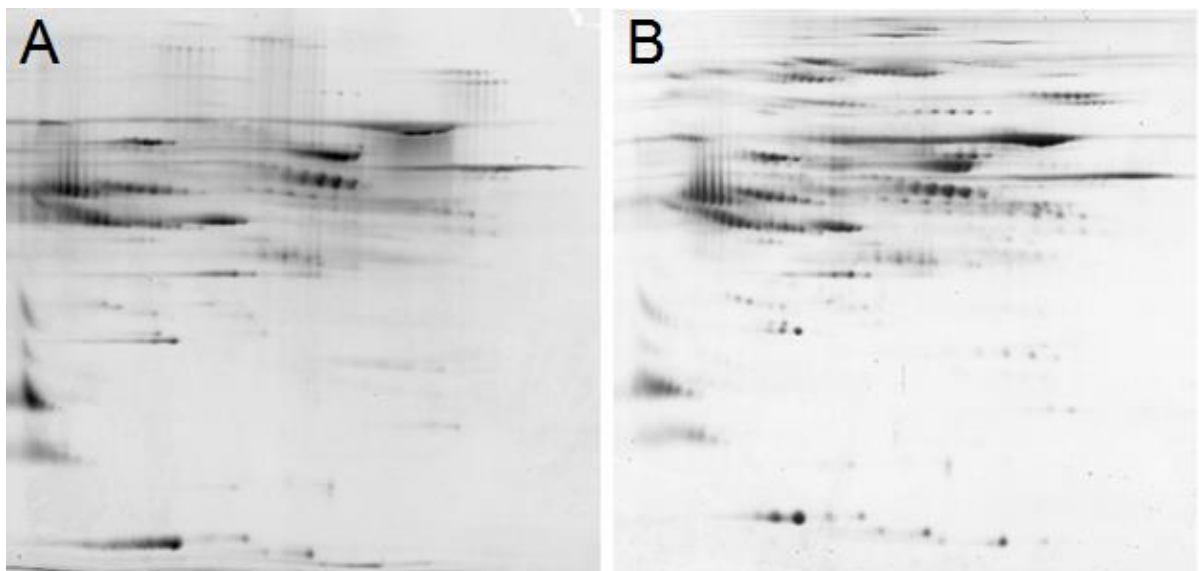


Figure 2-12. Trialing voltage gradients during IEF, large format.

This shows a comparison of 2D gels in which IPG strips were focused using different voltage gradients (see Figure 2-13) using 24 cm pH 3-10 NL IPG strips. 2nd dimension was 10% acrylamide.

Gel A used a strip which was focused with the recommended voltage gradient. The strip used for gel B was focused with a long voltage gradient. The protein load on both gels was 50 μg of depleted sheep plasma.

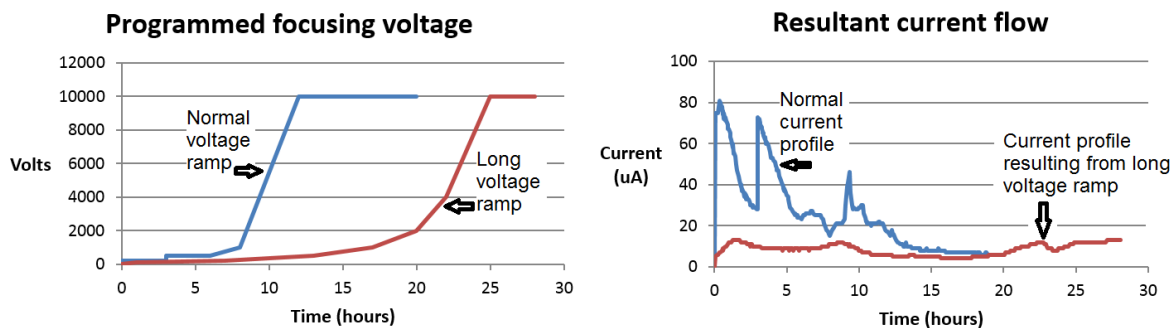


Figure 2-13. Voltage and resultant current profiles for 2 different IEF regimes.

See Figure 2-12 for gel images from these runs.

The gels shown in Figure 2-12 were run using a 50 μg protein load, and in the nature of DIGE, three times this load is required for each strip, *i.e.* 150 μg , which is higher than the recommended maximum analytical load of 60 μg for 24 cm ph3-10 IPG strips [246]. It is possible that this increased load may be the cause of the poor resolution seen in the first DIGE experiments.

Many of the methods that have been previously reported use an intermediate voltage range, *i.e.* a quicker ramp than that used previously in the present study but slower than that recommended by GE Healthcare. An extra-long run was compared with focusing done for an intermediate time to exaggerate the differences. As previously noted, water may be consumed during IEF due to electrolysis, a factor that may be exaggerated during extra-long runs. It was therefore decided to calculate the amount of water consumed.

Table 2-2 shows calculations for the amount of water consumed by electrolysis. For 50 hours at 75 μA this comes to 1.25 μL , which is an insignificant amount, especially when one considers that 150 μL is applied to each electrode wick. As the maximum current for the 50 hour run was approximately 15 μA (see Table 2-2) the amount of water consumed by electrolysis during the run was probably less than 1 μL per strip.

Value	Units	Method applied to determine value
75	μA	maximum current allowed per strip
7.5×10^{-5}	amps	μA/1,000,000
6.24×10^{18}	electrons per amp per second	Coulomb's constant
4.68×10^{14}	electrons used per second @ 75 μA	amps x Coulomb's constant
2.34×10^{14}	H ₂ O molecules used per second	two electrons required per molecule H ₂ O
6.02×10^{23}	molecules per mole	Avogadro's constant
3.89×10^{-10}	moles H ₂ O used per second	molecules H ₂ O used/Avogadro's constant
18.02	molar mass H ₂ O	g/mole
7×10^{-9}	mL H ₂ O used per second	moles H ₂ O used per second x molar mass H ₂ O
2.52×10^{-5}	mL H ₂ O used per hour	mL H ₂ O used per second x 3,600
0.025	μL H₂O used per hour	mL H₂O used per hour x 1,000

Table 2-2. Theoretical water consumption due to electrolysis during isoelectric focusing.

As the water consumption due to electrolysis was calculated to be minimal it was decided to proceed with the extra-long and intermediate length IEF experiment. Gels are shown in Figure 2-14 and as can be seen there appeared to be no advantage in using an extra-long IEF run and so an intermediate length run was adopted for the next DIGE experiment.

Second DIGE experiment

The DIGE experiment was repeated using a 90% acetone cleanup and an intermediate voltage ramp, but there was no improvement in the spot resolution. Again it was thought that an improvement in spot resolution was needed in order to achieve good quantitation. Images from DIGE gels lined up with post stained gels show the difference in resolution achieved, particularly at the acidic end of the IPG strips (see Figure 2-15). A variety of alternative methodologies were trailed in order to improve resolution, note that small format gels were often used for testing methods simply because they are quicker and easier to run.

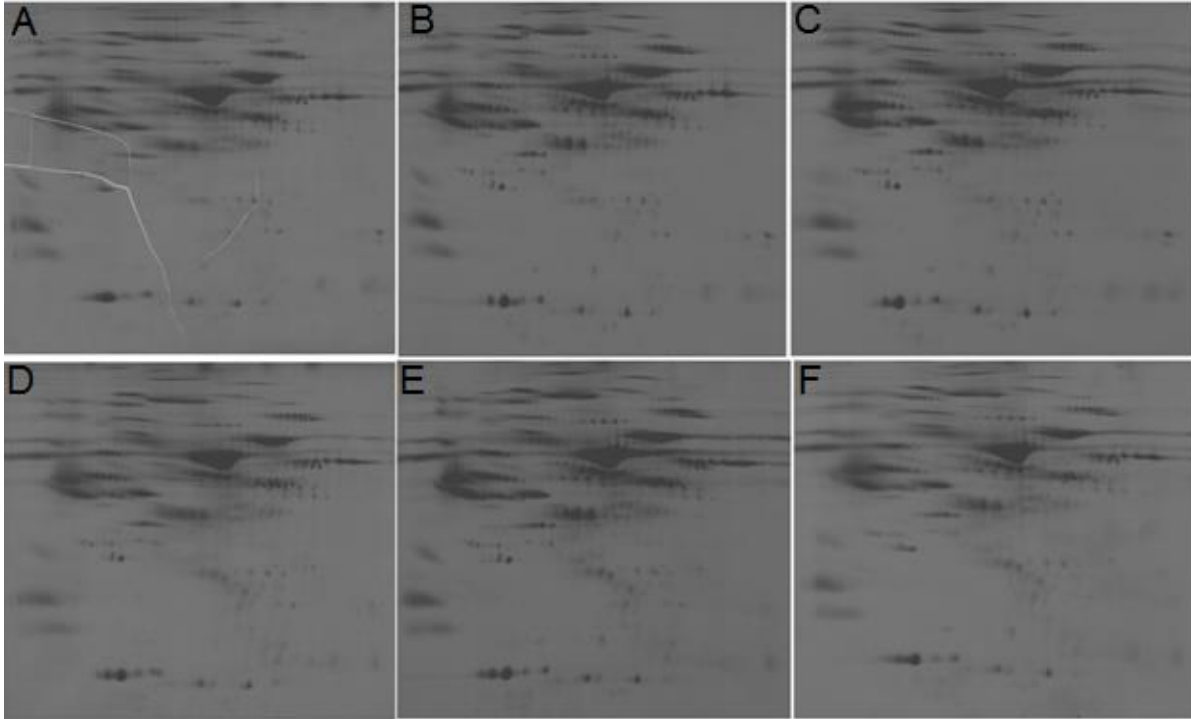


Figure 2-14. Intermediate voltage gradient vs an extra long voltage gradient during IEF. 2D PAGE gels loaded with non-depleted sheep plasma samples, 50 μ g protein per gel. IPG strips were pH 3-10 NL, 24 cm, 10% acrylamide in the second dimension. **Gels A, B and C** are from an intermediate length focusing run, whereas **gels D, E and F** had an extra long focussing time.

Increased protein load

As the IPG strips had to be able to handle a higher load than that used in Figure 2-12 it was decided that a greater improvement in resolution was required. A large number of experiments were carried out to improve 1st dimension resolution when using a higher than normal protein load. Firstly, after depletion, proteins were alkylated prior to IEF instead of using DeStreak in the 1st dimension and iodoacetamide during SDS equilibration, prior to the 2nd dimension run. Secondly, denaturing conditions used during alkylation prior to precipitation and focusing were investigated. To do this the alkylation step was done as before, but either in the presence of urea or in the presence of guanidine hydrochloride, with or without DeStreak in the isoelectric focusing buffer. It was found that alkylation in the presence of urea was effective in providing reasonable resolution, at least for the majority of proteins (Figure 2-16).

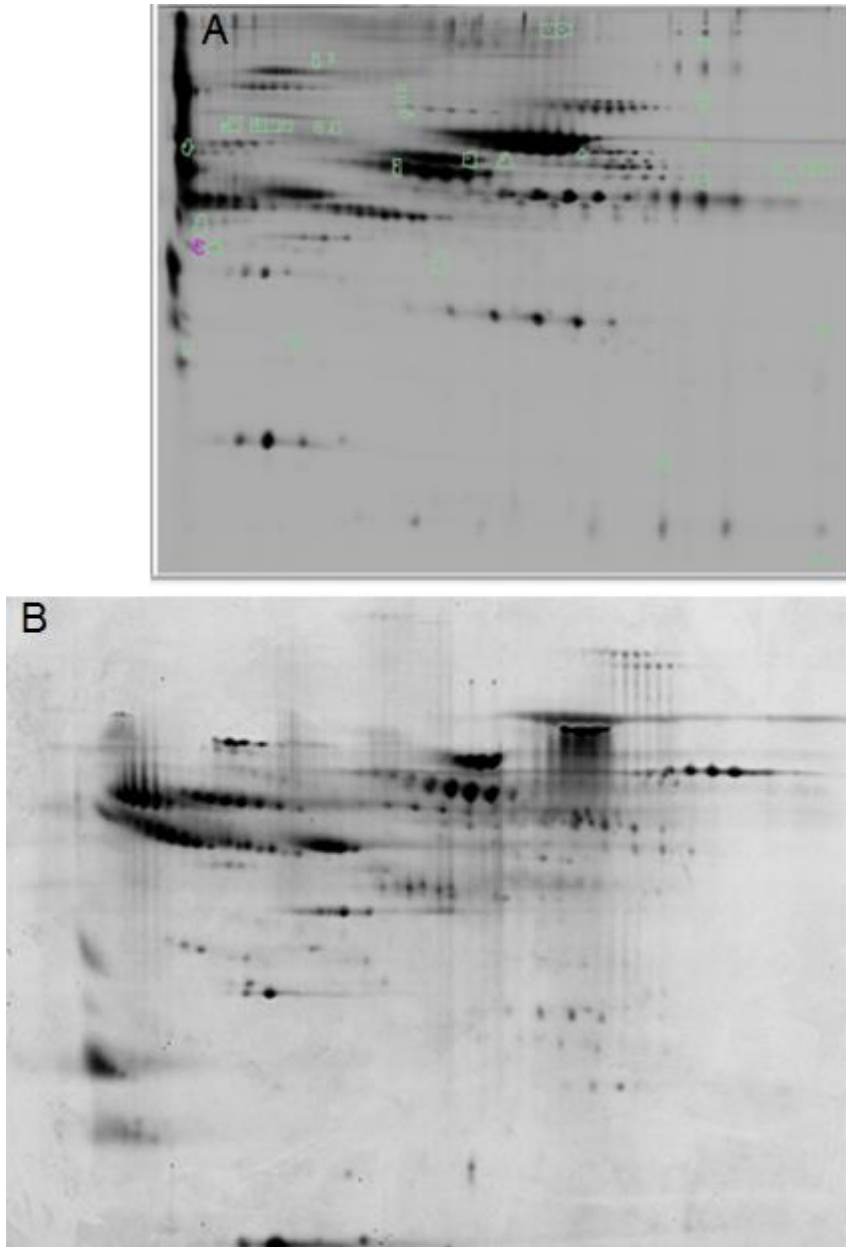


Figure 2-15. Aligning horizontal resolution of DIGE gel with non-DIGE gel.

2D PAGE gels, pH 3-10 NL 24 cm IPG strips. **Gel A** shows one of the three 50 μ g loads from the 1st DIGE experiment, note this gel was cropped on the left to facilitate spot detection as there were no resolved spots in this area. **Gel B** is a Sypro Ruby stained gel loaded with 50 μ g depleted sheep plasma. They are lined up vertically to show the disparity in horizontal resolution at the acidic (left) side. For the second dimension, gel A is a GE 12% acryamide gel using the 2nd dimension GE buffer system, whereas gel B is a 10% labcast gel run using the standard Tris/glycine buffer system.



Figure 2-16. Alkylation protocols and spot resolution.

Small format 2D PAGE gels each loaded with 10 μg of depleted sheep plasma using different alkylation procedures. Sample **A** was alkylated in the presence of urea, **B** with guanidine hydrochloride and **C** with guanidine hydrochloride followed by running with DeStreak in the rehydration solution. Strips were pH3-10 NL 7 cm, 2nd dimension was 10% acrylamide. Staining was with silver nitrate. Note the maximum recommended analytical load for these IPG strips is 6 μg [246].

Spin clean-up experiment

As it is considered possible that contaminants that affect IEF can co-precipitate with protein during sample clean-up [192] it was decided to investigate an alternative clean-up method. The protocol of Megan Penno *et al.* [249] was used. Their procedure focusses on reducing the salt contamination of samples with the use of spin columns along with testing sample purity by monitoring conductivity. A suitable conductivity meter was obtained (a Horiba Twin Cond B-173) and a spin column (Vivaspin™, 0.5 mL, 10 kDa cutoff) was used to wash the resuspended sample with 2D buffer until the conductivity reduced to less than 300 $\mu\text{S}/\text{cm}$ from 4.6 mS/cm (for 1.6 mg/mL protein in 50 μL). The sample was split, with one half put being aside on ice and the other half being washed using a spin column. The 25 μL sample was mixed with 175 μL 2D buffer and centrifuged at 12,000 g (4°C) until the volume was reduced to approximately 20 μL then 180 μL 2D buffer was added for the next spin. This process was repeated for 3 spin washes. Finally buffer was added to 100 μL and the conductivity retested and found to be 87 $\mu\text{S}/\text{cm}$.

The protein concentration of the samples was measured and the spin cleaned up sample was found to be more concentrated than the not spun sample, (46 μg *cf* 32 μg). This is difficult to explain, but possibly the volume was slightly less for the spun sample. From each sample 15 μg was loaded onto duplicate 7 cm 3-10 NL strips and focussed using an intermediate focus protocol. Figure 2-17 shows the spin washed samples, and Figure 2-18 shows the samples that were not spin washed. 15 μg was

loaded on each strip as this is approximately 3x the recommended analytical load for 7 cm strips and so reflects the 3x load on DIGE gels.

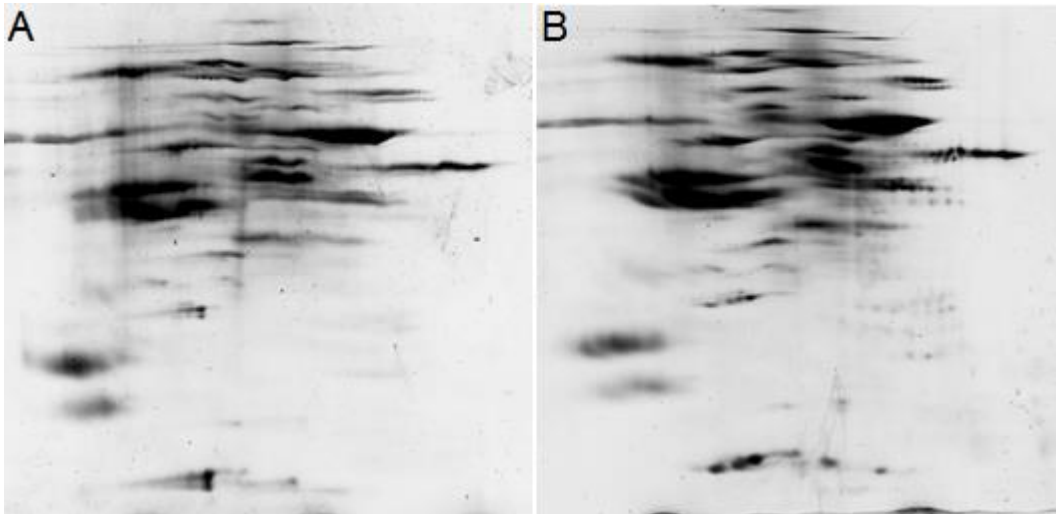


Figure 2-17. Spin clean up and spot resolution.

Duplicate 2D PAGE gels using samples prepared by spin clean up to reduce conductivity. 15 μ g depleted sheep plasma protein was loaded per 7 cm pH 3-10 NL IPG strip, 2nd dimension was 10% acrylamide.

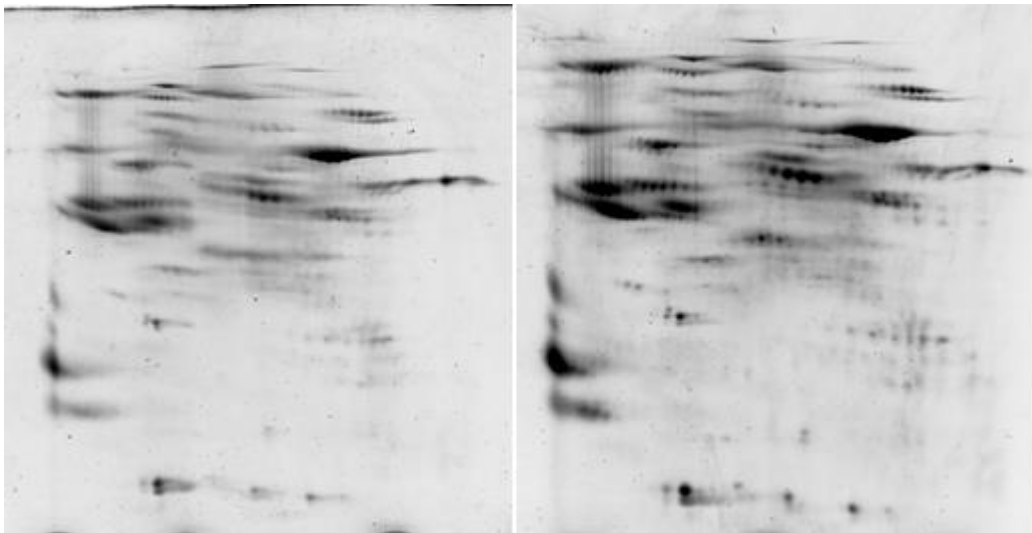


Figure 2-18. Acetone precipitation and spot resolution, small format.

Duplicate 2D PAGE gels with samples prepared using acetone precipitation without washing in spin columns. 15 μ g depleted sheep plasma protein was loaded per 7 cm pH 3-10 NL IPG strip, 2nd dimension was 10% acrylamide.

The gels from the samples prepared with acetone precipitation had better resolution than the gels with samples prepared with the spin column method, although spot resolution was still not consistent.

Equilibration time

An experiment was carried out to investigate the relationship between equilibration time (when the IPG strips are soaked in SDS detergent in preparation for the 2nd dimension) and spot resolution. Samples were prepared as before, with 10µg of depleted plasma protein being loaded onto each of 5 pH 3-10 7 cm IPG strips. During the equilibration step one strip was removed from its equilibration tube after one minute, rinsed with tank buffer and placed into the 2nd dimension gel. This process was repeated at two minutes, five minutes, ten minutes and thirty minutes. Note that no equilibration buffer change during equilibration was required as samples were alkylated prior to IEF. All 2nd dimension gels were 12% acrylamide, and stained with silver nitrate (Figure 2-19).

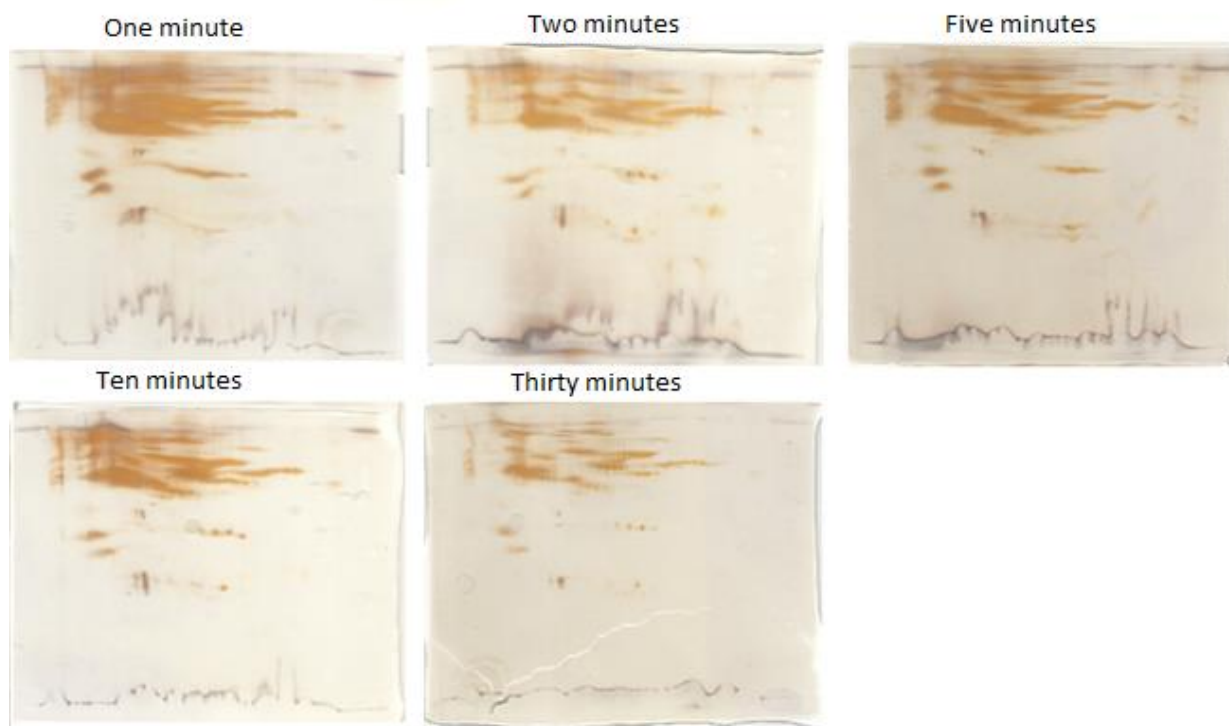


Figure 2-19. Equilibration time and spot resolution.

The effect of equilibration time on spot resolution on 2D PAGE gels. 10 µg of depleted sheep plasma was loaded onto 7 cm pH 3-10 IPG strips. Strips were placed into SDS equilibration buffer at the same start time and were progressively removed from the buffer and rinsed clean at the times stated. 12% acrylamide was used in the 2nd dimension and the gels were stained with silver nitrate.

As equilibration time appeared to have an effect on resolution it was reasoned that longer equilibration times were probably washing away poorly resolved proteins lying on the surface of the IPG strip and that better resolved proteins may lie deeper within the strip. This may be affected by the loading method employed.

In order to address loading concerns a cup loading experiment was carried out (Figure 2-20).

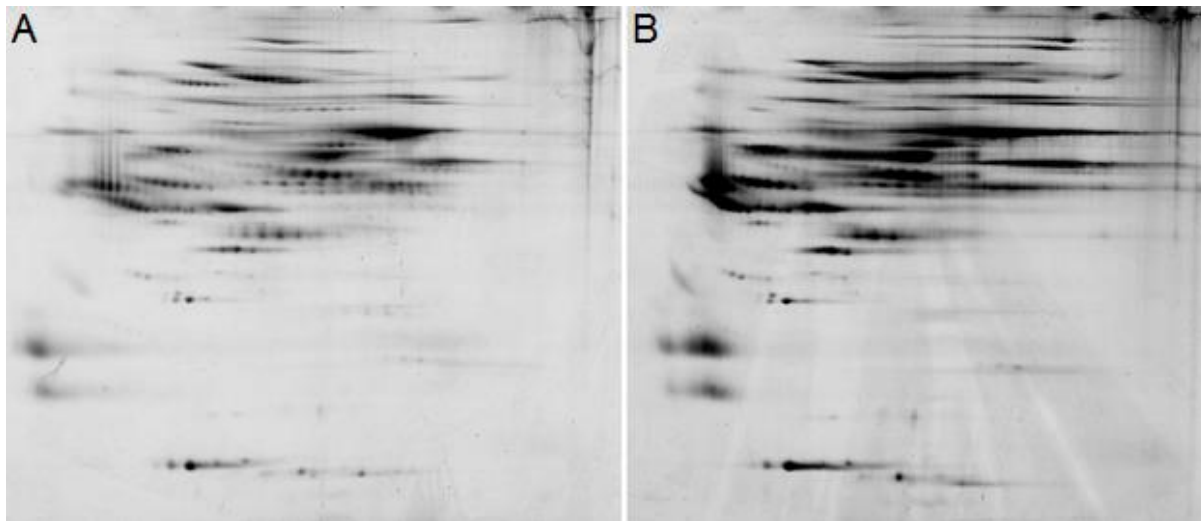


Figure 2-20. 2D PAGE cup loading experiment, large format.

A 50µg sample of depleted sheep plasma was cathodic (i.e. basic or right hand end) cup loaded onto 6.24 cm pH 3-10NL IPG strips. Six gels were run, but only the image shown in gel A has reasonable resolution. The other five resembled the image shown in gel B or worse.

Results from the cup loading experiment were variable and generally poor, only one gel of the 6 that were run had reasonable resolution.

Nature Protocols method (also using cup loading)

In order to test alternative published methods, a protocol following one published in the Journal Nature Protocols [163], was undertaken. As this method was designed for human plasma, ethical approval was obtained (HEC: Southern A application 13/37) and a human sample obtained. This was treated according to the published protocol as follows; 6.26 µL plasma was mixed with 10 µL 10% SDS, 150 mM DTE (dithio-1,4-erythritol), and heated for 5 minutes at 95°C in a water bath. After cooling to room temperature, it was diluted with 485 µL of a solution containing 8 M urea, 4% CHAPS, 65 mM DTE, 35 mM Tris and 1% bromophenol blue. 60 µL of this solution (containing 170

µg of protein) was loaded into cathodic sample cups on 24 cm pH 3-10 NL IPG strips that had been rehydrated overnight at 21°C in a disposable reswelling tray with 8 M urea, 2% CHAPS, 10 mM DTE, 0.4% bromophenol blue and 2% IPG buffer. As the Immobiline dry strip reswelling cassette recommended in the Nature Protocols procedure was not available, a disposable Immobiline dry strip reswelling tray was used.

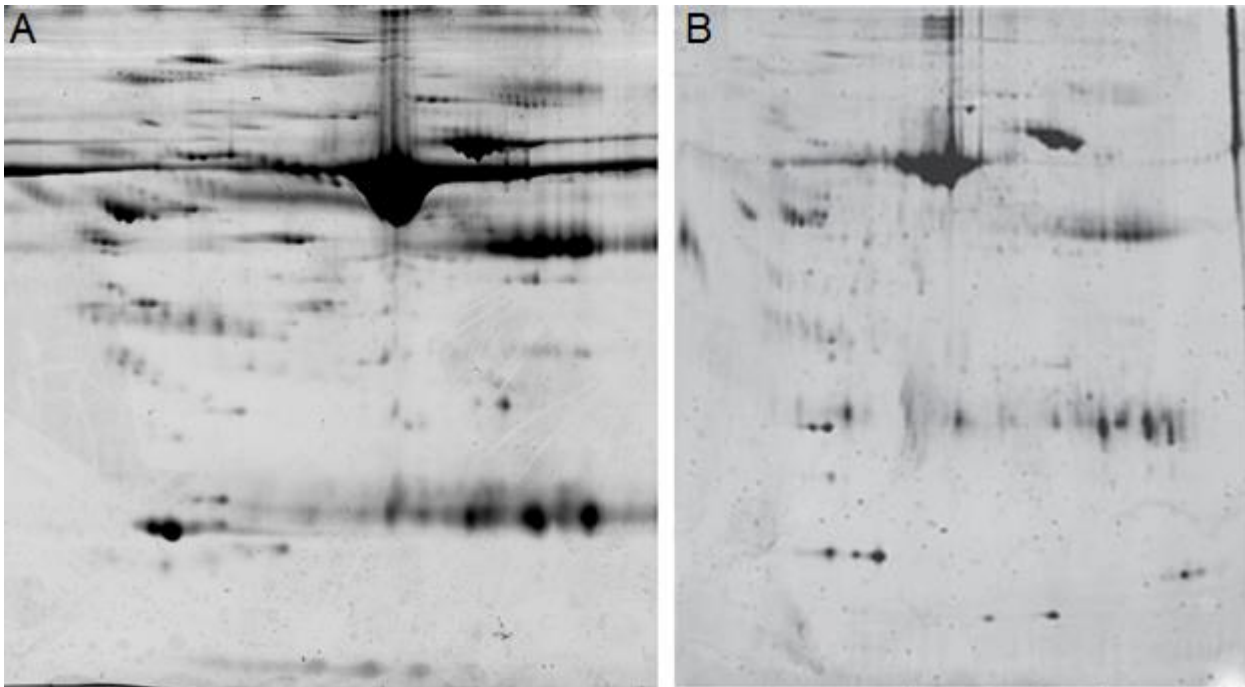


Figure 2-21. Evaluation of Nature Protocol method, large format.

2D PAGE with pH 3-10 NL 24 cm IPG strips, stained with Sypro Ruby. **Gel A** was cathodic cup loaded with 170 µg of human plasma protein, 2nd dimension 10% acrylamide. **Gel B** is a gel image, published in Nature Protocols, that had been cup loaded with 45 µg of human plasma protein, 2nd dimension was a gradient gel 8-16% acrylamide. (Reprinted by permission from Macmillan Publishers Ltd: Nature Protocols Vol 1, No 2, p820, copyright (2006)). See also Figure 2-22.

As shown in Figure 2-21 the Nature Protocols method sometimes produced reasonable quality gels, although again, resolution was not consistent. Figure 2-22 shows a poor quality gel prepared using the identical (Nature Protocols) method along with a gel prepared according to the basic method used previously but run with the human sample and cup loaded.

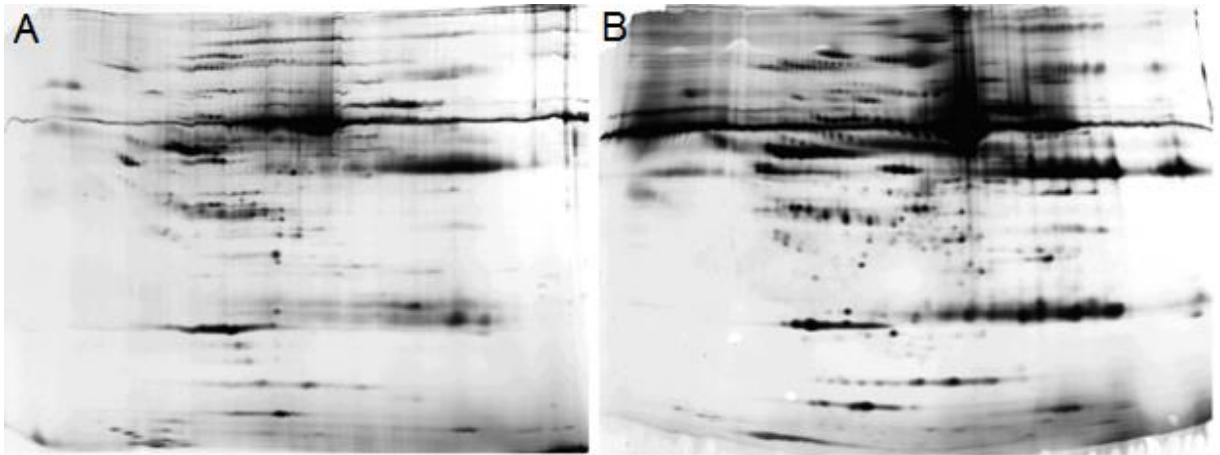


Figure 2-22. Further evaluation of Nature Protocol method, large format.

2D PAGE with pH 3-10 NL 24 cm IPG strips, loaded with 170 μg non-depleted human plasma. 2nd dimension was 8-16% acrylamide, ammoniacal silver staining. **Gel A** is an example of a poor resolution gel made using the Nature Protocols method (see also Figure 2-21). **Gel B** was run using the same human sample but with the previously used basic sample preparation method and cup loaded.

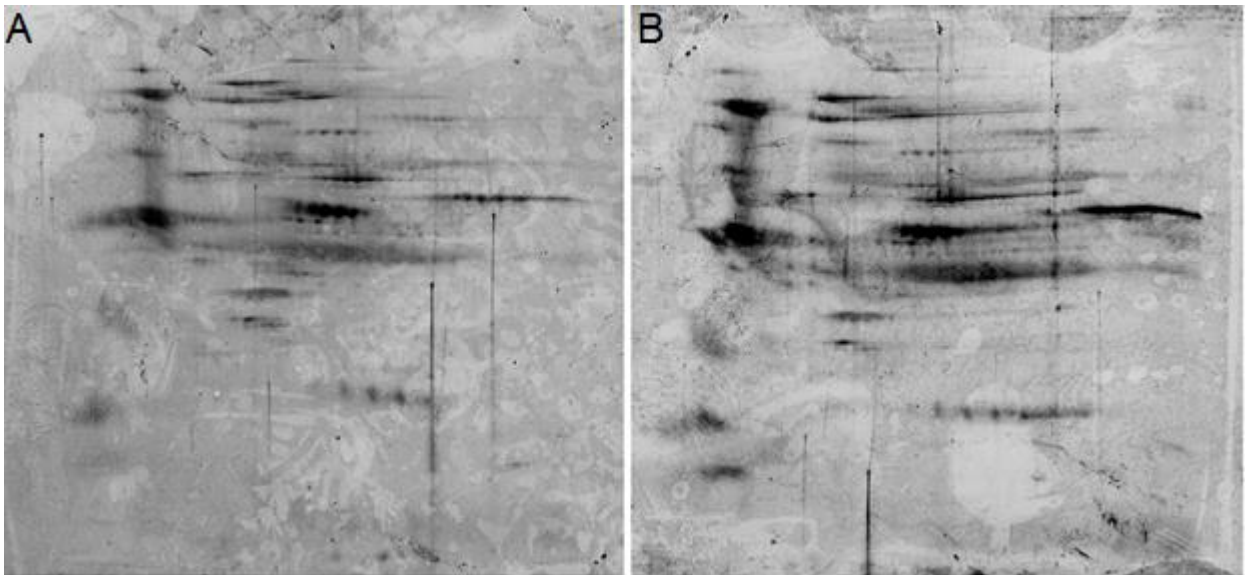


Figure 2-23. Reduced electrode wick water and spot resolution, small format.

Duplicate gels from 2D PAGE with 7 cm pH 3-10 IPG strips, loaded with 10 μg depleted sheep plasma using the basic method, except that electrode wicks had only 50 μL MQ water applied *i.e.* instead of 150 μL .

Reducing water flow by including hydrophilic agents such as glycerol and isopropanol was also not effective in producing gels of consistent good resolution (data not shown).

As cup loading had not shown a consistent improvement in spot resolution it was decided to use passive rehydration loading for the remainder of experiments. Work then began in an attempt to see if changes made at the electrodes affected the consistency of resolution. It was reasoned that the electrode wicks may be introducing excess water to the IPG strips during IEF, resulting in poor protein entry (into the IPG strip) of largely hydrophilic plasma proteins. A set of mini gel experiments was undertaken to see if reducing wick water would improve the consistency of resolution. Unfortunately these experiments generally failed to produce good quality gels. The recommended wick water volume is 150 μL and examples of gels run from strips focused using 50 μL wick water are shown in Figure 2-23.

Improved electrical connection

Initially conductivity was increased by raising the percentage of carrier ampholytes used in the rehydration solution. Carrier ampholytes are commercially available in specific pH ranges, the GE products for this purpose are known as IPG buffers. Technical data from GE suggests using either 0.5% IPG or 2% IPG buffers in the rehydration solution. As 0.5% IPG buffer had already been used in the basic method, both 1% and 2% IPG buffer were trialed. Again mini gels with 7 cm 3-10NL pH IPG strips were used for these trials, examples are shown in Figure 2-24.

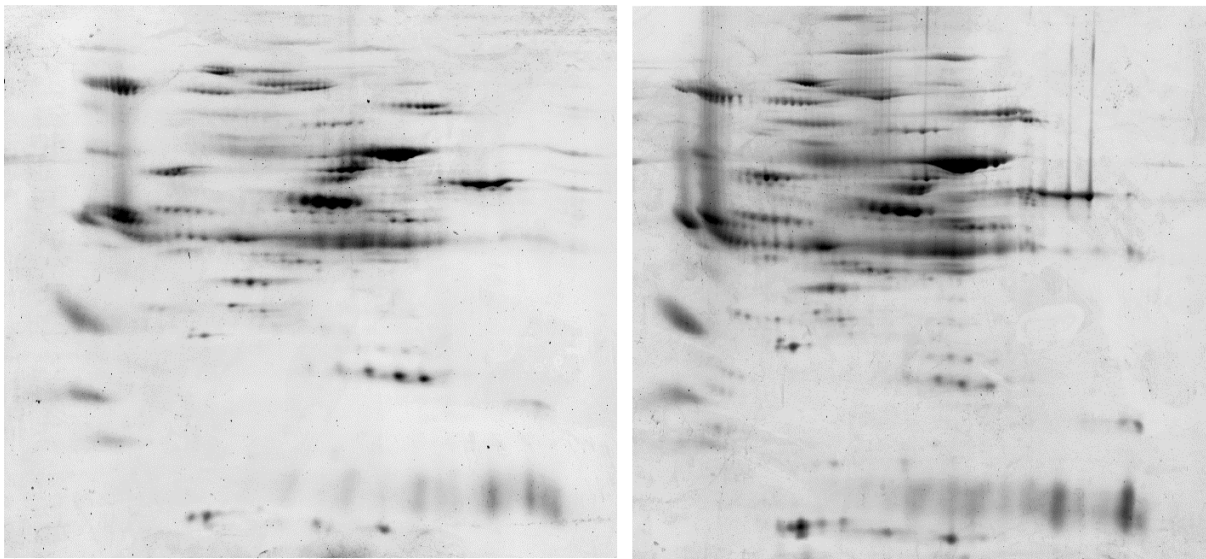


Figure 2-24. Increased carrier ampholytes, reduced wick water & spot resolution, small format.
Duplicate 2D PAGE gels using 7 cm pH 3-10 IPG strips loaded with 10 μg depleted sheep plasma. Strips were run with partially reduced wick water (100 μL instead of 150 μL) and had increased carrier ampholytes (1% IPG buffer instead of 0.5%).

As large format gels would be used for future quantitative work, subsequent experiments were carried out using these instead of small format gels. A set of experiments to determine if electrode wick and carrier ampholytes could be manipulated with the aim of producing consistent good quality large format gels. Figure 2-25 showed a marked improvement in spot resolution when IPG buffer was included in the wick solution when using non-depleted human plasma.

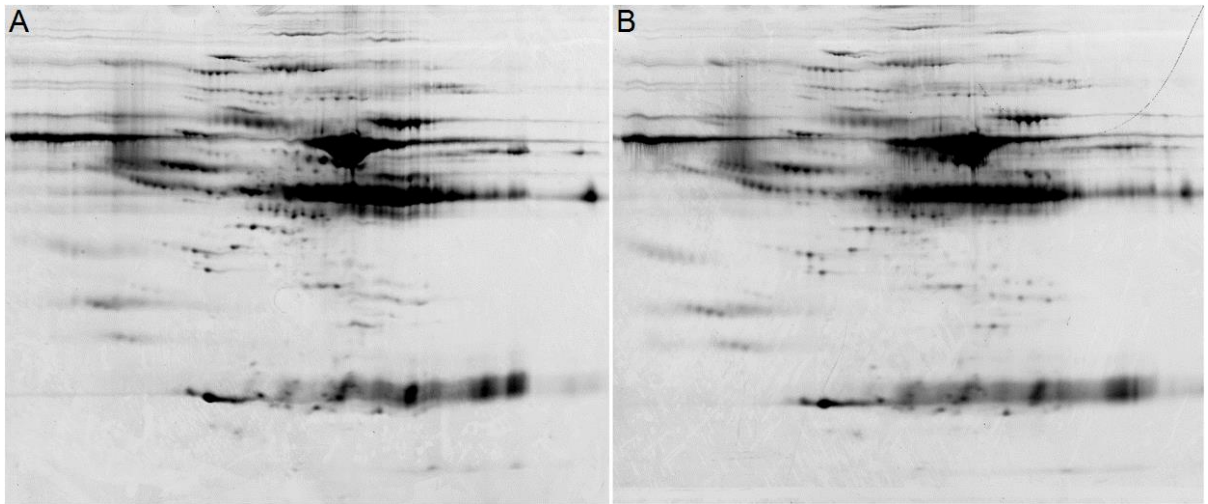


Figure 2-25. Carrier ampholytes in wick water, human plasma sample, large format.

2D PAGE gels with 24 cm pH 3-10 NL IPG strips loaded with 150 μ g of non-depleted human plasma protein. Both IPG strips had 0.5% IPG buffer in the rehydration solution and 2% IPG buffer (carrier ampholytes) in the wick water. The IPG strip for gel A had 100 μ L wick solution and the strip for gel B had 150 μ L wick solution.

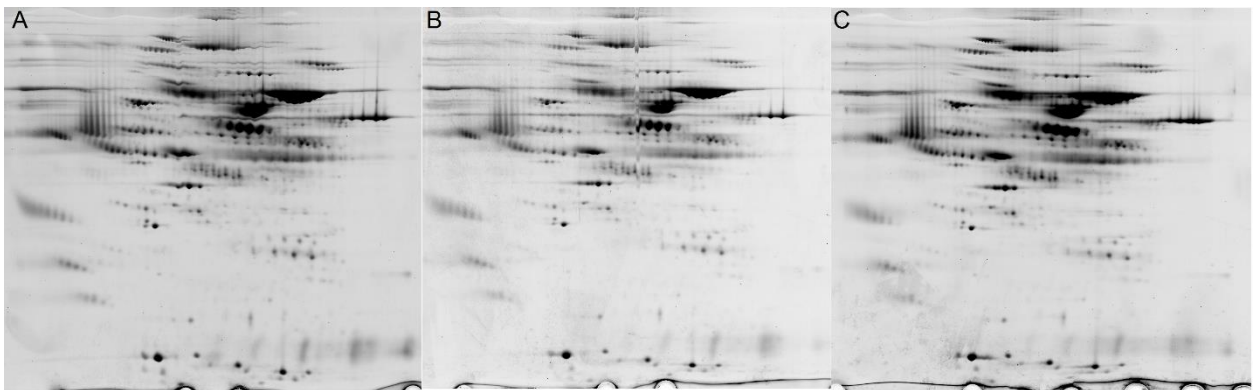


Figure 2-26. Carrier ampholytes in wick water, 150 μ g depleted sheep plasma, large format.

Triplicate large format 2D PAGE gels using 24 cm pH 3-10 NL IPG strips rehydration loaded with 150 μ g protein from pooled depleted sheep plasma samples resuspended in 30mM Tris. The rehydration buffer for the IPG strips contained 0.5% IPG buffer, and the electrode wicks contained 2% IPG buffer (carrier ampholytes). 2nd dimension was 10% acrylamide and staining was with Sypro Ruby.

Samples were then prepared for another DIGE experiment (see chapter 3 for details) and run using the improved method. The gels appeared to be consistent and of reasonable quality, see Figure 2-27. The only visible problem was with a second dimension gel where the water saturated butanol overlay had mixed with the top of the gel during casting on the left hand side of the gel. This gel appeared useable prior to running the second dimension but upon scanning it seems that butanol from the overlay had mixed with the gel (possibly from a too strong pipetting action while applying the overlay) on the left hand end of the gel during casting. Prior to running the second dimension the acrylamide/butanol mixture in this area had to be scraped off as it protruded up into the space required for the IPG strip. After running it appeared that the butanol/gel mix had prevented protein from properly entering the gel in this area (see Figure 2-32). This section was cropped from the scanned image prior to continuing with gel analysis, resulting in the loss of that sample's highly acidic proteins from the analysis.

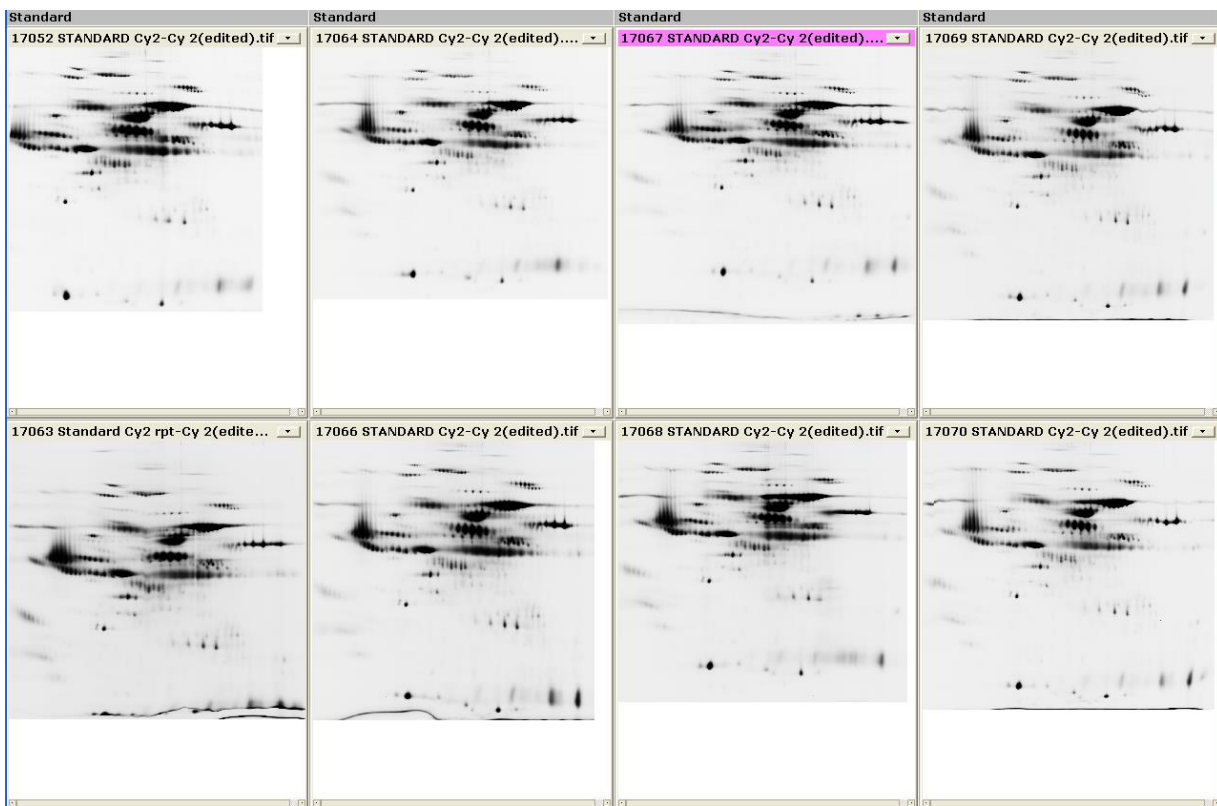


Figure 2-27. Standard images from DIGE experiment B.

All 2D PAGE gels in DIGE experiment B, showing reasonable and consistent resolution. The gel 17052 (top left) had a partially poorly cast second dimension gel (due to partial mixing of butanol overlay with acrylamide mixture, see Figure 2-32) and had to be cropped on the acidic (left) side. This

experiment is described in Chapter 3. IPG strips were 24 cm ph 3-10 NL, 2nd dimension was 10% acrylamide using the Ettan DALT large format system.

The standards images from two DIGE experiments, using both the basic and improved methods, were analysed for variance in order to determine the level of improvement in resolution, this is reported in Chapter 3 from page 76, under the heading “Evaluating the 2D PAGE methods”.

Gel casting issues

Numerous problems with casting large format gels were encountered, prominent among these were problems with generating a smooth top to gels. Figure 2-28 shows an example of a gel with an extremely poor top.

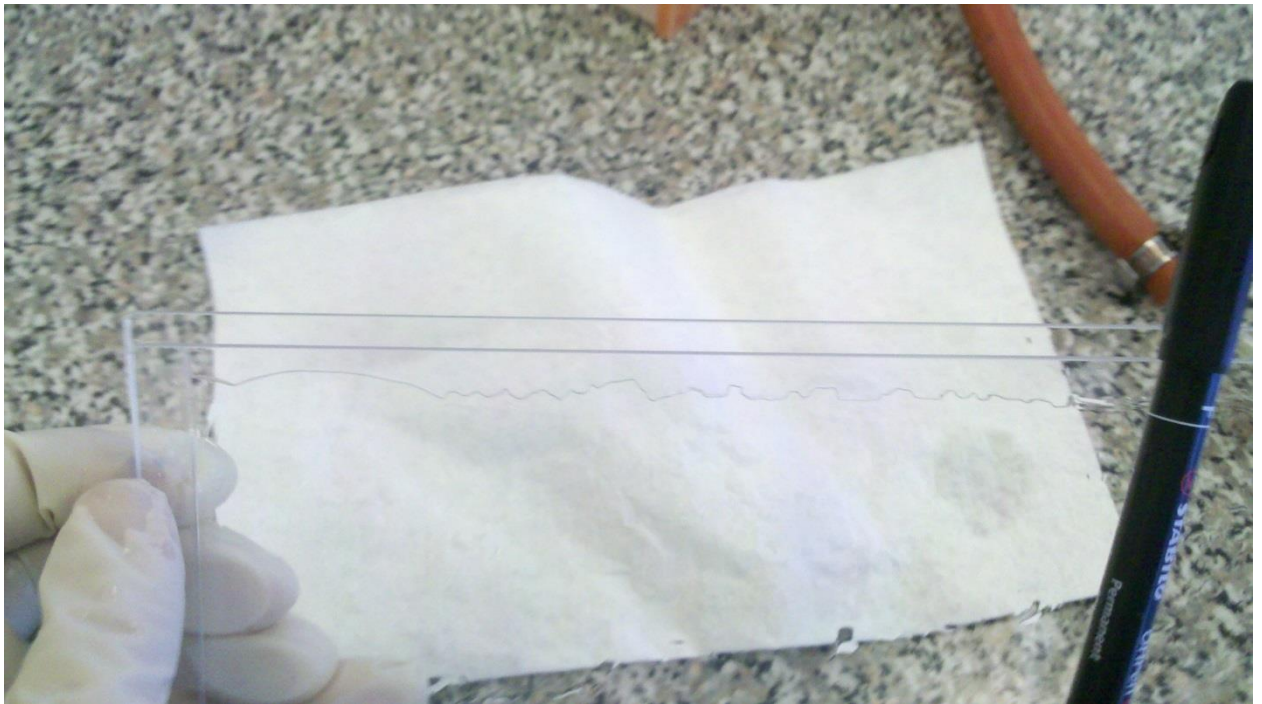


Figure 2-28. Example of an extremely wobbly top gel.

Within the casting tank, spacers are provided in order to reduce surplus caster volume, for example when 1 mm gels are cast (as opposed to 1.5 mm gels). The number of spacers was reduced from 6 to 5 which allowed the gel solution to flow more readily between the plates and into the gaps. This reduced the problem with uneven gel tops however it was still found that there was considerable waviness to the gels which affected the resultant gel image. Further, while some of the gel tops

were smooth, they had an uneven schlieren line underneath the top of the gel, with resultant uneven protein resolution, as shown in Figure 2-29.

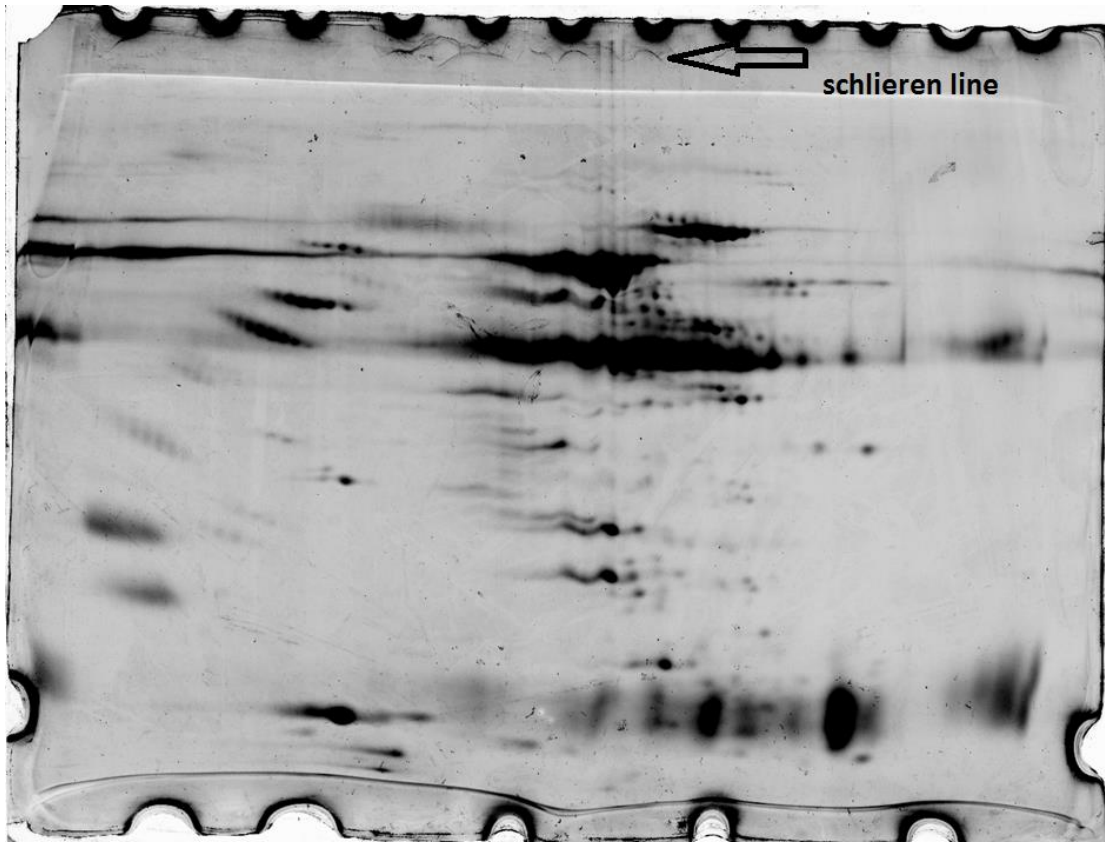


Figure 2-29. Uneven polymerisation.

Gel with uneven polymerisation towards the top of the gel (shown in a wavy schlieren line) resulting in horizontal waviness in stained proteins.

The line towards the top of the gel, known as the schlieren line, represents a change in the degree of polymerisation of the acrylamide due to inhibition by oxygen. Flushing the chamber with nitrogen before casting the gels reduced the unevenness of the schlieren line. However although the schlieren line became more uniform when using this method, it did nothing to eliminate the unevenness at the very top of the gels or the effect on protein resolution, but instead appeared to exaggerate it, as shown in Figure 2-30.

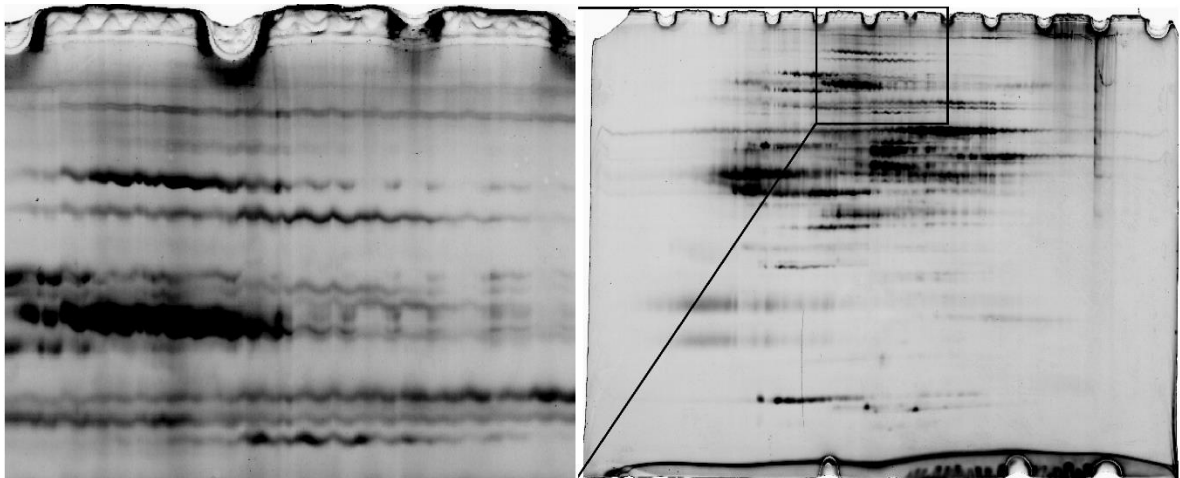


Figure 2-30. Effect of wobbly top gels on apparent protein resolution.

After testing a number of ways to remove this waviness it was concluded that it may be due to shrinkage during polymerisation. Polymerisation is known to cause shrinkage in other fields (*e.g.* dentistry) as covalent bonds have shorter bond lengths than non-covalent bond [250]. A method to supplement buffer into the bottom of the gel caster during polymerisation was devised in order to support the top of the gel as it shrunk during polymerisation. A displacement solution (375 mM Tris-HCl pH 8.8, 30% glycerol, a trace bromophenol blue) was put into a vessel connected to the bottom of the gel caster with a tube. It was found that the wedge shaped rubber block (used for casting homogenous gels) could remain in place at the bottom of the gel caster. Note that it is important to remove all air from the connecting tube prior to commencing gel casting otherwise air bubbles can be introduced into the gels. The level of the displacement solution was found to be critical, initially it needed to be about 1 cm below the required level of the top of gels as polymerisation solution may be drawn into the top of the gel plates by capillary action. As the gels polymerise the level of the supplementary solution was raised by a few mm to facilitate supporting the top of the gels. Entry of displacing solution into the bottom of the gel plates can be observed due to the inclusion of a trace amount of dye in the buffer (Figure 2-31).

After the polymerisation solution is poured into the gel caster, an overlay solution (often water saturated butanol) is usually applied to the top of the polymerising gels to prevent oxygen entering the top of the gels and inhibiting polymerisation. It commonly assumed these solutions are not miscible, however, it was found that they are and that it is important to be careful when applying the overlay solution so as not to mix the water saturated butanol with the polymerisation solution.



Figure 2-31. Supplementing buffer solution.

Unfortunately one gel in DIGE experiment B appeared to have some butanol mixed into the surface of the gel at the edge of the gel. Immediately prior to running the 2nd dimension part of the soft gel had to be scraped out between the glass plates to allow room for the IPG strip to be loaded. This affected partially the running of the second dimension (Figure 2-32).

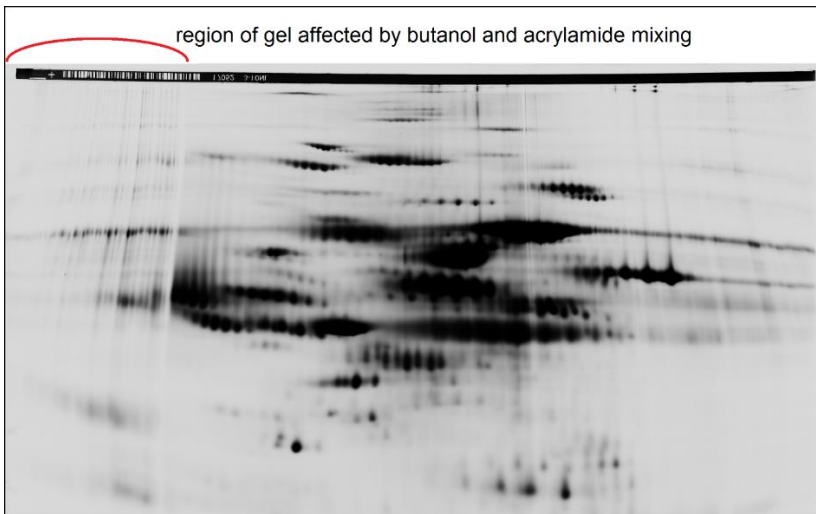


Figure 2-32. Gel from DIGE experiment B with a partial casting issue.

Gel 17052 (top left gel in Figure 2-27) from DIGE experiment B had an area where the water saturated butanol overlay mixed with acrylamide on the left hand side of the gel preventing proper entry of proteins into the gel and raising the top of gel in this region. This area had to be scraped level prior to loading the IPG strip in order to get the strip onto the top of the gel.

Chapter 3. DIGE methodology

As outlined in Chapter 2, an improved method for running 2D gels was developed. In order to be able to statistically compare the methods, data from one of the DIGE experiments resulting in poor resolution gels (the 3rd DIGE experiment) was chosen (now termed DIGE A) along with data from the 4th DIGE experiment (now termed DIGE B). Briefly, three changes from recommended practice as outlined in the GE Healthcare 2D PAGE manual [246] and used in DIGE experiment A, were made for DIGE experiment B. These were; 1) samples were acidified (with HCl to pH 2.5) prior to precipitation with acetone, 2) the focusing step used a long slow voltage ramp, and, 3) carrier ampholytes were included in the electrode wick water.

Samples used were those collected as described at the beginning of Chapter 2 *i.e.* sheep plasma collected from in lamb ewes (carrying multiple foetuses) towards the end of pregnancy.

Labelling

Note the same protein labelling methodology, based on manufacturer's recommendations, was used for all DIGE experiments undertaken in this study. Briefly, after precipitation samples were resuspended in 50 μ L labelling buffer, containing 2 M thiourea (GE Healthcare, stored in a vacuum desiccator), 7 M urea (GE Healthcare PlusOne), 2% CHAPS (Bio-Rad) and 30 mM Tris base (GE Healthcare PlusOne) and placed on ice. A solid state micro pH probe (Lazarlab, Los Angeles, USA) attached to a volt meter was used to determine the pH of the cooled samples (which were on ice) using a standard curve that had been calculated from pH standards (Fisher Chemical). The pH of standards was checked to see if they maintained the appropriate pH when placed on ice. Cleaning of the solid state probe was required between each sample measurement in order to prevent excessive pH drift. The pH of samples was adjusted to approximately 8.5 by the addition of microliter amounts of either 50 mM hydrochloric acid or 70 mM Tris base (Appendix '[1 - 3rd DIGE \(A\) expt sample prep.xlsx](#)' and '[2 - 4th DIGE \(B\) expt sample prep.xlsx](#)'). After pH adjustment protein concentrations were calculated in triplicate using the EZQ protein quantitation kit (Invitrogen) and typically ranged from 4 to 6 mg/mL.

Volumes of samples required for 50 μ g of protein were calculated and pipetted into microfuge tubes (Axygen) on ice. A pooled standard was made up using 25 μ g of protein from each of the samples

making up a single DIGE experiment, and was labelled with Cy 2. The bearing and non-bearing samples were randomly assigned labels so that half were labelled with Cy 3 and half with Cy 5, with an equal number from each group (control and bearing).

The CyDyes were reconstituted in dimethylformamide (DMF, Merck) that was stored in a glass jar with a SeccoSept® access lid to prevent hydration. The dyes were reconstituted by the addition of DMF to a 1 mM stock solution and then further diluted in DMF to a 0.4 mM working solution immediately before labelling. Storage, mixing and labelling were done according to the manufacturer's recommendations for minimal labelling. 1 µL of working solution dye (400 pmol) was added to each 50 µg sample and the samples incubated on ice in the dark for 30 minutes. After this time the reaction was quenched by the addition of 1 µL of 10 mM lysine and incubated for a further 10 minutes on ice to stop the reaction. An equal volume of rehydration buffer (2 M thiourea, 7 M urea, 2% CHAPS) was then added to each sample, so that each sample had the volume double that prior to mixing. The pooled standard was labelled as above, except for the use of an appropriate volume for the combined pool. Thus for a 6 gel experiment, 6 µL of Cy 2 was used. Each strip (and thus each gel) contained two 50 µg samples, each labelled with Cy3 and Cy 5 respectively, along with a pooled sample (also 50 µg per strip) labelled with Cy 2 (Appendix '[1 - 3rd DIGE \(A\) expt sample prep.xlsx](#)' and '[2 - 4th DIGE \(B\) expt sample prep.xlsx](#)').

IEF

Samples were randomly allocated to IPG strips so that there would be one Cy 3, one Cy 5 and one standard Cy 2 per strip. As rehydration loading was used, the volume added from each sample and standard was subtracted from the 450 µL required for each strip in order to calculate the volume of additional rehydration buffer required. 0.5 % carrier ampholytes (IPG buffer, pH 3-10 NL, GE Healthcare) was used for each strip *i.e.* 2.25 µL per 24 cm strip. As samples had been alkylated (with 4-vinylpyridine) during sample preparation, reducing agents were not added to the rehydration buffer. 24 cm pH 3-10 NL IPG strips were used and rehydrated with 450 µL of rehydration buffer that included the mixed sample. Care was taken so that the rehydration buffer was evenly distributed along the bottom of the rehydration tray, and there was a complete absence of air bubbles. After a few minutes of rehydration the strip was carefully moved to and fro along the tray to ensure an even distribution of rehydration fluid underneath the length of the strip. Care was also taken to ensure the rehydration tray was level on the lab bench. Rehydration was done in either a

disposable rehydration tray (and not covered with oil) and within an IPG box (GE Healthcare) or in a 24 cm Immobiline Drystrip reswelling tray and covered with Drystrip cover fluid (GE Healthcare) for overnight rehydration, in the dark at room temperature.

Rehydrated IPG strips were transferred to an Ettan IPGphor II manifold for face up IEF at 20°C. For all DIGE experiments except DIGE experiment B, 150 µL of Milli-Q water was evenly applied to the electrode wicks. For DIGE experiment B 150 µL of Milli-Q water containing 2% carrier ampholytes (IPG buffer, 3-10 NL) was evenly applied to the wicks. Wicks were positioned over the strips as shown in Figure 3-1, with a large portion of the wicks overhanging the ends of the strips, and the electrode wire on the inner end. The IEF focusing program used for DIGE experiments A and B is shown in Table 3-1. The IPGPhor II was covered to protect strips from light and after focusing was complete the strips were stored at in the dark -70°C until required for 2nd dimension separation.

Focusing protocol used for DIGE A	Long gradient protocol used for DIGE B
75 µA maximum current per strip:	20 µA maximum current per strip:
Step at 200 V - 3 hours	Gradient to 100 V - 1 hour
Step at 500 V - 3 hours	Gradient to 200 V - 6 hours
Gradient to 1,000 V - 2 hours	Gradient to 500 V - 6 hours
Gradient to 10,000 V - 4 hours	Gradient to 1,000 V - 4 hours
Step at 10,000 V - 8 hours	Gradient to 2,000 V - 3 hours
(105.6 kWh or 20 hours)	Gradient to 4,000 V - 2 hours
	Gradient to 10,000 V - 3 hours
	Step at 10,000 V - 3 hours
	(67.55 kWh or 28 hours)

Table 3-1. Voltage profiles used for isoelectric focusing in two DIGE experiments.

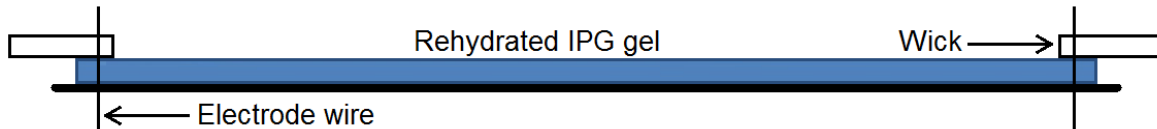


Figure 3-1. Diagram showing the relative positions of the IPG strip, wicks and electrode wires.

Second dimension

For the second dimension, large format 10%, 1mm thick, acrylamide gels were cast in an Ettan DALTsix gel caster, using low fluorescent glass plates. As discussed in Chapter 2, it was found to be necessary to provide positive pressure to the bottom of the gel caster in order for gels to have a smooth upper surface. This was done by connecting a tube to the bottom of the gel caster to a flask containing displacing solution (375 mM Tris-HCl pH 8.8, 30% glycerol, a trace of bromophenol blue) so that the level of the solution in the flask was just below the level required for the top surface of the gels. Otherwise casting was carried out according to the manufacturer's protocol for casting 1 mm gels [251]. Water saturated butanol was used to overlay the gels after they were poured. Gels were stored in gel storage solution (375 mM Tris-HCl pH 8.8, 0.1% SDS) at 4°C for several days until convenient for running the second dimension.

The focused IPG strips were thawed and equilibrated for 30 minutes in the recommended SDS equilibration buffer [246], except that neither reducing or alkylating reagents were included as the samples had been reduced and alkylated prior to IEF, thus there was no buffer change during equilibration. After removal from the gel storage buffer, the IPG strip slot was rinsed with tank buffer prior to insertion of the strip. After equilibration in SDS buffer, the IPG strips were carefully inserted into the space at the top of gels. Surplus tank buffer was poured off, with care being taken to prevent any air bubbles forming between the strip and gel. 1 mL per gel of molten agarose containing 0.002% bromophenol blue was pipetted over each strip to form a seal between the strip and the top of the glass plates and to provide a dye front so that electrophoresis could be followed.

An Ettan DALTsix electrophoresis unit (with an improved upper buffer tank) connected to a Bio-Rad 4860 refrigerated recirculator set to 20°C was used for the second dimension run. Power was supplied by a Bio-Rad 3000Xi computer controlled electrophoresis power supply, and programmed to run overnight according to manufacturer's recommendations. The upper buffer tank temperature was monitored (with an immersion thermometer) which showed that the temperature never reached 30°C at any point during the run. The next day, the run was extended until the dye

fronts were close to the bottom of the gels. Gels (still within glass plates) were rinsed and placed either on ice or in a chiller until they could be scanned later in the day.

Image acquisition, spot detection, editing and matching

Gel plates were dried and the gels while still within the glass plates were scanned with a Typhoon FLA 9000 scanner (GE Healthcare) according to the manufacturer's recommendations. A 473 nm (blue) laser and BPB1/530DF30 emission filter were used to obtain Cy 2 images, a 532 nm (green) laser and BPG1/570DF20 emission filter were used to obtain Cy 3 images, and a 635 nm (red) laser and LPR/R665 emission filter was used to obtain Cy 5 images. Pre-scanning was of each channel was carried out in order to set the photomultiplier tube (PMT) voltage so that there was close to, but no saturation of any protein spots. For the main scans, the resolution was set to 100 μ M. Gel images were cropped using the DeCyder Image Loader to remove extraneous material and then loaded into the Differential In-gel Analysis (DIA) module of the DeCyder 7.0 software (GE Healthcare). The DeCyder spot detection algorithm 6.0 was used to detect spots.

A value of 2,500 estimated spots was chosen as using the recommended 10,000 expected spots value resulted in a large number of very small spots being detected as well as many spots that were clearly single were being subdivided. The recommended 30,000 exclude filter was used to remove very low abundance spots and small dust particles.

The DeCyder Biological Variation Analysis (BVA) software was used for spot matching, spot editing and initial univariate analysis. Gel images were assigned to the appropriate experimental groups (standard, bearing or control) and gels were matched. A representative gel was chosen to be the master gel, the gel to which all other gels are matched and on which spot matching and numbering is based. As manual matching found some incorrectly matched spots, further inspection was carried out. Adding landmarked spots did not help as the problem was not due to differences in spot location but rather to differences in the spot detection between gels. An example of a spot that was split in some gels is shown in Figure 3-2. The spot highlighted in red was split in 5 out of 8 gels. Split spots were manually combined to make spots appear similar.

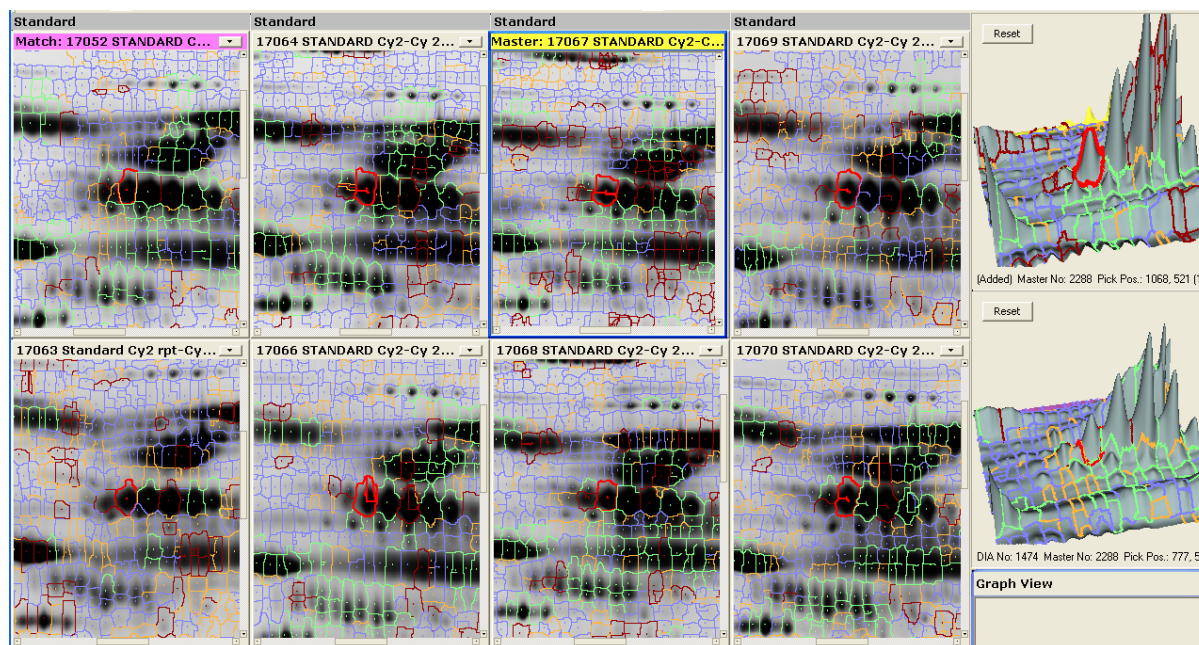


Figure 3-2. Inconsistent spot boundaries identified in DeCyder 7.0.

The image shows a zoomed in section of standard gel images plus 2 3D views in match mode of DeCyder 7.0 BVA software. The spot highlighted in red is one which was split in 5 out of 8 gels. Lines extending into the center of these spots indicate split spots that required merging (in gels 17064, 17067 (the master), 17069, 17066 and 17070).

Spot matching was verified as follows. Spots were examined in the 3D viewer and had to have a visibly discernible bump over surrounding pixel intensity to be regarded as a true spot. Note that for some spots, the 3D view was “zoomed in” to detect faint spots. This was especially required when faint spots were close to highly abundant spots, as when highly abundant spots are within the 3D viewer field of view, the scale is automatically reduced. If spots could be detected and matched in more than half of the gels, they were marked to be included in the analysis.

Unfortunately the software outlined and matched a great many spots that appeared to be not real protein spots despite the filtering process, as shown in Figure 3-3. There were also spots that had to be split to be correctly matched. All spots in all gels were manually examined to determine which spots were real and which were not. Examples of spot inclusion and exclusion are shown in Figure 3-4 and Figure 3-5. This manual spot checking process resulted in only 208 spots being included for analysis out of 2184 spots being accepted by DeCyder 7.0 for DIGE experiment A and 428 out of the 2384 spots for DIGE experiment B. Figure 3-6 shows the 428 visibly discernible matched spots found

in DIGE experiment B. Figure 3-7 shows the 208 visibly discernible matched spot found in DIGE experiment A.



Figure 3-3. Example of spot rejection.

A spot that was judged not to be a real spot is highlighted in red. Note there was also incorrect matching of the position of this spot in the highlighted gel (pink banner, gel.17063).

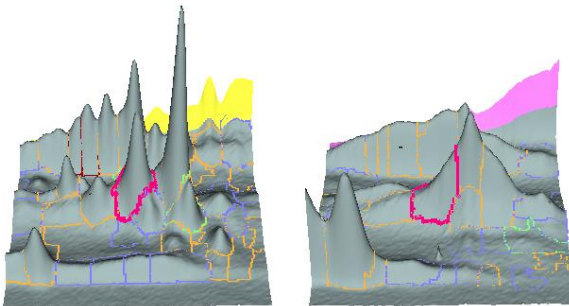


Figure 3-4. Further example of spot rejection.

The spot outlined in pink in the left image (the master) was included whereas the spot on the right was not because it could not be confidently matched to the master. If less than half of the spots could be matched to the master then none of the matched spots were included.

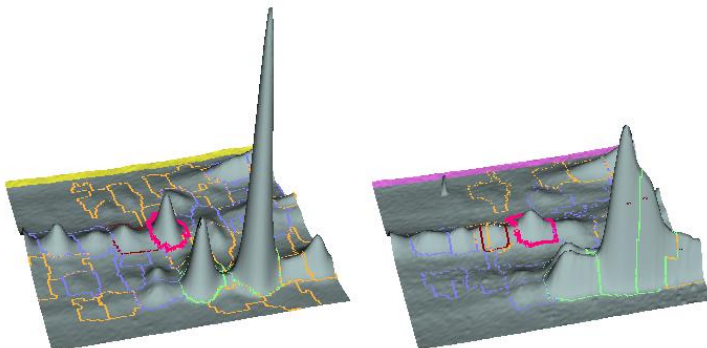


Figure 3-5. Example of spot inclusion.

The spots outlined in pink were visibly discernible spots and they could be matched, and were included.

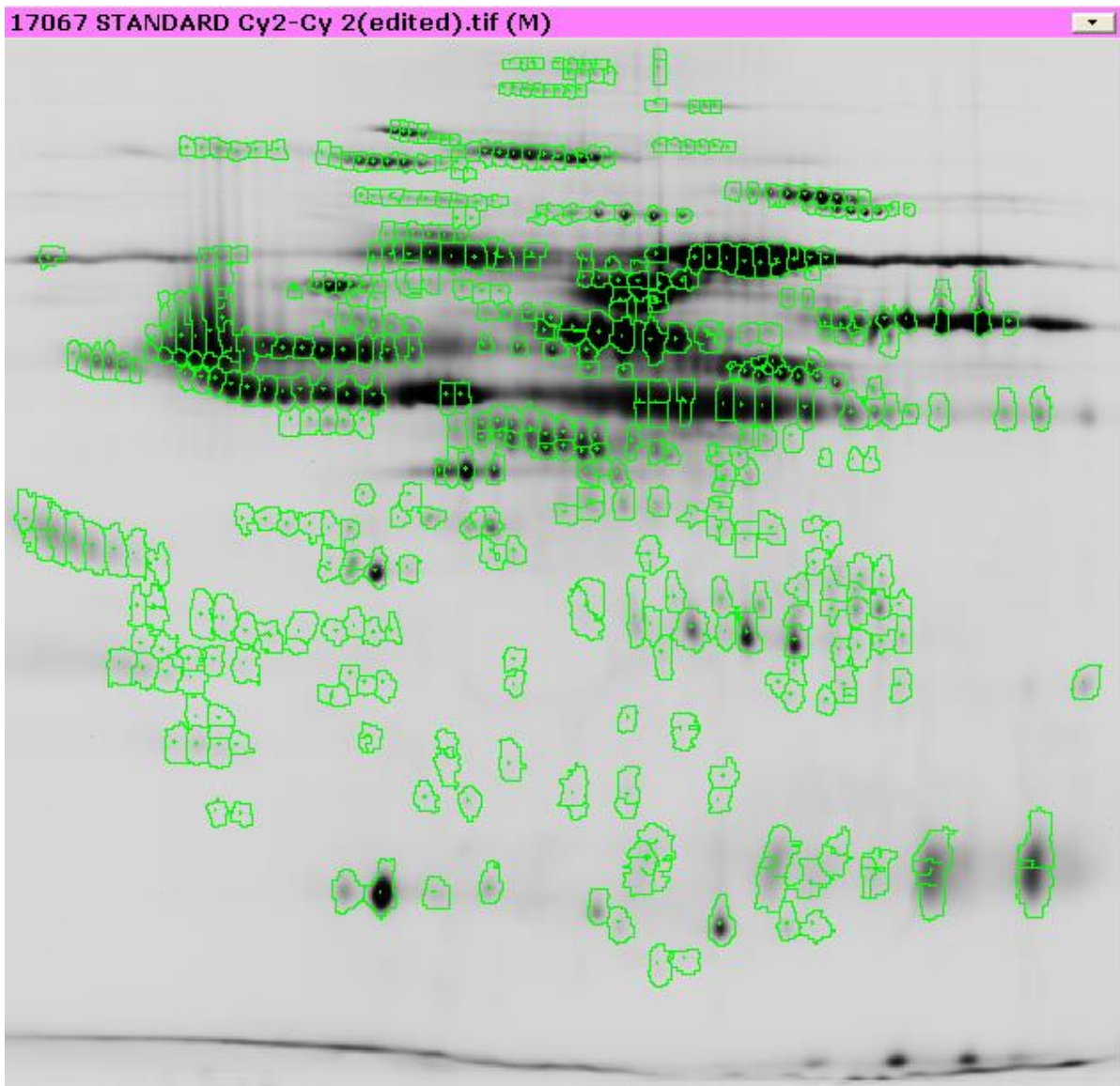


Figure 3-6. 428 matched spots representing visibly discernible spots were found in DIGE B.
The master gel standards image is shown, spots are outlined.

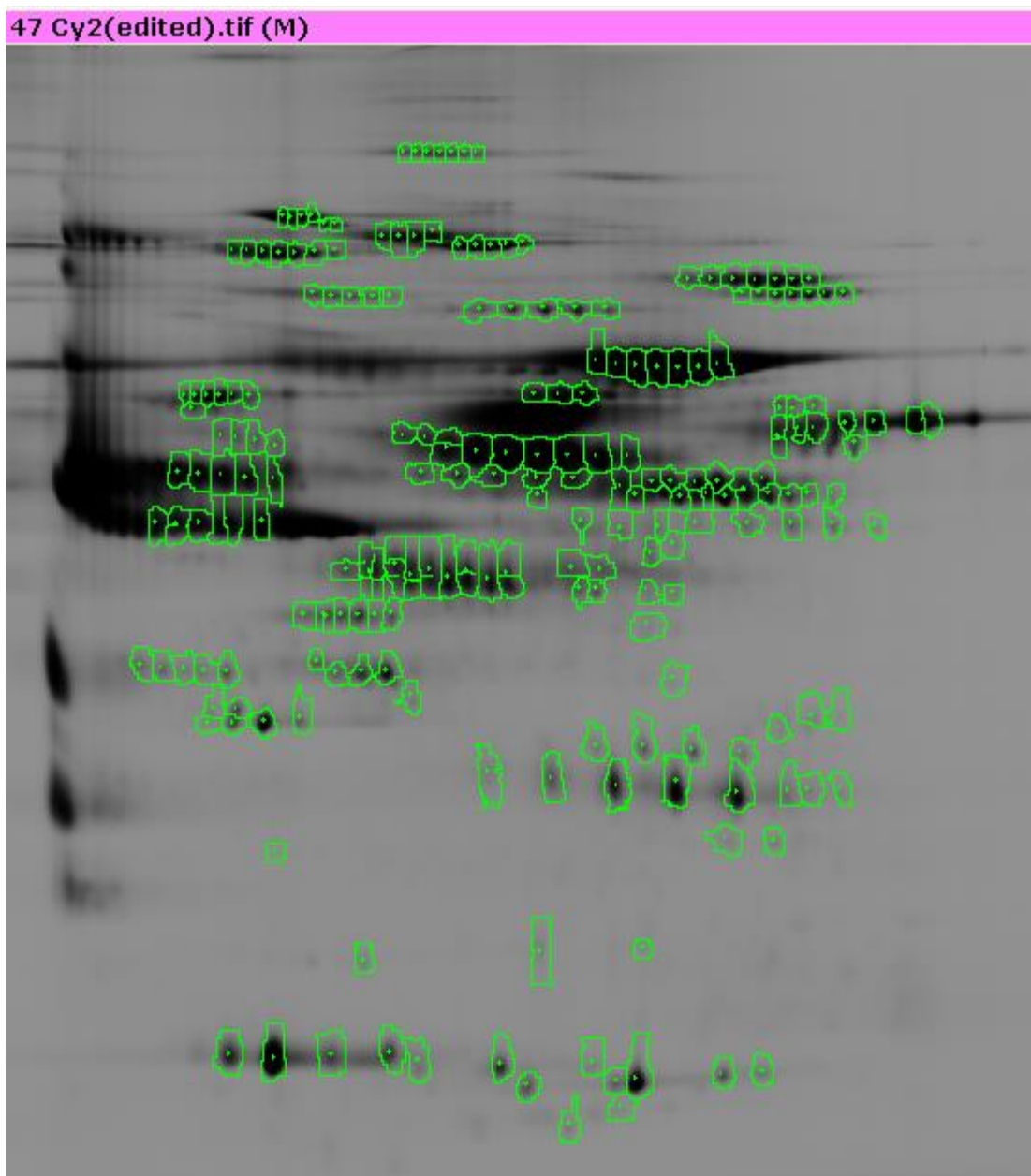


Figure 3-7. 208 matched spots representing visibly discernible spots were found in DIGE A.
The master gel standards image is shown, spots are outlined.

In order to evaluate the qualitative differences between the two DIGE experiments reported here an analysis of the data variation between gels was undertaken. Standard data was used to assess variation as the same standards are used on each gel within an experiment. Standard data is not normalised within DeCyder as the standardisation process accommodates differences in the values of standard data between gels. In the present study, comparison between the standards was required and so normalisation was necessary.

Data comparison – DIGE A and DIGE B

Extracting standard data

Standard data was extracted from DeCyder 7.0 by cutting and pasting. Using the BVA module in appearance mode, spots were selected one at a time and data tables copied and pasted into an Excel spreadsheet. The cutting and pasting was done individually for each spot of interest on the master gels for both DIGE experiments. Within Excel the master numbers were retained along with standard volume data. Care was taken to ensure spots with missing values were attributed to the correct gel. Missing values were left empty and no attempt to impute or replace missing values was made. Any calculations that produced a '0' value or a '#DIV/0!' result, due to missing values, were blanked so that missing values did not skew the calculations.

Extracting experimental data

Protein spots that were deemed to be real spots (by manual examination, see above) were marked as "proteins of interest" (POI's) and the associated data was exported as a text file from the BVA module of DeCyder. The resultant text file was imported into Excel. Volume data was used for renormalisation.

Normalisation

Normalisation is a process used to accommodate whole gel differences between images. These differences might be due to variation in labelling efficiency, imperfections in PMT voltage optimisation or loading differences. Normalisation can be thought of as fine tuning of the total protein load to ensure it is the same on each gel. It should be noted that if there was only one spot per gel, the effect of normalisation would be to reduce variation to zero. The more spots there are, the less the variation between the matched spots in different gels is reduced by normalisation. The minimum number of spots recommended for normalisation is 100 [252].

In DeCyder, normalisation is done in the DIA module (prior to matching in the BVA module) and is used to produce normalised abundances of sample spots (but not standards) within each gel. To do this, the assumption that most spots will not differ in abundance is made. Normalisation of standards between gels is not necessary for DeCyder analysis, as differences between gels is accommodated by standardisation. For the method analysis it was necessary to normalise standards

between gels as it was only by comparing the variation of standards between gels that the 2D methods could be quantitatively assessed.

Note that a variety of different normalisation methods were used in order to evaluate the main result and these are reported in Chapter 5. In order to evaluate the new IEF method and compare it to the previously used method, a simple linear normalisation approach was chosen that used data from spots that were present on all gels. For this analysis the average volume of spots present on all gels was calculated for each gel, and a scale factor calculated. All the spots on each gel were then scaled so that the average volume of spots on each gel was the same (Appendix, '[3 - DIGE A 208 standards, with 2 normalisation methods.xlsx](#)' and '[4 - DIGE B 428 standards, with 2 normalisation methods.xlsx](#)').

Unfortunately, only 50 spots could be matched on all gels in DIGE experiment A (304 spots were matched on all gels in DIGE experiment B). As this analysis of methodology used the standard data, which is all based on the same sample *i.e.* with no inherent biological variation, this method of normalisation was assumed to be valid for the analysis of the 2D method.

Although individual sample data (such as control and experimental data) is normalised in DeCyder, it was normalised again, as described in chapter 4 and chapter 5 because a variety of different normalisation methods were able to be used. Furthermore, the DeCyder manual recommends the re-normalisation of data if a large number of spots are removed, presumably because the inclusion of poorly resolved proteins could skew the normalisation. Many of the spots that were detected by the DeCyder DIA, but that didn't appear to represent real or well resolved proteins, were not included in this analysis and so re-normalisation was carried out.

As the main analysis (see chapter 5 for details) involved samples with natural variation, it was decided to adopt a normalisation process that would use all protein spots, *i.e.* more than 100 spots per gel as recommended. Note that the gel with the least number of spots still had more than 100 spots (a gel in DIGE A had only 106 spots) but only 50 spots could be matched across all the gels in that experiment. This method of normalisation (using all spots) involved calculating the abundance of each spot relative to the average for that spot for each experiment, and then calculating a grand average relative spot abundance for each gel. The grand average was then used as an adjusting

factor. For instance, if a gel had a grand average spot abundance of 1.1, then each spot was divided by 1.1 to make each gels grand average 1. Note that this normalisation method (using all spots) weights the importance of all spots equally, so that weak spots have the same effect on the grand average as highly abundant spots. With the normalisation method that only uses spots that are present on all gels, highly abundant spots have a larger effect, in a similar way to a loading adjustment where highly abundant proteins have a large effect on protein quantity. Note that both normalisation methods used here to compare 2D methods use a linear adjustment *i.e.* all spot volumes on the same image are adjusted by the same numerical factor.

Evaluating the 2D PAGE methods

The two normalisation methods were used to normalise standard protein spots and then coefficients of variation (CVs) were calculated. CVs for the 174 spots that could be matched between DIGE experiments A and B were calculated as well as the CVs for all spots also using data normalised with both methods.

When the two normalisation methods were used on standard spots that were matched between both DIGE experiments (A and B) and compared the results were very similar, *i.e.* the difference in Coefficient of Variation (CV) of standard spots matched between the experiments remained statistically significant at the 0.001 level. The *p* value was calculated to be 0.0007 (in a paired two tailed student's t-test comparing the 174 spot volumes that were matched between the DIGE experiments) when normalisation was done only with spots that were present on all gels, and 0.0008 when normalisation was done with all spots (Appendix, '[5 - Matched DIGE A & B, with 2 normalisation methods.xlsx](#)'). When CVs were compared using all spots, although the CV was slightly lower using the new method (in DIGE B) it was not statistically significant.

Finally, to put the technical variation in context, the biological variation of the control sample was investigated. This showed that the variation of the smaller data set (six samples with 208 master gel spots *c.f.* eight samples with 428 master gel spots) was less, *i.e.*, 0.32 *c.f.* 0.38 (volume CVs for experiments A and B, respectively). Removing standardisation increased the CVs substantially in both experiments (from 0.32 to 0.41 for experiment A and from 0.38 to 0.46 for experiment B). See Table 3-2 for a summary of results, (Appendix folder '[6 - method analysis data](#)').

DIGE experiment	A	B
Number of gels	6	8
Number of quantifiable spots on master gel	208	428
Number of quantifiable spots matched on all gels	50 (123 on 5/6 gels)	303 (411 on 7/8 gels)
Average number of spots matched to master	163	410 (p<0.001)
Spots not found on other master (174 spots matched)	34	254
Average CV of standard volumes	0.25	0.24
Average CV of log of standard volumes	0.019	0.019
Average CV of matched spots, volumes (174 spots)	0.24	0.20 (p<0.001)
Average CV of matched spots, log of volume (174 spots)	0.018	0.015 (p<0.01)
Correlation of CVs with average log volumes	-0.33	-0.45
Average CV of standardised control sample spots , vol (Not Std)	0.32 (0.41)	0.38 (0.46)
Average CV of standardised control sample spots, log (Not Std)	0.024 (0.032)	0.028 (0.035)

Table 3-2. Summary table comparing spot resolution in DIGE A and DIGE B.

Normalisation was done using spots present on all gels (Appendix folder '[6 - Method analysis data](#)').

Correlations were done between the average matched spot volumes in both DIGE experiments using both normalisation methods. It was found that the correlation between the two experiments was very similar when normalisation with all spots was used than if normalisation was done only with spots present on all gels (0.9735 as compared to 0.9728). (see cell DK179 in sheet 'Norm. by spots on all gels' and cell BI179 in sheet 'Norm. by all spots' in Appendix '[5 - Matched DIGE A & B, with 2 normalisation methods.xlsx](#)'). Note that a few spots in DIGE experiment B were combined to enable matching to DIGE experiment A.

Scatter plots were created to investigate the relationship between CV and spot volume (Figure 3-8). These showed a negative correlation between CV and the log of spot volume for both experiments, with experiment B having a slightly stronger relationship than experiment A (-0.33 cf. -0.45 for experiments A and B, respectively). Both correlations were statistically significant ($p < 0.001$).

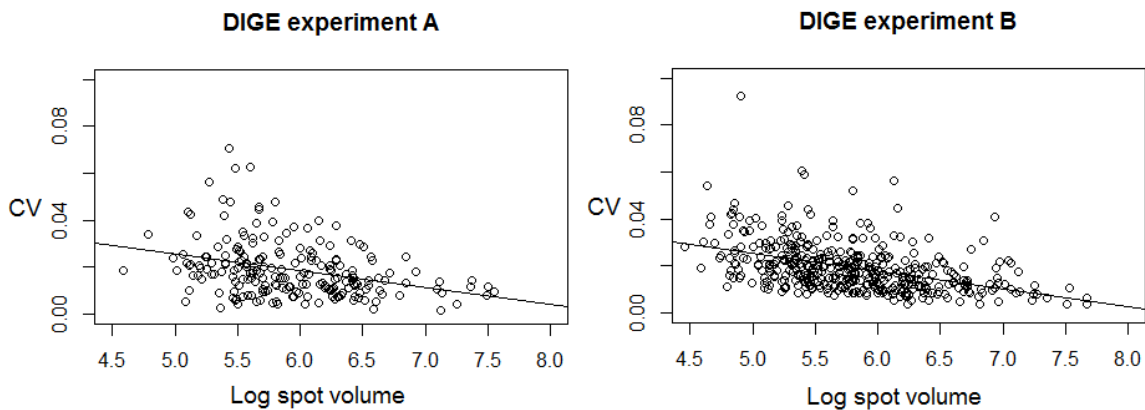


Figure 3-8. Correlation of spot variation (CV) with spot volume of the internal standards.

Data for the two DIGE experiments analysed are shown as scatter plots along with fitted lines.

Finally, to put the technical variation in context, the biological variation of control sample was investigated. This showed that the variation of the smaller data set (six samples with 208 master gel spots cf. eight samples with 428 master gel spots) was less, *i.e.*, 0.32 c.f. 0.38 (volume CVs for experiments A and B, respectively). Removing standardisation increased the CVs substantially in both experiments (from 0.32 to 0.41 for experiment A and from 0.38 to 0.46 for experiment B). See also the results in chapter 5 where same samples spots are correlated between the two DIGE experiments analysed.

Note that a haptoglobin validation experiment is described in Chapter 5 which showed there was a high degree of correlation ($r^2 = 0.87$) between combined haptoglobin spot volumes and a haptoglobin activity assay. The correlation was higher when values were log (base 2) transformed ($r^2 = 0.91$), see Figure 5-43.

Chapter 4. Data analysis

As the aim of this project was to identify plasma proteins that were differentially regulated prior to prolapse occurring (*i.e.* in apparently healthy sheep) a sensitive method of analysis that retained biomarker information was required. In order to do this, accuracy in terms of data analysis was necessary, and so an evaluation of normalisation methods was undertaken. Two methods for evaluating normalisation methods were employed; ratio-intensity plots and variance ratio analysis. These are explained below. Note that the aim of normalisation is to reduce unwanted noise or variation from the data so that true signals can be more clearly observed. This principle was based on the assumption that good quality normalisation would result in more reliable, higher quality data due to less background variation. A number of different normalisation methods were applied and tested. Data distribution was also examined in order to determine if transformation was necessary.

Data extraction: obtaining standard data

As outlined in chapter 3 using the DeCyder 7.0 BVA module in appearance mode, standard spots that had been deemed to represent real spots were selected one at a time, and their corresponding data tables copied and pasted into a Microsoft Excel spreadsheet. Within Excel the master numbers were retained along with standard volume data and care was taken to ensure spots with missing values were attributed to the correct gel. No attempt was made to impute or replace missing values. Any calculations that produced a '0', a '#NUM!' or a '#DIV/0!' result, due to missing values, were blanked so they did not skew the calculations. The only exception to this practice occurred when quantile normalisation (a non-linear normalisation method that requires no missing values) was carried out (as well as for variance stabilising normalisation (VSN), done with the R package 'vsn' for comparison) because the quantile method requires that there are no missing values. In this case, any missing values were replaced with the average value across both groups. Note that although the calculations done to compare VSN normalisation with quantile normalisation were made with missing values replaced, the VSN calculations done to determine proteins of interest were made without replacing missing values.

Normalisation of the volume data was carried out as described above. The Microsoft Excel statistical function 'stdeva' (which returns the standard deviation based on the data being a sample) was used to calculate standard deviation (SD). SD was divided by the mean to give CV.

Data extraction: obtaining control and bearing ewe data

Within DeCyder, control and bearing ewe data were extracted by marking the spots that had been noted as representing real spots (see the chapter 3) as proteins of interest. Quantitative data from these proteins of interest spots were exported from DeCyder into a text file which was then imported into Microsoft Excel and any extraneous data removed (such as unnecessary column headings). Again missing values were left blank so as not to skew calculations. The data were normalised as described below then subjected to a student's t-test analysis. Ratios were calculated in the same manner as DeCyder *i.e.* if the average volume of the bearing sample spots were increased (above controls), the ratio was reported as a positive number (> 1) and if the average volume of the bearing sample spots was decreased, a negative number was reported (< -1). Note also that ratios were calculated with (re-normalised) volume data rather than log volume data, as is done in DeCyder. (Appendix '[7 - DIGE A, with 2 normalisation methods.xlsx](#)' and '[8 - DIGE B, with 2 normalisation methods.xlsx](#)').

Normalisation

Normalisation can be thought of as the removal of non-biological sources of variation in experimental data. There are two basic types of normalisation processes, linear and non-linear normalisation. Linear normalisation is simply a factor adjustment used to accommodate whole gel differences between images. These differences might be due to imperfections in PMT voltage optimisation or loading differences. Linear normalisation can be thought of as fine tuning of the total protein load to ensure the load is the same on each gel so that any observed changes are not a result of different protein loads. Non-linear normalisation is more sophisticated, and reflects inconsistent technical errors, such as those that can arise from sample preparation or labelling conditions. Examples are differences in temperature or pH which can affect dye labelling efficiency. A number of non-linear normalisation methods have been developed particularly for high density oligonucleotide array data. Some of these originally developed for gene expression arrays, have also been co-opted for use with 2D gel data. Examples are quantile normalisation or variance stabilising normalisation both of which are described below. Regarding the effect of normalisation on biological variation it should be noted that if there was only one data point per sample, the effect of normalisation would be to reduce the variation to zero. The more data points there are, the less

variation is reduced by normalisation, and 100 spots is regarded as the minimum number for 2D gel normalisation [252].

In DeCyder, normalisation is done in the DIA module (prior to matching in the BVA module) and is used to produce normalised abundances of sample spots (but not standards) within each gel. To do this the assumption is made that most spots will not differ in abundance. Normalisation between gels is not necessary for DeCyder analysis, as differences between gels is accommodated by standardisation. For method analysis, however, it was necessary to normalise standards between gels as it was only by comparing the variation between gels that the 2D methods could be quantitatively assessed. For this analysis the average volume of spots that were present on all gels was calculated for each gel, and scaling factors were calculated and applied so that the average spot volume (for spots present on all gels) on each gel became the same. The adjustment factors ranged from 0.71 to 1.30 for DIGE experiment A and from 0.87 to 1.23 for DIGE experiment B. (Appendix '[7 - DIGE A, with 2 normalisation methods.xlsx](#)' and '[8 - DIGE B, with 2 normalisation methods.xlsx](#)').

Unfortunately only 50 spots could be matched on all gels in DIGE experiment A, in contrast to DIGE experiment B where 304 spots were matched on all gels. However, as the method analysis used the standard data, which is all based on the same sample *i.e.* with no biological variation, it is valid to use this method of normalisation for the method analysis [253]. Note that although sample data (such as control and experimental data) is normalised in DeCyder, these data were normalised again for the present study. This was partly because a different method of normalisation was required for the method analysis, and because a large number of spots were removed. Many of the spots identified by the DeCyder DIA that didn't appear to represent real or well resolved proteins, were not included in this analysis necessitating re-normalisation.

As analysis of the experimental data involved the analysis of samples with natural variation, a normalisation process that used all the protein spots, (*i.e.* more than 100 spots per gel) was adopted. As mentioned earlier this process was relevant for DIGE experiment A, as only 50 spots could be matched on all gels. This new method of normalisation involved calculating the abundance of each individual spot relative to the average for matched spots in each experiment, and then calculating a grand average spot abundance for each gel. The grand average was used as an adjusting factor. For example, if a gel had a grand average spot abundance of 1.1, then each spot was divided by 1.1

to make each gels grand average 1. When data from all spots were used, the adjustment factors ranged from 0.81 to 1.23 for DIGE experiment A and from 0.87 to 1.23 for DIGE experiment B. (Appendix, '[7 - DIGE A, with 2 normalisation methods.xlsx](#)' and '[8 - DIGE B, with 2 normalisation methods.xlsx](#)').

When the method analysis calculation was repeated using the new normalisation processes, the results were very similar, *i.e.* the improvement in Coefficient of Variation (CV) of spots matched between the experiments was still statistically significant at the 0.001 level. Normalisation using spots present on all gels gave a p-value of 0.0007 (in a paired two tailed student's t-test comparing the CVs of 174 spots matched between the DIGE experiments), while normalisation using all spots gave a very similar but slightly higher of 0.0008 (see cell C1180 in sheet 'Norm. by spots on all gels' and cell BE180 in sheet 'Norm. by all spots' in Appendix '[5- Matched DIGE A & B, with 2 normalisation methods.xlsx](#)'). Note that a few spots in DIGE experiment B were combined to enable matching to single spots in DIGE experiment A.

A number of non-linear normalisation methods have been co-opted from transcriptomic normalisation processes [254], and although most have not been empirically tested for variance, variance stabilising normalisation (VSN) and quantile normalisation have been shown to be effective for at least some 2D gel data [255]. Both methods involve adjusting individual data intensities in order to overcome technical variation with the aim of revealing biological data distribution. With any normalisation process there is a danger that important data may be lost, or artefacts accidentally introduced. The ratio-intensity plot described by Menuier [256] has been used in the assessment of normalisation methods by Artigaud *et al.* who found that quantile normalisation was slightly better at recentering data than VSN [255].

Another issue in data variation is that it is sometimes observed that variation increases with the level of protein expression [257], and so a variance vs intensity plot is sometimes used to assess normalisation methodology [258]. More recently an algorithm in the R package 'quantro' has been developed to quantitatively assess the appropriateness of quantile normalisation for a particular data set [259]. Quantile normalisation requires missing values to be imputed (see below for details) which is common practice in 2D gel data analysis [260] therefore to enable a fair comparison

between the two non-linear normalisation methods employed, missing values were also replaced for VSN normalisation.

Normalisation before or after standardisation

The present study uses 3 dye DIGE, which enables a standardisation step, and so the option of whether to normalise either before or after standardisation arises. Linear normalisation techniques were applied prior to standardisation as any variance is assumed to be related to loading or PMT voltage adjustment *i.e.* events closely related to electrophoresis which standardisation accommodates so it makes sense to apply standardisation after linear normalisation. Non-linear normalisation adjustment can cope with a wider variety of errors, not only those related to electrophoresis, and on this basis, it was also applied last. Both points of application of non-linear normalisation are reported below.

Evaluation of normalisation

Note firstly that the evaluation of normalisation methods described were applied primarily to DIGE B data because there was substantially more data points and so one would expect the variance to be larger. Artigaud *et al.* [255] proposed that ratio-intensity plots (known in microarray analysis as MA-plots) are useful for evaluating the effects of normalisation in 2D gels. In a ratio-intensity plot the log base 2 ($\log(2)$) of the ratio of means for each spot is plotted against the log base 10 ($\log(10)$) of the product of the means. Ratio-intensity plots were graphed for the two linear normalisation methods used, as well as the standardisation, and are shown in Figure 4-1 (Appendix, [‘8 - DIGE B, with 2 normalisation methods.xlsx’](#), ‘normalised by all spots’ tab). Note that the term intensity used for the ratio-intensity plots reflects spot volume. Spot volumes are an arbitrary unit, reflecting spot area and staining intensity, as described in the introduction.

As can be seen, for these methods at least, the ratio-intensity plots are very similar. Artigaud *et al.* suggested that the way to evaluate these plots is to observe if the cloud of intensity is off-centered (reflecting less well normalised data). However in the present study, despite the inclusion of a line of best fit, any difference in position of the cloud of intensity is difficult to evaluate.

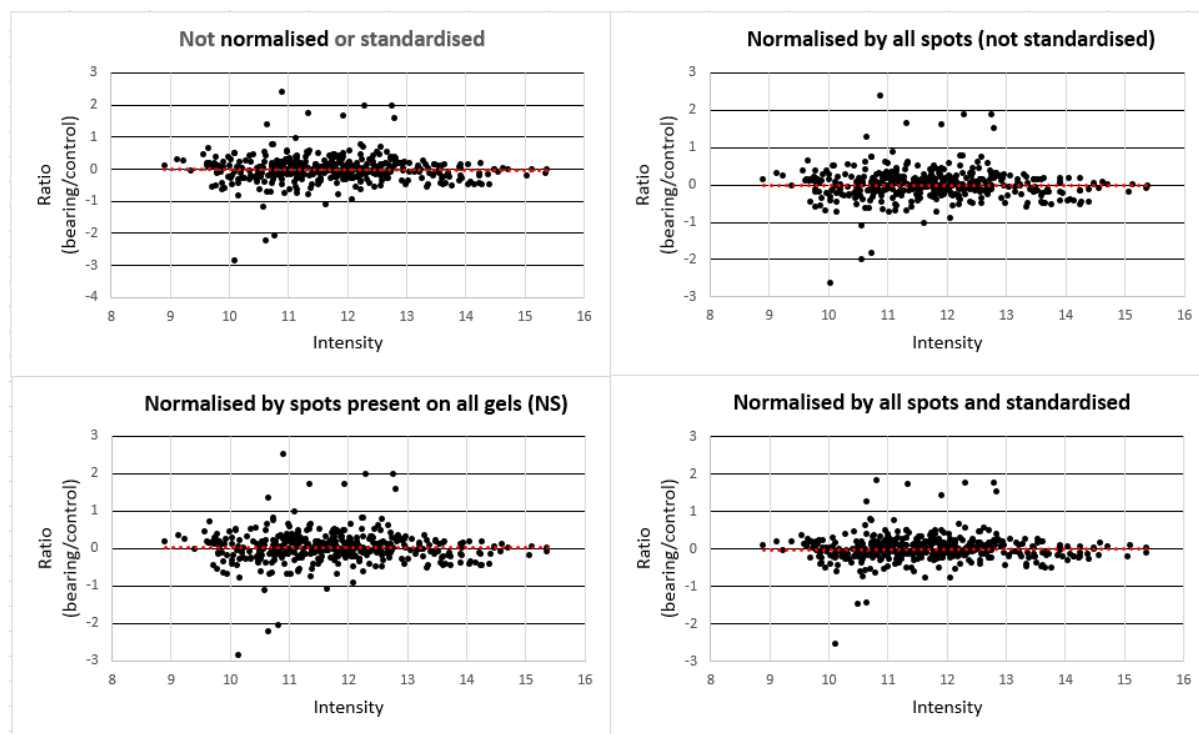


Figure 4-1. Ratio-intensity plots to evaluate linear normalisation methods.

The dotted red line is the line of best fit. Note ratios are calculated from the $\log(2)$ of average spot volume ratios (bearing/control) and intensity is calculated from the $\log(2)$ of spot volume. Note all plots for evaluating data normalisation and distribution in this chapter use DIGE experiment B data.

Microarray data analysis uses very similar statistical techniques to those used in 2D gel data analysis, especially as they both can be applied to the evaluation of protein expression. An issue in protein expression has been that variation can rise proportionally with the level of protein expression. As a result, plots of variance vs intensity began to be used to evaluate expression analysis processes [257]. Bolstad *et al.* [254] plotted variance ratios (e.g. data point X normalised by technique A/same data point normalised by technique B) against intensity to evaluate different normalisation techniques. The resultant plots were used to show whether array variation varied with data intensity, and also to examine the variation resulting from the use of the various normalisation techniques, in order to identify methods that results in the lowest data variation.

Variance ratio plots were used to assess the normalisation and standardisation methods used in this study, and are shown in Figure 4-2 (Appendix; [8 - DIGE B, with 2 normalisation methods.xlsx](#), bottom of 'Normalisation check' tab). Note that these plots differ from the ones shown in Figure 4-1. In Figure 4-1, the ratios shown are the intensity ratios between the experimental groups

(bearing/control) one plot for each of the different methods, whereas in Figure 4-2 the variance ratios are used to compare the differences in variances produced between two different methods on one plot. A negative value indicates that variance in the numerator is less than the denominator. Figure 4-2 shows that normalisation using all spots produced less variation than normalisation using only spots present on all gels. It is also clear that standardisation reduced the variation even further. There was only minor effects of spot intensity on variance.

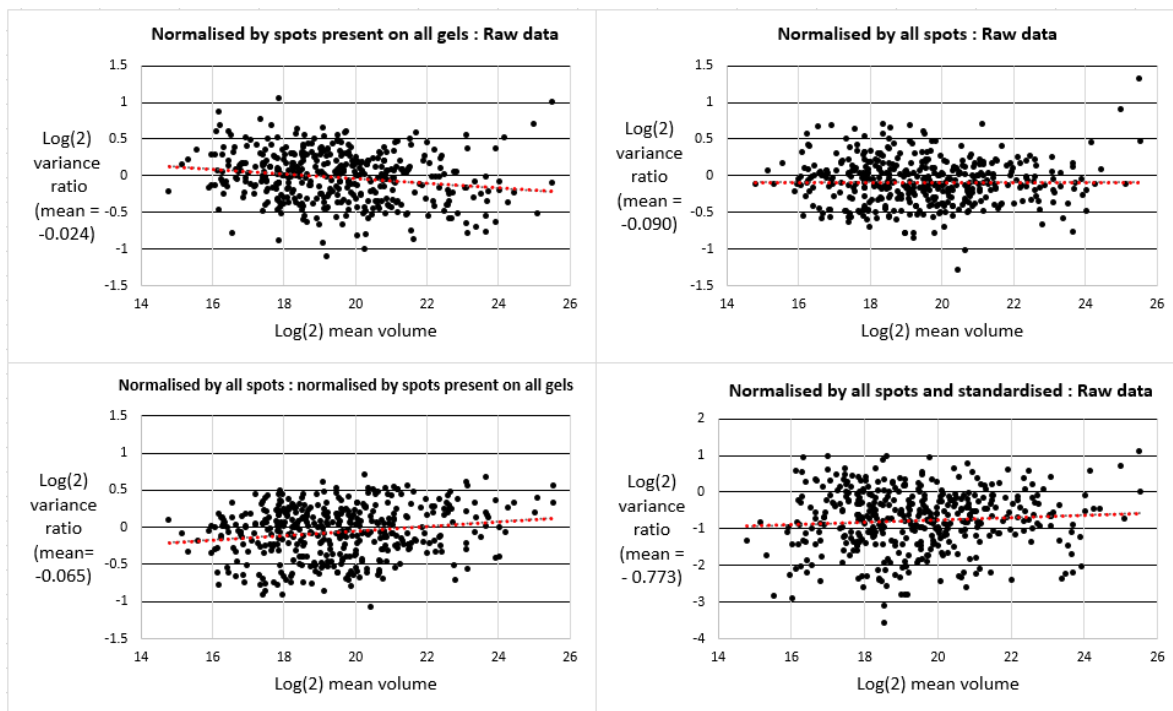


Figure 4-2. Variance ratio plots to evaluate the linear normalisation methods used.

These plots compare data variance between the two linear normalisation methods used, along with standardisation by the preferred method. The title for each graph shows the two methods being compared, in terms of numerator : denominator. A number below zero in the variance ratio reflects a lower variance in the numerator method. Mean values are shown in the Y axis title.

As standardisation had the largest effect of reducing variation (as shown in Figure 4-2 D), it was possible this was caused by cross talk between dyes on the same gel, as has been suggested by Karp *et al.* [166]. Cross talk is where the fluorescent signal from one dye influences the signal from another, *i.e.* from the same place in the gel. This can be caused by quenching failure after dye labelling [261] by or poor quality fluorescent filters within the scanner. If there was cross talk between dyes, then one would expect that the variation on the same gel would be less than variation between gels.

Cross talk was tested with a variation ratio evaluation between spots on the same gel and spots on different gels. A normalised (by all spots) and standardised data set was used to allocate 8 pairs of sets of spots that had been run on the same gel and 8 pairs of sets of spots that had not. Variation between the 8 pairs of spots was averaged and plotted on a variance ratio vs spot intensity graph, as shown in Figure 4-3 (Appendix '[9 - cross talk variance.xlsx](#)'). The mean variation within each gel was slightly less than the mean variation between gels, indicating that there may have been a small amount of cross talk between spots on the same gel. This analysis cannot distinguish cross talk between samples and between standards and samples. However, it is reassuring to note that the reduction in variation due to the use of standards was larger than the reduction in variation arising from spots within gels. Because different biological samples were used in this analysis, this result should be viewed with caution. To truly test cross talk requires the use of one sample applied both within and across gels, which was done by the developers of DIGE technology [205].

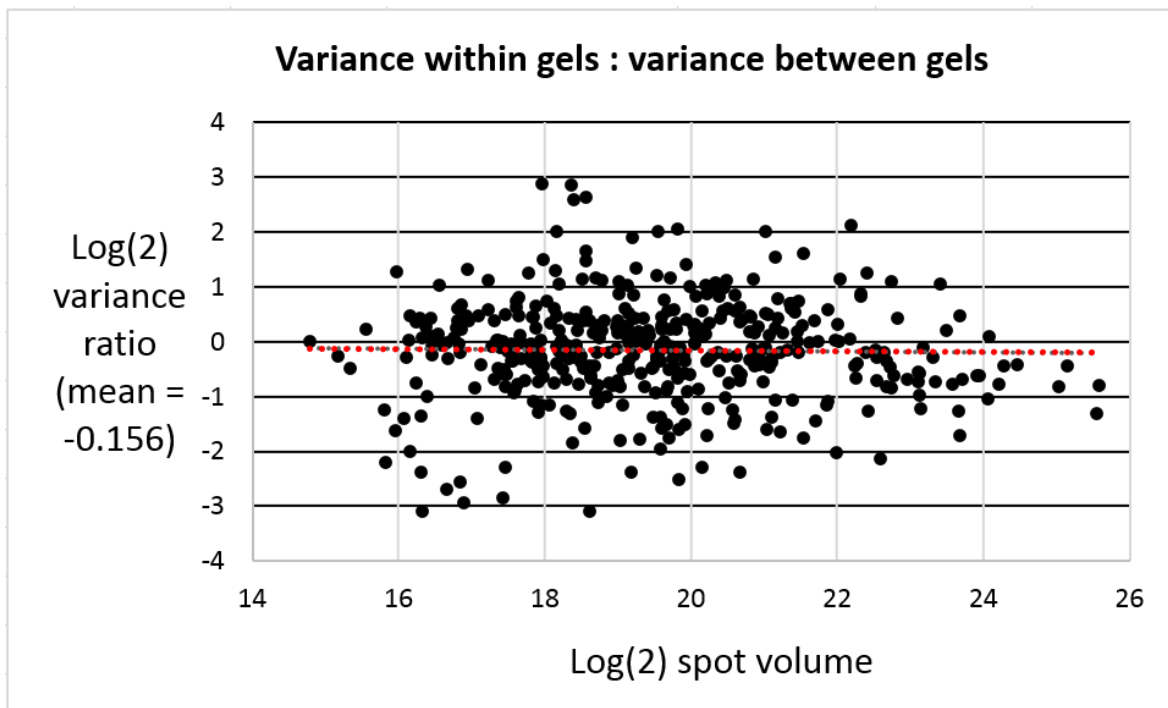


Figure 4-3. Variance between gels was compared to variance within gels.

An alternative way of looking at the effect of normalisation is to examine box plots of individual samples. Given that in the present study, only 16 samples were evaluated, it was possible to plot all samples on one graph using both linear normalisation methods. Medians were more uniform after

normalisation with all spots, and variation was further reduced with standardisation, as can be seen in Figure 4-4 (Appendix '[10 - variance – box plots.xlsx](#)').

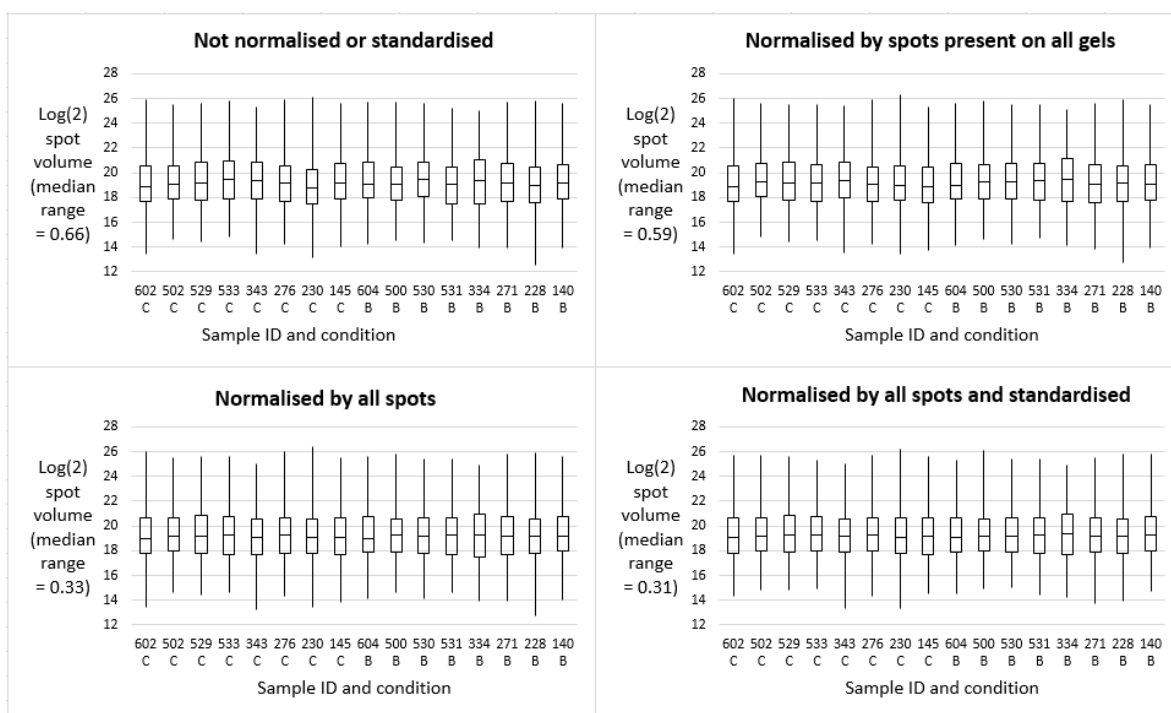


Figure 4-4. Box plots showing data variation before and after each normalisation method.

Quartile distributions are shown as boxplots with median values at the center. Sample ID and condition are shown where C = control and B = pre-prolapse sample.

Non-linear normalisation

Variance stabilising normalisation (VSN) and quantile normalisation, both non-linear normalisation methods used for normalising 2D gel data in another study [255], were trialed. As quantile normalisation is intolerant of missing values, an average for each matched spot was calculated across both groups (bearing and control) and used to fill missing values. To enable a fair comparison (between VSN and quantile normalisation) the VSN normalisation also used the same missing value filled data set (*i.e.* where missing values were filled with averages). Note that 'vsn' is an R package that returns VSN data after what is known as a glog transformation. This is essentially a log base 2 transformation (although values near 0 have a greater spread than they do with a log(2) transformation) [262]. Quantile normalisation can be done using either volume data or log transformed data, and in the present study it was done with both using Microsoft Excel.

Both methods of non-linear normalisation were used in this study, both before and after standardisation, and then evaluated in order to see the effect of using these normalisation methods on data distribution and variance ratios.

Non-linear normalisation applied after standardisation

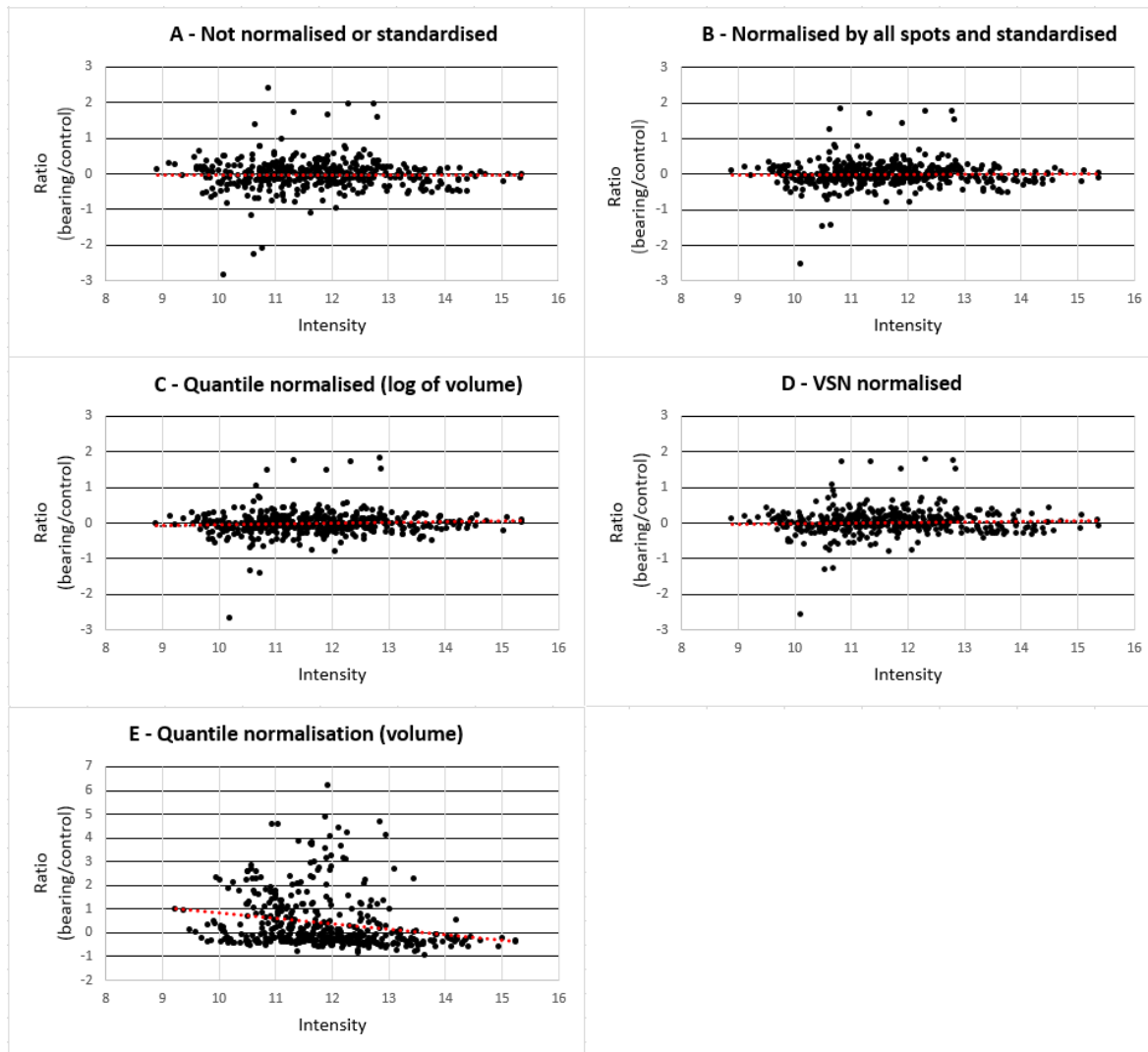


Figure 4-5. Ratio-intensity plots for the evaluation of non-linear normalisation methods.

The non-linear normalisation methods applied here were done after standardisation. The dotted red line is the line of best fit.

Ratio-intensity plots were generated for the non-linear normalisation methods, and are shown in Figure 4-5. In order to enable a fair comparison, the logged VSN and quantile normalisation data was unlogged prior to calculating the data for the graphs shown in Figure 4-5 (see the digeb_vsn tab

in Appendix '[11 - digeb_vsn.xlsx](#)') but not for the results shown in Figure 4-6 as these all contain log data (where the quantile normalised volume data was converted to a logarithmic scale prior to plotting, Appendix '[12 - digeb vols qnorm.xlsx](#)').

As was the case for linear normalisation, the ratio-intensity plots are difficult to interpret as the graphs are all very similar, except for the quantile normalisation of volume data (Figure 4-5 E), which was quite different as the cloud of points had a much greater spread.

Variance ratio vs intensity plots were generated to compare variance from the non-linear normalisation methods to that from linear normalisation (Figure 4-6) (Appendix [11 - digeb_vsn.xlsx](#) and [12 - digeb vols qnorm.xlsx](#)). The quantile normalisation was done using Microsoft Excel, but the VSN was done using the R packages 'vsr' [258] and 'rlang' [263] and the results imported into Microsoft Excel for variance analysis (Appendix '[13 - analyse_spots_script.txt](#)' for R script).

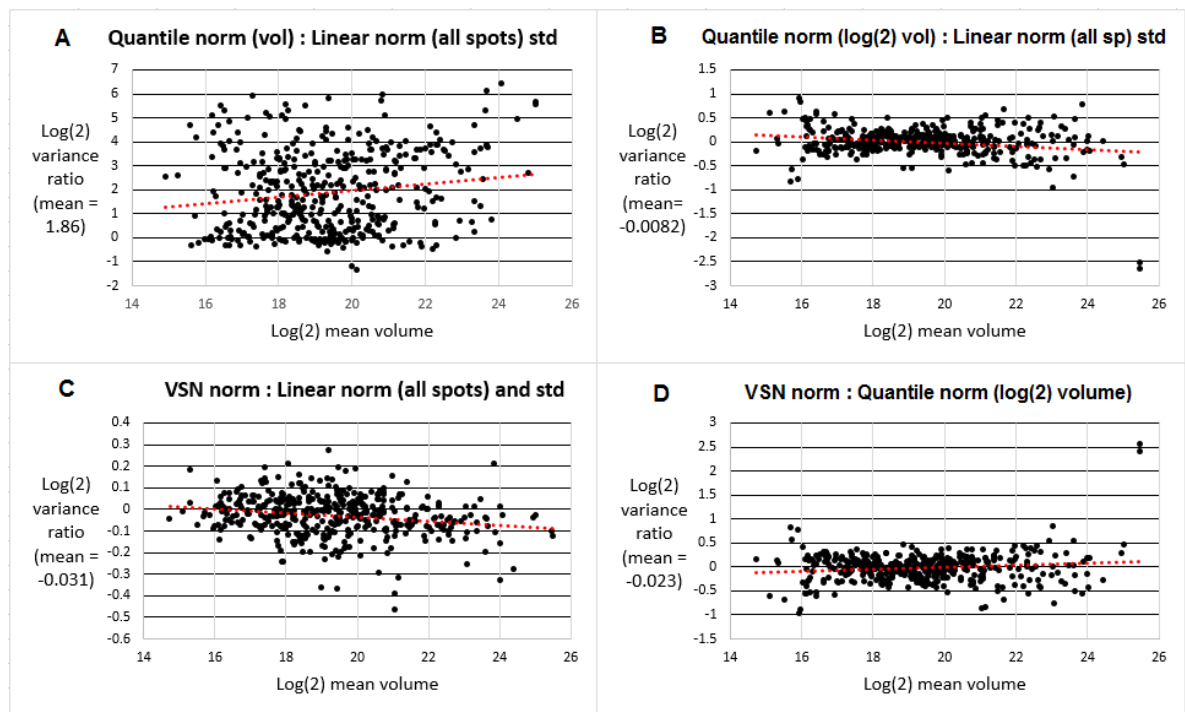


Figure 4-6. Variance ration plots for the non-linear normalisation methods.

The variance ratio plots shown compare the data variance produced using the two non-linear normalisation methods applied after standardisation. The title of each graph shows the two methods being compared, in terms of numerator : denominator. A number below zero in the mean of the variance ratio reflects lower mean variance in the numerator method than in the denominator method. Means are shown in the Y axis title.

The quantile normalisation of volume data increased the variance compared to that occurring from linear normalisation. Quantile normalisation using log(2) data reduced the variance slightly, and using VSN reduced it a little more. A comparison between the two methods also showed that using VSN reduced the variance more than using a quantile normalisation of log(2) volume data (Figure 4-6 D).

Non-linear normalisation applied before standardisation

Ratio-intensity plots generated for the two non-linear normalisation methods used, are shown in Figure 4-7 (Appendix '[14 - VSN before std.xlsx](#)', VSN before std tab and '[15 - Q norm before std.xlsx](#)', Std of Q norm tab).

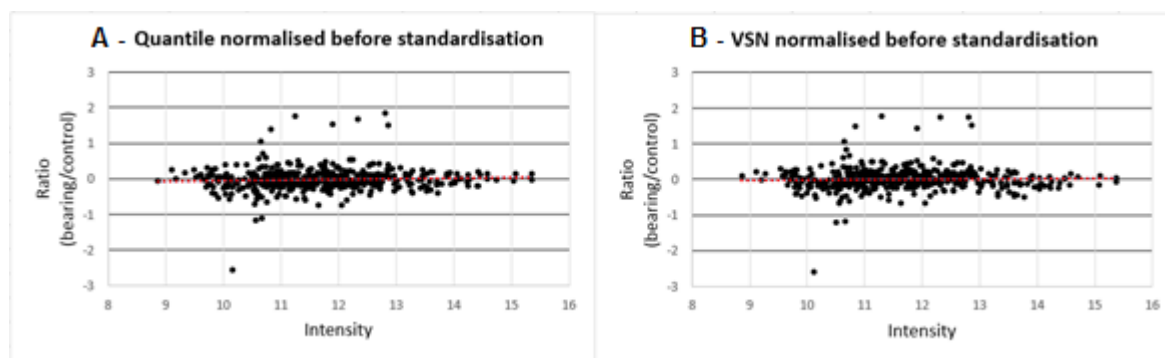


Figure 4-7. Ratio-intensity plots for non-linear normalisation applied before standardisation.

Variance ratio plots, generated to evaluate whether using the non-linear normalisation before standardisation (as opposed to after it) reduced variance, are shown in Figure 4-8 (Appendix '[14 - VSN before std.xlsx](#)', variance ratios tab and '[15 - Q norm before std.xlsx](#)' variance ratios tab).

Applying VSN normalisation prior to standardisation resulted in a small reduction in variance compared to the ratio resulting from linear normalisation (with all spots) and a slightly larger reduction when VSN was used after standardisation. This was reflected in a reduced variance ratio in the VSN after standardisation variance over the VSN before standardisation variance (-0.053, Figure 4-8 B). The VSN normalisations applied subsequently (*i.e.* in Results) were done after standardisation. Applying quantile normalisation before standardisation resulted in an increased variance ratio in comparison to linear normalisation (with all spots) as well as an increased variance

ratio in comparison to applying quantile normalisation after standardisation. Again the quantile normalisations applied subsequently (*i.e.* in Results) were done after standardisation.

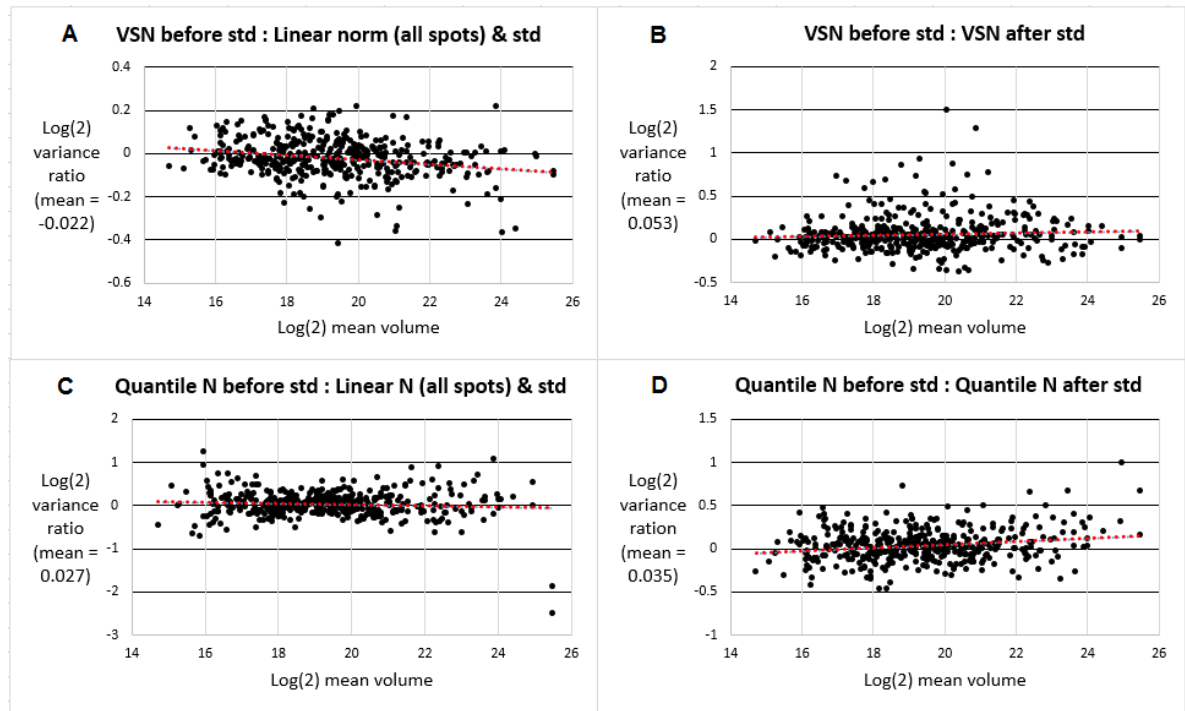


Figure 4-8. Variance ratio plots, non-linear normalisation applied before/after standardisation.

As a check on VSN normalisation, a VSN calculation was made with missing values not imputed and with the same missing values removed from quantile normalisation calculations. VSN normalisation calculated without missing values being imputed showed reduced variation when compared to both linear and quantile normalisation with missing values removed (Figure 4-9) (Appendix '[16 - VSN from norm \(all spots\) and standardised vols with blanks included.xlsx](#)'). Only small differences in mean values were observed when missing values were not imputed with VSN and were smaller than when missing values were allowed (*cf* Figure 4-6). Subsequent analysis (*i.e.* in Results) allowed the imputation of missing values with VSN.

Box plots generated for the two non-linear normalisation methods employed (after standardisation) are shown in Figure 4-10 (Appendix '[10 - variance - box plots.xlsx](#)'). While quantile normalisation reduced the average sample variation to low levels (the median is reduced to 0) the goal of the exercise is to reduce unnecessary individual spot variation which quantile variation did not achieve, as reflected in the variance ratio plots.

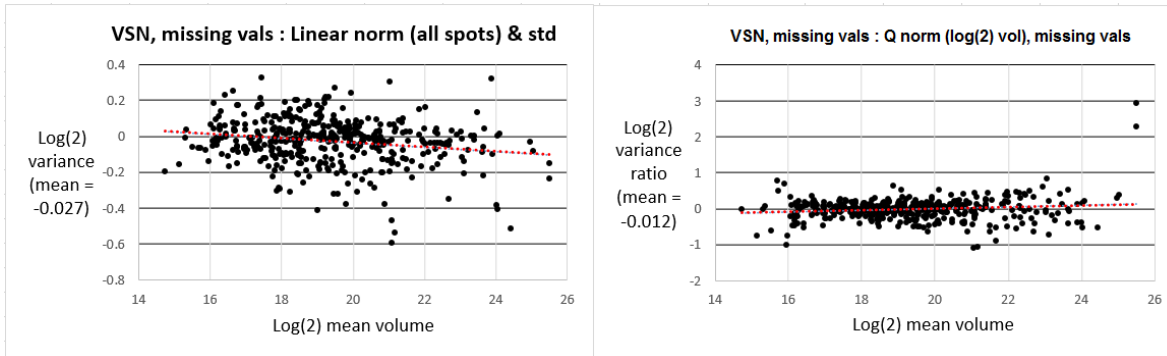


Figure 4-9. Variance ratio plots for VSN normalisation applied with missing values allowed. This was compared to linear normalisation (using all spots) and quantile normalisation with missing values removed. (Note quantile normalisation can only be done with missing values imputed).

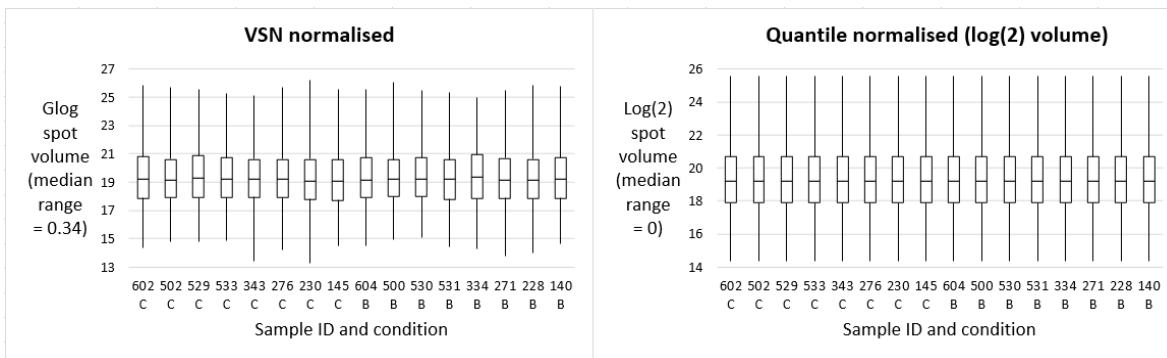


Figure 4-10. Box plots showing data distribution after two non-linear normalisation methods. Quartile distributions are shown as boxplots with median values at the center. Sample ID and condition are shown where C = control and B = pre-prolapse sample.

The only normalisation method that appeared to behave noticeably poorly was quantile normalisation by spot volume. This method had a much more unevenly distributed cloud of spots in the ratio-intensity plot (Figure 4-5 E) and substantially increased data variance (Figure 4-6 A) and so was not used further. This principle was based on the assumption that normalisation should reduce variance, resulting in more reliable, higher quality data. The other methods were deemed to be acceptable normalisation methods that could be used for data analysis. While VSN normalisation had a slightly lower mean variance than both quantile normalisation by log(2) spot volume and linear normalisation (all spots) the difference was considered minor. Both methods were subsequently applied after standardisation as this resulted in a lower mean variance (Figure 4-8).

Other normalisation methods were also included in the results analysis for completeness (see Alternate normalisation methods, page 122). These were; the DeCyder DIA normalisation, and three other alternative normalisation methods *i.e.* albumin adjustment (linear adjustment after main spots albumin data removal) CV adjustment (adjustment by spots with the lowest 10% of CVs after linear normalisation), and a blank filling adjustment that replaces missing values with adjusted values prior to calculations for linear normalisation using all spots. Variance ratios for these were all compared to linear normalisation with all spots as shown in Figure 4-11. The mean variance ratios were close to zero or positive, indicating that these methods were not particularly useful in reducing variance, however data using these methods was included in the spots of interest table for completeness (Table 5-15).

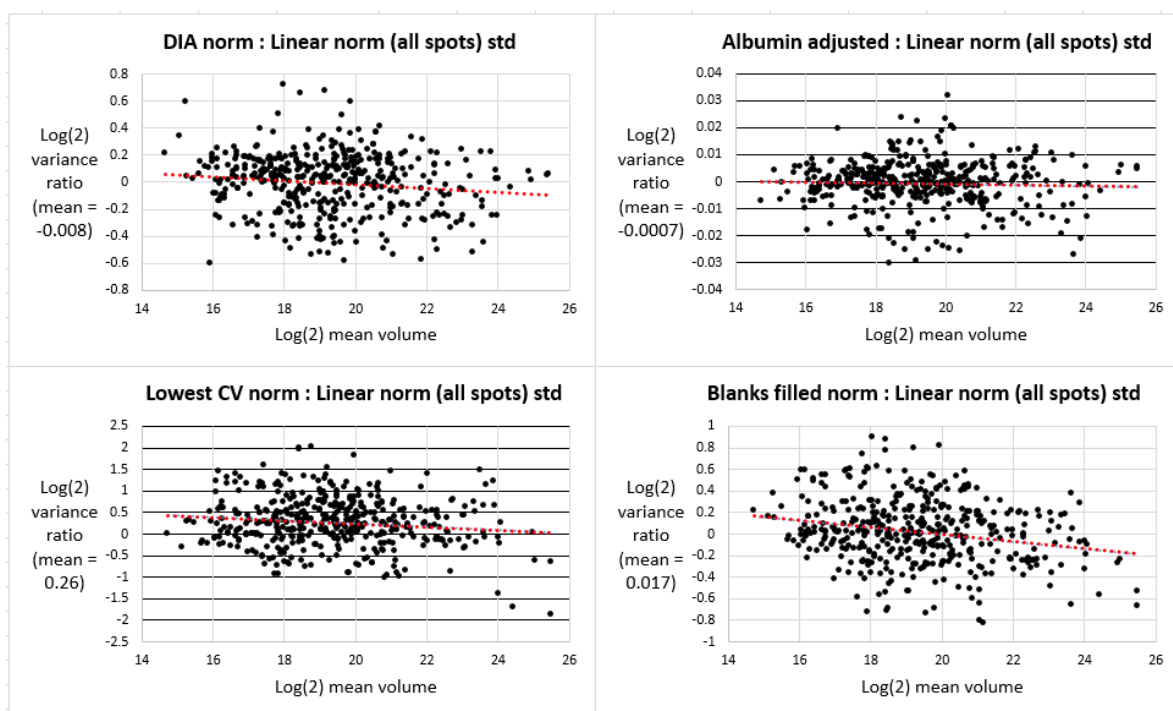


Figure 4-11. Variance ratio plots for DIA and alternative normalisation methods.

DIA normalised data was exported from DeCyder 7.0 in the form of log standardised abundance (LSA). This was converted to log(2) volume data for the variance ratio plots as shown in Appendix [‘33 - DIA LSA values - DIGE B.xlsx’](#). Albumin adjustment normalisation calculations can be found in Appendix [‘21 - albumin adjustment.xlsx’](#). Lowest CV normalisation calculations can be found in Appendix [‘22 - lowest CV norm, from spots present on all gels.xlsx’](#). Calculations for normalisation using blanks filled prior to linear normalisation with all spots can be found in Appendix [‘23 - DIGE B renorm by all spots, with blanks filled.xlsx’](#).

Data distribution

The primary requirement in data analysis, particularly for student's t-tests, is that data be normally distributed. This was checked using data that had been normalised with all spots and then standardised. A scatter plot was used to take an initial look at the data (Figure 4-12).

As can be seen in Figure 4-12, the distribution of the data is concentrated around low spot volumes making it difficult to assess the distribution of individual spots using this plot. Note that there are 428 different protein spots, and 6560 data points (428 spots x 16 samples, less 288 missing values) represented. In order to visualise large amounts of data, distribution histograms are often used. However because 428 data distributions have to be assessed, all with different mean values this method requires some refinement in order to be applied.

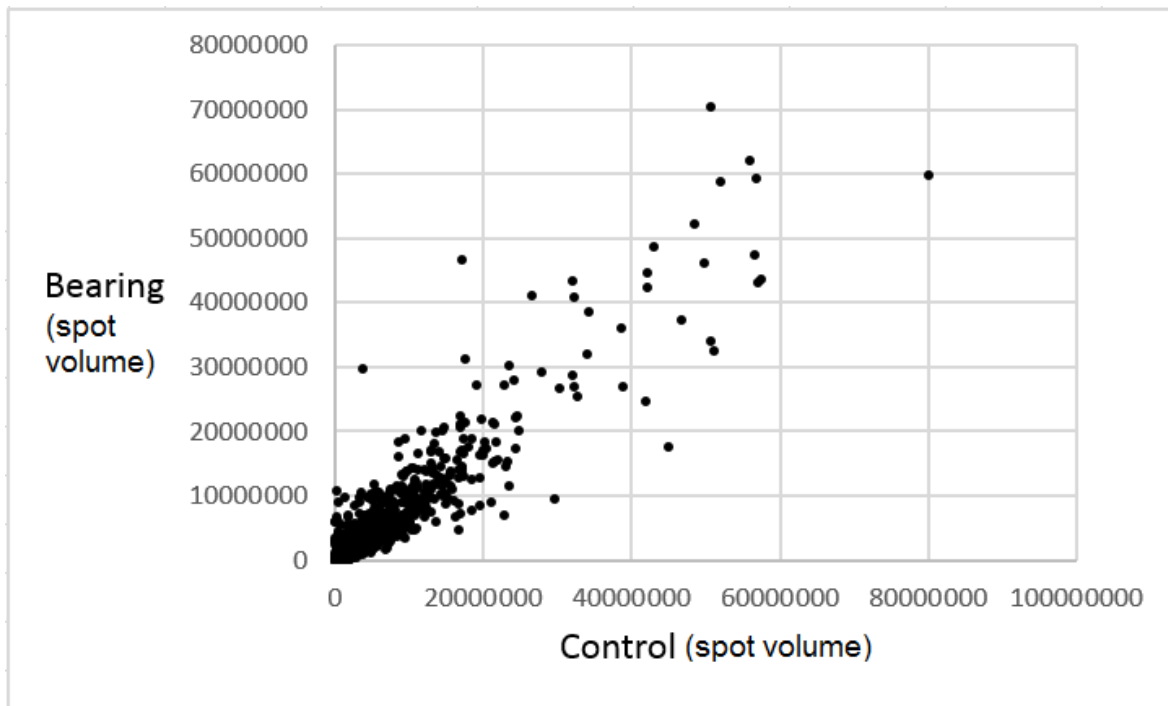


Figure 4-12. Scatter plot of paired Bearing vs Control samples.

Spot volume is shown, data was normalised by all spots.

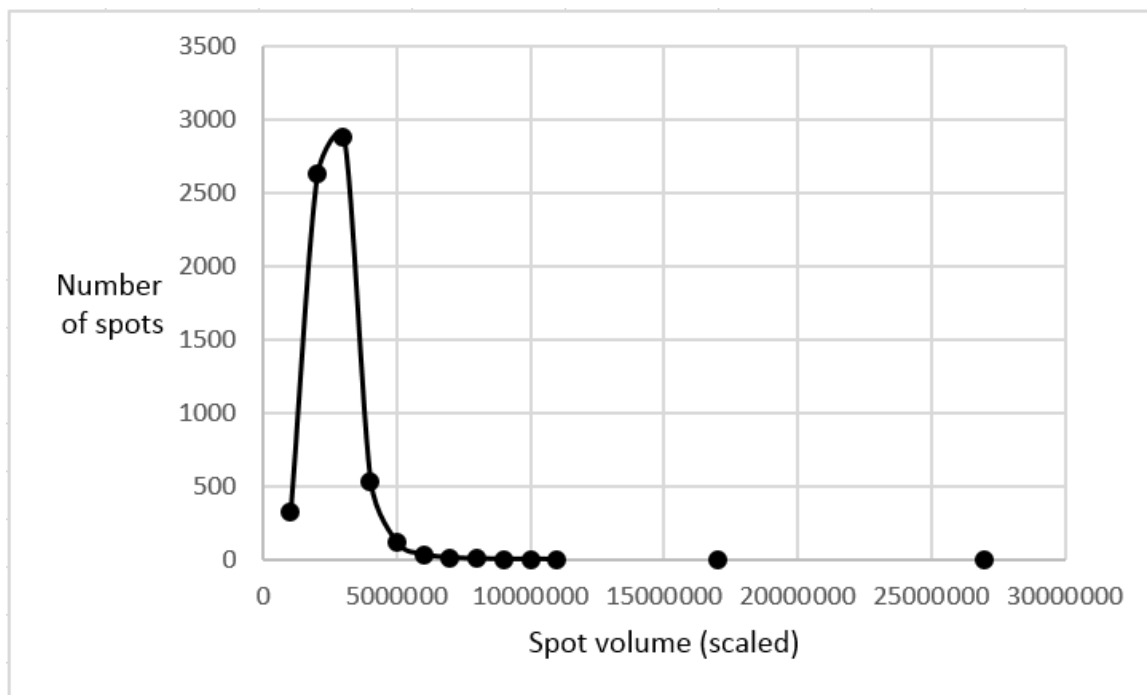


Figure 4-13. Distribution histogram for scaled spot volumes.

Distribution histogram of the normalised (by all spots) and standardised spot volumes. Spots were scaled to the average volume. A bin volume of 1,000,000 was used.

As the present study is multi-dimensional, all the protein spots have different means and so a single distribution histogram would be meaningless, as one would be required for each matched spot. However if the data is scaled so that each matched spot has the same mean the data distribution, the data set as a whole can be analysed on a single histogram. The average spot volume for each spot (across both controls and bearing samples) was calculated, then this data was used to calculate an average volume for all spots. Spots were then scaled uniformly across groups so that the average for each spot was the same. It should be noted that scaling doesn't change data distribution, as the SD as a percentage of mean remains the same (see the Dist 2 tab of Appendix ['8 - DIGE B, with 2 normalisation methods.xlsx'](#)). The resultant distribution histogram is shown in Figure 4-13, and as can be seen, the distribution of the volume data is skewed towards low values and does not follow a normal bell shaped distribution.

A data transformation such as a logarithmic transformation can be used to improve data distribution characteristics and is often used for 2D spot data. One of the issues when examining data distribution in multi variable analyses is that different transformations may be required (or not) for different variables. In this study, although a large dynamic range was observed for each protein spot,

all are from one source (plasma protein) indicating that applying a uniform (or none) transformation across all spots may be useful. Furthermore, it is normal practice to only use one type of transformation in spot analysis [252]. The need to use only one type of transformation was therefore investigated using data from all protein spots.

In order to test the data transformations used, quantile comparison plots (Q-Q plot) were constructed using the R package 'car' and the function 'qqPlot' [264, 265]. Normalised (with all spots) and standardised spot volumes from DIGE experiment B were used. These were converted to long form with the 'gather' function in R (in the 'tidyr' package) and plotted with 'qqPlot' (Figure 4-14).

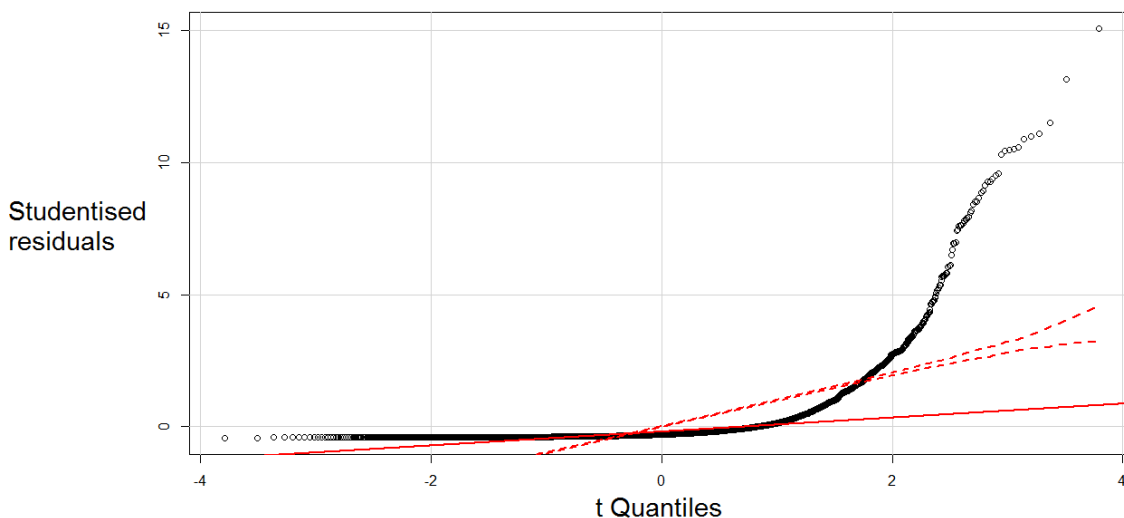


Figure 4-14. Quantile comparison plot of normalised and standardised spot volume data.

Normalisation was by all spots. The solid red line is the line of best fit, and the dashed lines are at the 95% confidence interval.

As the distribution of a large proportion of the data in the Q-Q plot was asymmetric and well outside of the 95% confidence intervals, the data was transformed using log base 2 and analysed with a Q-Q plot (Figure 4-15). While some values are outside the 95% confidence interval, the curve is very similar to one reported as acceptable [266]. It is noted that these graphs represent the distribution of a large amount of data, *i.e.* from 428 proteins with 6560 data points (428 spots x 16 samples, less 288 missing values).

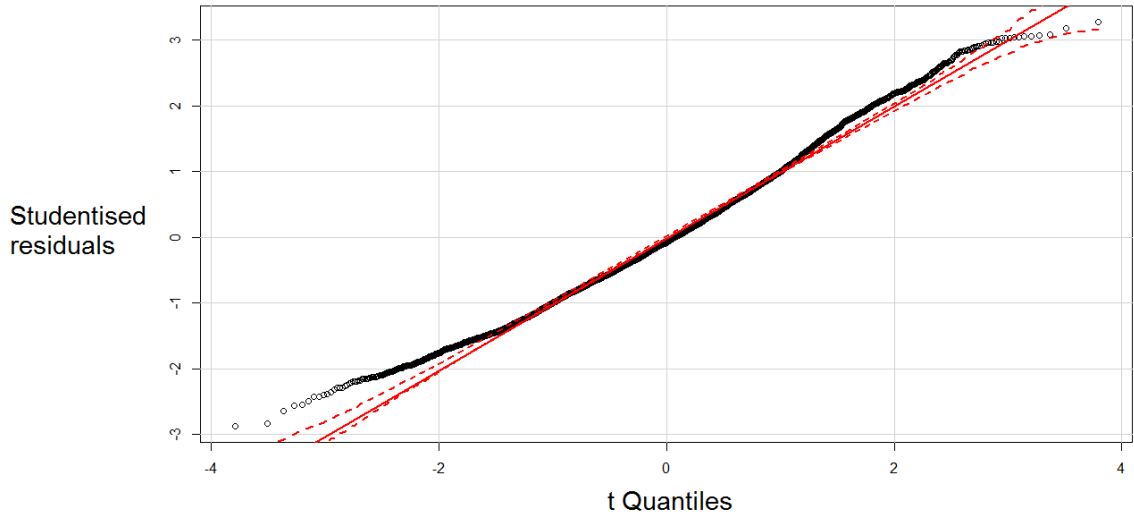


Figure 4-15. Quantile comparison plot of $\log(2)$ normalised & standardised volume data.
Normalisation was by all spots. Solid red line is line of best fit, and dashed lines are at the 95% confidence interval.

A Q-Q plot was generated for the VSN normalised data, this is shown in Figure 4-16.

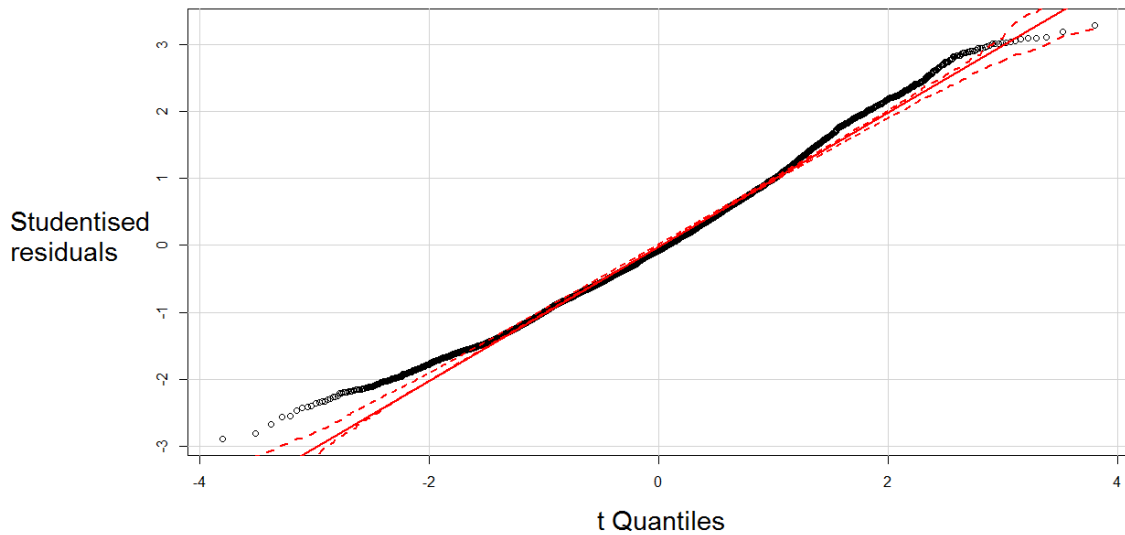


Figure 4-16. Quantile comparison plot of VSN normalised data.
The solid red line is the line of best fit, and the dashed lines are at the 95% confidence interval.

A Q-Q plot was generated for the quantile normalised $\log(2)$ data (Figure 4-17).

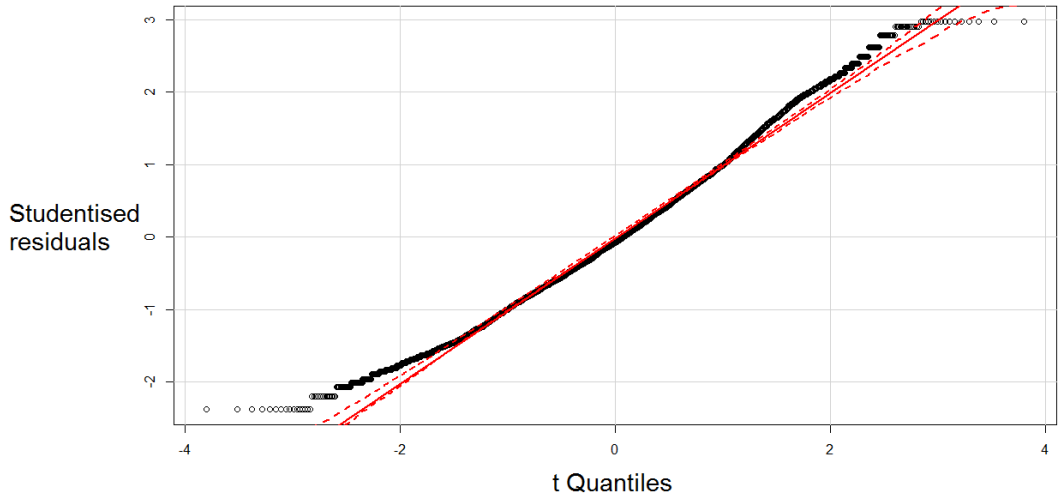


Figure 4-17. Quantile comparison plot of quantile normalised log(2) data.

The solid red line is the line of best fit, and the dashed lines are at the 95% confidence interval.

A log (base 2) distribution data set was calculated in a similar manner to the scaled volume data set (calculations are shown in the Dist 2 tab of the '[DIGE B, with 2 normalisation methods.xlsx](#)' file). The resultant distribution (Figure 4-18) is much more symmetrical, even when outliers are included.

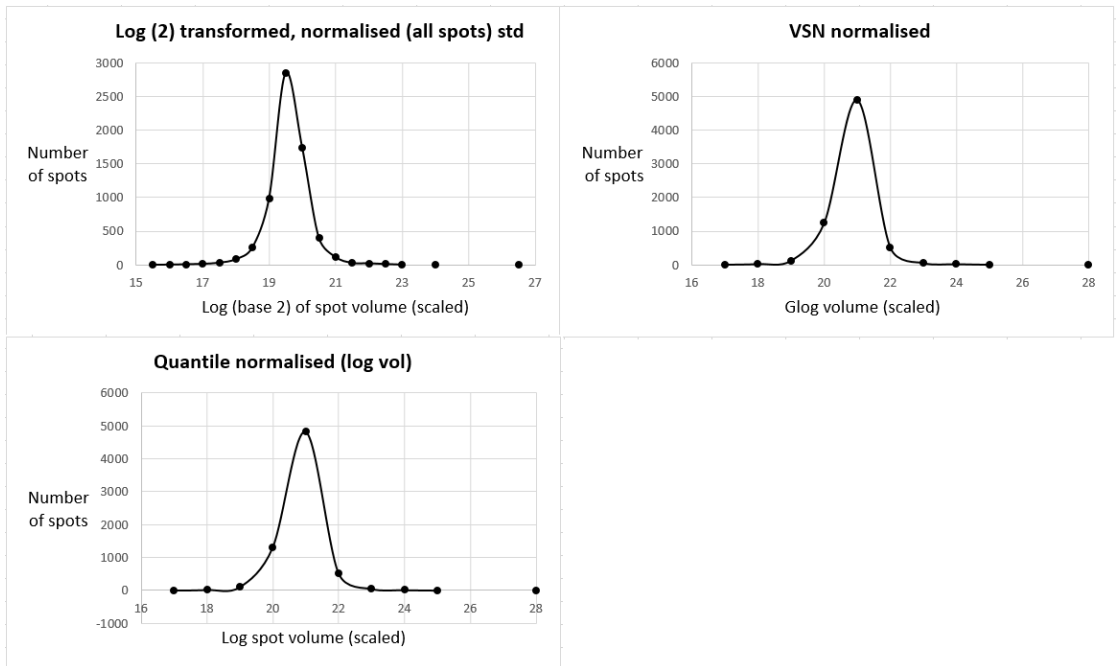


Figure 4-18. Distribution histograms for log transformations and normalisations.

Shown are data distributions for log (base 2) transformation of spot volumes, VSN and quantile (log volume) normalised data, using a bin size of 0.5. Spots were scaled to have the same mean.

Data distribution was further visualised using scatter plots (Figure 4-19), but only very minor differences could be seen between the different normalisation methods after data transformation. See Figure 4-12 for a non-transformed scatter plot.

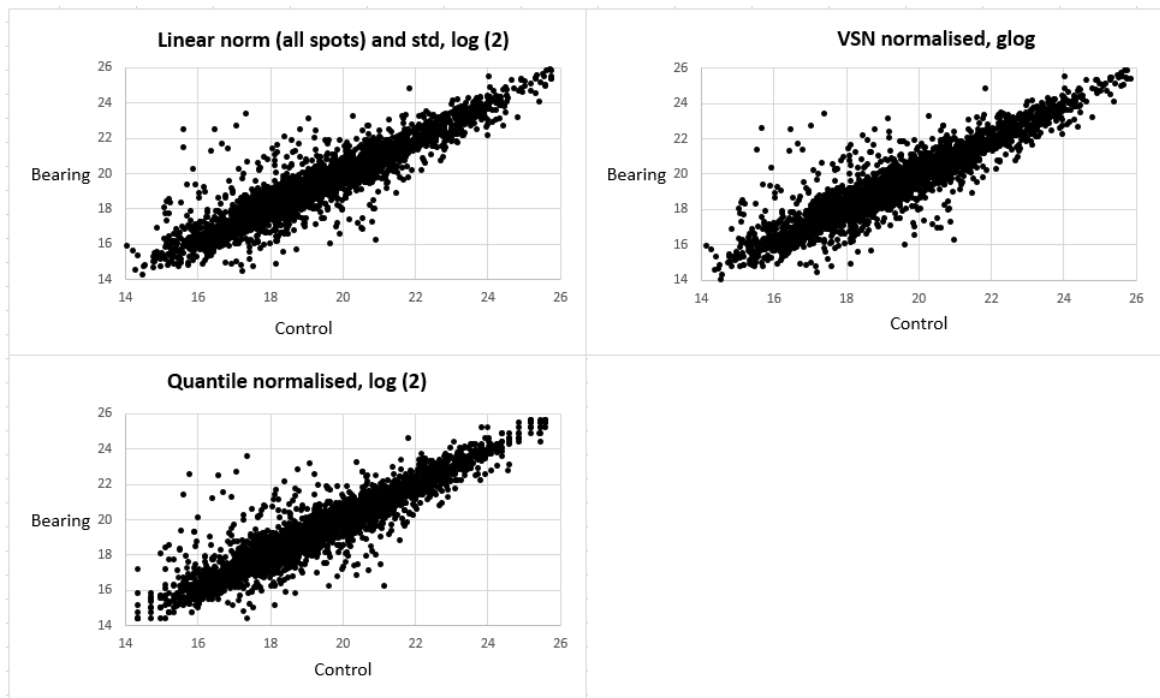


Figure 4-19. Scatter plots for transformed paired spots, bearing vs control. Linear normalised (by all spots) and standardised, and quantile normalised (log volume) methods used a log base 2 transformation, whereas VSN normalisation used a glog transformation.

Summary graphs of paired averages (bearing vs control) are shown volume in Figure 4-20.

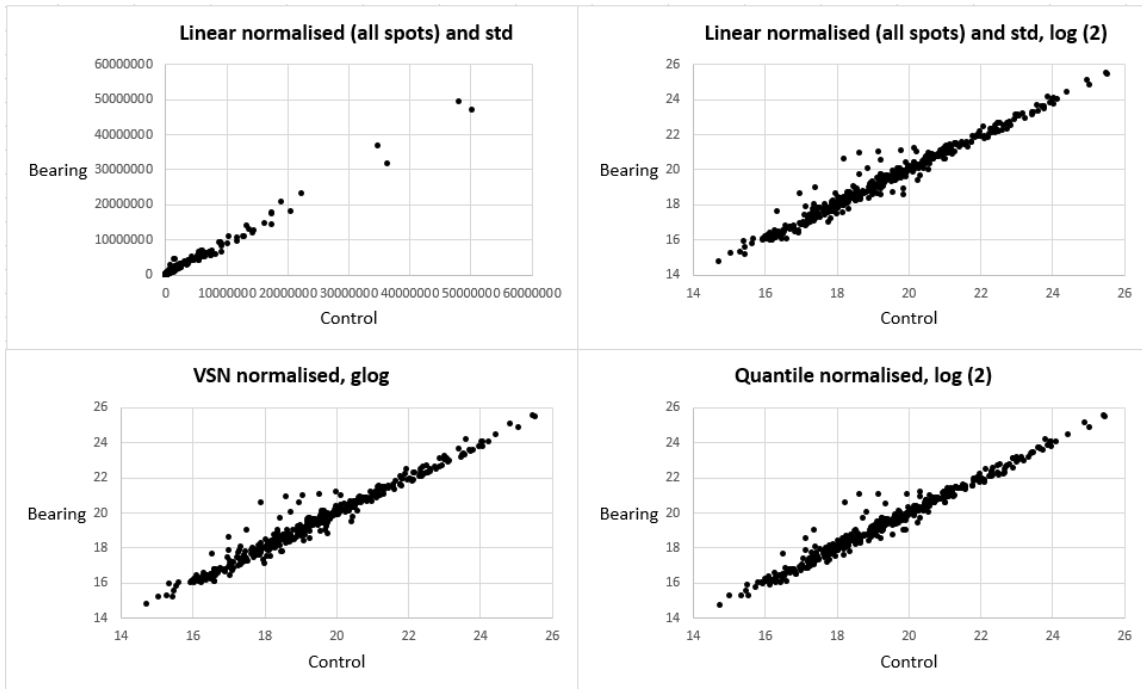


Figure 4-20. Scatter plots showing average spot volumes, bearing vs control.

Transformed and not transformed data are shown.

Given the improved distribution, particularly as seen in the distribution histograms (Figure 4-18) the decision was made to continue with data analysis using log (base 2) transformed data for linear and quantile normalised data as well as the glog output of the VSN normalisation.

Chapter 5. Results

Prolapse occurrence

Of the 650 ewes that had blood sampled, 28 subsequently prolapsed, although one sample tube from a prolapsed ewe could not be found. Figure 5-1 shows the distribution of prolapse occurrence. The first two occurred on day 10 (from blood sampling) and the last one observed was on day 47. Sample collection is described at the beginning of Chapter 2.

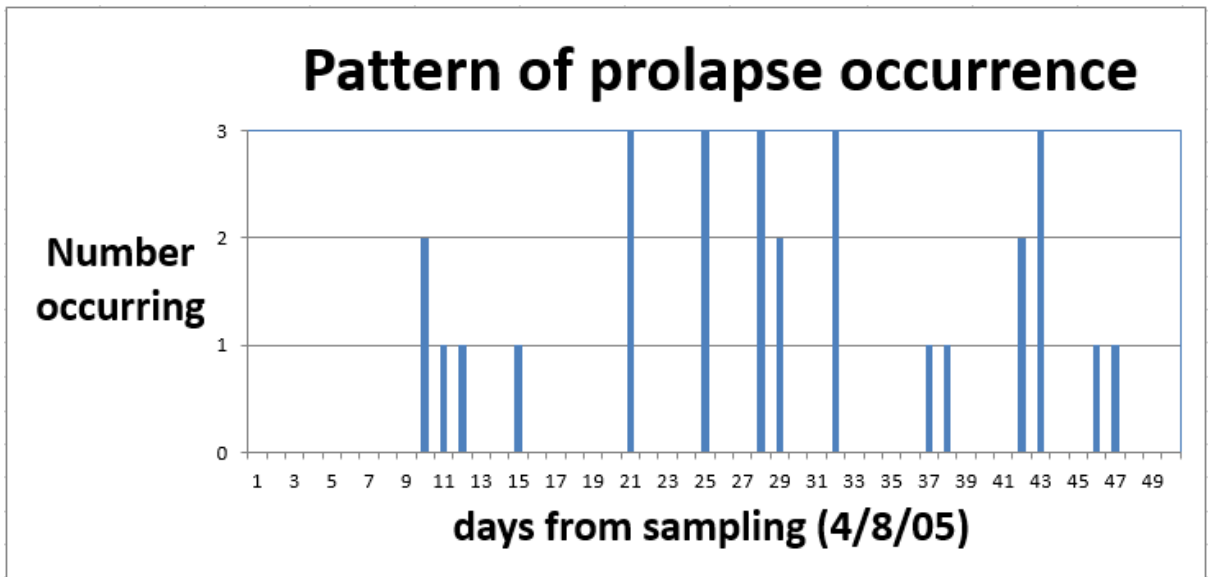


Figure 5-1. Distribution of prolapse occurrence.

Two DIGE experiments (using slightly different methodology) and two sets of cortisol data (using the same methodology) were analysed during the course of the study. The DIGE experiments are termed DIGE experiment A and B for the purposes of comparison. Controls for all experiments were selected from samples with numbers numerically close to the numbers of prolapsed samples in an attempt to control for time of day of sampling. As only a limited number of samples could be analysed by DIGE technology, twelve samples were analysed in DIGE A (6 control and 6 pre-prolapse) and sixteen (8 control and 8 pre-prolapse) in DIGE B. All pre-prolapse samples analysed by DIGE prolapsed within 21 days of blood sampling.

DIGE experiment A had poor resolution in the first dimension, the master gel can be seen in Figure 5-2. Note that a master gel is determined in DyCyder purely for the purposes of assigning spot numbers for identification and matching purposes. DIGE experiment B used an improved

methodology, as detailed in Chapter 2. The master gel from DIGE experiment B gel image can be seen in Figure 5-4, and this experiment became the main focus of the data analysis, although both sets of DIGE data are reported here.

DIGE data analysis

Analyses for both DIGE experiments were initially done using DeCyder 7.0 BVA software (GE Healthcare Life Sciences) that automatically carries out a log (base 10) transformation of normalised volume data before proceeding with the statistical analysis. In the DeCyder biological variation analysis (BVA), 5 spots were found that had statistically significant differences ($p < 0.05$) in DIGE experiment A and 8 in DIGE experiment B (Table 5-1, Table 5-2 and Figure 5-4).

Spot ID	Appearance	T-test	Av. ratio	Spot ID	Appearance	T-test	Av. ratio
-----DIGE experiment A-----				-----DIGE experiment B-----			
A 1160	15 (18)	0.015	-1.26	B 1417	24(24)	0.5	-1.12
A 781	9 (18)	0.020	1.47	B 885	24(24)	0.25	1.09
A 1166	15 (18)	0.030	-1.59	NA			
A 792	9 (18)	0.035	1.45	B 904	24(24)	0.97	-1.00
A 788	12 (18)	0.049	1.66	B 893	24(24)	0.94	1.01
A 1172	15 (18)	0.053	-1.59	B 2281	24(24)	0.24	-1.19
A 1162	15 (18)	0.056	-1.31	B 1421	24(24)	0.5	-1.08
A 1155	12 (18)	0.098	-1.29	B 1410	24(24)	0.32	-1.11

Table 5-1. Initial data analysis for DIGE experiment A using DeCyder 7.0.

Protein spots including those matched to experiment B are listed by p value up to 0.1. The student's t-test calculations for p value are from two tailed t-tests with homoscedastic (equal) variance after DIA normalisation and log(10) transformation. The average ratios (Av. ratio) represent values found in bearing/control samples using non-transformed volume data, positive values indicate an increased spot volume in bearing samples and negative values represent a decrease. An average ratio of 1.00 indicates no change. NA = data not available because the matching spot could not be identified. Appearance indicates the number of images the spots was found in, *e.g.* to appear in 15(18) means that the spot appeared in 15 images (*i.e.* 5 bearing, 5 control and 5 standard) out of the possible 18 images (6 bearing, 6 control and 6 standard).

Within the DeCyder differential in-gel analysis (DIA) module, normalisation is calculated automatically using data from all spots detected. However in the present study many spots could not be included in the analysis because of overlap, so it was necessary to renormalise the data. This was done as outlined in chapter 4. Student's t-test p values were re-calculated using log (base 2)

data that had been re-normalised using two methods, linear normalisation (using all spots) and VSN normalisation (after standardisation).

Spot ID	Appearance	T-test	Av. Ratio	Spot ID	Appearance	T-test	Av. Ratio
-----DIGE experiment B-----				-----DIGE experiment A-----			
B 2366	21 (24)	0.0016	3.70	NA			
B 746	24 (24)	0.019	-1.53	NA			
B 1629	24 (24)	0.020	1.34	NA			
B 1071	21 (24)	0.029	1.25	NA			
B 1611	24 (24)	0.033	1.40	A 1284	12(18)	0.54	1.54
B 1588	24 (24)	0.034	3.15	A 1490	18(18)	0.49	2.4
B 1577	24 (24)	0.040	2.62	A 1268	15(18)	0.18	2.79
B 1635	21 (24)	0.044	-1.46	NA			
B 2338	21 (24)	0.052	1.70	NA			
B 2368	24 (24)	0.055	3.16	NA			
B 2268	24 (24)	0.059	-1.19	NA			
B 765	24 (24)	0.061	-1.48	A 660	9(18)	0.67	1.08
B 891	21 (24)	0.074	-1.17	A 750	18(18)	0.32	-1.14
B 2271	24 (24)	0.075	-1.21	NA			
B 1233	21 (24)	0.075	-1.20	NA			
B 1039	21 (24)	0.076	1.48	NA			
B 2336	24 (24)	0.078	1.38	A 1262	15(18)	0.18	2.06
B 1012	21 (24)	0.078	1.48	NA			
B 1078	24 (24)	0.081	1.19	NA			
B 997	21 (24)	0.093	1.43	NA			
B 1048	21 (24)	0.094	1.43	NA			
B 1135	24 (24)	0.097	-1.17	NA			
B 2052	21 (24)	0.098	1.27	A 1435	15(18)	0.51	1.05
B 1060	21 (24)	0.099	1.39	NA			
B 1102	21 (24)	0.099	-1.40	NA			

Table 5-2. Initial data analysis for DIGE experiment B using DeCyder 7.0.

DeCyder 7.0 analysis for DIGE experiment B showing protein spots listed by *p* value to 0.1 and the values obtained for spots that matched in DIGE experiment A. As in Table 5-1, DeCyder DIA normalisation was used, followed by log(10) transformation. Student's *t*-test *p* value results are from two tailed *t*-test calculations with homoscedastic (equal) variance. Ratios represent values found in bearing/control samples using non-transformed volume data. Positive values indicate an increase in bearing samples and negative values represent a decrease. An average ratio of 1.00 indicates no change.

Data re-normalisation

Table 5-3 and Table 5-4 show the data that has been re-normalised using the linear method (using all spots) while Table 5-5 and Table 5-6 show data re-normalised with VSN.

Spot ID	Appearance	T-test	Av. Ratio	Spot ID	Appearance	T-test	Av. Ratio
-----DIGE experiment A-----				-----DIGE experiment B-----			
A 1160	15(18)	0.0042	-1.3	B 1417	24(24)	0.464	-1.1
A 781	9(18)	0.017	1.4	B 885	24(24)	0.288	1.1
A 1162	15(18)	0.017	-1.4	B 1421	24(24)	0.492	-1.1
A 1166	15(18)	0.019	-1.7	NA			
A 792	9(18)	0.025	1.4	B 904	24(24)	0.950	-1.0
A 1172	15(18)	0.030	-1.7	B 2281	24(24)	0.275	-1.2
A 788	12(18)	0.054	1.6	B 893	24(24)	0.972	1.0
A 1155	12(18)	0.068	-1.3	B 1410	24(24)	0.337	-1.1
A 1457	9(18)	0.074	-3.2	NA			
A 1169	15(18)	0.086	-1.6	B 1428	24(24)	0.398	-1.3

Table 5-3. T-test p values using linear normalised log(2) transformed data, from DIGE A.

Spots matched in DIGE experiment B (also with linear normalised log(2) data) are also shown.

Spot ID	Appearance	T-test	Av. Ratio	Spot ID	Appearance	T-test	Av. Ratio
-----DIGE experiment B-----				-----DIGE experiment A-----			
B 2366	24(24)	0.0016	3.6	NA			
B 746	24(24)	0.012	-1.5	NA			
B 1635	21(24)	0.020	-1.5	NA			
B 1588	24(24)	0.032	3.4	A 1490	18(18)	0.498	2.3
B 1577	24(24)	0.034	2.7	A 1268	15(18)	0.199	2.6
B 1629	24(24)	0.037	1.3	NA			
B 2338	21(24)	0.047	1.7	NA			
B 2368	24(24)	0.050	3.3	NA			
B 765	24(24)	0.054	-1.5	A 660	9(18)	0.856	1.0
B 1611	24(24)	0.055	1.4	A 1284	12(18)	0.53	1.4
B 1071	21(24)	0.057	1.2	NA			
B 2336	24(24)	0.058	1.4	NA			
B 2271	24(24)	0.058	-1.2	NA			
B 789	24(24)	0.062	-1.1	NA			
B 1233	24(24)	0.062	-1.2	NA			
B 2268	24(24)	0.070	-1.2	NA			
B 1435	24(24)	0.083	-1.2	A 1164	18(18)	0.218	-1.3
B 1102	21(24)	0.083	-1.4	NA			
B 1039	21(24)	0.086	1.5	NA			
B 1012	21(24)	0.086	1.5	NA			
B 1668	21(24)	0.087	-1.7	NA			
B 1622	21(24)	0.095	-1.5	NA			
B 1683	21(24)	0.098	-1.7	NA			
B 1135	24(24)	0.098	-1.2	NA			
B 2373	24(24)	0.098	3.4	A 1493	15(18)	0.567	2.3

Table 5-4. T-test p values using linear normalised log(2) transformed data, DIGE B.

Spots matched in DIGE experiment A (using linear normalised log(2) data) are also shown.

Spot ID	Appearance	T-test	Av. Ratio	Spot ID	Appearance	T-test	Av. Ratio
-----DIGE experiment A-----				-----DIGE experiment B-----			
A 1160	15(18)	0.0040	-1.3	B 1417	24(24)	0.481	-1.1
A 1166	15(18)	0.019	-1.7	NA			
A 1162	15(18)	0.020	-1.4	B 1421	24(24)	0.511	-1.1
A 1172	15(18)	0.033	-1.7	B 2281	24(24)	0.278	-1.2
A 792	9(18)	0.036	1.4	B 904	24(24)	0.959	1.0
A 781	9(18)	0.052	1.4	B 885	24(24)	0.198	1.1
A 1155	12(18)	0.055	-1.3	B 1410	24(24)	0.352	-1.1
A 788	12(18)	0.071	1.6	B 893	24(24)	0.929	1.0
A 1457	9(18)	0.081	-3.2	NA			
A 1169	15(18)	0.095	-1.6	B 1428	24(24)	0.396	-1.2

Table 5-5. T-test p values using non-linear (VSN) re-normalised data, DIGE A.

Spots matched in DIGE experiment B (using VSN re-normalised data) are also shown.

Spot ID	Appearance	T-test	Av. Ratio	Spot ID	Appearance	T-test	Av. Ratio
-----DIGE experiment B-----				-----DIGE experiment A-----			
B 2366	24(24)	0.0017	3.7	NA			
B 746	24(24)	0.0091	-1.5	NA			
B 1635	21(24)	0.026	-1.4	NA			
B 1071	21(24)	0.031	1.2	NA			
B 1588	24(24)	0.032	3.4	A 1490	18(18)	0.50	2.2
B 1577	24(24)	0.036	2.7	A 1268	15(18)	0.20	2.6
B 1629	24(24)	0.041	1.3	NA			
B 2338	21(24)	0.046	1.7	NA			
B 765	24(24)	0.048	-1.5	A 660	9(18)	0.83	1.0
B 2368	24(24)	0.051	3.4	NA			
B 1611	24(24)	0.055	1.4	A 1284	12(18)	0.78	1.0
B 2336	24(24)	0.070	1.4	NA			
B 2271	24(24)	0.074	-1.2	NA			
B 2268	24(24)	0.079	-1.2	NA			
B 1039	21(24)	0.079	1.5	NA			
B 198	24(24)	0.080	1.2	A 213	12(18)	0.37	1.2
B 1012	21(24)	0.081	1.5	NA			
B 1435	24(24)	0.089	-1.2	A 1164	18(18)	0.20	-1.3
B 1078	24(24)	0.090	1.2	NA			
B 789	24(24)	0.090	-1.1	NA			
B 1135	24(24)	0.090	-1.2	NA			
B 1668	21(24)	0.096	-1.7	NA			
B 1102	21(24)	0.097	-1.4	NA			
B 997	21(24)	0.097	1.4	NA			
B 2373	24(24)	0.098	3.5	A 1493			
B 1233	24(24)	0.098	-1.2	NA			
B 1048	21(24)	0.099	1.4	NA			

Table 5-6. T-test p values using non-linear (VSN) re-normalised data, DIGE B.

Spots matched in DIGE experiment A (using VSN re-normalised data) are also shown.

Summaries of spot p values using the three different normalisation methods trialed are shown in Table 5-7 and Table 5-8.

Spot ID	DIA	Linear	VSN
A 1160 (15/18)	0.015 (-1.3)	0.0042 (-1.3)	0.0040 (-1.3)
A 781 (9/18)	0.020 (+1.5)	0.017 (+1.4)	0.052 (+1.4)
A 1166 (15/18)	0.030 (-1.6)	0.019 (-1.7)	0.019 (-1.7)
A 792 (9/18)	0.035 (+1.5)	0.025 (+1.4)	0.036 (+1.4)
A 788 (12/18)	0.049 (+1.7)	0.054 (+1.6)	0.071 (+1.6)
A 1172 (15/18)	0.053 (-1.6)	0.030 (-1.7)	0.033 (-1.7)
A 1162 (15/18)	0.056 (-1.3)	0.017 (-1.4)	0.020 (-1.4)

Table 5-7. Summary table of student's t-test p values and ratios, DIGE A.

Spots with student t-test p values below 0.05 are shown using three different normalisation methods (DIA, linear (using all spots) and VSN). Ratio values are shown in brackets next to p values. The numbers in brackets in the ID column are the number images the spot was present on, out of the total of 18. P values that differ from DIA normalisation at threshold points (0.01 and 0.05) are highlighted in bold.

Spot ID	DIA	Linear	VSN
B 2366 (24/24)	0.0016 (+3.7)	0.0016 (+3.6)	0.0017 (+3.7)
B 746 (24/24)	0.019 (-1.5)	0.012 (-1.5)	0.0091 (-1.5)
B 1629 (24/24)	0.020 (+1.3)	0.037 (+1.3)	0.041 (+1.3)
B 1071 (21/24)	0.029 (+1.3)	0.057 (+1.2)	0.031 (+1.2)
B 1611 (24/24)	0.033 (+1.4)	0.055 (+1.4)	0.055 (+1.4)
B 1588 (24/24)	0.034 (+3.2)	0.032 (+3.4)	0.032 (+3.4)
B 1577 (24/24)	0.040 (+2.6)	0.034 (+2.7)	0.036 (+2.7)
B 1635 (21/24)	0.044 (-1.5)	0.020 (-1.5)	0.026 (-1.4)
B 2338 (21/24)	0.052 (+1.7)	0.047 (+1.7)	0.046 (+1.7)

Table 5-8. Summary table of student's t-test p values and ratios, DIGE B.

Spots with student t-test p values below 0.05 are shown using three different normalisation methods. Ratio values are shown in brackets next to p values. The numbers in brackets in the ID column are the number images the spot was present on, out of the total of 24. P values that differ from DIA normalisation at threshold points (0.01 and 0.05) are highlighted in bold.

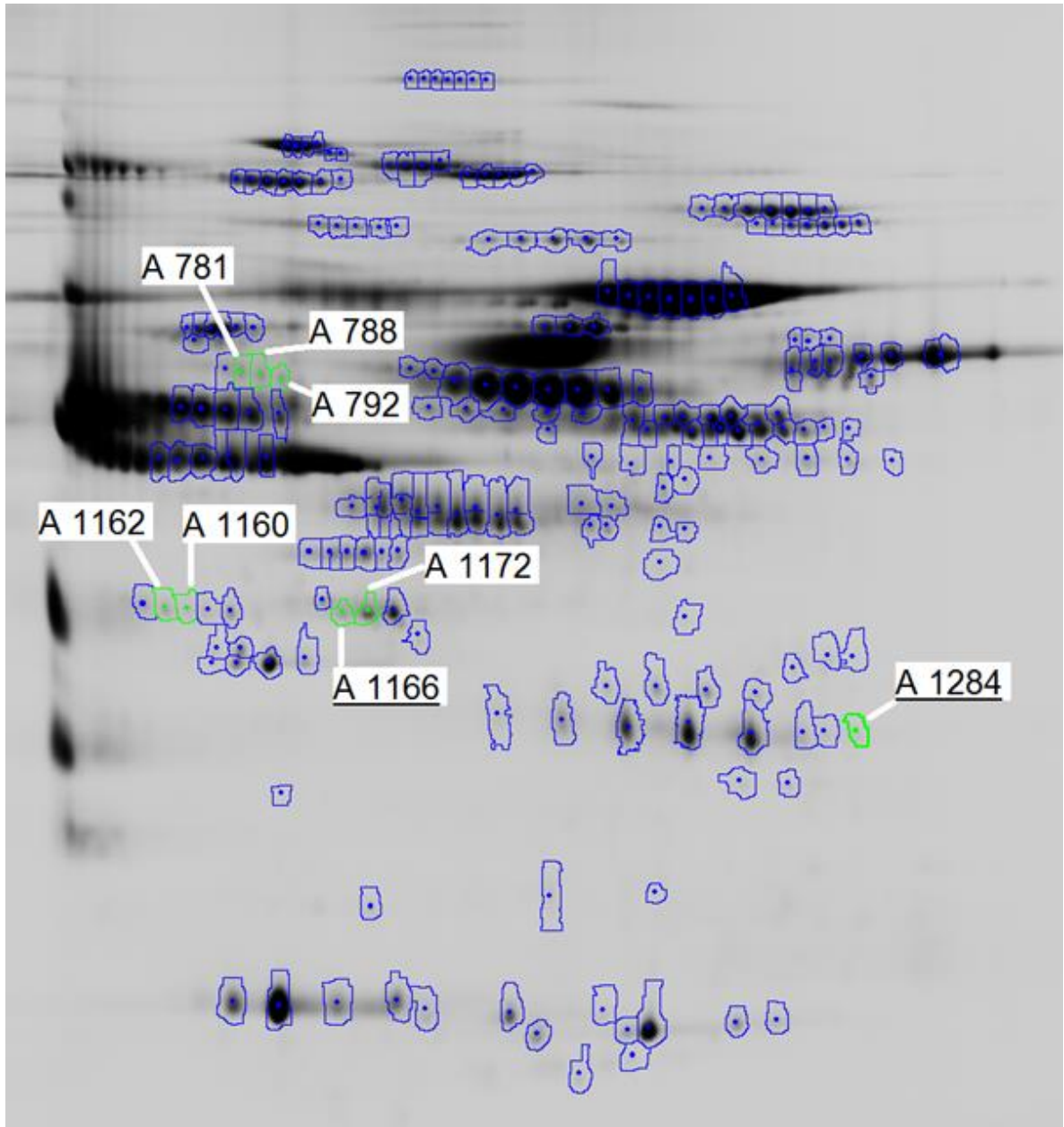


Figure 5-2. The master gel from DIGE experiment A.

All spots included in the analysis are outlined. Spots outlined in green have statistical significance as found using the initial DeCyder 7.0 BVA analysis (without renormalisation) and are labelled. Labels that are not underlined represent spots that were found in DIGE experiment A to have statistically significant differences between control and bearing samples as a result of applying the student's t-test ($p < 0.05$). Labels underlined represent spots that were found to be significantly different between bearing and control samples on the basis of FDR (False Discovery Rate) testing. Spot A 1166 was found to be significantly different between bearing and control samples on the basis of both a t-test and FDR test (see Table 5-10).

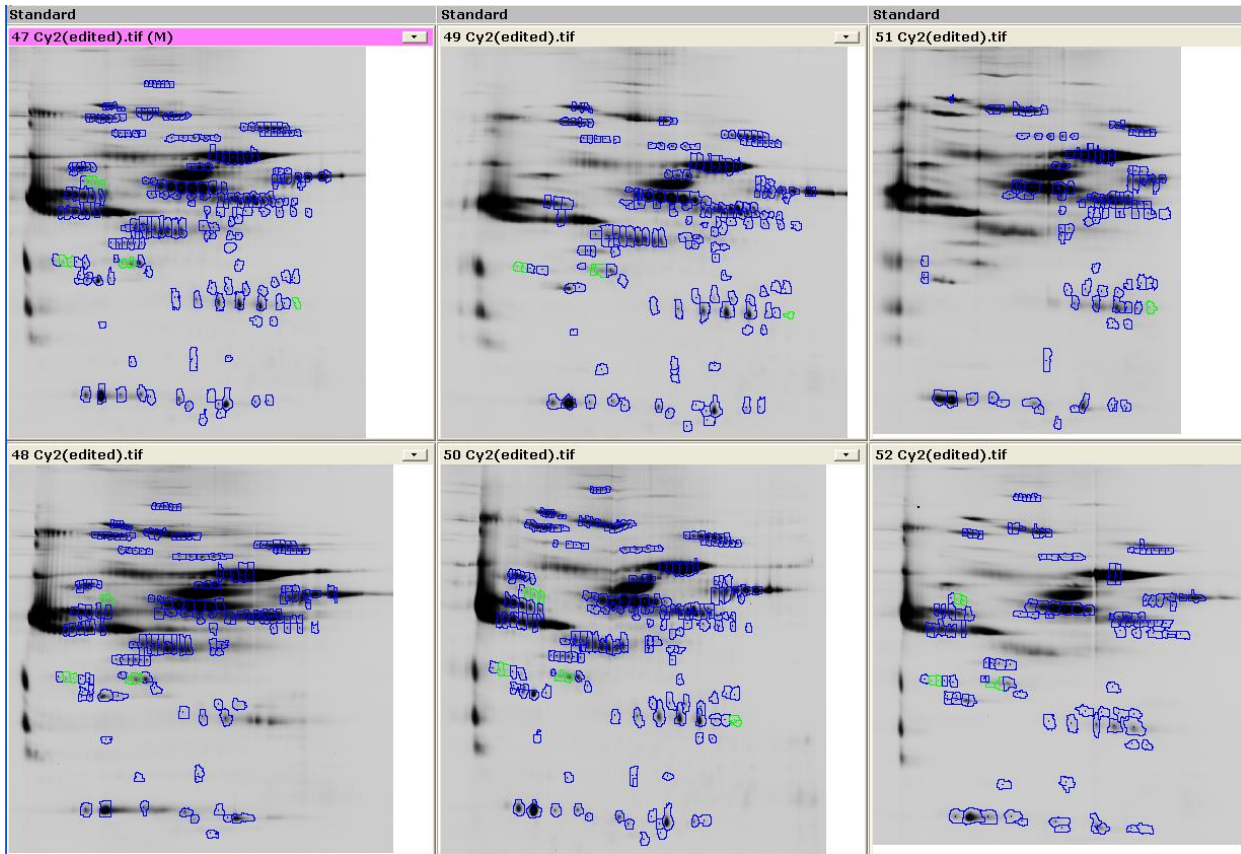


Figure 5-3. Standard images for all gels from DIGE experiment A.

All quantified spots are outlined in either blue or green. Spots outlined in green have significance as described Figure 5-2. Images from the pooled standard is shown for all gels in DIGE experiment A. The master gel heading is highlighted in pink.

As none of the spots matched between the experiments showed p levels below 0.05 in both experiments, a Person's correlation was carried between the standards used in each experiment. A correlation of 0.97 ($p < 0.001$) was found between the average volume of the 174 standard spots matched between the two DIGE experiments, indicating a high level of correlation. This was calculated using linear normalised standard data. When calculated with VSN data, the correlation was slightly lower at 0.92 ($p < 0.001$). When this was unlogged, however, a very similar correlation was found (0.97, $p < 0.001$) (Appendix '[17 - Matched standards – VSN data \(incl blanks\).xlsx](#)' and '[5 - Matched DIGE A & B, with 2 normalisation methods.xlsx](#)' 'Norm. by all spots' tab).

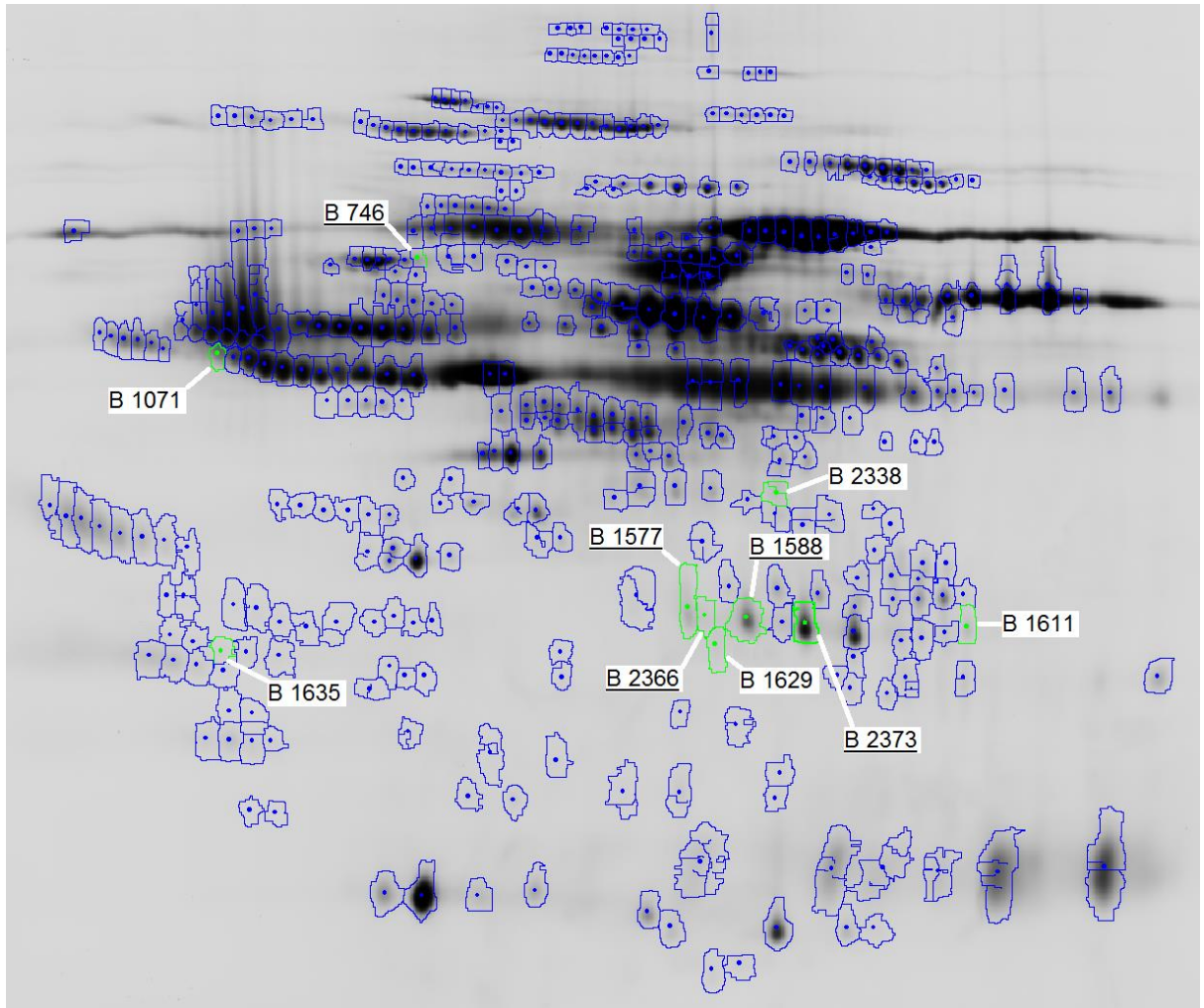


Figure 5-4. The master gel from DIGE experiment B.

All spots included in the analysis are outlined in either green or blue. Spots outlined in green have statistical significance as found using the initial DeCyder 7.0 BVA analysis (without renormalisation) and are labelled. Spots that are labelled without underlining were shown to have statistically significant differences between control and bearing samples in DIGE experiment B as a result of applying the student's t-test ($p < 0.05$). Spots with underlined labels were found to have significant differences between bearing and control samples after FDR testing. Spots B 746, B 1577, B 1588 and B 2366 were found to be significantly different between the two groups of samples on the basis of both the t-test and FDR test.

As there were some (seven) samples in common to both experiments, these samples were individually correlated using linear normalised (all spots) volume data. The average Pearson's correlation coefficient was 0.95 with a range of 0.92 – 0.98. The lowest correlation coefficient had the lowest matched spot count (87) and the highest correlation coefficient had the highest matched spot count (172). All correlations were statistically significant (Appendix, ['18 - Correlations.xlsx'](#)).

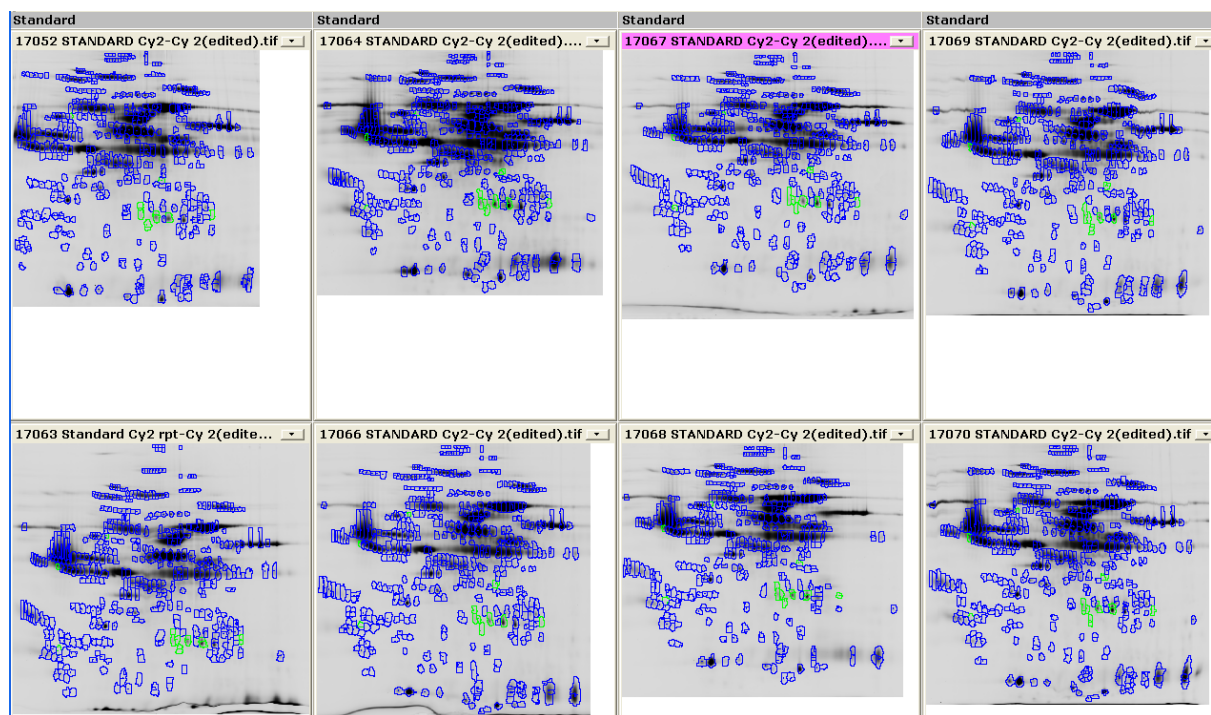


Figure 5-5. Standard images for all gels from DIGE experiment B.

All quantified spots are outlined in either green or blue. Spots outlined in green are significant as described in Figure 5-4. Images from the pooled standard is shown for all gels in DIGE experiment B. The master gel heading is highlighted in pink. Note as mentioned in chapter 2 (see page 64) the gel in the upper left (17052) had to be cropped on the acidic (left) side as there was poor protein transfer in this region due to the overlay partially mixing with acrylamide during casting.

False discovery; Benjamini & Hochberg FDR and q values

Multiple hypothesis testing is where many statistical tests are run concurrently on the same small number of subjects. For example, if 20 student's t-tests with a statistical threshold for p of 0.05 were undertaken using a normally distributed data set, then because $0.05 \times 20 = 1$, this means that one of the 20 tests is likely to be called true purely by chance. In order to counter this false discovery, it is recommended that the distribution of p values is examined, especially when q values are used [233]. P value distribution histograms and q values were produced using the R package 'qvalue' [267]. Results are shown in Figure 5-6 to Figure 5-13.

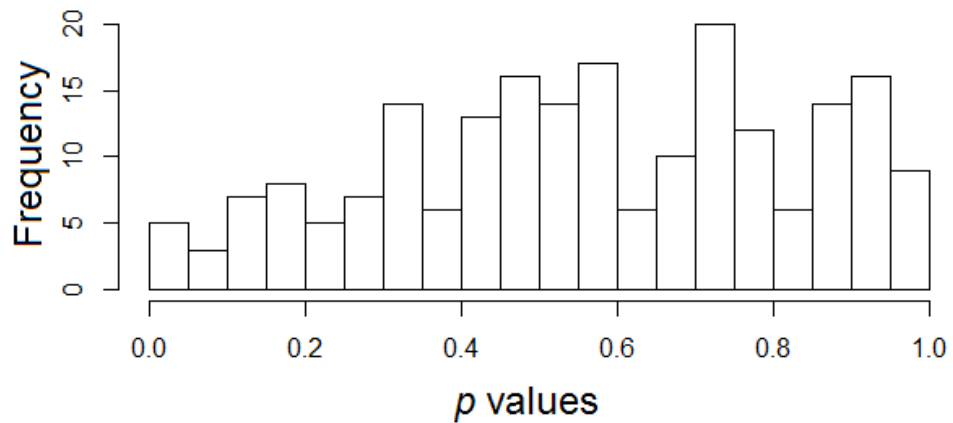


Figure 5-6. Distribution of p values for DIGE experiment A, from DIA analysis.

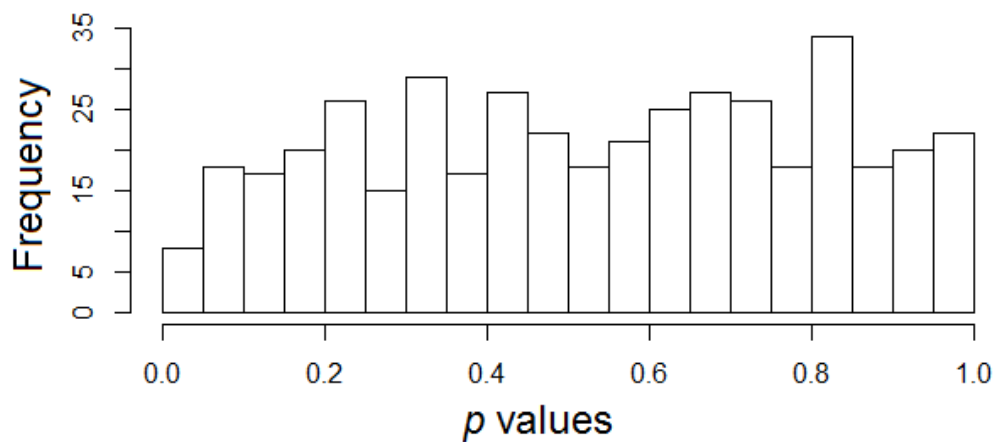


Figure 5-7. Distribution of p values for DIGE experiment B, from DIA analysis.

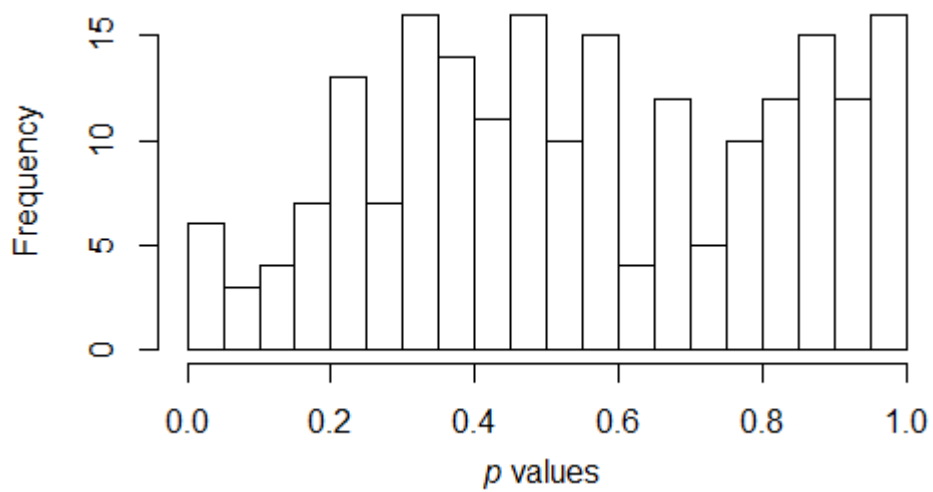


Figure 5-8. Distribution of p values for DIGE experiment A, linear normalised (all spots).

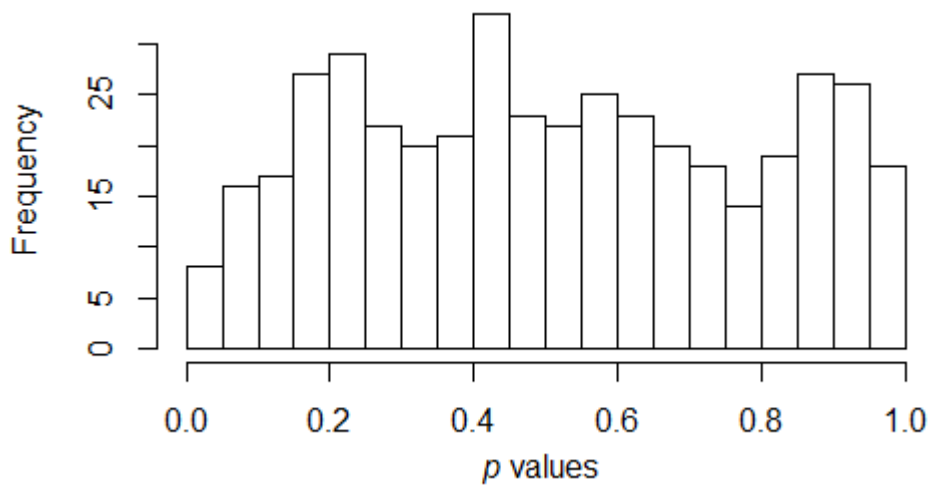


Figure 5-9. Distribution of p values for DIGE experiment B, linear normalized (all spots).

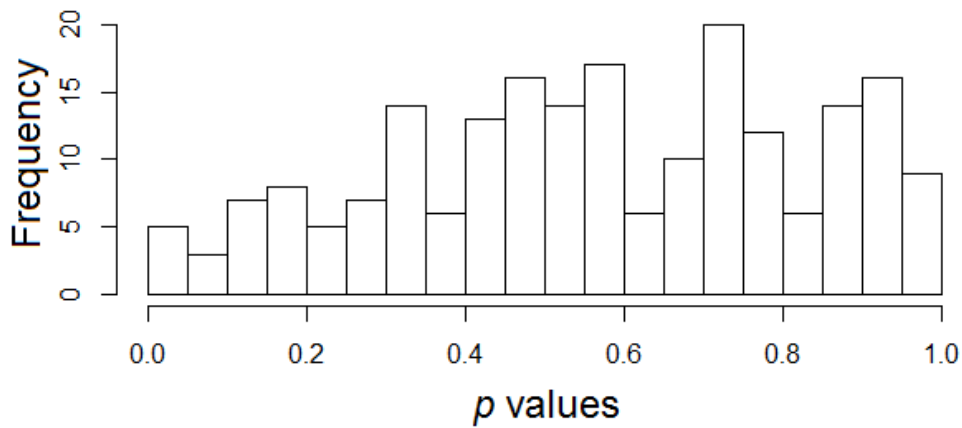


Figure 5-10. Distribution of p values for DIGE experiment A, VSN normalisation.

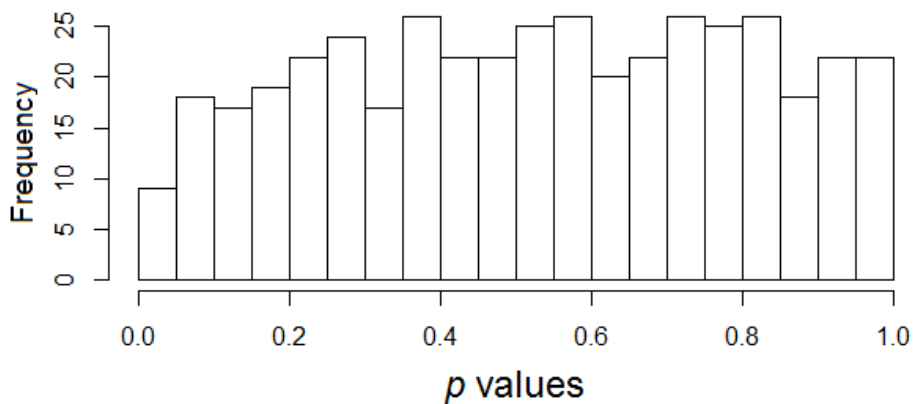


Figure 5-11. Distribution of p values for DIGE experiment B, VSN normalisation.

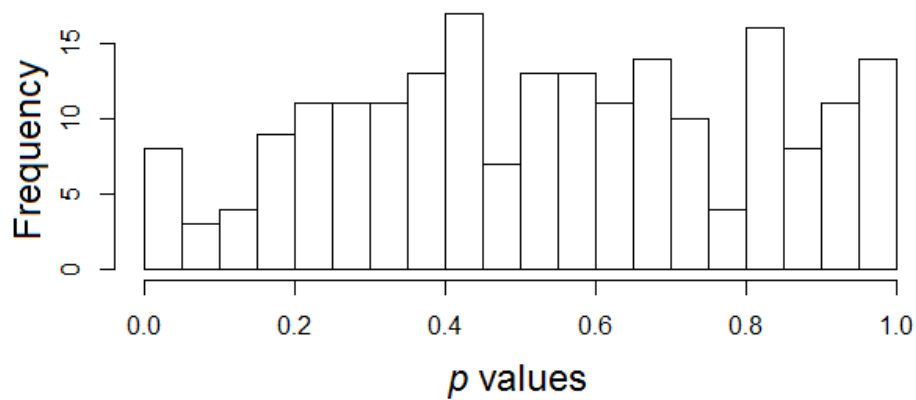


Figure 5-12. Distribution of p values for DIGE A, quantile normalisation of volume.

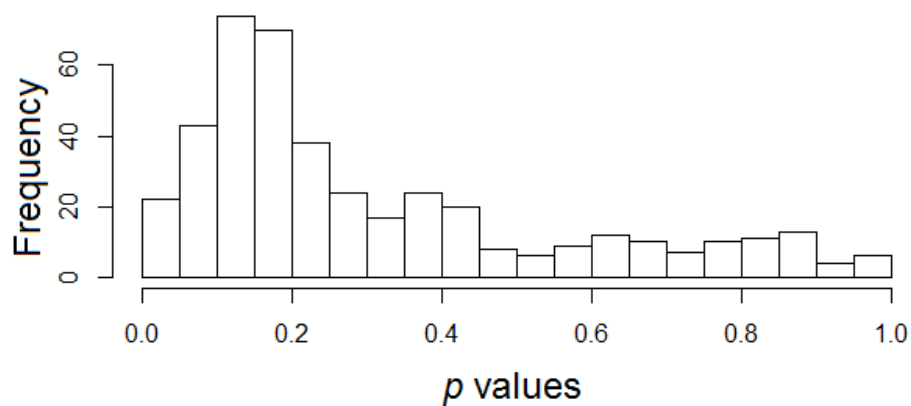


Figure 5-13. Distribution of p values for DIGE B, quantile normalisation of volume.

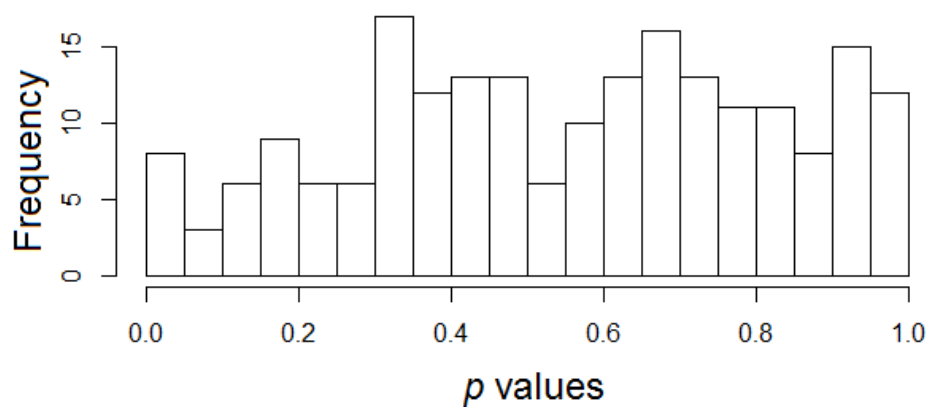


Figure 5-14. Distribution of p values for DIGE A, quantile normalisation of $\log(2)$ volume.

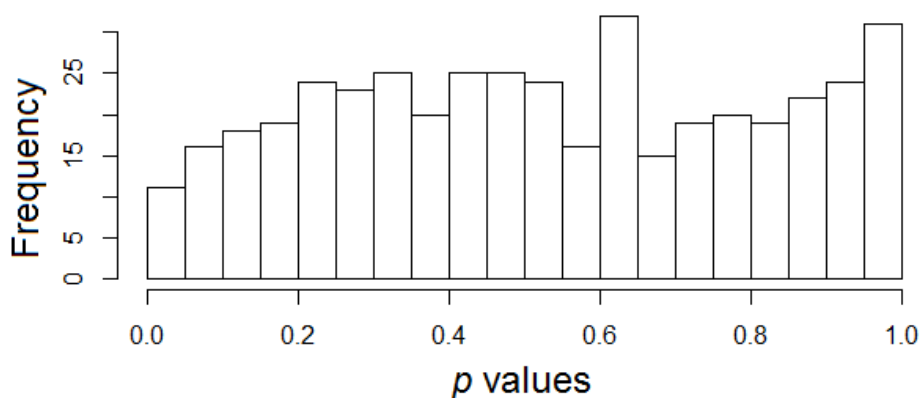


Figure 5-15. Distribution of p values for DIGE B, quantile normalisation of $\log(2)$ volume.

As can be seen in the p value histograms, values are not evenly distributed across the range of values for both experiments as p values in the lower range, especially below 0.05 (the left most bar) are poorly represented. Such poor distribution of p values at the low end did not occur in the case of quantile normalisation by volume of DIGE B data as shown in Figure 5-13. Quantile normalisation by volume of the DIGE B data resulted in 22 p values (out of 428) less than 0.05 and 65 p values less than 0.1, far more than were obtained using the other normalisation methods. Even so, the p values were clearly not evenly distributed. For DIGE A with 208 spots, 10.4 (208/20) would be the average expected number of spots per 5% distribution (assuming an even distribution of p values) and for DIGE B with 428 spots, 21.4 would be the average expected number. By a purely visual assessment, the most even distribution of p values was obtained using the VSN normalised DIGE B data, as shown in Figure 5-11.

Karp *et al.* [166] suggested that biological data should show an even distribution of p values and that in three dye DIGE experiments there is a bias towards low proportions of low p values. This suggestion was supported by a study that used repeats of identical samples which produced small proportions of low p values. Along with some data simulations, this led the authors to assert that the DIGE three dye system produces data that is incorrectly inherently biased towards small proportions of low p values. However, because the same samples were repeatedly used for this research [166] there should be no differences between samples, and so any differences found have to be due to technical error rather than actual group differences. Although a few authors have voiced concerns about 3 dye DIGE technology [268], it is generally well accepted in proteomic studies [269].

One of the reasons for examining p value distributions is that some studies have shown a high proportion of low p values indicating that there are large differences between experimental groups. This can result from genetic differences between groups, such as a gene knockout [166]. The present study is a search for predictive markers for the later onset of a condition that has no known genetic differences between groups. Therefore, any differences between groups may be small and difficult to detect and, low levels of differences between the groups is expected.

Spot ID	DIA		Linear		VSN		Q (log(2))		Q (volume)		
	p vals	B&H p & q	p vals	B&H p & q	p vals	B&H p & q	p vals	B&H p & q	p vals	B&H p	q value
-----DIGE A-----											
A 1160	0.015	0.99	0.0042	0.87	0.0040	0.84	0.0016	0.33	0.0020	0.42	0.42
A 781	0.020	0.99	0.017	0.99	0.052	1.00	0.013	0.52	0.0094	0.58	0.58
A 1166	0.030	0.99	0.019	0.99	0.019	1.00	0.015	0.52	0.020	0.58	0.58
A 792	0.035	0.99	0.025	1.00	0.036	1.00	0.0088	0.52	0.0058	0.58	0.58
A 788	0.049	0.99	0.054	1.00	0.071	1.00	0.11	0.99	0.15	1.00	1.00
A 1172	0.053	0.99	0.030	1.00	0.033	1.00	0.021	0.58	0.033	0.86	0.86
A 1162	0.056	0.99	0.017	0.99	0.020	1.00	0.012	0.52	0.015	0.58	0.58
A 920	0.54	0.99	0.26	1.00	0.31	1.00	0.015	0.52	0.015	0.58	0.58
A 1155	0.97	0.99	0.068	1.00	0.055	1.00	0.022	0.58	0.017	0.58	0.58
-----DIGE B-----											
B 2366	0.0016	0.67	0.0016	0.68	0.0017	0.73	0.0023	1.00	0.12	0.39	0.11
B 746	0.019	0.98	0.012	0.99	0.0091	0.99	0.0060	1.00	0.048	0.39	0.11
B 1629	0.020	0.98	0.037	0.99	0.041	0.99	0.070	1.00	0.064	0.39	0.11
B 1071	0.029	0.98	0.057	0.99	0.031	0.99	0.13	1.00	0.64	0.75	0.21
B 1611	0.033	0.98	0.055	0.99	0.055	0.99	0.082	1.00	0.071	0.39	0.11
B 1588	0.034	0.98	0.032	0.99	0.032	0.99	0.034	1.00	0.10	0.39	0.11
B 1577	0.040	0.98	0.034	0.99	0.036	0.99	0.030	1.00	0.079	0.39	0.11
B 1635	0.044	0.98	0.020	0.99	0.026	0.99	0.020	1.00	0.25	0.43	0.12
B 2338	0.052	0.98	0.047	0.99	0.046	0.99	0.038	1.00	0.13	0.39	0.11
B 765	0.06	0.98	0.054	0.99	0.048	0.99	0.048	1.00	0.037	0.39	0.11
B 2286	0.22	0.98	0.23	0.99	0.21	0.99	0.30	1.00	0.0033	0.39	0.11
B 2282	0.25	0.98	0.26	0.99	0.24	0.99	0.19	1.00	0.0092	0.39	0.11
B 1075	0.13	0.98	0.10	0.99	0.10	0.99	0.055	1.00	0.012	0.39	0.11
B 891	0.074	0.98	0.11	0.99	0.15	0.99	0.024	1.00	0.018	0.39	0.11
B 2274	0.16	0.98	0.17	0.99	0.15	0.99	0.20	1.00	0.021	0.39	0.11
B 789	0.18	0.98	0.062	0.99	0.090	0.99	0.052	1.00	0.023	0.39	0.11
B 2373	0.10	0.98	0.098	0.99	0.098	0.99	0.086	1.00	0.023	0.39	0.11
B 1097	0.21	0.98	0.19	0.99	0.20	0.99	0.14	1.00	0.024	0.39	0.11
B 773	0.20	0.98	0.18	0.99	0.16	0.99	0.12	1.00	0.025	0.39	0.11
B 1170	0.44	0.98	0.32	0.99	0.41	0.99	0.15	1.00	0.030	0.39	0.11
B 656	0.21	0.98	0.20	0.99	0.22	0.99	0.085	1.00	0.031	0.39	0.11
B 695	0.31	0.98	0.34	0.99	0.34	0.99	0.21	1.00	0.033	0.39	0.11
B 653	0.33	0.98	0.36	0.99	0.45	0.99	0.18	1.00	0.034	0.39	0.11
B 992	0.34	0.98	0.25	0.99	0.25	0.99	0.14	1.00	0.036	0.39	0.11

Spot ID	DIA		Linear		VSN		Q (log(2))		Q (volume)		
	<i>p</i> vals	B&H <i>p</i> & <i>q</i>	<i>p</i> vals	B&H <i>p</i>	<i>q</i> value						
B 652	0.32	0.98	0.30	0.99	0.36	0.99	0.20	1.00	0.041	0.39	0.11
B 1135	0.097	0.98	0.098	0.99	0.090	0.99	0.16	1.00	0.043	0.39	0.11
B 861	0.23	0.98	0.15	0.99	0.21	0.99	0.090	1.00	0.043	0.39	0.11
B 697	0.42	0.98	0.43	0.99	0.44	0.99	0.31	1.00	0.045	0.39	0.11
B 1625	0.14	0.98	0.13	0.99	0.13	0.99	0.14	1.00	0.049	0.39	0.11
B 269	0.21	0.98	0.18	0.99	0.20	0.99	0.12	1.00	0.050	0.39	0.11

Table 5-9. *P* values, adjusted *p* values and *q* values for spots where *p* < 0.05.

Adjusted *p* values (calculated using the Benjamini and Hochberg (B&H) [229] method) and *q* values for spots with *p* values less than 0.05 from both DIGE experiments using a variety of different normalisation methods (Q = quantile normalisation). *Q* values were the same as the B&H adjusted *p* values for all methods except for those normalised using the quantile by volume method. Note the order of spots is according to their *p* value up to 0.05 in the DIA normalisation, and then by spots with *p* values less than 0.05 in the other normalisation methods.

One way to deal with low *p* values occurring randomly (rather than reflecting true differences between groups) in multiple hypothesis testing, is to adjust the *p* values according to the number of variables being tested. Adjusted *p* values were calculated using the R function ‘*p.adjust*’ using the method of Benjamini and Hochberg [229] (B&H). Spots with *p* values less than 0.05 from both DIGE experiments are shown in Table 5-9 along with B&H adjusted *p* values for the same spots. As can be seen after the Benjamini and Hochberg adjustments there are no longer any *p* values less than 0.05.

FDR testing

Another way to address multiple hypothesis testing is to apply a FDR test. A *q* value false discovery test was applied to the results found in the re-normalised data, using the R package ‘*qvalue*’ [233]. Most *q* values were found to be the same as the B&H adjusted *p* values except for DIGE B data that had been quantile normalised by volume (Appendix folder ‘[19 - B & H *p* adjustment](#)’).

The ‘*qvalue*’ package in R provides a plot function showing *p* value distributions and local FDR estimations. This was used with quantile normalised volume data from DIGE experiment B (Figure 5-16) and DIGE experiment B data that had been linearly normalised (Figure 5-17). The *q* value indicates the proportion of true null hypotheses for a variable when that variable is called significant. Prior to evaluating *q* values and FDR it is recommended that the first step is to check the *p* value distribution. Inspection of the *p* values shown in Figure 5-16, calculated using quantile normalised

data, shows again there is an uneven distribution, with the distribution of p values skewed towards lower values. The plot also provides a calculated local FDR threshold for the p values showing that many of the p values are above the FDR threshold. Because these samples were collected from otherwise healthy ewes, at the time of sample collection, this is unlikely to be correct. Inspection of the p values shown in Figure 5-17 reveals a more even distribution with few p values at the lowest end. The FDR calculation shows only a few p values pass the FDR test, this is more likely to be correct and presumably reflects a more reliable normalisation method.

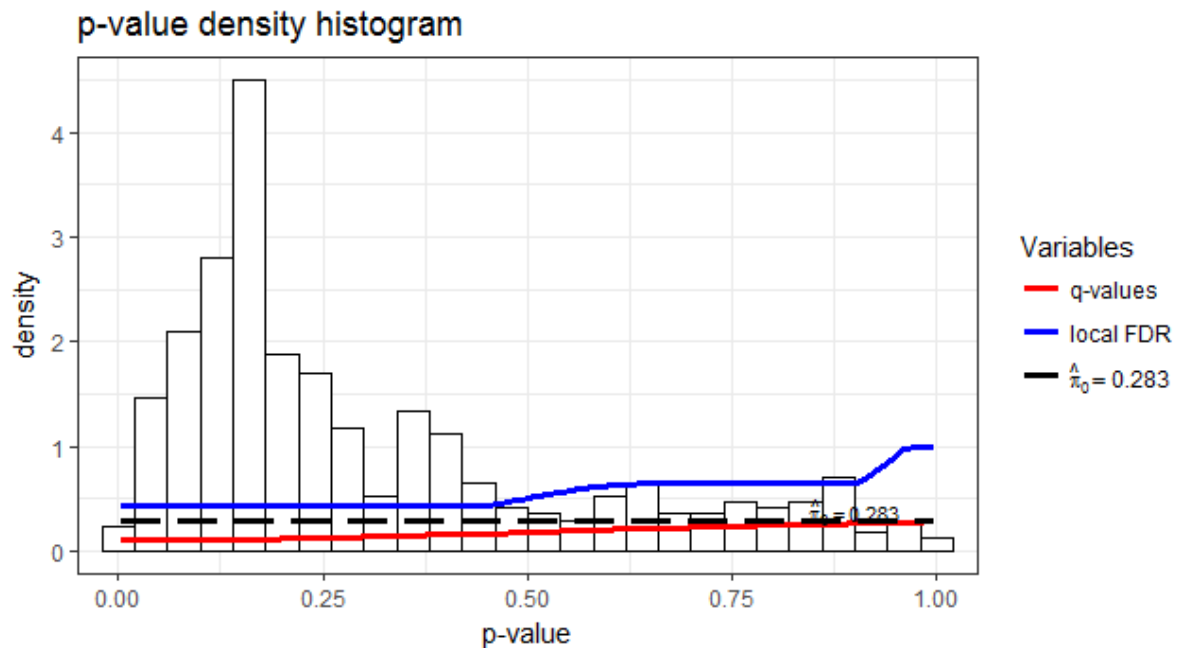


Figure 5-16. P value distribution using quantile normalised volume, FDR and q values. FDR is estimated local FDR as plotted by the R package 'qvalue', DIGE B data used.

As can be seen in Figure 5-16 and Table 5-9 q values for quantile normalised DIGE B volume data spots with p values less than 0.05 are 0.11. This indicates that the minimum FDR incurred in calling these values significant is 0.11 *i.e.* a 11% FDR, however as stated, the p value distribution is poor, calling into doubt the normalisation method. Looking at Figure 5-17 and Table 5-9, the lowest q value is 0.67 (*i.e.* a FDR of 67%) which although high has a more acceptable p value distribution and thus provides more confidence in the linear normalisation used.

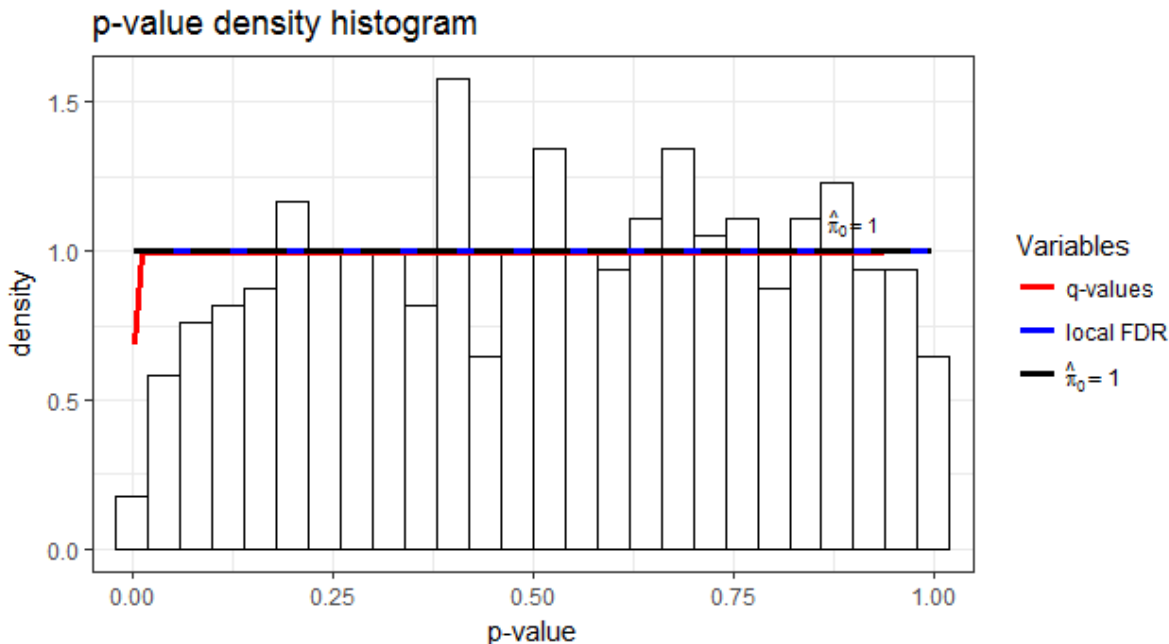


Figure 5-17. P value distribution using linear normalised (all spots) data, FDR and q values.
 FDR is estimated local FDR as plotted by the R package ‘qvalue’, DIGE B data used.

In order to more correctly determine p values a variety of improved t-tests that take account of all variables in question (rather than individually) have been developed [270]. The moderated t-test [271] is one that has emerged as being useful in correctly identifying genes and proteins of interest in both microarray and proteomic data [272]. Recently an R package, ‘prot2D’ was written to facilitate the application of the moderate t-test to 2D gel data [255] and was used to analyse the data from the two DIGE experiments reported here. The identification of spots which passed the ‘prot2D’ FDR test were produced as a text and so the output is not shown here but the results are summarised in Table 5-10 and Table 5-11. Plots with p values vs FDR were generated by ‘prot2D’, and some examples are shown in Figure 5-18 (Appendix folder ‘20 - FDR plots’).

DIA	Linear	VSN	Quantile (log(2))
A 1166	A 1166	A 1166	A 1166
A 1284	A 1284	A 1284	A 1284

Table 5-10. FDR spots using the ‘prot2D’ R package, DIGE A data.

Spots found to be significantly different (bearing vs control) in DIGE A after FDR testing using the ‘prot2D’ R package. Note that as the DIA data used was log(10) standardised abundance (LSA, as exported from DeCyder) this data was converted to log(2) volume data and the spots that passed FDR testing were found to be the same as when LSA data was used, with the same FDR plot. All other data used were log(2). Column headings indicate the normalisation methods used.

DIA	Linear	VSN	Quantile (log(2))
B 746	B 746	B 746	B 746
B 1577	B 1577	B 1577	B 1577
B 1588	B 1588	B 1588	B 1588
B 2366	B 2366	B 2366	B 2366
B 2373		B 2373	B 2373

Table 5-11. FDR spots using the ‘prot2D’ R package, DIGE B data.

Spots found to be significantly different (bearing vs control) in DIGE B after FDR testing using the ‘prot2D’ R package. As for Table 5-11, as the DIA data used was log(10) standardised abundance (LSA, as exported from DeCyder) this data was converted to log(2) volume data. Spots that passed FDR testing were found to be the same as when LSA data was used, with the same FDR plot. All other data used was log(2). Column headings indicate the normalisation methods used.

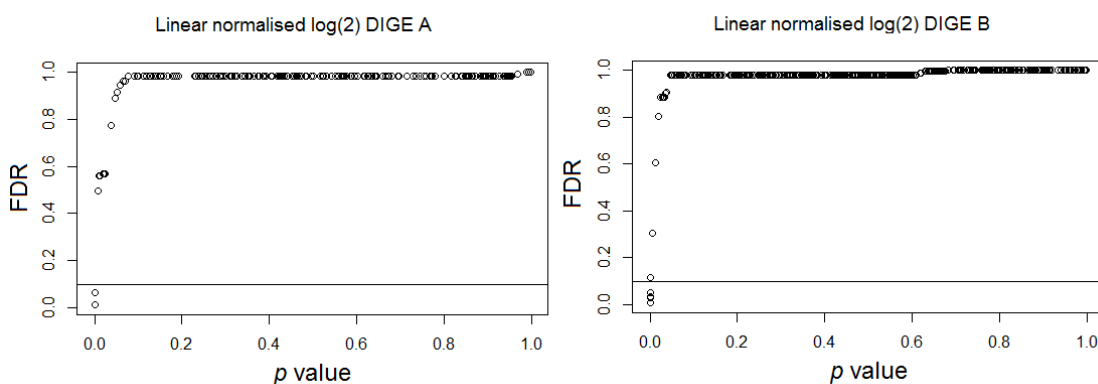


Figure 5-18. Example FRD plots generated in the R package ‘prot2D’.

Plots shown used linear normalised data. Spots below the line have passed the FDR test as shown in Table 5-10 and Table 5-11.

Data distribution

In order to examine the distribution of data for spots passing the FDR test, boxplots showing quartile divided data distribution were generated along with scatter distributions for each of the normalisation methods used (Figure 5-19 and Figure 5-20). Note that the data distribution of all spots collectively was examined in chapter 4.

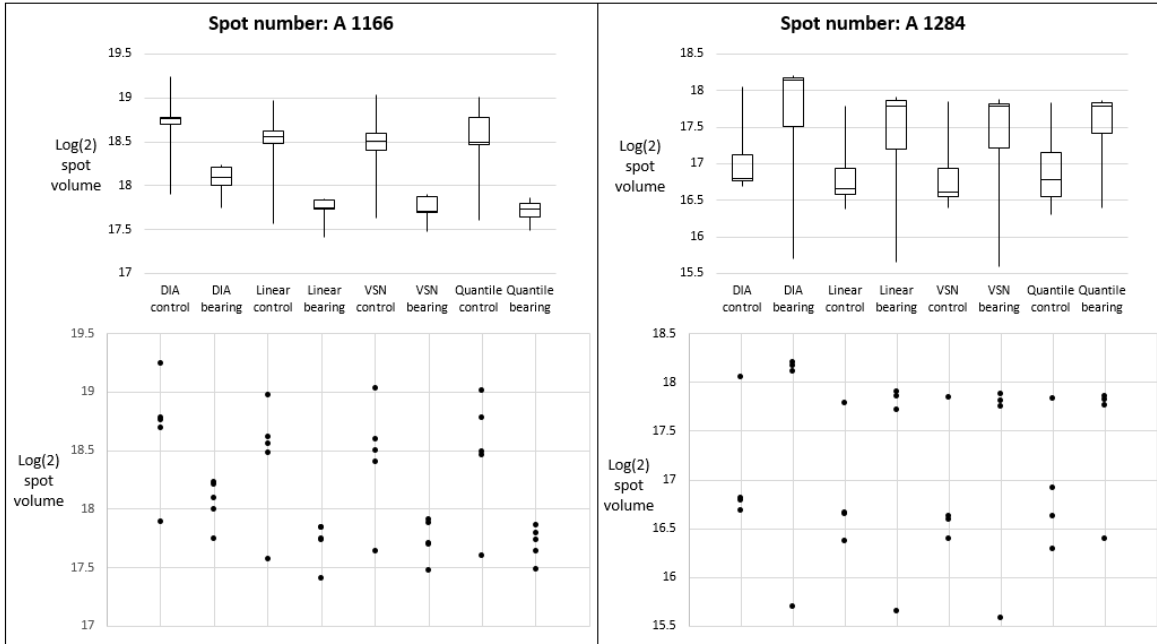
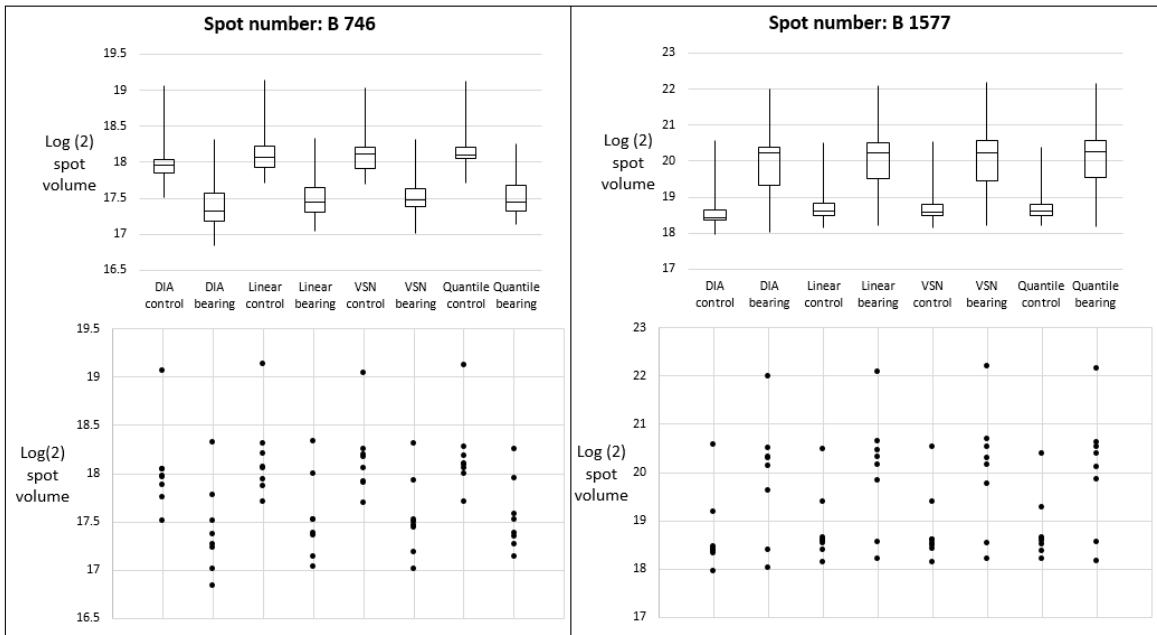


Figure 5-19. Distribution boxplots and scatter plots for FDR spots from DIGE A.

Boxplots (showing quartile data distribution) and scatter plots showing distribution of $\log(2)$ spot volume data for spots from DIGE experiment A that met the FDR calculation requirements of the B&H method when moderate t-test statistics were applied. Note some of the data points overlap in the scatter plots so that two data points appear as one. Spot 1166 had 5 data points for each condition and spot 1284 had only 4 data points for each condition.



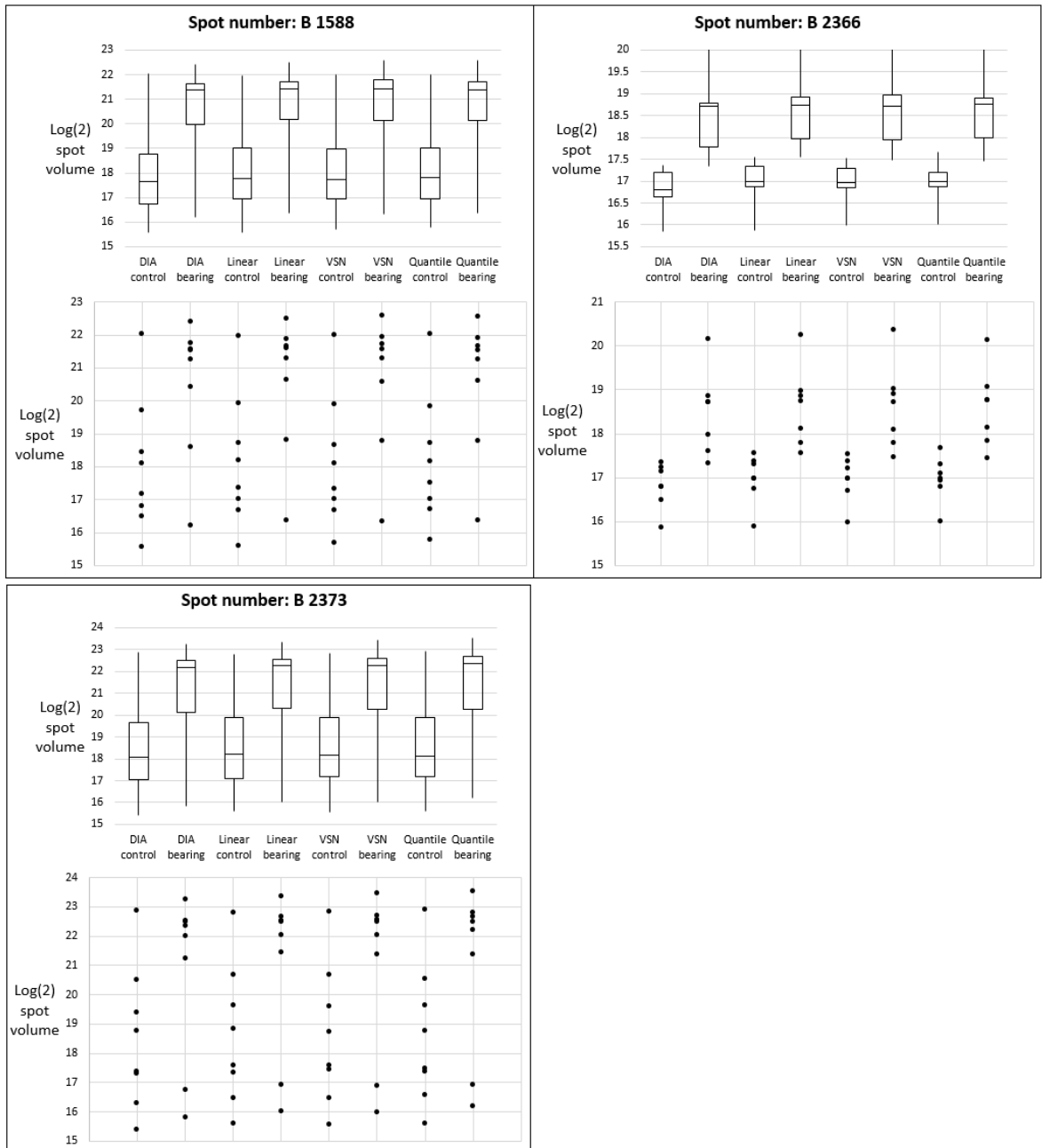


Figure 5-20. Distribution boxplots and scatter plots for FDR spots from DIGE B.

Boxplots (showing quartile distribution) and scatter plots of log(2) spot volume data for spots from DIGE experiment B that met FDR calculation requirements of the B&H method when moderate t-test statistics were applied. Note that the linear normalisation of spot number 2373 did not meet the FDR requirements, but normalisation with other methods did. Note as before some of the data points overlap in the scatter plots so that two data points appear as one. All spots shown here had 8 data points per condition except for spot number 2366 which had 7.

Alternate normalisation methods

Effect of albumin depletion variability

As a check on the variability of albumin depletion on the results obtained from DIGE experiment B, the data from 3 spots determined (initially by visual assessment of gels and subsequently confirmed by MS) to be albumin were removed. These were spot numbers 2302, 2303 and 2377 (see Figure 5-21 for spot positions). The gel data for all spots were then renormalized using two linear methods (by spots present on all gels and by all spots) and the student's t-test results were recalculated. This calculation resulted in only very minor changes in the p values of spots, and no change in the order of spots for spots with p values less than 0.05. The recalculated values were run through the R package 'prot2D' and the same spots were found to have passed the FDR test that passed it without albumin removal. See Table 5-12 for a summary of significant p values (Appendix '[21 - albumin adjustment.xlsx](#)').

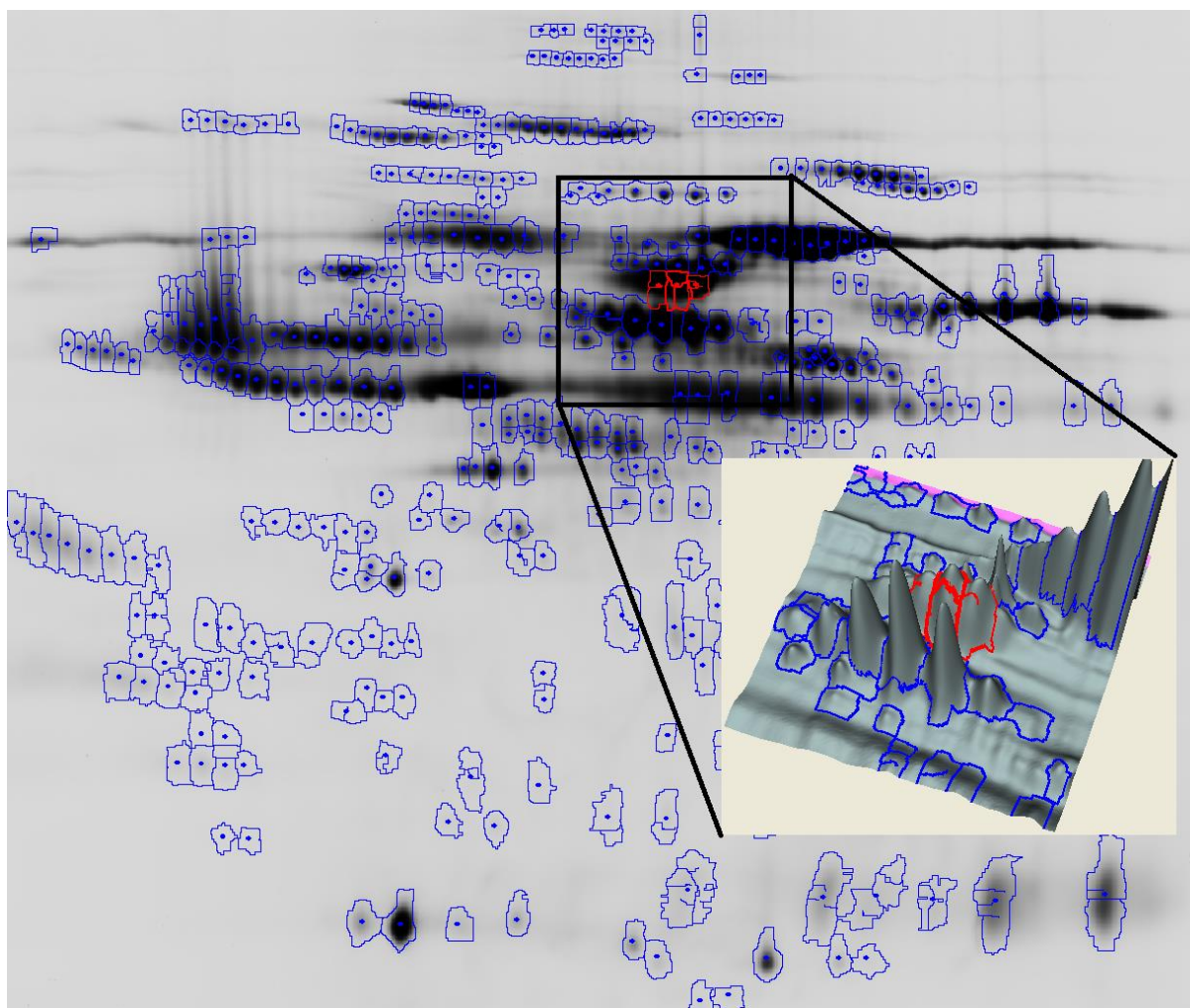


Figure 5-21. Location of albumin spots removed for depletion variability check.

The master gel from DIGE experiment B is shown along with a 3D representation of the central albumin spots as produced by DeCyder 7.0.

Loading control normalisation - using spots with the lowest variation

As a loading control approach is sometimes used for normalisation of proteomics experiments [273] it was decided to trial using spots with low variation as an alternative normalisation method. Spots to use for this normalisation were chosen by virtue of being in the lowest 10% of CVs after linear normalisation using spots present on all gels. It was decided to use spots present on all gels for this calculation, as this should more closely reflect equal protein loading than using all spots. Note that an iterative approach was required as the spots used for normalisation also became adjusted and therefore did not necessarily remain in the group with the lowest variation. After two rounds of adjustment using spots with the lowest 10% of CV from the previous round a point was reached where spots in the lowest 10% of CV didn't change. After standardisation, using standards that were also normalised in the same manner, only four spots had student's t-test p values less than 0.05 (Table 5-12) (Appendix '[22 - lowest CV norm, from spots present on all gels.xlsx](#)'). When this data was run through the R package 'prot2D', it was found that three spots (B1577, B2366 and B 2373) passed the false discovery test. Note that after DIA, VSN and quantile log(2) normalisation, the same three spots also passed the 'prot2D' false discovery test as shown in Table 5-11.

Normalising with all spots – with blanks filled to calculate normalisation factor

A normalisation method where the volumes of all spots were used, but where missing spots were filled with averages that were adjusted by factors calculated from spots present on all gels. The difference between this method and linear normalisation using all spots is that it aims to calculate the total protein load using information from all spots, whereas the other method calculated an average loading ratio for each spot. Thus highly abundant spots contribute more to the calculation (as they do when an equal load calculation is used) whereas in the ratio method each spot contributes equally. The results from both methods were similar, except that once again, only spots B 1577, B 1588 and B 2366 (*i.e.* not B 746) were found to be significantly different between the groups when linear adjusted data was tested for false discovery using 'prot2D' (Table 5-12) (Appendix '[23 - DIGE B renorm by all spots, with blanks filled.xlsx](#)').

	Linear, using all spots	Albumin adjusted	Low CV adjusted	Loading adjusted
Spot ID	T-test <i>p</i> value	T-test <i>p</i> value	T-test <i>p</i> value	T-test <i>p</i> value
B 2366	0.0016	0.0015	0.0043	0.0013
B 746	0.012	0.015	0.013	0.019
B 1629	0.037	0.028	0.10	0.021
B 1071	0.057	0.033	0.16	0.035
B 1611	0.055	0.043	0.11	0.033
B 1588	0.032	0.030	0.033	0.030
B 1577	0.034	0.034	0.051	0.032
B 1635	0.020	0.058	0.070	0.076
B 2338	0.047	0.047	0.061	0.038
B 765	0.054	0.045	0.032	0.053
B 2368	0.050	0.050	0.058	0.049

Table 5-12. Summary table for alternative normalisation methods.

Summary of student's t-test *p* values found for spots in DIGE experiment B that were adjusted by three alternate linear normalisation methods. Spots are shown if one of the *p* values is less than 0.05. The first column (Linear, using all spots) contains the same data as shown in Table 5-8 and Table 5-9.

Correlation with days to prolapse

In order to investigate any relationship between spots that passed the 'prot2D' FDR test and time to prolapse, charts were generated plotting abundance against days to prolapse for prolapsed samples along with boxplots for control data. Note that all the days to prolapse graphs generated here use linear normalised data (from all spots). The charts are shown in Figure 5-22 and Figure 5-25. Correlations were calculated for both DIGE experiments along with their *p* values and are shown for proteins of interest for DIGE experiment A in Table 5-13 and for DIGE experiment B in Table 5-14. None of spots that tested positive in the 'prot2D' FDR test had statistically significant correlations with days to prolapse. Correlation data was generated in R with the use of the 'Hmisc' package [274] (Appendix, '[13 - analyse spots script.txt](#)' for R script).

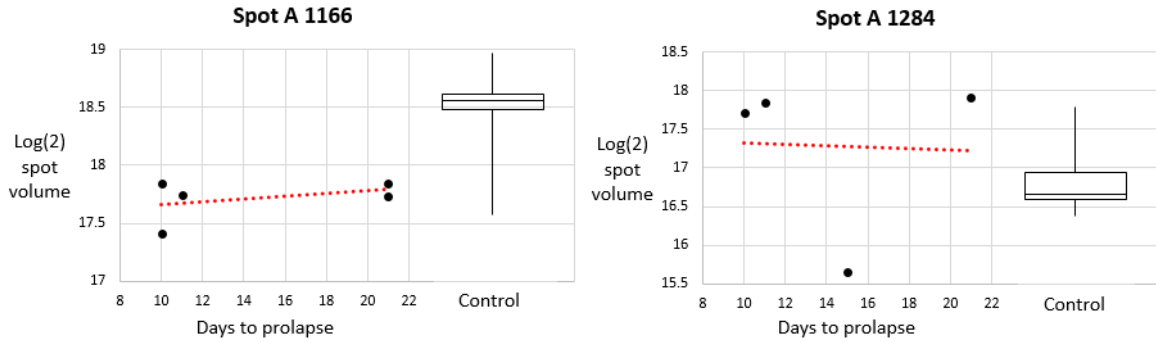


Figure 5-22. Days to prolapse vs abundance & control boxplots for FDR spots, DIGE A.

Log(2) spot volume versus days to prolapse and control boxplots for the two spots found to be significant after FDR testing (after using the moderate t-test) for DIGE experiment A. Fitted lines are shown as a red dotted line.

As well as looking for a correlation with time amongst spots that passed the FDR test, an examination of correlation was undertaken amongst other spots. Spots that had a statistically significant correlation were examined for a fit with controls. Figure 5-23 and Figure 5-24, for DIGE A, and Figure 5-26 and Figure 5-27, for DIGE B, show days to prolapse graphs and control boxplots for spots that have statistically significant correlations with days to prolapse.

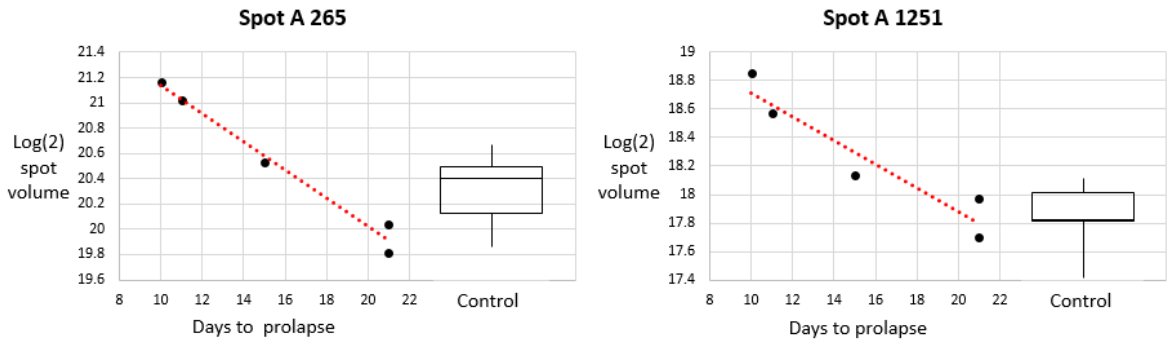


Figure 5-23. Days to prolapse vs abundance & control boxplots for correlated spots, DIGE A.

Log(2) spot volume versus days to prolapse in DIGE experiment A. Spot A 265 was the only spot with a correlation with days to prolapse with $p < 0.01$. For correlations with days with $p < 0.05$ spot A 1251 was the only spot which had a control boxplot that approximated the 3 week sample values.

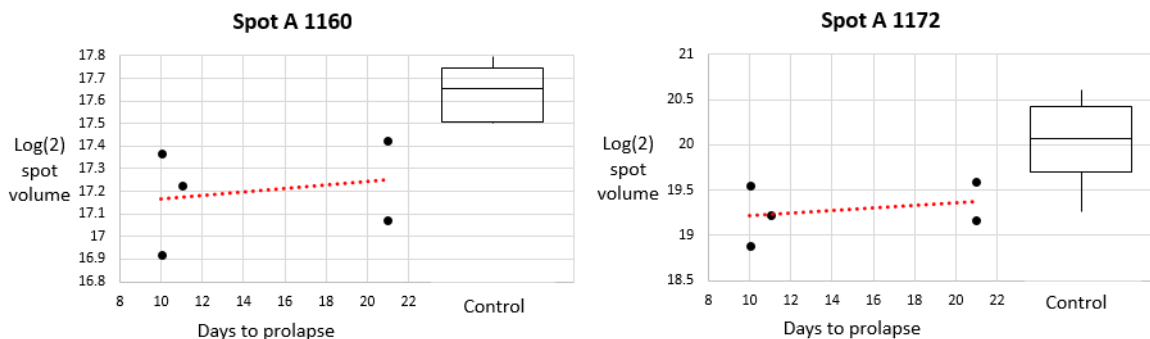


Figure 5-24. Days to prolapse vs abundance and control boxplots where controls fit correlation.
 Log(2) spot volume versus days to prolapse in DIGE experiment A for weak correlations but where control values may correspond to an extension of the fitted line.

Spot ID	Correl.	Correl. p value	T-test p value (days 10-21)	T-test p value (days 10-12)	Matched ID	Correl.	Correl. p value	T-test p value (days 10-21)	T-test p value (days 10-12)
A 265	-0.99	0.001	0.52	0.024	B 268	-0.10	0.81	0.54	0.44
A 262	-0.95	0.011	0.67	0.061	B 272	0.07	0.88	0.52	0.48
A 1487	-0.95	0.013	0.41	0.026	B 276	0.14	0.74	0.64	0.70
A 1251	-0.95	0.015	0.13	0.010	B 1572	0.03	0.94	0.41	0.33
A 672	-0.95	0.015	0.77	0.94	B 747	-0.19	0.68	0.42	0.62
A 957	0.89	0.017	0.66	0.38	NA	NA	NA	NA	NA
A 694	0.92	0.027	0.91	0.27	NA	NA	NA	NA	NA
A 1071	0.96	0.037	0.34	0.11	B 1290	0.37	0.37	0.41	0.61
A 677	-0.90	0.038	0.98	0.63	B 766	-0.36	0.39	0.91	0.78
A 946	0.88	0.051	0.21	0.032	NA	NA	NA	NA	NA
A 1166	0.40	0.50	0.019	0.055	NA	NA	NA	NA	NA
A 1172	0.30	0.63	0.067	0.030	B 2281	0.07	0.87	0.27	0.39
A 1160	0.22	0.73	0.0093	0.0042	B 1417	0.73	0.040	0.46	0.16
A 1284	-0.04	0.96	0.012	0.53	B 1611	-0.57	0.14	0.043	0.055

Table 5-13. Spots from DIGE experiment A that correlate with days to prolapse.

Data is shown for spots from DIGE experiment A that correlate with days to prolapse ($p < 0.05$) along with student's t-test results for all control vs bearing samples (*i.e.* samples from ewes that prolapsed from days 10 – 21) and control vs samples from ewes that prolapsed early *i.e.* days 10-12. Results are in order of correlation p value, spots below the thick line have correlation p values greater than 0.05, but have control values that fit the correlation as shown in Figure 5-22 and Figure 5-24. Linear normalised data used (all spots). Note NA indicates spots not found in DIGE experiment B. Correl. = correlation.

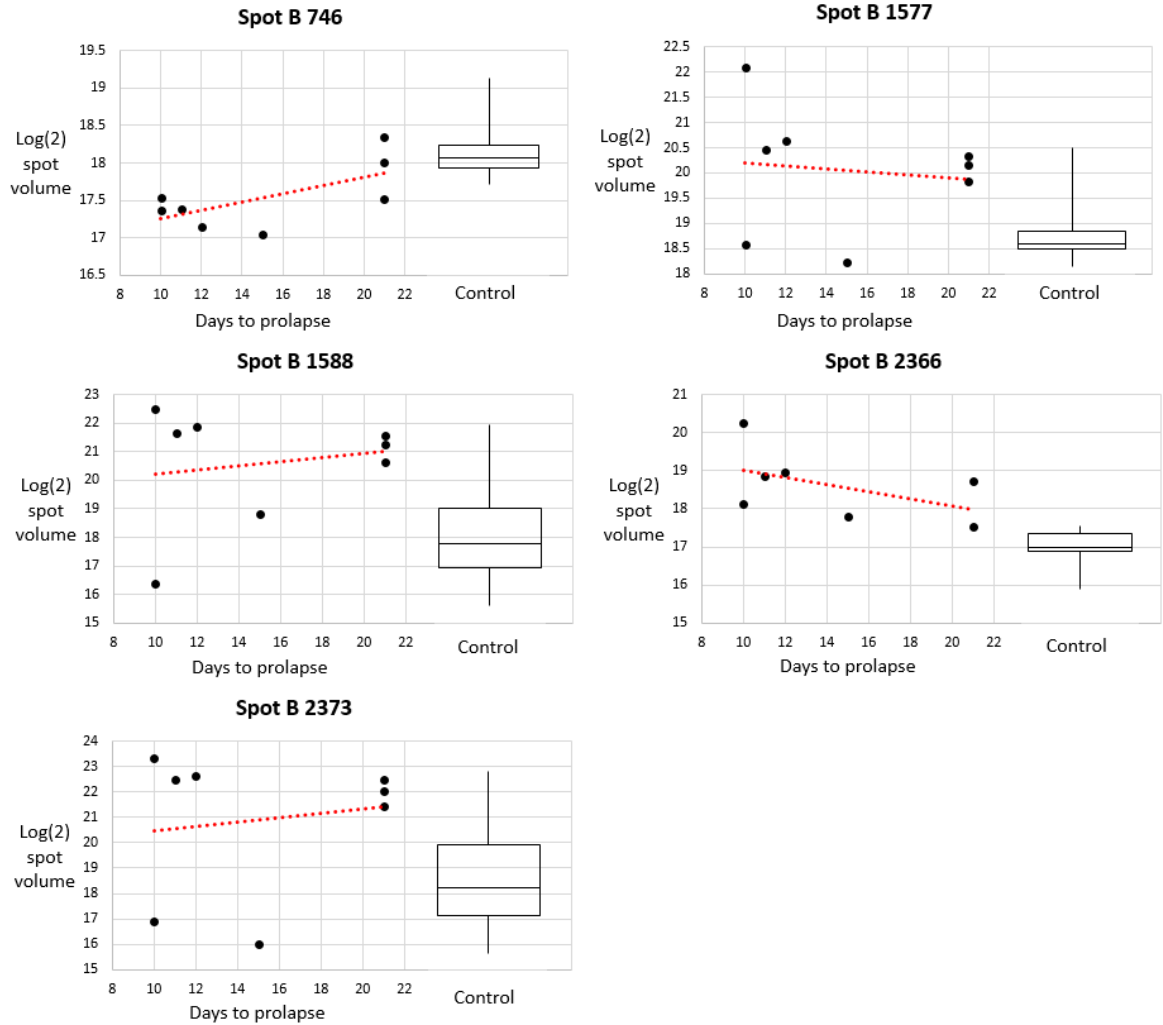
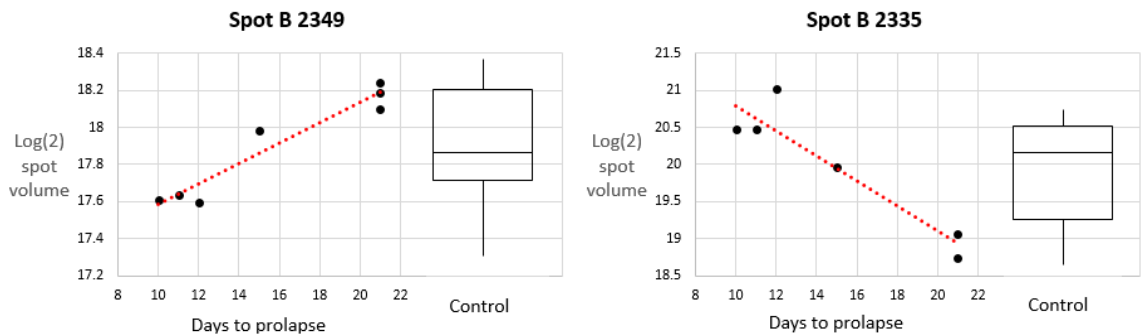


Figure 5-25. Days to prolapse vs abundance and control boxplots for FDR spots, DIGE B.

Log(2) spot volume versus days to prolapse and control boxplots for the five spots found to be significant after FDR testing (after using the moderate t-test) for DIGE experiment B. Fitted lines are shown as a red dotted line. Note that none of the correlations with days had statistical significance at the 0.05 level, see Table 5-14 for details.



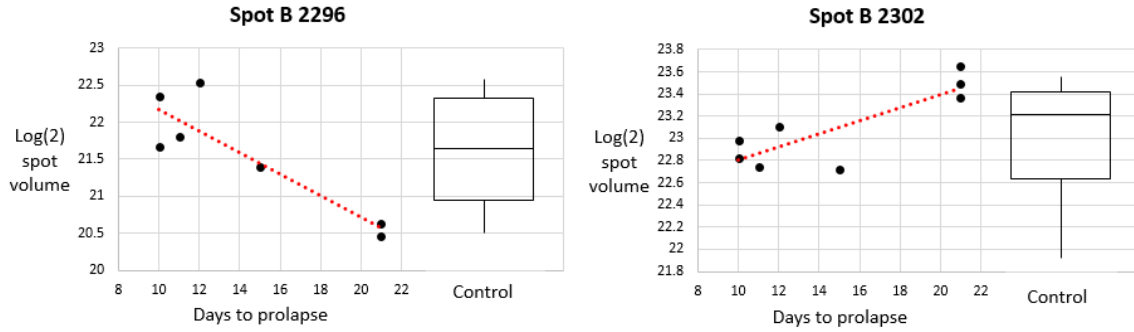


Figure 5-26. Days to prolapse vs abundance and control boxplots for correlated spots, DIGE B. Spots from DIGE experiment B that correlate with days to prolapse ($p < 0.01$) along with box plots for control values.

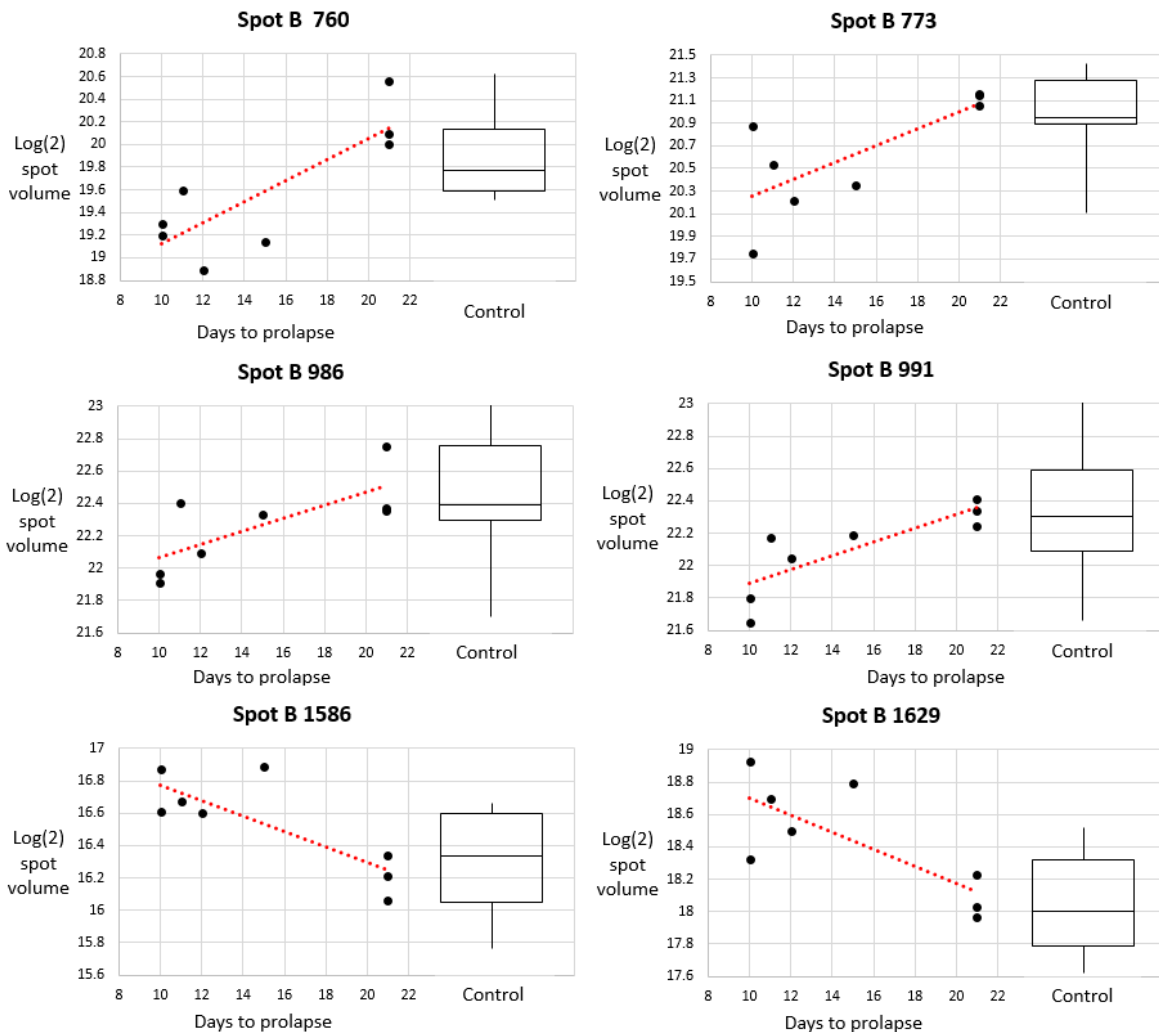


Figure 5-27. Days to prolapse vs abundance and control boxplots for correlated spots, DIGE B. Spots from DIGE experiment B that correlate with days to prolapse ($p < 0.05$) and that have control box plots that approximated the 3 week sample values.

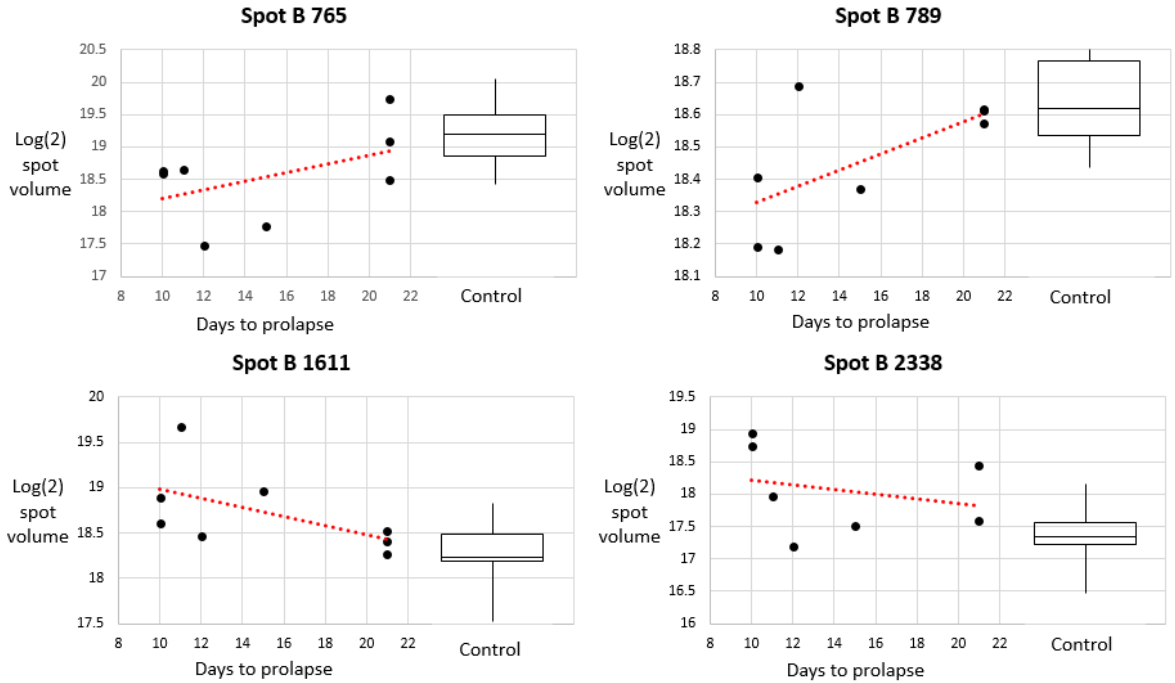


Figure 5-28. Days to prolapse vs abundance and control boxplots for correlated spots, DIGE B. Spots from DIGE B that had a significant difference between controls and the samples from sheep that prolapsed from days 10-12 ($p < 0.05$) and had control boxplots similar to the ewes that prolapsed later.

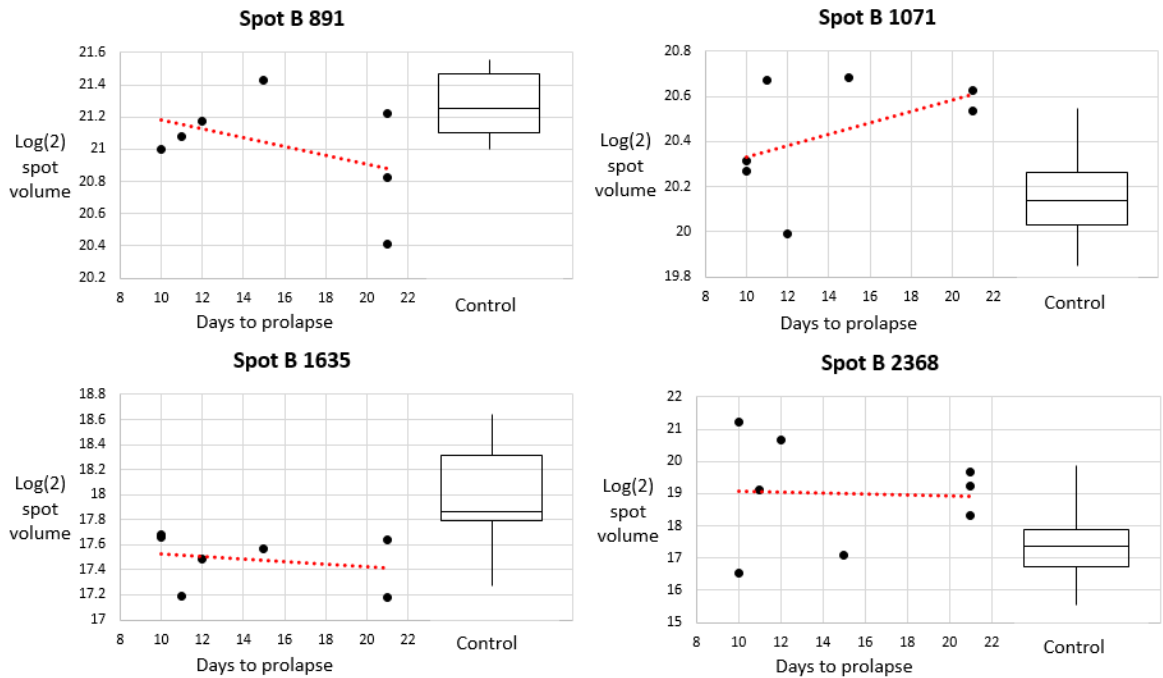


Figure 5-29. Days to prolapse vs abundance and control boxplots for correlated spots, DIGE B. Spots from DIGE experiment B with p values (prolapse vs control) less than 0.05 but with poor fit of control to days to prolapse correlation.

In order to aid the search for spots that correlate with days to prolapse and also fit with control values, samples were searched for a statistically significant difference ($p < 0.05$) between samples that prolapsed first and control values. Positive results are shown in Figure 5-28.

Spots that had a statistically significant difference between all prolapse samples and controls but which did not have control values that fit with a correlation with time to prolapse are shown for completeness in Figure 5-29.

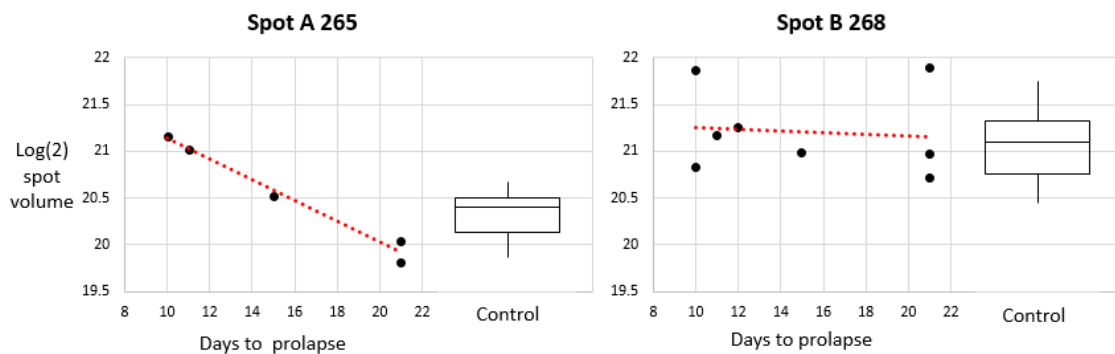
Spot ID	Correl.	Correl. p value	T-test p value (days 10-21)	T-test p value (days 10-12)	Matched ID	Correl.	Correl. p value	T-test p value (days 10-21)	T-test p value (days 10-12)
B 2349	0.96	0.001	0.99	0.23	NA	NA	NA	NA	NA
B 2335	-0.94	0.006	0.89	0.19	NA	NA	NA	NA	NA
B 2296	-0.89	0.007	0.89	0.32	NA	NA	NA	NA	NA
B 2302	0.84	0.009	0.62	0.81	NA	NA	NA	NA	NA
B 991	0.83	0.011	0.26	0.12	A 852	0.72	0.17	0.39	0.14
B 760	0.82	0.013	0.24	0.02	A 668	0.12	0.92	0.86	0.92
B 1586	-0.81	0.014	0.15	0.05	NA	NA	NA	NA	NA
B 2348	0.81	0.015	0.58	0.52	NA	NA	NA	NA	NA
B 446	0.85	0.015	0.33	0.60	A 427	0.73	0.27	0.94	0.66
B 2334	-0.89	0.019	0.72	0.35	NA	NA	NA	NA	NA
B 56	0.82	0.024	0.71	0.22	NA	NA	NA	NA	NA
B 2301	-0.81	0.029	0.79	0.51	NA	NA	NA	NA	NA
B 950	0.76	0.029	0.59	0.23	A 822	-0.40	0.43	0.88	0.75
B 1629	-0.76	0.030	0.04	0.01	NA	NA	NA	NA	NA
B 986	0.75	0.032	0.34	0.16	A 848	0.84	0.16	0.80	0.35
B 773	0.75	0.033	0.17	0.04	A 681	-0.002	1.0	0.91	0.93
B 60	0.74	0.034	0.78	0.27	NA	NA	NA	NA	NA
B 59	0.74	0.036	0.73	0.24	NA	NA	NA	NA	NA
B 992	0.74	0.037	0.25	0.10	A 861	0.62	0.26	0.81	0.41
B 2337	-0.78	0.038	1.00	0.35	NA	NA	NA	NA	NA
B 2297	-0.73	0.040	0.90	0.50	NA	NA	NA	NA	NA
B 1417	0.73	0.040	0.46	0.16	A 1160	0.22	0.72	0.0042	0.0093
B 2317	-0.77	0.042	0.72	0.62	NA	NA	NA	NA	NA
B 1183	-0.72	0.044	0.80	0.67	NA	NA	NA	NA	NA
B 746	0.66	0.075	0.0055	0.012	NA	NA	NA	NA	NA
B 789	0.65	0.08	0.035	0.062	NA	NA	NA	NA	NA
B 1611	-0.57	0.14	0.043	0.055	A 1284	-0.04	0.96	0.53	0.12
B 765	0.49	0.22	0.026	0.054	A 660	0.78	0.43	0.86	0.80
B 2366	-0.50	0.25	0.0009	0.0016	A 1209	0.30	0.70	0.37	0.45
B 2338	-0.27	0.56	0.055	0.047	NA	NA	NA	NA	NA
B 1588	0.19	0.65	0.12	0.032	A 1490	0.14	0.78	0.50	0.46
B 2373	0.16	0.71	0.113	0.098	A 1493	-0.10	0.88	0.57	0.16
B 1577	-0.12	0.78	0.028	0.034	A 1268	0.10	0.87	0.20	0.37

Table 5-14. Spots from DIGE experiment B that correlate with days to prolapse.

Spots from DIGE experiment B that correlate with days to prolapse ($p < 0.05$) along with student's t-test p value results for all control vs bearing samples (*i.e.* that prolapsed from days 10 – 21) and control vs samples that prolapsed early *i.e.* days 10-12. Results are in order of correlation p value, spots below the thick line have correlation p values greater than 0.05, but have control values that fit the correlation as shown in Figure 5-25 and Figure 5-28. Linear normalized data was used (all spots). Highlighted in bold are spots with both statistically significant correlations for correlation with time to prolapse and for t-test p values for early prolapsed samples (days 10-12 vs controls), $p < 0.05$. Correl. = correlation. As in the plotted charts linear normalised data was used (all spots).

Spots of interest from DIGE A and matched spots in DIGE B

Levels of abundance and days to prolapse for spots of interest from DIGE A and matching spots from DIGE B are shown in Figure 5-30. Only one of the two spots that passed the 'prot2D' FDR test is shown (A 1284) as the other spot (A 1166) was not present in either DIGE B or the MS prep gels. A spot from DIGE A that had a p value less than 0.05 and with the lowest p value in DIGE B is shown (A 1172) as well as three other spots where control values may correlate with days to prolapse as shown in Figure 5-23 and Figure 5-24. The spot with the lowest p value in DIGE A (A 1160) was faintly present in DIGE B (B 1417) but was not visible on MS prep gels and is shown here for completeness. The spot abundance levels for spots shown in Figure 5-30 are similar between the two sets of data, with most control and trend data broadly following the same pattern between the DIGE experiments. Note it was initially thought that spot (B 891) may constitute a spot of interest as it appeared in both experiments after DIA normalisation although the p value was not less than 0.05 and had a positive result with quantile normalisation by volume (see Table 5-9). It was decided, however, that quantile normalisation by volume alone did not justify its inclusion (see chapter 4).



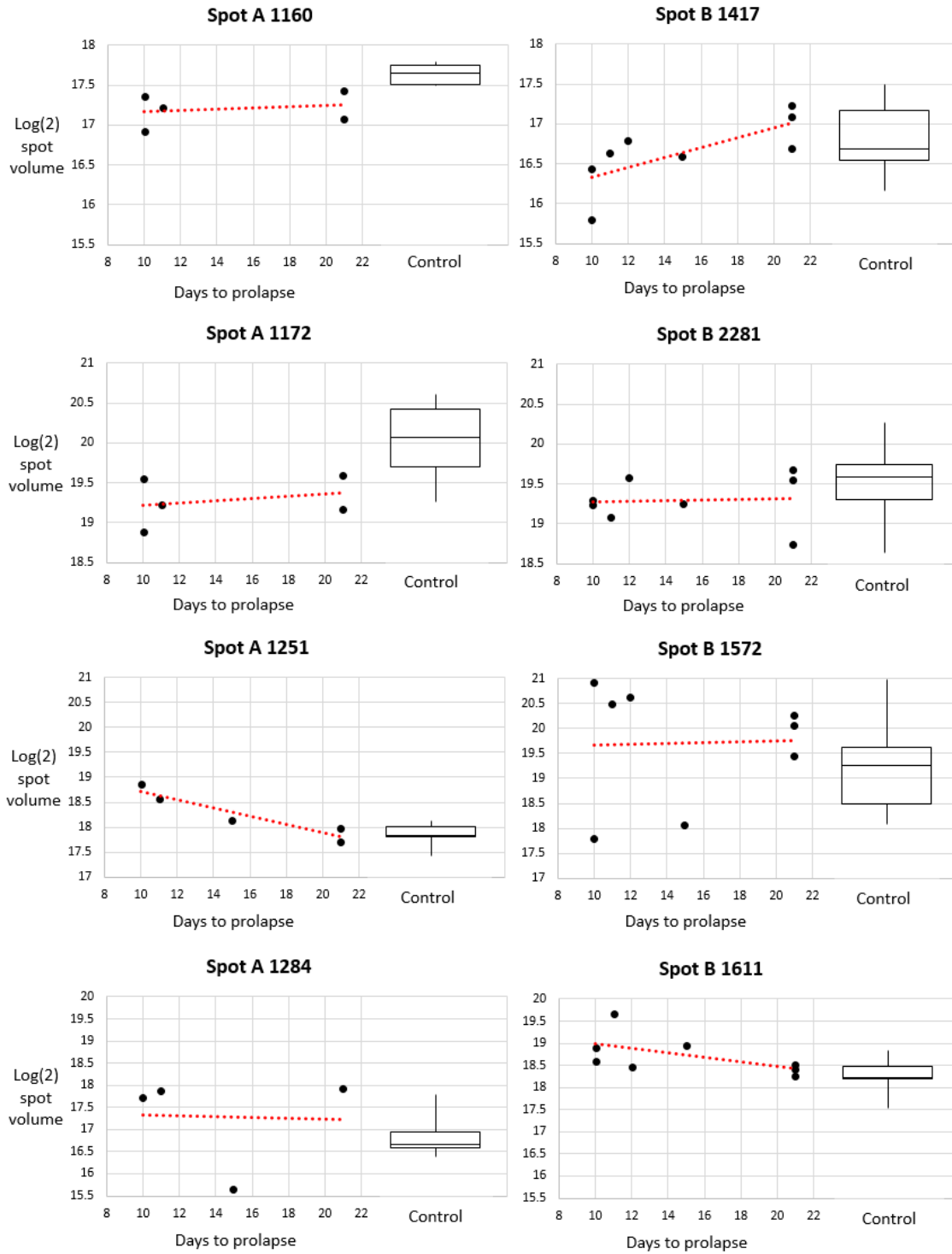
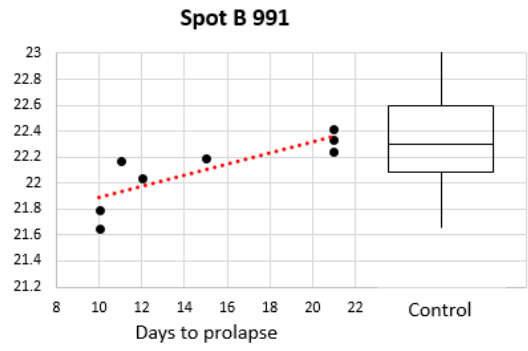
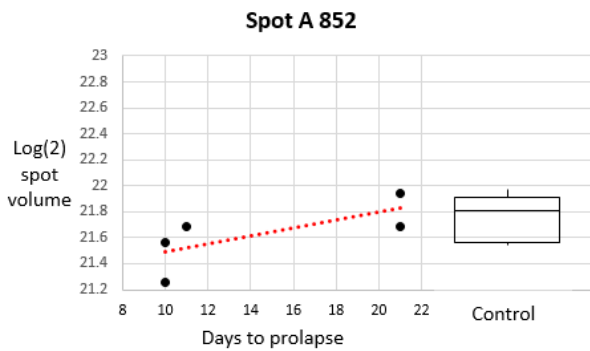
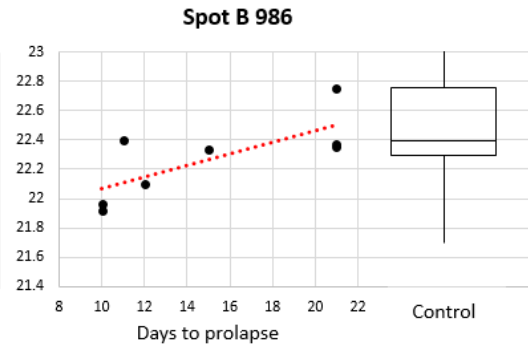
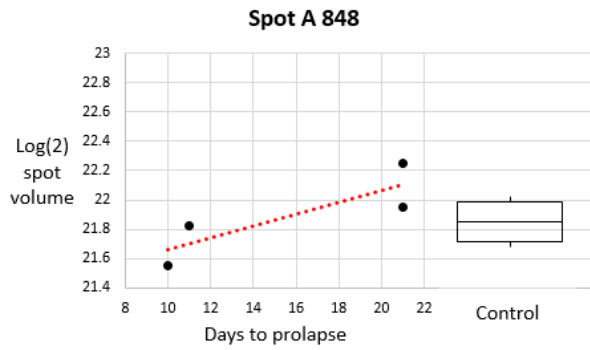
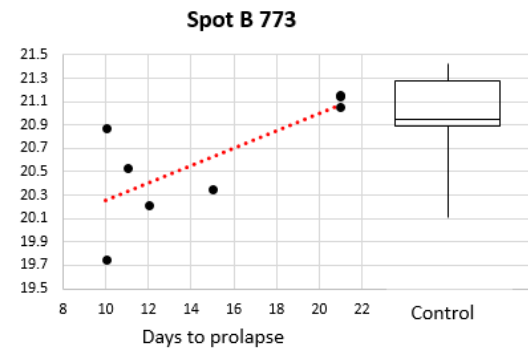
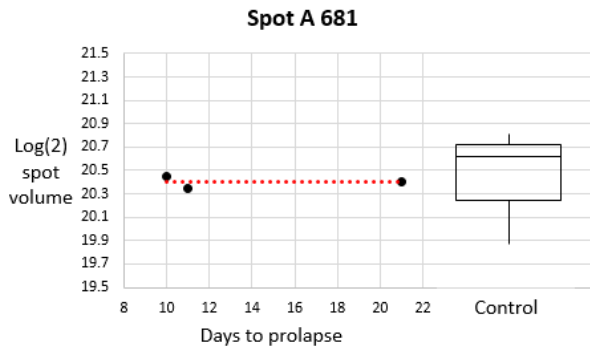
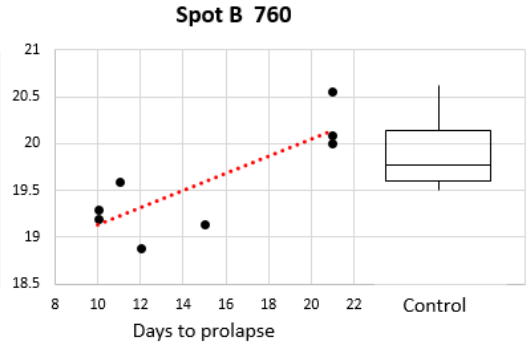
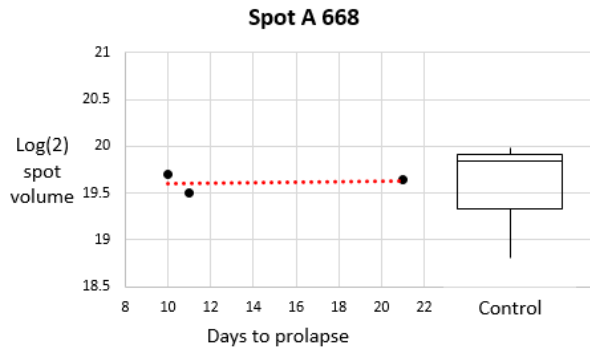
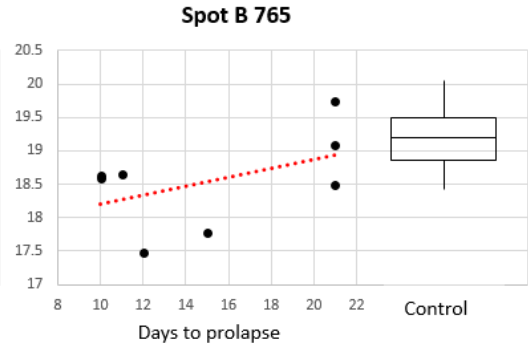
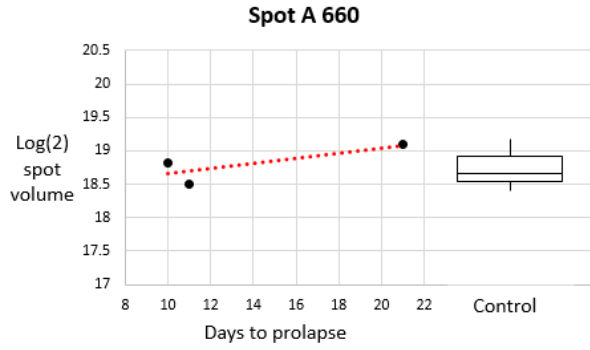


Figure 5-30. Days to prolapse vs abundance and control boxplots for matching spots.

Spot abundance for spots of interest found in DIGE A in comparison to the levels found for matched spots in DIGE B. On the left are DIGE A spots and on the right are the matching spots from DIGE B.



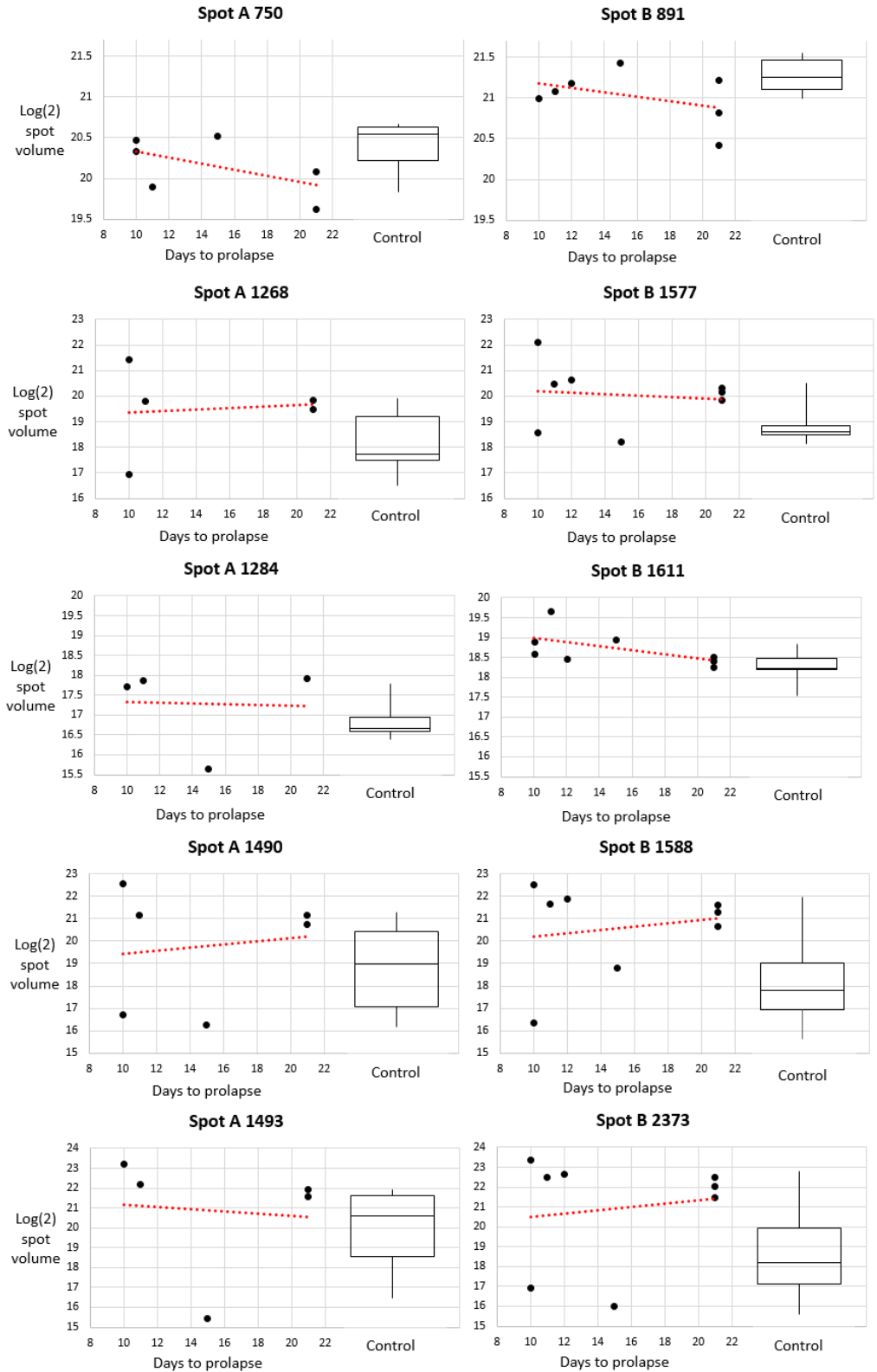


Figure 5-31. Days to prolapse vs abundance and control boxplots for matching spots.

Spot abundance for spots of interest found in DIGE B in comparison to the levels found for matched spots in DIGE A. On the left are DIGE A spots and on the right are the matching spots from DIGE B.

Spots of interest from DIGE B and matched spots in DIGE A

Levels of abundance and days to prolapse for spots of interest from DIGE B and matching spots from DIGE A are shown in Figure 5-31. Note that only spots of interest from DIGE B with matches to spots in DIGE A are shown. One matched spot is repeated from Figure 5-30 (B 1611) as it is a spot of interest in both experiments. Spots shown in Figure 5-26 (spots in DIGE B that correlate with days to prolapse with $p < 0.01$) were not included as the control values did not fit into an extension of the correlation.

Spots of interest for identification by mass spectrometry

Spot ID (DIGE B)	FDR	$p < 0.01$	$0.01 > p > 0.05$	Control fits correlation with days	Spot of interest in DIGE A	Ratio (linear norm.)
B 746	√	VSN, Q	DIA, Lin, Al adj, CV adj, L adj	√		-1.5
B 760				√		-1.2
B 765			Al adj, CV adj	√		-1.5
B 773				√		-1.2
B 1071			DIA, VSN, Al adj, L adj			1.2
B 1417					√	-1.1
B 1577	√		DIA, Lin, VSN, Q, Al adj, L adj	√		2.7
B 1588	√		DIA, Lin, VSN, Q, Al adj, CV adj, L adj			3.4
B 1611			DIA, Al adj, L adj	√	√	1.4
B 1629			DIA, Lin, VSN, Al adj, L adj	√		1.3
B 1635			DIA, Lin, VSN, Q			-1.5
B 2338			Lin, VSN, Q, Al adj, L adj	√		1.7
B 2366	√	DIA, Lin, VSN, Q, Al adj, CV adj, L adj		√		3.6
B 2373	√					3.4

Table 5-15. Spots of interest.

Spots of interest for identification by mass spectrometry and reasons for inclusion. Acceptance that the control fits with correlation with days does not imply that the correlation had a particular significance level as a fit with control values was also required (see Table 5-14 for details). DIA = normalisation in DeCyder 7.0 prior to manual spot exclusion, Lin = linear normalisation by all spots, VSN = variance stabilising normalisation, Q = quantile normalisation of log(2) data, Al adj = linear adjustment after albumin data removal, CV adj = adjustment by spots with the lowest 10% of CVs after linear normalisation, L adj = a loading adjustment that replaces missing values with adjusted values. Ratio data is also included and was calculated using linear normalisation from all spots.

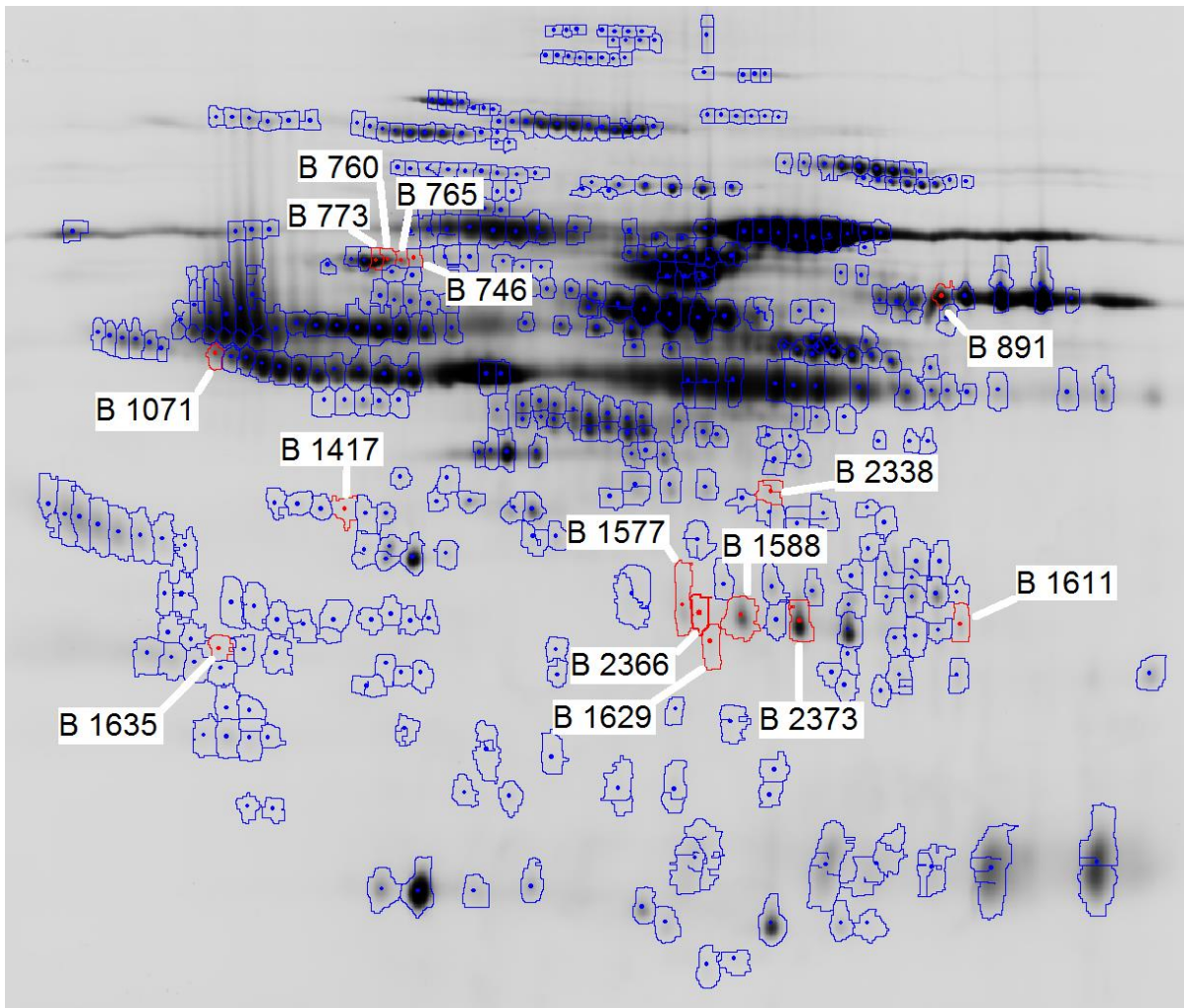


Figure 5-32. The master gel from DIGE B showing positions of the spots of interest.

These spots are listed in Table 5-15. Note B891 was removed as a spot of interest after renormalisation.

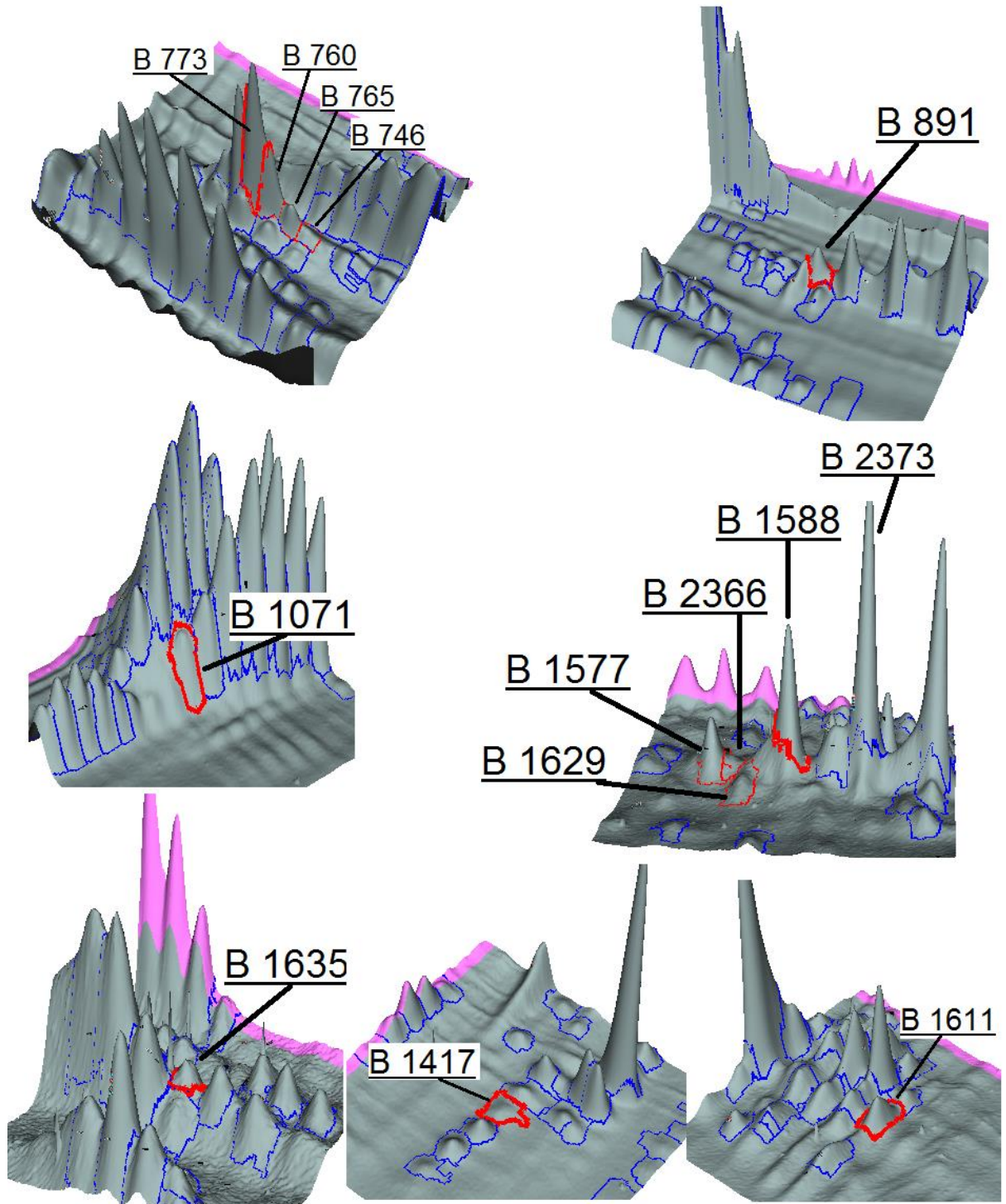


Figure 5-33. Spots of interest in 3D view.

Images were taken from the 3D viewer in the BVA module of DeCyder 7.0, DIGE B, where the vertical dimension reflects stain intensity. The 3D view is orientated to facilitate viewing spots of interest. Note the pink banner indicates which gel the image is taken from, in this case the master gel, as well as helping to indicate the degree of horizontal rotation used for the 3D image.

Mass spectrometry (MS)

Spots were picked from the colloidal Coomassie stained gels (Figure 5-41) with a Proteome Works Plus spot cutter (Bio-Rad) that was set up within a fluorescent enclosure. The spot cutter was calibrated according to the manufacturer's instructions and fitted with a 14 gauge cutting tip. The cutting area had a cutting mat and a clean cutting sheet inserted. Gels were placed on the cutting sheet along with two stainless steel holding bars to ensure it did not move during cutting. Once in place the gel was liberally covered with MQ water to assist spot pick up. Gels were imaged and spots of interest marked for picking. The spot cutter removed the required spots and placed them into water filled wells of a 96 well plate.

The gel spots were then transferred into 0.5 mL protein LoBind tubes (Eppendorf) and destained with several 200 μ L washes of 50% methanol, 5% acetic acid. The strongly stained spots were sonicated in a sonicating water bath and heated at 37°C for 30 minutes to assist the destaining process. Once destained, the gel pieces were dehydrated by the addition of 200 μ L acetonitrile and after 5 minutes incubation, the solution was carefully removed with a pipette. They were then dried in a Savant DNA110 SpeedVac for 5 minutes before being rehydrated in 200 μ L of digest buffer (50 mM ammonium bicarbonate, 1 mM calcium chloride) for 10 minutes. Trypsin was prepared by dissolving 20 μ g trypsin (Sigma) in 100 μ L of 1mM HCl to make a stock solution containing 200 ng/ μ L trypsin. The trypsin stock solution was diluted 10x in digest buffer to make up a working solution of 20 ng/ μ L trypsin. Spots were dehydrated as before and then 30 μ L of the trypsin working solution (containing 600 ng trypsin) was added and the sample placed on ice for 10 minutes for rehydration, before being incubated overnight at 37°C.

In order to extract peptides from the gel spots 30 μ L of extraction buffer (50% acetonitrile, 5% formic acid and 45% distilled water) was added to each tube then incubated for 10 minutes at room temperature with occasional vortexing. The supernatants were transferred into new 0.5 mL LoBind tubes (Eppendorf) and another 30 μ L of extraction buffer was added to each gel spot then incubated for a further 10 minutes (with vortexing). The volume in each peptide extraction mix was reduced to approximately 20 μ L in a SpeedVac. The samples were then centrifuged at 14,000 *g* for 15 minutes, to pellet any insoluble material, and the supernatants transferred to 0.1 mL glass micro inserts, which were then placed into 2 mL glass vials with ultraclean caps (with rubber centre holes) ready for mass spectrometry.

Samples were analysed by the Massey University Mass spectrometry Centre on a Thermo Scientific Q Exactive Plus™ Hybrid Quadrupole-Orbitrap™ mass spectrometer coupled to a nanoflow capillary peptide HPLC. Samples passed through a reversed phase peptide trap for desalting before being separated on a 50 cm C18 Acclaim reversed phase column. This was coupled to an on-line Q Exactive Plus mass spectrometer equipped with higher-energy collisional dissociation (HCD), an Orbitrap mass analyser and a Nano Flex ion source (ThermoFisher Scientific, Waltham, MA USA).

Samples were run using data dependent acquisition for tandem MS data. MS1 scans were collected over a mass range of 375-1,600 m/z at a resolution of 70,000 and MS2 data collected with a resolution of 17,500. Fragment ion data was taken with a resolution setting of 17,500. The top ten most abundant ions were selected for fragmentation and fragment ion spectra were detected at 1.4 m/z ion width (Appendix [‘24 - LCMS description for Stuart Brown.docx’](#)).

A pecora (even toed ruminants) protein database was generated and downloaded from the NCBI database on the 23/8/2018. A contaminant database was obtained from WEHI (Walter + Eliza Hall Institute of Medical Research). Both databases were searched with Proteome Discoverer 2.20.388 (Thermo Fisher Scientific) with the following amino acid modifications. A fixed modification on cysteine of +105.058 Da (alkylation with 4-vinylpyridine). Variable modifications were methionine +15.995 Da (oxidation), asparagine and glutamine +0.984 Da (deamidation), histidine, serine, threonine and tyrosine +79.966 Da (phosphorylation) and N-terminal acetylation +42.011 Da. The search was done using trypsin as the enzyme allowing for 2 missed cleavages, a minimum peptide length of 7 residues, a maximum of 144 residues, a precursor mass tolerance of 10 ppm and a fragment mass tolerance of 0.02 Da. A decoy database search (using reverse sequences) was done with the false discovery rate set to 1% or less. Protein IDs from the PD Sequest HT search (with hits in *Ovis aries* and a minimum of two distinct peptides) are shown in Table 5-16 to Table 5-20 (for coverage see Appendix folder [‘25 - MS data using Proteome Discoverer 2.2’](#)).

MS results were also analysed using the TPP search engine [275]. An *Ovis aries* protein database was generated and downloaded from the NCBI database on the 21/5/2018. The resultant *Ovis aries* database, along with a previously generated contaminant database was searched using a LabKey

server and the TPP search engine with the same amino acid modifications used for the Proteome Discoverer search.

In LabKey Peptide Prophet was used to determine sensitivity from the minimum probability of error. A minimum error probability of 0.05 was chosen and the sensitivity estimated from the Peptide Prophet score for each sample. This sensitivity was copied into the peptide filter with a filter type of 'greater than or equal to'. With peptides thus filtered the protein (legacy) report was used to determine which proteins matched the MS data. Samples of the peptide spectral matches (PSM) were examined to ensure they reflected the peptides belonging to the specified protein. As an example, the spectrum from peak m/z 674.1074 originating from spot B 2373 is shown in Figure 5-34. Most peaks are covered by peptides found in the sequence. Also note there are more peaks found that are +1 ions, less +2 ions and only one +3 ion was seen. A summary of LabKey results can be seen in Appendix folder '[26 - MS data using labkey](#)' and are almost identical to those found using PD, with only the percentage coverage and number of distinct peptides being different. Note that in Peptide Prophet the terms peptides and unique peptides correspond to PSMs (peptide spectrum matches, which includes redundant peptides) and distinct peptides respectively in PD.

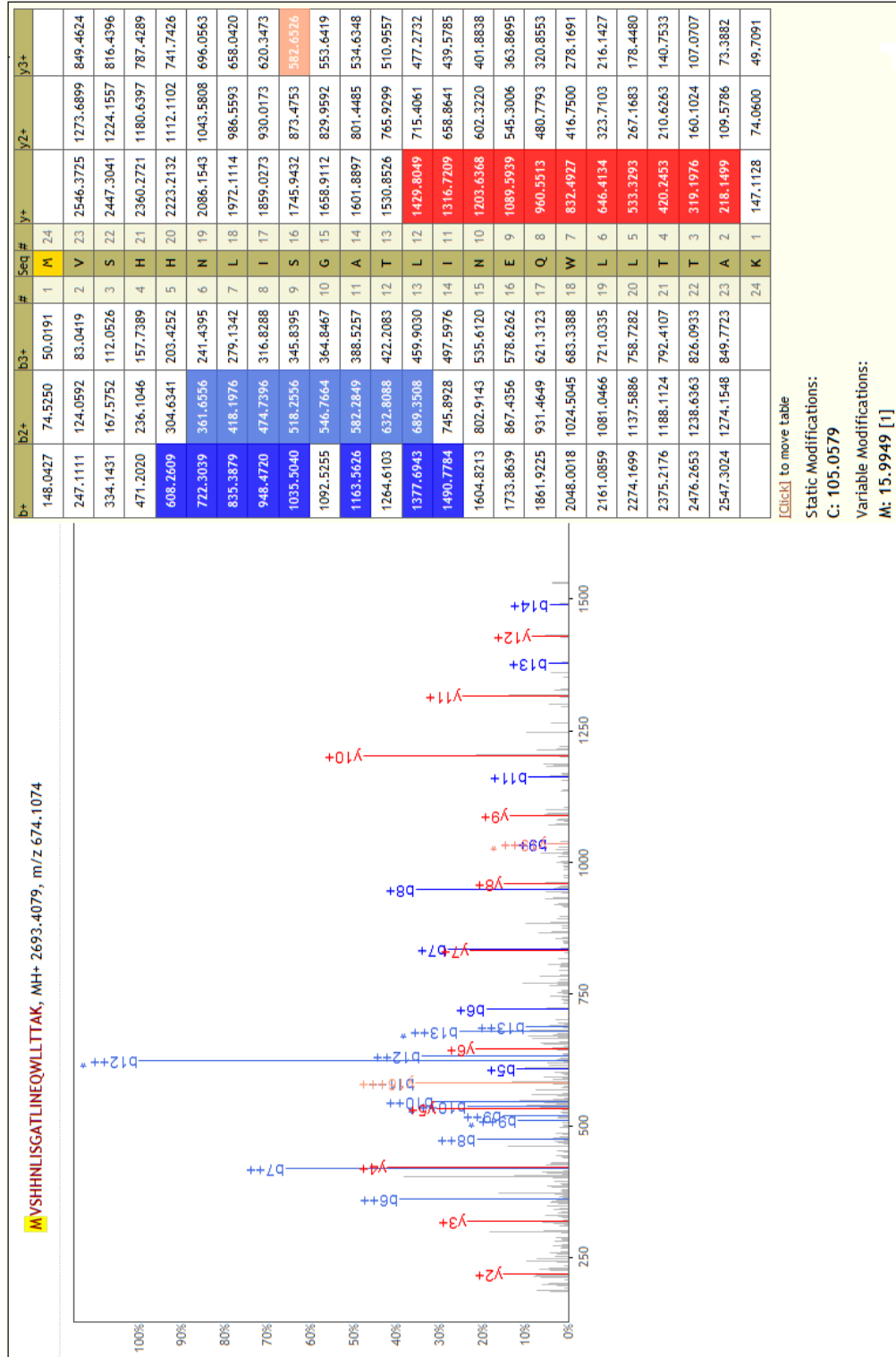


Figure 5-34. Example MSMS spectrum.

This MSMS spectrum of m/z 674.1074 was obtained from the tryptic digest of spot B 2373. B ions are highlighted (in the spectra as well as the sequence) in dark blue and y ions in dark red.

Unidentified ions are grey. As well as the modifications noted at the bottom of the table and covered in the text, a neutral loss of NH₃ is marked with *.

Protein	Cal. Mass (kDa)	Cal. PI	Distinct peptides	AA coverage	PSM's	Sum PEP score	Score Sequest HT	Description
MS spot 1								
P14639.1	69.1	6.15	45	68%	2053	439.9	4112	Albumin (<i>Ovis aries</i>)
MS spot 2								
P14639.1	69.1	6.15	44	67%	2733	NA	5320	Albumin (<i>Ovis aries</i>)
MS spot 3								
P14639.1	69.1	6.15	62	76%	3801	896.7	9461	Albumin (<i>Ovis aries</i>)
MS spot 4								
P14639.1	69.1	6.15	47	69%	2844	648.2	5537	Albumin (<i>Ovis aries</i>)
MS spot 5								
P14639.1	69.1	6.15	41	64%	1717	NA	3163	Albumin (<i>Ovis aries</i>)

Table 5-16. Protein IDs for spots 1-5.

See Figure 5-35 for locations of spots. Cal. Mass = calculated mass, Cal. PI = calculated isoelectric point, Distinct peptides = unique peptides, PSM's = number of peptide spectrum matches, Sum PEP score = sum posterior error probability (only available for some results), Score Sequest HT = sum of the Xcorr peptide scores from the Sequest HT search.

Protein	Cal. Mass (kDa)	Cal. PI	Distinct peptides	AA coverage	PSM's	Sum PEP score	Score Sequest HT	Description
Spot B 765 (MS spot 6)								
XP_014955832.1	44.1	6.92	19	48%	750	175.1	1789	Predicted: Low quality protein: alpha-1B-glycoprotein X1 (<i>Ovis aries</i>)
P14639.1	69.1	6.15	22	45%	316	117.6	607	Albumin (<i>Ovis aries</i>)
MS Spot 7								
XP_014955832.1	44.1	6.92	19	48%	746	NA	1804	Predicted: Low quality protein: alpha-1B-

								glycoprotein X1 (<i>Ovis aries</i>)
P14639.1	69.1	6.15	17	40%	185	NA	331	Albumin (<i>Ovis aries</i>)
MS spot 8								
XP_014955832.1	44.1	6.92	19	48%	782	205.5	1877	Predicted: Low quality protein: alpha-1B-glycoprotein X1 (<i>Ovis aries</i>)
P14639.1	69.1	6.15	18	40%	195	98.8	350	Albumin (<i>Ovis aries</i>)

Table 5-17. Protein IDs for spots close to and including B 765.

See Figure 5-35 for locations of spots and Table 5-16 for abbreviations.

Protein	Cal. Mass (kDa)	Cal. PI	Distinct peptides	AA coverage	PSM's	Sum PEP score	Score Sequest HT	Description
MS spot 9								
P29701.1	45.4	5.38	12	43%	522	NA	1364	Alpha-2-HS-glycoprotein (<i>Ovis aries</i>)
P14639.1	69.1	6.15	2	4%	5	NA	4	Albumin (<i>Ovis aries</i>)
MS spot 10								
P29701.1	45.4	5.38	11	43%	416	58.6	1234	Alpha-2-HS-glycoprotein (<i>Ovis aries</i>)
P14639.1	69.1	6.15	2	4%	5	3.3	8	Albumin (<i>Ovis aries</i>)
MS spot 11								
P29701.1	45.4	5.38	11	43%	315	NA	790	Alpha-2-HS-glycoprotein (<i>Ovis aries</i>)
XP_011954394.1	46.6	5.73	7	29%	19	NA	22	Predicted: Serpin A3-8 isoform X1 (<i>Ovis aries</i>)
MS spot 12								
P29701.1	45.4	5.38	12	43%	437	NA	1138	Alpha-2-HS-glycoprotein (<i>Ovis aries</i>)
XP_011954394.1	46.6	5.73	11	42%	53	NA	81	Predicted: Serpin A3-8 isoform X1 (<i>Ovis aries</i>)

P14639.1	69.1	6.15	2	4%	4	NA	2	Albumin (<i>Ovis aries</i>)
MS spot 13								
P29701.1	45.4	5.38	11	43%	207	NA	484	Alpha-2-HS-glycoprotein (<i>Ovis aries</i>)
XP_011954394.1	46.6	5.73	9	28%	35	NA		Predicted: Serpine A3-8 isoform X1 (<i>Ovis aries</i>)
Spot B 1071 (MS spot 14)								
XP_011954394.1	46.6	5.73	16	57%	76	NA	147	Predicted: Serpine A3-8 isoform X1 (<i>Ovis aries</i>)
P29701.1	45.4	5.38	11	43%	162	NA	415	Alpha-2-HS-glycoprotein (<i>Ovis aries</i>)

Table 5-18. Protein IDs for spots close to and including B 1071.

See Figure 5-35 for locations of spots and Table 5-16 for abbreviations.

Protein	Cal. Mass (kDa)	Cal. PI	Distinct peptides	AA coverage	PSM's	Sum PEP score	Score Sequest HT	Description
Spot B 2373 (MS spot 15)								
XP_011966076.1	46.2	7.74	16	49%	526	NA	1384	Predicted: haptoglobin (<i>Ovis aries musimon</i>)
P14639.1	69.1	6.15	2	4%	7	NA	9	Albumin (<i>Ovis aries</i>)
Spot B 1588 (MS spot 16)								
XP_011966076.1	46.2	7.74	19	51%	911	NA	2275	Predicted: haptoglobin (<i>Ovis aries musimon</i>)
P14639.1	69.1	6.15	2	4%	8	NA	7	Albumin (<i>Ovis aries</i>)
Spot B 1577 (MS spot 17)								
XP_011966076.1	46.2	7.74	19	51%	317	67.1	892	Predicted: haptoglobin (<i>Ovis aries musimon</i>)

Table 5-19. Protein IDs for protein spots B 2373, B 1588 and B 1577.

See Figure 5-35 for locations of spots and Table 5-16 for abbreviations.

Protein	Cal. Mass (kDa)	Cal. PI	Distinct peptides	AA coverage		PSM's	Sum PEP score	Score Sequest HT	Description
Spot B 891 (MS spot 18)									
XP_004017.232.2	91.8	6.14	28	30%		1059	215.1	2077	Predicted: fibrinogen alpha chain isoform X1 (<i>Ovis aries</i>)
P14639.1	69.1	6.15	2	4%		5	5.2	7	Albumin (<i>Ovis aries</i>)

Table 5-20. Protein IDs for protein spot B 891.

See Figure 5-35 for locations of spots and Table 5-16 for abbreviations.

The protein spots identified by mass spectrometry were also found on the published sheep serum 2D map [170], and were in good agreement in terms of location with respect to isoelectric point and molecular weight (Figure 5-36 and Figure 5-37).

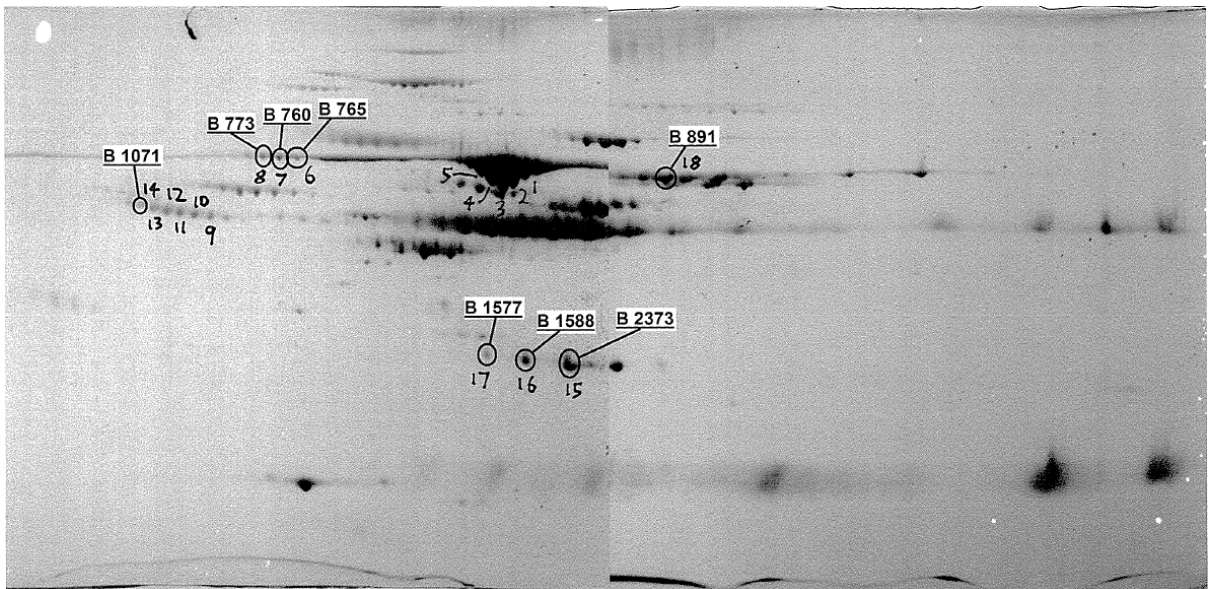


Figure 5-35. Locations of spots extracted for mass spectrometry.

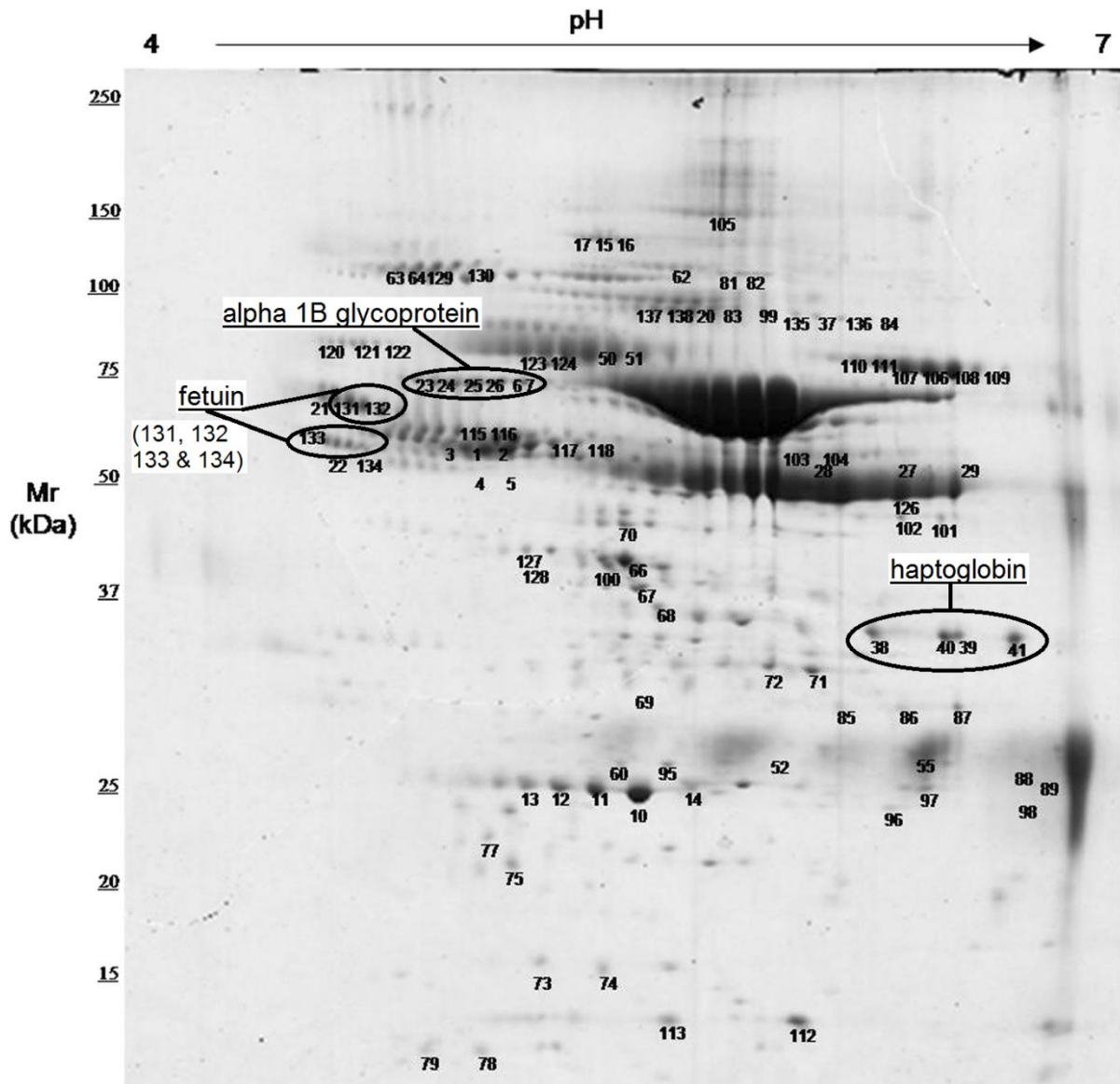


Figure 5-36. 2D reference map of sheep serum proteins, pH 4-7 [170].
Proteins of interest from the present study are labelled.

differentially regulated as discussed earlier. The positions of the globally quantified spots are shown in Figure 5-38.

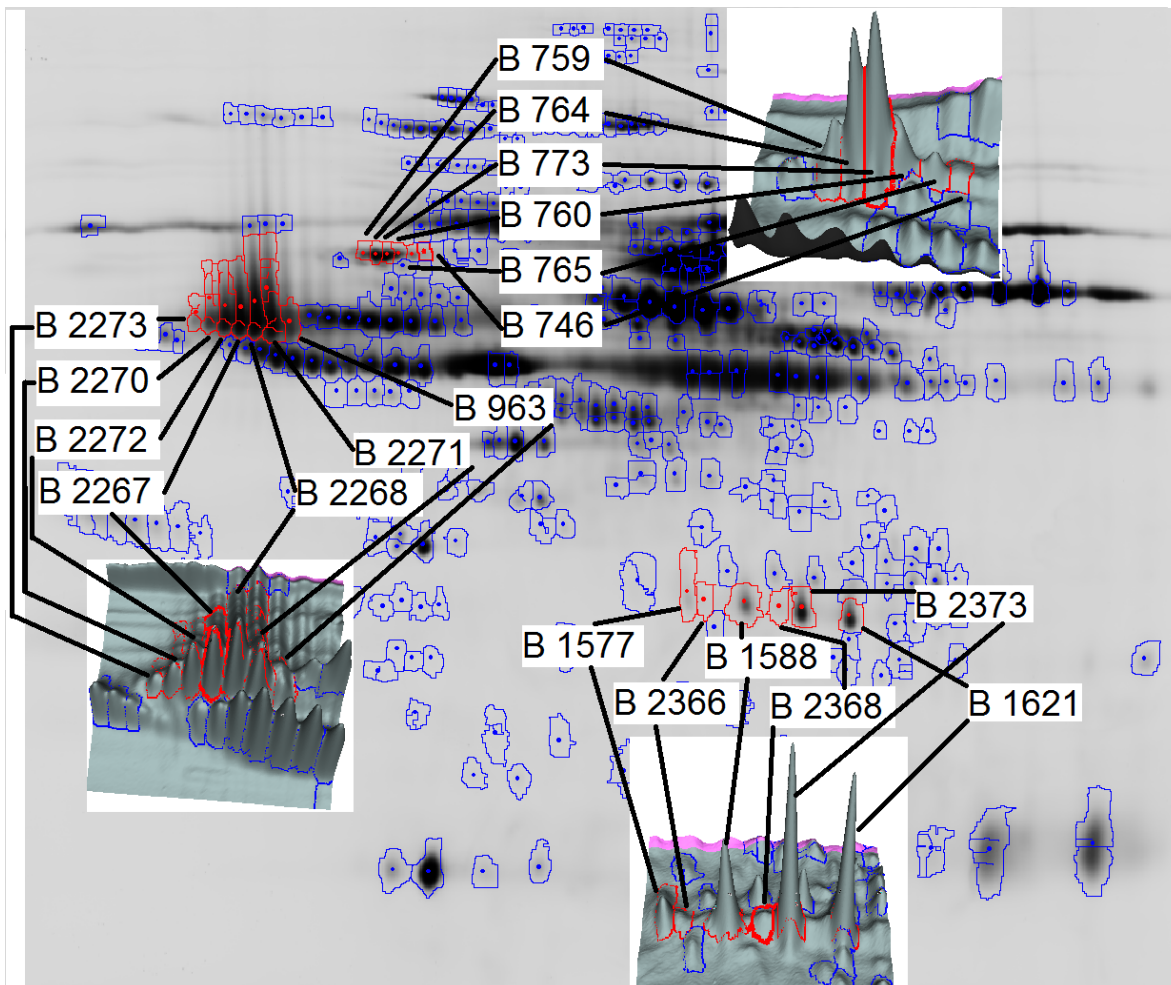


Figure 5-38. Spot positions and 3D views for globally quantified proteins.

For student t-test p values see Table 5-21, Table 5-22 and Table 5-23.

Spot ID	T-test p value	Av. Ratio (bearing/control)
B 1577	0.035	2.7
B 2366	0.0016	3.8
B 1588	0.031	3.5
B 2368	0.052	3.5
B 2373	0.097	3.5
B 1621	0.13	3.0
Combined:	0.044	3.2

Table 5-21. Haptoglobin spot changes, individual and combined results.

Linear normalised data are shown. Student's t-test results are based on log(2) spot volume. Combined results are based on the log(2) of combined spot volumes prior to t-test. (Appendix '[27 - Haptoglobin spots combined.xlsx](#)').

Spot ID (upper row)	T-test <i>p</i> value	Av. Ratio (bearing/control)	Spot ID (lower row)	T-test <i>p</i> value	Av. Ratio (bearing/control)
B 2273	0.91	1.01	B 1071	0.031	1.23
B 2270	0.23	-1.14	B 1078	0.057	1.19
B 2272	0.23	-1.14	B 1086	0.077	1.20
B 2267	0.22	-1.13	B 1099	0.204	1.15
B 2268	0.088	-1.19	B 1112	0.272	1.14
B 2271	0.090	-1.21	B 1113	0.371	1.11
B 963	0.26	-1.15	B 1122	0.569	1.06
Combined:	0.27	-1.16	Combined:	0.24	1.14
Rows combined:	0.52	-1.05			

Table 5-22. Two rows of fetuin spots and combined results (linear normalised).

Student's t-test results are based on log(2) spot volume. Combined results are based on spot volumes added together then log transformed prior to t-test. (Appendix '[28 - Fetuin spots.xlsx](#)').

Spot ID	T-test <i>p</i> value	Av. Ratio (bearing/control)
B 746	0.013	-1.56
B 765	0.044	-1.51
B 760	0.23	-1.19
B 773	0.16	-1.24
B 764	0.87	1.01
B 759	0.70	1.08
Combined:	0.14	-1.14

Table 5-23. Alpha-1B-glycoprotein spot changes, individual and combined results.

Linear normalised data is shown. Student's t-test results are based on log(2) spot volume. Combined results are based on spot volumes added together then log transformed prior to a t-test analysis (Appendix '[29 - Alpha-1B-glycoprotein spots.xlsx](#)').

Both the haptoglobin (Table 5-21) and alpha-1B-glycoprotein (Table 5-24 and Figure 5-39) spots appear to exhibit global regulation *i.e.* all spots in the group appear to be similarly regulated prior to prolapse, rather than just one or a few isoforms [276]. A haptoglobin assay was obtained from Tridelta Development Ltd, Maynooth, Ireland [277]. Unfortunately the purchase of an alpha-1B-glycoprotein quantitative assay was not possible due to limitations of both time and budget.

Spot ID	Correl.	Correl. <i>p</i> value	T-test <i>p</i> value (days 10-12)	Ratio (bearing days 10-12/control)	Matched spot ID	Correl.	Correl. <i>p</i> value	T-test <i>p</i> value (days 10-12)	Ratio (bearing Days 10-12/control)
B 746	0.67	0.075	0.012	-3.7	NA				
B 765	0.55	0.22	0.054	-3.7	A 660	0.78	0.43	0.80	-1.6
B 760	0.82	0.013	0.018	-3.2	A 668	0.12	0.92	0.92	-1.5
B 773	0.79	0.033	0.040	-3.1	A 681	-0.002	1.0	0.93	-1.6
B 764	0.31	0.43	0.93	-2.0	A 680	0.73	0.48	0.47	-1.7
B 759	0.26	0.60	0.98	-2.0	A 679	-0.78	0.43	0.66	-1.4
Combined:	0.84	0.0086	0.0079	-2.6	Combined:	0.20	0.87	0.77	-1.6

Table 5-24. Correlation between alpha-1B-glycoprotein and days to prolapse.

Linear normalised data was used. Student's t-test results are based on log(2) spot volume from samples ewes that prolapsed within 12 days of sampling compared to controls. At the bottom are combined results for each DIGE experiment separately.

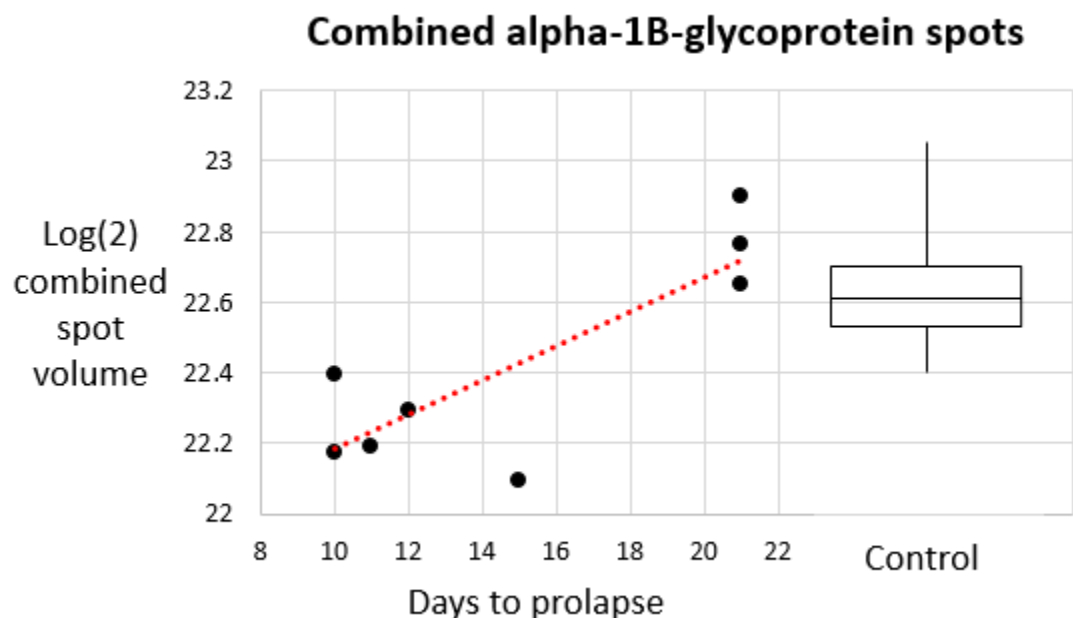


Figure 5-39. Combined alpha-1B-glycoprotein spots, days to prolapse and control boxplot.

DIGE B alpha-1B-glycoprotein log(2) combined spot volume versus days to prolapse and control data distribution (linear normalised). The red dotted line is a fitted line.

Preparatory gels used for spot identification

Samples for mass spectrometry preparatory gels were prepared using the improved method as outlined in chapter 3 except that samples were not depleted and an increased volume of plasma was used in order to increase the intensities of the spots. Duplicate samples were prepared by mixing 30 μ L plasma with 1470 μ L TBS. Each of these plasma/TBS samples was added to separate

15 mL Nunc tubes containing 7.2 mg TCEP, 19.7 mg Tris, 1.2 g urea and 100 mg Triton X-100 resulting in final concentrations of 10 mM TCEP, 65 mM Tris, 8 M urea, 4% Triton X-100 and a pH of around 8.5. The tubes were mixed end-over-end for approximately 30 minutes to ensure the buffer solids had completely dissolved. Then 125 μ L 25% 4-vinylpyridine (in water) was added to each tube to alkylate all cysteine residues. After mixing by inversion, insoluble material and foam was removed by centrifugation at 3000 *g* for 30 seconds before each tube was flushed with N₂ and incubated for 2 hours in the dark at room temperature. Approximately 26 μ L 6 M HCl was then added to each tube to lower the pH to approximately 2.9. Acetone was added to 15 mL (to get 90% acetone) and the samples incubated overnight at -20°C.

After acetone precipitation, tubes were centrifuged (3000 *g* for 10 minutes) and the supernatant drained off and discarded. To precipitate the protein, 10 mL 90% ice cold acetone was added to each tube, then vortexed before incubation for a minimum of two hours at -20°C. The spinning/washing process was repeated twice before the pellets were lyophilised overnight. Pellets were resuspended in 250 μ L of a solution containing 7 M urea, 2 M thiourea, 2% CHAPS (Bio-Rad), and 30 mM Tris (TR buffer) by repeated flicking (but were not vortexed). The samples were combined and the protein concentration obtained using an Invitrogen EZQ protein quantitation kit was 15 mg/mL.

The IPG strips (24 cm, pH 4-7 and pH 6-9, GE Healthcare) were rehydrated overnight at room temperature in disposable GE Healthcare IPG trays, inside an IPG rehydration box. Each strip was rehydrated in 450 μ L TR buffer containing 0.5 % IPG buffer (pH 4-7 or pH 6-11, GE Healthcare) evenly distributed in a single channel. The IPG strips were placed into the appropriate channel and carefully moved up and down in order to evenly distribute the buffer under each strip.

In order to load a high protein load onto the IPG strips, cathodic paper bridge loading was used. 50 μ L of sample (containing 750 μ g protein) was mixed with 50 μ L TR buffer containing 40 mM DTT and 4% IPG buffer. The final concentration of DTT and IPG buffer on the paper bridge was 20 mM and 2% respectively, along with 750 μ g protein in each 100 μ L applied per paper bridge. The relative position of the paper bridge to the IPG strip and electrodes is shown in Figure 5-40.

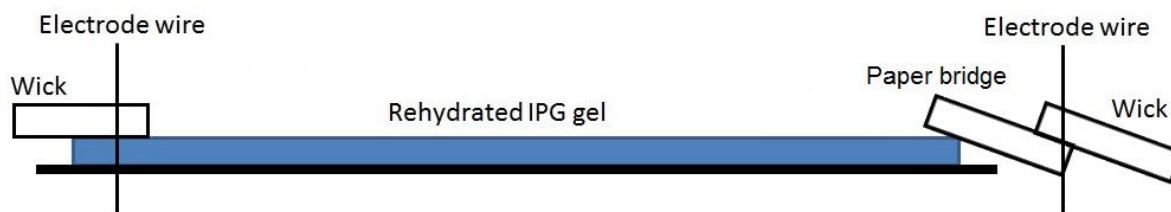


Figure 5-40. Schematic showing the location of the paper bridge, IPG strip and electrode wick.

Gels were cast, loaded and run as described in chapter 3 after which they were stained using colloidal Coomassie G250 according to the protocol of Simpson 2003 [195]. Two individual preparatory gels are shown in Figure 5-41. A combined image generated from the gels shown in Figure 5-41 was matched to the DIGE B master gel, to show the positions of spots of interest (Figure 5-42). Unfortunately several low abundance spots of interest did not show up in the preparatory gels.

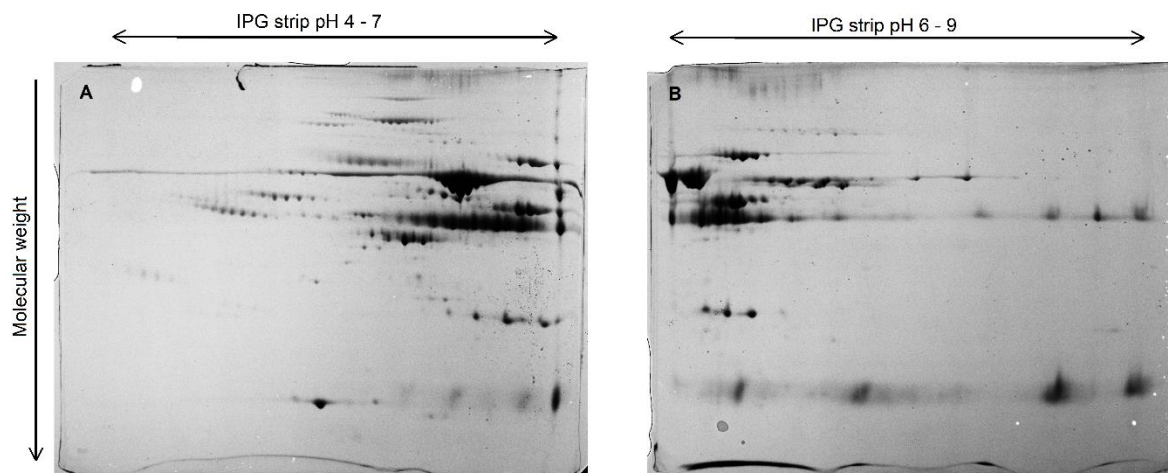


Figure 5-41. Preparatory 2D PAGE gels for mass spectrometry.

Both gels were cathodic paper bridge loaded with 750 μ g non-depleted sheep plasma with 2% IPG buffer (ampholytes) added to the electrode wicks. After electrophoresis the gels were stained with colloidal Coomassie G250 and then scanned on a Typhoon FLA 9000 scanner at 532nm with a fluorescent plate overlaying the gels.

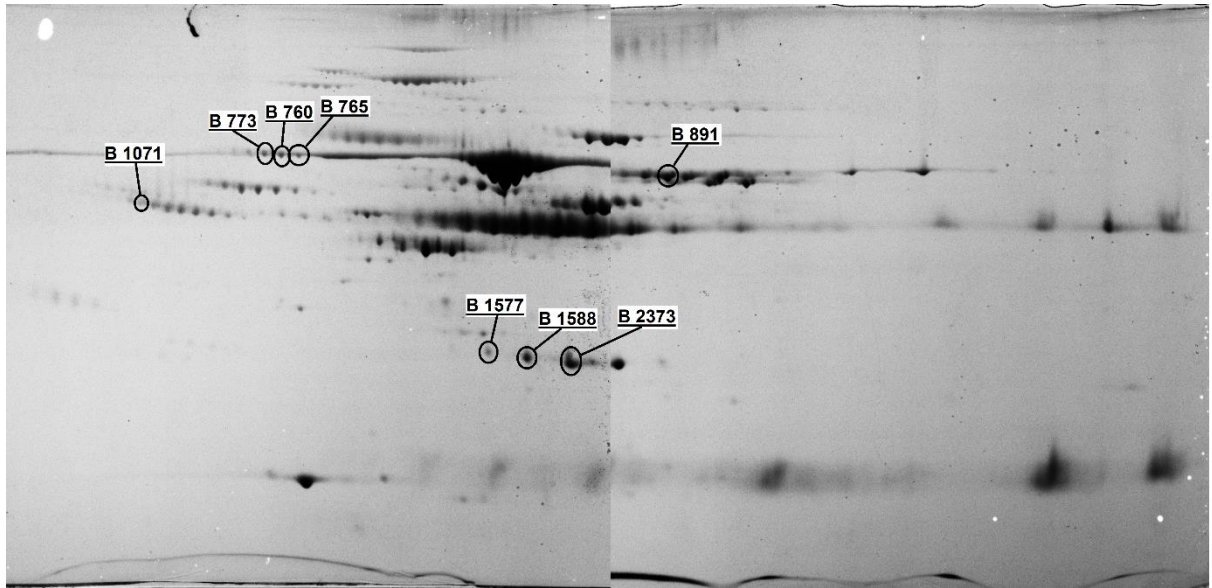


Figure 5-42. Combined preparatory gel images.

The gel images shown in Figure 5-41 were combined and labelled with the spots of interest that could be matched from DIGE B.

Haptoglobin assay

This assay is based on the principle that free haemoglobin has peroxidase activity which is inhibited at low pH. If haptoglobin is present in the given sample then it binds free haemoglobin and preserves its peroxidase activity at low pH. The assay is carried out at low pH in the presence of an oxidisable chromogen which changes colour as it is oxidised, and so can be measured spectrophotometrically [278].

Bearing samples and controls were assayed in duplicate along with standards and external controls. Samples were initially diluted 2x (in the supplied dilution buffer). Those that required further dilution in order to lie within the linear portion of the standard curve were diluted 5x or 10x as appropriate. A standard curve was computed and haptoglobin concentration determined (Appendix '30 - Haptoglobin assay.xlsx', '2x dilution' and '5x and 10x dil' tabs).

Figure 5-44 shows haptoglobin concentrations from the same samples used in DIGE experiment B. The difference between numerically matched controls and bearing samples was just above statistical significance at the $p < 0.05$ level ($p = 0.057$). The average haptoglobin concentration in bearing samples was approximately twice (2.15x) the level of that in matched controls. When all controls ($n = 27$) were used there was no statistically significant difference between samples that

prolapse from days 10 – 21 and controls or between all prolapse samples and all controls (Appendix [‘30 - Haptoglobin assay.xlsx’](#), ‘Combined’ tab).

The correlation coefficient between the assayed log(2) transformed haptoglobin concentrations and that of combined haptoglobin spots determined in DIGE B was 0.95 ($p < 0.001$) with an r^2 of 0.91 see Figure 5-43 (Appendix [‘30 - Haptoglobin assay.xlsx’](#), ‘Correlation with spot volume’ tab, normalised with all spots).

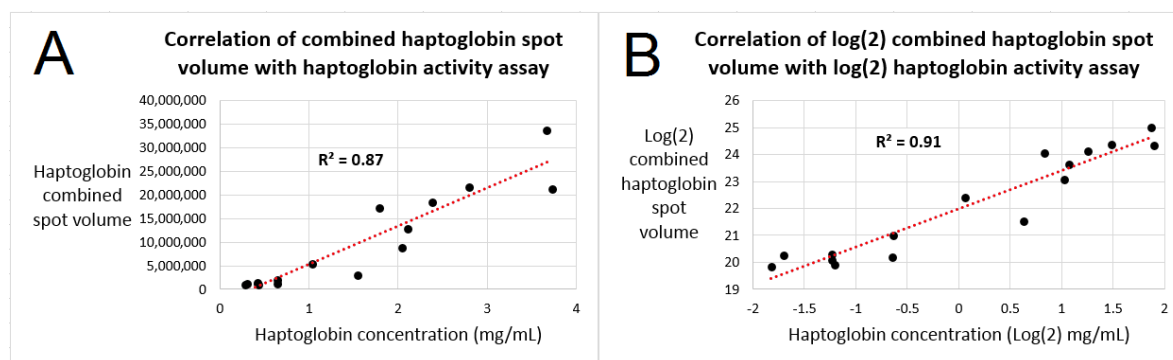


Figure 5-43. Correlation of combined haptoglobin spot volume with haptoglobin assay. Correlation plots show; **A**, untransformed data (volume vs concentration) and **B**, log transformed data (log(2) volume vs log(2) concentration). R^2 values are shown.

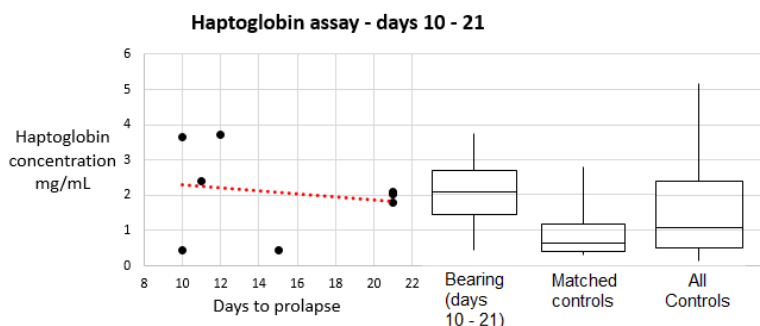


Figure 5-44. Haptoglobin assay, same samples as DIGE B, correlation with days and boxplots. Haptoglobin concentration versus days to prolapse and quartile distribution boxplots showing control and bearing samples for samples used in DIGE B along with all controls. The weak negative correlation of haptoglobin concentration with days to prolapse was not statistically significant.

Figure 5-45 shows the haptoglobin concentration for all samples along with controls. There was no statistically significant difference between pre-prolapse samples and control samples although average pre-prolapse concentrations were higher than those from control animals.

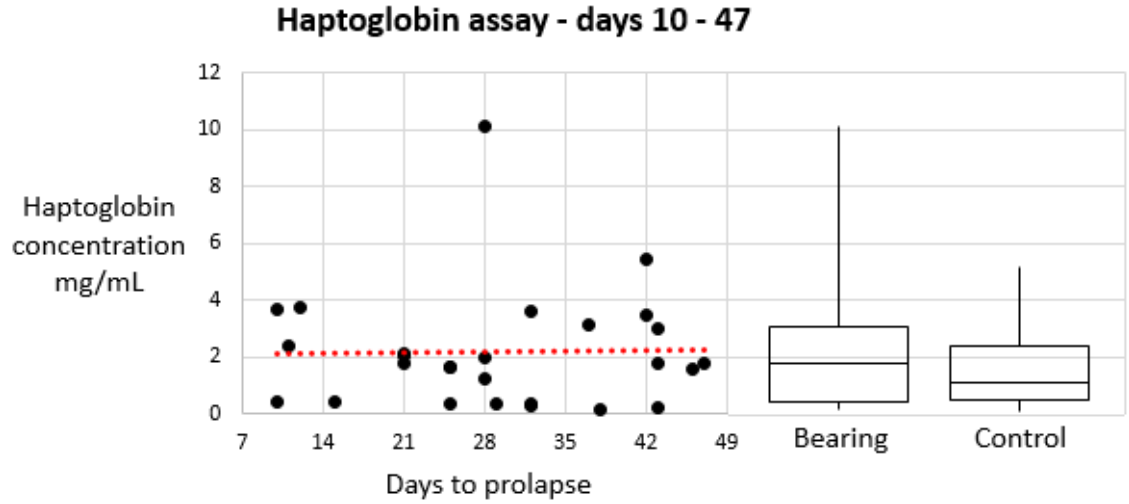


Figure 5-45. Haptoglobin assay, all pre-prolapse samples, correlation with days and boxplots. Haptoglobin concentration versus days to prolapse and quartile distribution boxplots showing control and bearing samples for all samples.

Phosphate assay

An epidemiological study reported in 2002 that serum phosphate concentrations were different in bearing samples and controls [4]. Sample collection dates are not provided but were collected in the year 2000 prior to lambing. Analysis was undertaken by the AgriQuality Animal Health Laboratory in Palmerston North. See Figure 5-46 for results.

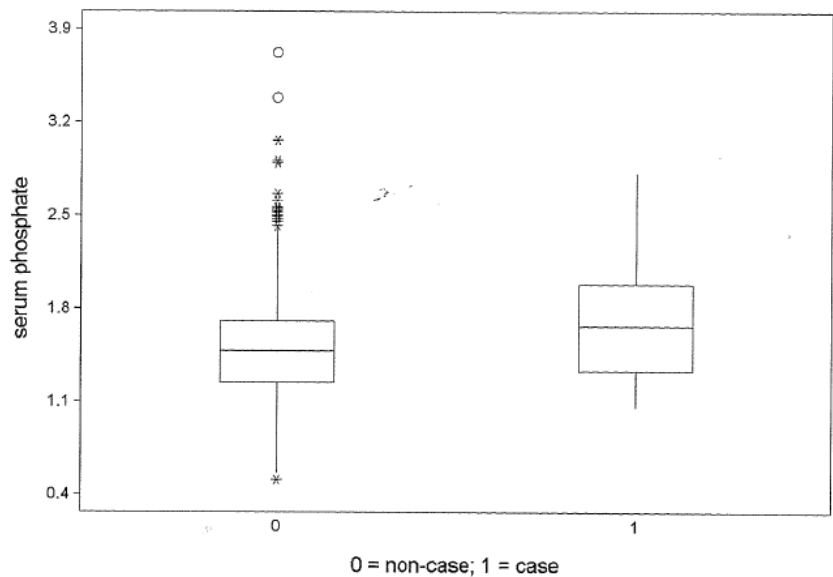


Figure 5-46. Box and whisker plot of serum phosphate levels as found by Hilson *et al.* [4].

Box and whisker plot of serum phosphate concentrations from 976 control samples (non-case) and 18 bearing samples (case) collected for an epidemiological study into pre-partum vaginal prolapse (reproduced with permission) [4].

An inorganic plasma phosphate test was undertaken by the Nutrition Laboratory, Massey University (Figure 5-47).

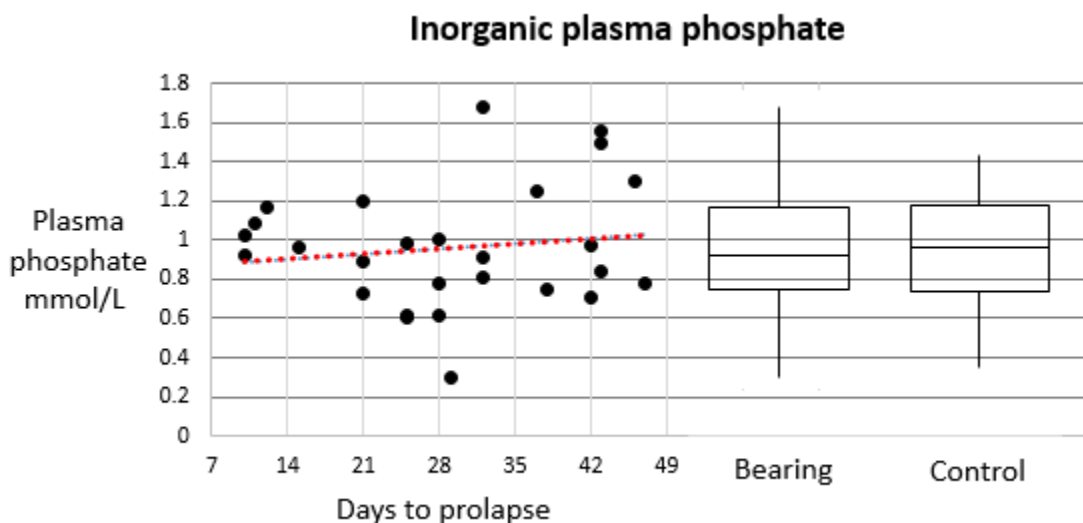


Figure 5-47. Plasma phosphate, days to prolapse and boxplots.

After undertaking the inorganic plasma phosphate test (Figure 5-47) it was subsequently determined that ethylenediaminetetraacetic acid (EDTA) used in the sample collection tubes interferes with the widely used ammonium molybdate assay used to determine inorganic plasma phosphate levels [279] and so the accuracy of these results is in doubt.

Cortisol assay

Plasma cortisol concentration was determined in duplicate by coated tube radioimmunoassay by the Massey University Institute of Food Nutrition and Human Health. Two sets of samples were run as it was not possible to fit all 27 samples in duplicate plus controls and standards on one 96 well test plate. For samples that were repeated an average of both sets of duplicates was taken (Appendix folder '[31 - Cortisol](#)').

Boxplots showing the quartile distribution of the cortisol data are shown in Figure 5-48.

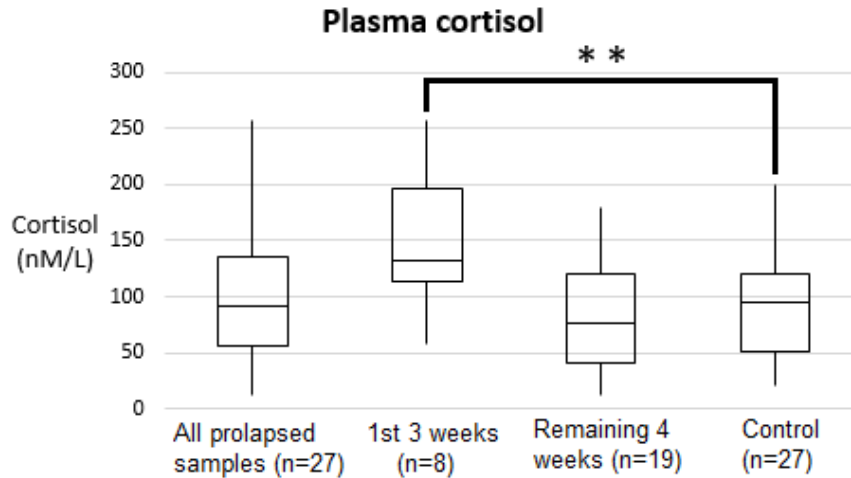


Figure 5-48. Plasma cortisol boxplots, all pre-prolapse samples, 1st 3 weeks and control.

Distribution boxplots are shown depicting plasma cortisol levels in samples taken from all ewes that prolapsed, in samples taken from ewes that prolapsed within three weeks of sampling, in samples taken from ewes that prolapsed after this time (*i.e.* samples from ewes that prolapsed from days 22-47) and control samples. Differences between all prolapsed samples and controls were not statistically significant, but there was a significant difference between samples collected from ewes that prolapsed within three weeks of sampling and controls ($p < 0.01$).

It was found there was no significant difference when all the prolapsed samples were compared to controls, however for ewes that prolapsed within three weeks of sampling there was a significant difference ($p < 0.01$). There was some concern that the data appeared to be not normally distributed (Appendix '[32 - Cortisol results ordered by days.xlsx](#)', dist tab) so a log(2) transformation was done. The results were very similar except that the p value for the difference between samples from ewes that prolapsed within 3 weeks of sampling and controls was greater but still statistically significant at the 0.05 level (Figure 5-49).

It was found that there was a negative correlation between cortisol concentration and days to prolapse from sampling, $r^2 = 0.36$ ($r = -0.6$), $p < 0.01$ (Figure 5-50). As normality of data distribution is not a requirement for correlation, the data was not transformed. The proportion of variability in cortisol values that can be explained by days to prolapse (*i.e.* r^2) was found to be 0.36, although this does not include control values which roughly approximate the prolapsed sample values furthest from sampling and so are in agreement with the correlation.

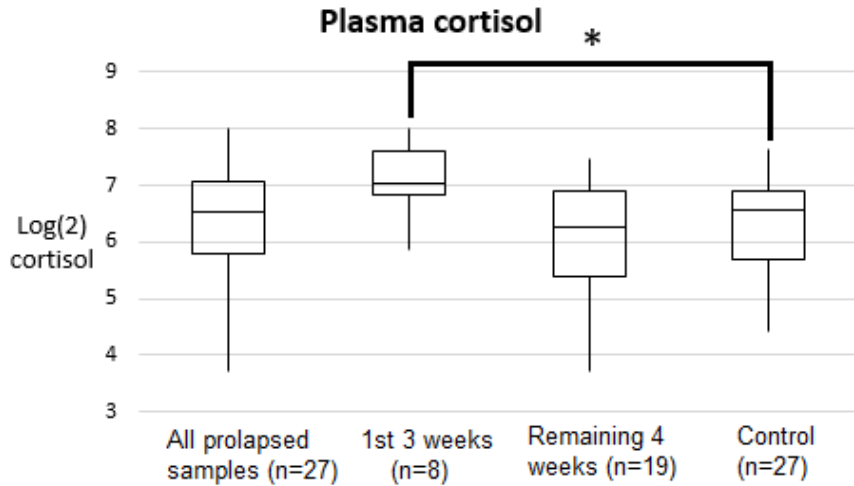


Figure 5-49. Log(2) transformed plasma cortisol, 1st 3 weeks and controls.

Boxplots showing data distribution of the same dataset as shown in Figure 5-48, except that in this figure, the data was subjected to a log(2) transformation in order to address possible issues of non-normal data distribution. Again differences between all prolapsed samples and controls were not statistically significant, but there was a significant difference between samples that prolapsed within three weeks of sampling and controls ($p < 0.05$).

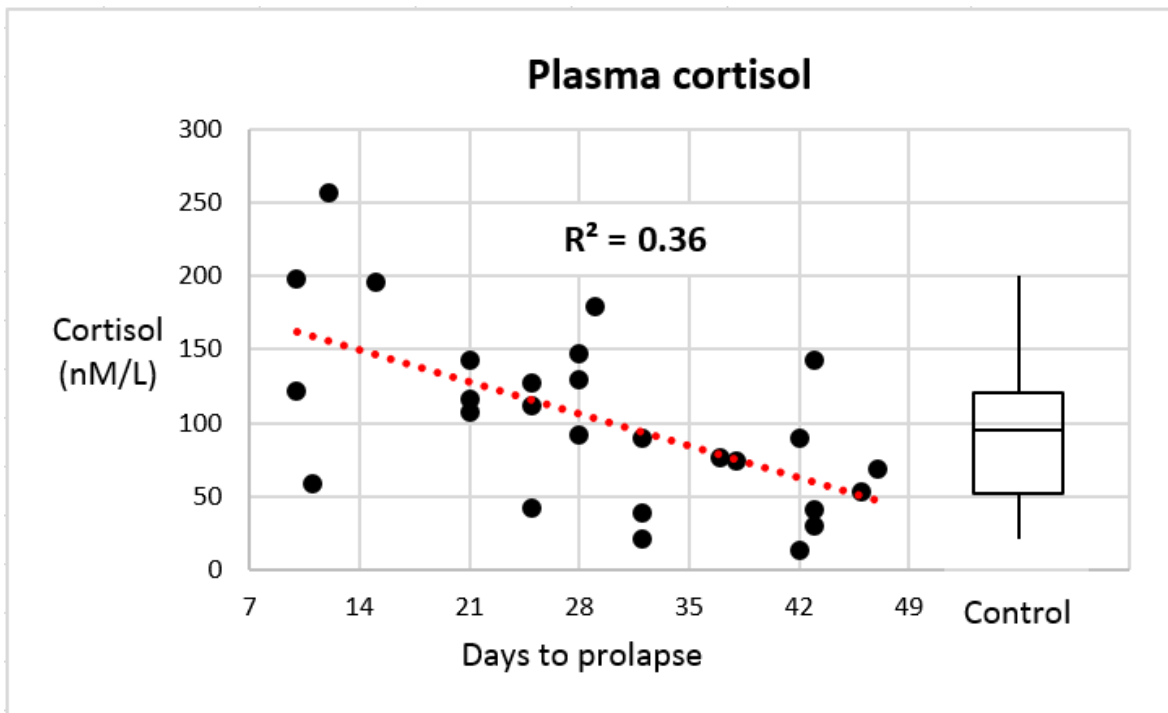


Figure 5-50. Plasma cortisol, days to prolapse vs abundance and control boxplot.

Cortisol concentration plotted against days to prolapse, with trend line. Sampling was done at day 0. An r^2 value of 0.36 was found, however this doesn't include control values.

Chapter 6. Discussion and conclusion

Summary of analysis and results

Because it was anticipated any predictive signal that was available in the days and weeks leading up to prolapse would be relatively weak both 2D DIGE method development and data analysis methodology focused on identifying methods that would increase sensitivity. A large variety of methods for improving spot resolution in 2D gels were trialed. Similarly a variety of methods for preparing data for analysis were evaluated. The focus of this study was to identify any differences in abundance of plasma proteins in an attempt to link a biochemical process to the aetiology of prolapse. For this reason complex multivariate data analysis methods, such as principle component analysis (PCA) or decision trees, were not employed other than as a rudimentary test of sample ID mismatch as suggested in the DeCyder 7.0 software.

Method development began with trialing albumin and IgG depletion methods. Cibacron Blue was not found to be an effective depletion method for albumin. Other methods were tested and it was found that an IgY albumin depletion method was effective. This combined with a protein G method, for IgG depletion, was used to deplete the sheep plasma samples. When depleted samples were run with standard 2D sample preparation and running conditions in DIGE experiments, resolution was very poor. An improved method was developed, evaluated and resulted in gels that had substantially more spots that could be quantified and lower CVs for standard spots that were matched between the experimental methods.

A variety of normalisation methods were also evaluated. Apart from one method (quantile normalisation because it appeared to increase variation) normalisation methods were applied in an inclusive approach *i.e.* spots that passed more than one student's t-test from any of the normalisation methods (apart from quantile normalisation by volume) were included as spots of interest. Spots that both correlated with days to prolapse (with a p value less than 0.05) and had a student's t-test p value for samples that prolapsed the earliest (from days 10-12 after sampling) less than 0.05 were also of interest. The rationale for including these was that it allowed for the inclusion of spots which only changed in abundance close to prolapse occurring.

Spots of interest were determined by three methods. Firstly, by applying a student's t-test, comparing prolapse samples with controls, to each of the normalisation methods and then sorting by p value to find spots with p values less than 0.05. Secondly, spots of interest were determined by correlation with days to prolapse along with an assessment of the relative distribution of control values. Thirdly, spots that passed a FDR test using a moderated t-test were included.

Spots of interest that could be matched on preparative gels were excised and identified by MS. For sets of spots that had more than one spot with differential abundance (between bearing and control) and for which positional and/or MS data suggested they were isoforms of the same protein, spot volumes were added together, so that global abundance changes could be calculated. Two proteins identified by MS, alpha-1B-glycoprotein and haptoglobin, had global changes. The global alpha-1B-glycoprotein differences were confined to ewes that prolapsed within 15 days of sampling.

The global haptoglobin differences calculated from the combined spots volume from DIGE B did not correlate with days to prolapse. The haptoglobin concentration assay correlated well with the combined haptoglobin spot volume however increasing the number of samples ($n = 16$ for DIGE experiment B, $n = 54$ for the haptoglobin assay) resulted in the statistical difference between prolapse samples and controls disappearing. The assay also failed to demonstrate a correlation between days to prolapse and haptoglobin concentration. What the assay could not validate (or otherwise) was the association of some isoforms of haptoglobin with prolapse. However the assay did demonstrate that the total haptoglobin spot volume calculations were in agreement with assay results suggesting that the DIGE B haptoglobin spot volumes were correct and that increases in the concentrations of isoforms of haptoglobin may be associated with pre-prolapse samples.

There was one individual spot that was identified by MS and deemed to be a spot of interest, this was an isoform of fetuin (otherwise known as alpha-2-HS-glycoprotein).

The only non-protein biomarker evaluated in this study was cortisol which was found to be upregulated in ewes close to prolapse.

Alpha-1B-glycoprotein

Alpha-1B-glycoprotein (A1BG) was found to be decreased in abundance in ewes within 15 days of prolapse. The A1BG protein is thought to be secreted in the plasma of all mammalian species. Understood to be a member of the immunoglobulin superfamily of proteins [280] the function of A1BG is not yet known, although it is known to bind another poorly understood protein, CRISP-3, in many mammalian species [281]. CRISP-3 is expressed in neutrophilic granulocytes and is thought to play a role in innate immunity with a positive local effect via release from neutrophilic granulocytes. As some CRISP proteins are neurotoxic it has been suggested that the binding of circulating CRISP-3 by A1BG may play a protective role [282].

A1BG has been found to be upregulated in a number of human cancers [283, 284] as well as in human endometriosis [285]. Studies have also found changes in glycosylation of A1BG in association with cancer [286] along with shifts in isoelectric point [287] and the introduction of unusual glycosylation site [288].

A1BG has been shown to be down regulated in blood samples of at least two studies. It was shown to have lower concentrations in the plasma of farmers with musculoskeletal disorders [289] and in the plasma of rheumatoid arthritis patients [290]. Conversely another study found that A1BG was upregulated in the synovial fluid of rheumatoid arthritis sufferers and that antibodies to A1BG were also found in those patients *i.e.* A1BG was acting as an autoantigen [291]. In a rat model of rheumatoid arthritis it has also been found that A1GB is upregulated in synovial fluid [292].

Two studies have been reported in regard to A1BG levels in sheep disease. Firstly, A1BG was found to be down regulated in the gastric efferent lymph of immune 10 month old lambs that had been recently exposed to *Teladorsagia circumcincta* infective (L3) larvae [248]. It is not understood how this is related to nematode immunity or infection although it was noted that A1BG was unlikely to play a role in nematode immunity because the “immune exclusion of the worms had already occurred [by the time the change in A1BG levels had occurred]”. Another study found A1BG was upregulated in sheep suffering from rhino-tracheo bronchitis, a common respiratory infection in sheep [170].

A genome wide search for associations between SNPs and cardiovascular outcomes found a SNP in the A1BG gene that was associated with increased risk of cardiovascular disease [293]. While no clear mechanisms of action were identified in this study it was of interest that all SNPs found were in genetic regions associated with immune function.

In summary, changes in A1BG plasma concentration are known to be associated with some diseases, and particularly some cancers where it is upregulated. It is only down regulated in blood for a small number of diseases, notably in rheumatoid arthritis in humans and in the gastric lymph of immune lambs after exposure to infective worm larvae. On the basis of these observations it is difficult to determine a physiological connection between these diseases and the finding that A1BG was lowered close to prolapse.

Haptoglobin

DIGE experiment B found that global plasma haptoglobin levels were increased in ewes prior to prolapse. When the same samples were analysed by a haptoglobin activity assay there was a good correlation between the global levels found by DIGE experiment B and those found using the haptoglobin activity assay. When all available samples were analysed (using the activity assay) the difference in total haptoglobin level between pre-prolapse samples and controls reduced, and although haptoglobin levels remained higher in pre-prolapse samples compared to controls it was no longer statistically significant. However, the finding that the more acidic isoforms of haptoglobin are upregulated prior to prolapse remains valid.

In humans circulating haptoglobin is made up of two subunits linked by disulfide bonds. The subunits are encoded by one gene and are post translationally modified by proteolytic cleavage to form a disulfide bridge linked protein prior to release into circulation [294]. Sample preparation for 2D electrophoresis involves the use of reducing agents so that disulfide linked proteins can be separated. From the MS results in this study it appears that the haptoglobin gel spots identified represent the beta subunit of haptoglobin (Appendix folder '[25 - MS data using Proteome Discoverer 2.2](#)' and [295]). The authors of the published 2D sheep map [170] did not comment on which subunit was found but given that the spot positions on their 2D gels approximated the positions of those in the present study it seems likely that the haptoglobin on the published map was also the beta subunit. While the haptoglobin subunits have not been reported to date in sheep,

in cattle (as in humans) circulating haptoglobin is made up of two polypeptide chains linked by disulfide bonds [294] and is also present as polymers associated with albumin [296]. While albumin associated proteins may be removed during depletion, any haptoglobin removal in this study was at least proportional to that which remained as verified by the correlation of haptoglobin spot volume to the haptoglobin assay, for which albumin depletion was not performed.

Haptoglobin was discovered to be a haemoglobin binding protein in 1938 [297], and this protein-protein interaction is one of the strongest known [298]. Free circulating haemoglobin is a damage associated molecular pattern molecule (DAMP) and in humans can be increased due to a range of clinical syndromes such as burns, trauma or infection [299]. Haptoglobin binds free haemoglobin and forms a complex that is too large to pass through the kidneys. The stable complex is then taken up by monocytes or macrophages. The benefit of this is that the organism is protected from oxidative damage by free haemoglobin and access to free iron is restricted away from iron dependent bacteria. Haptoglobin has other anti-inflammatory roles such as monocyte and macrophage binding as well the suppression of T cell proliferation. Haptoglobin is also known to have angiogenesis effects and acts as an extracellular chaperone [300].

A number of studies have looked at haptoglobin levels in ruminants in relation to a variety of disease states as haptoglobin (along with serum amyloid A) is described as one of the two most important acute phase proteins in these animals [110]. Levels of haptoglobin can be elevated 100 times normal levels in cattle [301] whereas in humans, there may only a 2-4% increase in circulating haptoglobin associated with inflammatory conditions [302]. In ruminants elevated levels of haptoglobin have been found to be associated with: mastitis in dairy cows [303], *mycoplasma bovis* infection in calves [304], post-partum uterine inflammation (both endometritis and metritis) in dairy cows [305, 306], dystocia in sheep [307, 308] and dairy cows [309], placental retention in dairy cows [309], traumatic reticuloperitonitis in cows [310], inflammation around the heart in cows (both pericarditis and endocarditis) [311], hoof disorders in dairy cows [110, 312], ketosis in sheep [313] goats [314] and dairy cows [315], during transport stress in sheep [316], heat stress in goats [317], *corynebacterium pseudotuberculosis* infection in sheep [318], gastro intestinal parasite infection in lambs [319] and goats [320], coccidiosis infection in goats [321], rhino-tracheo-bronchitis in sheep [170] and acidosis in goats [322]. Haptoglobin has also been found to be upregulated close to lambing [170].

Few studies have assessed variations in the concentration of isoforms due to the difficulties associated with it, although they do hold promise as disease biomarkers [323]. There is, however, an increasing interest in this area due to a growing awareness of the effects of post-translation modification such as glycosylation of proteins [324]. Most of the studies looking at the regulation of isoforms of haptoglobin are limited to humans however a study looking into haemolytic anaemia in dogs using isoelectric focusing found a change in the levels of isoforms of haptoglobin compared to controls. The shift in PI was attributed to a reduction in the sialic acid content of the oligosaccharides attached to haptoglobin [325].

Aberrantly fucosylated and sialylated haptoglobin is known to be related to a number of different human diseases, particularly cancer [326]. By using a lectin-antibody enzyme linked immunosorbent assay system Takeda *et al.* [327] found that increased haptoglobin fucosylation levels in colorectal cancer patients was linked to poorer outcomes to treatment. Haptoglobin glycosylation levels in serum were investigated from patients with either chronic hepatitis C, hepatitis C induced liver cirrhosis or hepatocellular carcinoma. It was found that levels of haptoglobin sialylation were different between the diseases and that analysis of haptoglobin glycosylation could predict liver disease outcomes without the need for biopsy [328].

Another form of haptoglobin modification that affects the isoelectric point of haptoglobin is deamidation. Protein deamidation occurs when asparagine or glutamine amino acids are converted to either aspartic acid or glutamic acid respectively. This process is due to the loss of the amine group converting the amino acid to an acid, thus changing the PI of the protein, and generally reflects its molecular age [329]. Haptoglobin has been found to have differing levels of deamidated haptoglobin in association with small cell lung cancer [330] and in leprosy patients that are in treatment [331].

One study [295] has reported that variations in spot position of human haptoglobin in 2D gels has been found to be caused by three major allelic variants two of which have similar molecular weight but differ in their isoelectric point. The other allele differs in its molecular weight. They also found that that all alleles could change in their PI due to deamidation of an asparagine residue and by the retention of a (charged) C terminal arginine residue that is normally enzymatically removed [332]. It should be noted that the genetic variation that translated into differences in spot position in 2D

gels was found in the alpha subunit of haptoglobin, whereas the variation found in the present study appears to be in spots identified as being beta subunit spots.

Fetuin A and Serpin

Spot B 1071, which was found to be slightly up regulated, appears to represent two different proteins, fetuin A and serpin in approximately equal amounts, at least from the qualitative information available from MS. Fetuin A, otherwise known as alpha-2-HS-glycoprotein, is capable of carrying a wide range of different molecules including calcium phosphate and in humans appears to influence free plasma phosphate levels [333]. Increased plasma phosphate was found to be increased in association with prolapse in the Hilson *et al.* study [4]. Plasma phosphate could not be accurately evaluated in the present study as the samples were collected in EDTA tubes and unfortunately EDTA (ethylenediaminetetraacetic acid) interferes with the widely used ammonium molybdate assay used to determine inorganic plasma phosphate levels [279]. An alternative would be to use NMR spectroscopy to evaluate phosphate level as EDTA does not interfere with this approach [334].

Serpins are proteins found in all kingdoms of life and have protease inhibitor activity with more than 3000 members [335]. There are a large number of different serpins which have been found to be involved in a range of biological functions including blood pressure regulation, sperm development and hormone transport [336]. Changes in circulating levels of serpins have not been reported for many conditions in sheep although they are associated with seasonal weight loss [337] and lactation [338]. In humans, changes in serpins have been found to be associated with obesity [339], Parkinson's disease [340], cardio vascular disease [341] schistosomiasis [342], premature delivery [343], skin attributes [344], and a number of different cancers [345].

Cortisol

The statistically most significant finding of this study was that plasma cortisol was the highest in ewes that were closest to prolapse (*i.e.* a correlation between days to prolapse and plasma cortisol levels) and that control levels of cortisol approximated the levels of ewes that prolapsed the furthest from blood sampling. The reasoning for the claim that it is the statistically most significant finding is firstly, that the plasma cortisol test was not exposed to multiple hypothesis testing. Only one test of this kind was done and so there was no searching amongst variables for statistically significant

results meaning there is no need to consider adjusting the p value due to multiple hypothesis testing. Secondly, a greater number of samples were tested for this result, *i.e.* $n = 54$ as opposed to 16 for the proteomic analysis. Higher sample numbers always gives more statistically reliable results.

It should be noted that plasma cortisol levels fluctuate during the day [346] and fluctuate in response to acute stress, such as experienced by the ewes during blood sampling. Note that controls were matched to prolapsed ewes by the time of day of sampling. The time plasma cortisol takes to come down in response to acute stress is a matter of hours, at least in humans [347]. In the present study an association was found between ewes that had high cortisol and prolapsing within 3 weeks of that time, well after the time one would expect a cortisol response to sampling to fall. This could indicate one of several things. Firstly, the high plasma cortisol at sampling time was a marker of damage that was happening at the same time *e.g.* to tissue that retains the vagina in place such as the constrictor vestibuli muscle (the plain muscle that surrounds the vaginal opening). Secondly, the high plasma cortisol at sampling time could be associated with another unknown condition (as covered below), such as an infection, that is causative for prolapse via an unknown mechanism. Thirdly, the high plasma cortisol could be an indication of ongoing high cortisol, such as is suffered under chronic stress or anxiety, and prolapse could be a direct and current consequence of chronic stress via for example, raised intra-abdominal pressure. Fourthly, the cortisol result could be purely due to random chance, and not associated with prolapse at all.

Assuming the cortisol result is real, a question that can be asked is; could the cortisol result be affected by the ewes being closer to lambing than the controls? Levels found in the 8 ewes that prolapsed within 3 weeks of blood sampling averaged 150 ± 63 nmol/L, which after applying a student's t-test was found to statistically significantly different to the 27 controls evaluated ($p < 0.01$) (Appendix '[32 - Cortisol results ordered by days.xlsx](#)'). Published cortisol levels from twinning ewes late in pregnancy have been found to average 87 ± 42 nmol/L [348], similar to the control levels found in this study which averaged 91 ± 48 nmol/L. The reference range for plasma cortisol in normal healthy non-pregnant sheep is 42-82 nmol/L. The reference range refers to the average ± 2 standard deviations *i.e.* covering 95% of the data points in a normally distributed dataset. For sheep plasma, the average cortisol concentration has been found to be 62 ± 10 nmol/L [349]. This is slightly lower than that found in ewes in late pregnancy. However, a closer look at the published literature on the subject of cortisol during pregnancy reveals that cortisol is higher in early pregnancy, falls

during pregnancy, and is at its lowest close to lambing [350]. It falls more in twinning ewes than singles [348]. This would indicate that pre-prolapse ewes that are higher in cortisol than controls are not simply closer to lambing.

Assuming the cortisol result represents a real difference between pre-prolapse samples and controls *i.e.* that ewes close to prolapse did have a higher level of cortisol, the next question is; what could this mean? Cortisol is a marker of stress, and in the present study was collected by jugular venipuncture, itself a stressful process. The response seen, if real, is that ewes that were closest to lambing had a larger cortisol response to blood sampling than controls.

One possibility is that a disease or condition that the prolapsing ewes were suffering from could be causing the increased cortisol. Cortisol increases are associated with a large number of diseases. One of these is ketosis, a metabolic condition common in heavily pregnant ewes and one that is known to be associated with increased cortisol [351]. Ketosis, otherwise known as pregnancy toxemia in sheep, leads to increased plasma β hydroxybutyrate [352] but as discussed in chapter 1, is not thought to be causative of prolapse. Increased cortisol is also known to be associated with gastrointestinal parasitism [353], lameness [354], flystrike [355], bacterial infection [356] and increased methane production [357, 358] amongst other things.

Gastrointestinal parasitism, lameness and flystrike are all things commonly dealt with on a day to day basis by sheep farmers and sheep research scientists alike. One would think that if there was an association if these diseases and prolapse then this would have been observed and reported. It remains possible that sub-clinical conditions of these diseases are associated with prolapse or that they are only partially associated with prolapse but at least superficially it seems unlikely or at most just weakly associated. Bacterial infection may be more difficult to detect by the casual observer and is discussed further below in the section entitled combined biomarker discussion. Increased methane production may be relevant in that it is associated with increased internal pressure in the fore stomach of sheep, although it is unclear if this would translate to increased pressure near the pelvis [359].

Another possibility is that the cortisol biomarker result reflects a stress condition that is associated with prolapse. Given that indications are that the elevated cortisol levels were present in the sheep

sampled up to 3 weeks prior to prolapse this is more likely to represent chronic stress rather than acute stress. The question then arises, how could chronic stress cause prolapse?

One possibility is that chronic stress affects muscles or processes that function to retain the vaginal structure internally, such as weakening of the constrictor vestibuli muscle. Research on this condition in sheep is almost non-existent, although in humans there appears to be an association between environmental stressors and urinary control [360] as well as a defecation reflex in the presence of stress [361].

As discussed in the introduction, another mechanism for chronic stress to be involved in prolapse is that stress may raise intra-abdominal pressure, putting increased pressure on the internal end of the vagina. It was noted by the researchers in the 1950's that intra-abdominal pressure in the standing relaxed ewe was negative and that upon physically restraining ewes for measurement it took several minutes for levels to fall to stable levels, suggesting that the psychological state of relaxation in the ewe affects IAP [15]. It was found that the IAP of ewes lying down was positive, and higher for ewes lying on a slope with buttocks downhill, leading to research in this area [16]. An interest in the association between farm topography and prolapse began which has persisted through much prolapse research [3, 31, 32]. However, no published studies have reported on the relative position ewes are actually in when prolapse occurs. It can be noted at this point that the author of this thesis has observed that ewes can prolapse whilst standing. Given that a relaxed standing ewe has negative intra-abdominal pressure, prolapsing whilst standing could only occur if intra-abdominal pressure is positive, indicating that the ewes in question may not be relaxed. Over what time frame or to what degree, the psychological state of relaxation affects intra-abdominal pressure and thus prolapse is unknown, however it does appear to be a reasonable line of enquiry.

The literature search suggests that predator stress could biochemically limit rates of reproduction in other species, notably the snowshoe hare [362]. If we accept that stress is a factor contributing to bearings in ewes and that while stress may not be affecting reproduction in the same way as it does with the snowshoe hare (as with bearing ewes both the mother and unborn fetuses die whereas in the case of the snowshoe hare fecundity is reduced) it does appear that in both cases reproductive gain is less than it could be due to stress. This raises a question about how such a stress response could arise from an evolutionary perspective. In the case of the snowshoe hare it has been

justified in terms of a survival advantage for offspring [363] however it is difficult to see an adaptive advantage in a system that results in both mother and offspring dying. Genetic selection for reduced cortisol has been attempted in the pig, however it was found that although cortisol levels were reduced, glucocorticoid receptors became hypersensitive in the low cortisol line [364] indicating that cortisol responsiveness is resistant to reduction. It can also be noted that the rate limiting step of cortisol production is undertaken in the mitochondria so that the regulation of cortisol production is not under simple genetic control [365]. Further, regulation of cortisol is clearly important in early mammalian development [366] and so is therefore likely to be difficult to genetically regulate without negatively affecting other aspects of reproduction.

Future directions

Assuming the samples used in the present study remain available it would be useful to validate the alpha-1B-glycoprotein result *i.e.* with a quantitative assay to check if the global differences detected with 2D DIGE can be repeated with an alternative method such as an ELISA assay. It may also be useful to examine plasma phosphate using a method that is not affected by EDTA, such as NMR spectroscopy, to see if the plasma phosphate levels in this study match the results of the Hilson *et al.* study [4]. A liquid based chromatography MS/MS method to look for protein markers of prolapse as liquid based methods can complement gel based methods [367, 368] without the need to depleting samples of abundant proteins. Note that the albumin depletion used in the present study is occasionally suspected of depleting associated proteins thus reducing biomarker availability and so it could be useful to use a non-depleted sample set in a liquid chromatography assay [152].

Increasingly biochemists are interested in molecular markers other than proteins such as those sought in a metabolomics study [369]. Non-protein bio-markers such as lipid isomers or alternative glycan structures are increasingly being found to be associated with a huge range of diseases and conditions [370] and pursuit of such a search strategy could prove fruitful to further pursue an understanding of the etiology of prolapse.

Lastly, in regards to the cortisol result, it would be useful to know if cortisol levels were associated with increased IAP. To investigate this a cortisol test that is less prone to variation might be used, such as with the testing of cortisol in wool [371], which could be tracked over time. It would also be useful to see if rates of prolapse are affected by the intensity and type of farm management

practices that may affect stress levels in pre-lamb ewes, such as the herding of sheep with dogs, pre-lamb vaccination or winter crutching. These practices could be tested to check for association with chronic stress, IAP, and rates of prolapse. If it was found that prolapse was associated with stress then this would trigger a raft of research into the mechanism of this process. Veterinary pathologists could examine ewes that had predictive biomarkers (*e.g.* elevated cortisol) to investigate what other changes were occurring in the sheep. Animal behaviourists would want to know what particular kind of stress was involved, is it a type of anxiety disorder? Does it resemble post-traumatic stress disorder? How is it triggered? Is it a model for human stress disorders? Farmers would want to know, what are the best management practices to avoid prolapse? Is stress causing other problems on the farm?

Conclusion

It is important to acknowledge the limitations of any study. In the present study proteomics is open to problems with statistics and in particular multiple hypothesis testing *i.e.* the findings could be due to searching through variables that are affected by random variation. Random variation could also have influenced the cortisol result even though it was not the result of a search through variables. Sample size was also limited, particularly with the DIGE experiments. A larger sample size along with replicates from different farms, different seasons and from different breeds would be necessary for results to be more widely applicable. However that said, there is information to be gleaned from this study.

Many farmers and veterinarians think that affected ewes have simply eaten too much and so reduce feed allowance accordingly [372]. This study has found that there appear to be changes developing prior to prolapse occurring, *i.e.* isoform differences in haptoglobin, global differences in alpha-1B-glycoprotein as well as an increase in cortisol levels close to prolapse and that the most statistically significant is an increase in cortisol response in the days before it happens. This would indicate prolapse is probably not the result of a large gut fill immediately prior to prolapse and that some other factor is involved with causing prolapse. The cortisol finding alongside previous research that found that relaxed standing ewes are unlikely to prolapse (due to negative intra-abdominal pressure at the vagina) in conjunction with field observations that yarded standing ewes can prolapse, opens the possibility that increased cortisol may lead to increased intra-abdominal pressure and subsequent prolapse. The haptoglobin finding could be the result of some level of infection or injury

or it may rise as a result of high intra-abdominal pressure. It is unclear what the alpha-1B-glycoprotein finding indicates. An alternative explanation would be that the ewes about to prolapse are suffering from another condition, for which the markers are also associated with, such as an undetected infection. Further research is necessary to follow up these leads.

Bibliography

1. Edgar, D.E., *Vaginal eversion in the pregnant ewe*. The Veterinary Record, 1952. **52**(64): p. 852-858.
2. Noakes, D.E., *Prepartum cervico-vaginal prolapse in the ewe*. CPD Veterinary Medicine, 1999. **2**: p. 47-51.
3. Low, J.C. and H.K. Sutherland, *A census of the prevalence of vaginal prolapse in sheep flocks in the Borders region of Scotland*. The Veterinary Record, 1987. **120**: p. 571-575.
4. Hilson, R., et al., *An Epidemiological Study of Vaginal Prolapse in Ewes*. AgMardt, WoolPro and Meat NZ internal report. Massey University, 2002.
5. Laing, A.D.M.G., *"Sleepy sickness" and bearing trouble in ewes. Prevention by suitable methods of management*. New Zealand Journal of Agriculture, 1939. **58**: p. 465-470.
6. Ayen, E. and D.E. Noakes, *Displacement of the tubular genital tract of the ewe during pregnancy*. The Veterinary Record, 1997. **141**: p. 509-512.
7. Scott, P.R. and M.E. Gessert, *Ultrasonographic examination of 12 ovine vaginal prolapses*. Veterinary Journal, 1998. **155**(3).
8. Blood, D.C. and V.P. Studdert, *Saunders comprehensive veterinary dictionary*. 2nd ed. 1999, London: WB Saunders.
9. Kloss, S., et al., *Investigations about kind and frequency of mechanical dystocia in ewes with special regard to the vaginal prolapse ante partum*. Berliner Und Munchener Tierarztliche Wochenschrift, 2002. **115**(7-8): p. 247-251.
10. McLean, J.W., *Vaginal Prolapse in Ewes, Part VI: Mortality rate in ewes and lambs*. The New Zealand Veterinary Journal, 1959. **7**(5): p. 137-139.
11. Bassett, E.G. and S.M. Phillips, *Some observations on the pelvic anatomy of ewes with vaginal prolapse*. The New Zealand Veterinary Journal, 1955. **3** (4): p. 127-137.
12. Bassett, E.G. and D.S.M. Phillips, *Pelvic relaxation in sheep*. Nature, 1954. **174**(4439): p. 1020-1021.
13. McLean, J.W., *Vaginal Prolapse in Sheep*. The New Zealand Veterinary Journal, 1956. **4**(2): p. 38-55.
14. Davies, F.G., *Occurrence of Vaginal Eversion and Allied Disorders in Fat Ewes*. Research in Veterinary Science, 1970. **11**(1): p. 86-&.
15. McLean, J.W. and J.H. Claxton, *Vaginal Prolapse in Ewes, Part VII: The measurement and effect of intra-abdominal pressure*. The New Zealand Veterinary Journal, 1960. **8**(3): p. 51-61.
16. McLean, J.W., *Vaginal Prolapse in Ewes - Part III: The effect of topography on incidence*. The New Zealand Veterinary Journal, 1957. **5**(3): p. 93-97.
17. Ayen, E., *Intra-abdominal pressure changes in pregnant ewe*. Journal of the Faculty of Veterinary Medicine, University of Tehran, 2002. **57**(3): p. 97-101.
18. Watkins, J.D., *Nutritional factors associated with vaginal prolapse*. The Veterinary Record, 1991. **129**: p. 263.
19. Goddard, P.J. and W.E. Allen, *The use of catheter-tipped pressure transducers for chronic measurement of genital tract pressures in the ewe. II. Effects of oxytocin and prostaglandin F2 alpha*. Theriogenology, 1986. **25**(5).
20. Malbrain, M., et al., *Prevalence of intra-abdominal hypertension in critically ill patients: a multicentre epidemiological study*. Intensive Care Medicine, 2004. **30**(5): p. 822-829.
21. Malbrain, M., *Different techniques to measure intra-abdominal pressure (IAP): time for a critical re-appraisal*. Intensive Care Medicine, 2004. **30**(3): p. 357-371.
22. Drellich, S., *Intraabdominal pressure and abdominal compartment syndrome*. Compendium on Continuing Education for the Practicing Veterinarian, 2000. **22**(8): p. 764-769.
23. Ivatury, R.R., H.J. Sugerman, and A.B. Peitzman, *Abdominal compartment syndrome: recognition and management*. Advances in Surgery, 2001. **35**: p. 251-269.

24. Walker, J. and L.M. Criddle, *Pathophysiology and management of abdominal compartment syndrome*. American Journal of Critical Care, 2003. **12**(4): p. 367-371.
25. Hakobyan, R.V. and G.G. Mkhoyan, *Epidural analgesia decreases intra-abdominal pressure in postoperative patients with primary intra-abdominal hypertension*. Acta Clinica Belgica, 2008. **63**(2): p. 86-92.
26. De Waele, J.J., et al., *A role for muscle relaxation in patients with abdominal compartment syndrome?* Intensive Care Medicine, 2003. **29**(2): p. 332-332.
27. Carroll, D., et al., *Blood pressure reactions to stress and the prediction of future blood pressure: Effects of sex, age, and socioeconomic position*. Psychosomatic Medicine, 2003. **65**(6): p. 1058-1064.
28. Williams, J.H. and W.S. Barnes, *The Positive Inotropic Effect of Epinephrine on Skeletal-Muscle - a Brief Review*. Muscle & Nerve, 1989. **12**(12): p. 968-975.
29. Bayly, A., T.H. Hankin, and P. Haugh, *Eversion of the Vagina in Ewes*. New Zealand Journal of Agriculture, 1936. **53**: p. 19-27.
30. Risdons, H. and C. Lapford, *The relationship of serum calcium to prolapsed vagina and ringwomb*. The Veterinary Record, 1972. **90**(4): p. 100.
31. Jackson, R., et al., *Epidemiology of vaginal prolapse in mixed-age ewes in New Zealand*. New Zealand Veterinary Journal, 2014. **62**(6): p. 328-337.
32. Stubbings, D.P., *Observations on Serum Calcium Levels in Ewes in North-Lincolnshire in Relation to Prolapse of Vagina and Incomplete Cervical Dilatation*. Veterinary Record, 1971. **89**(11): p. 296-300.
33. Sobiraj, A., et al., *Investigations into the blood plasma profiles of electrolytes, 17 beta -oestradiol and progesterone in sheep suffering from vaginal inversion and prolapse ante partum*. British Veterinary Journal, 1986. **142**(3).
34. Hosie, B.D., et al., *Nutritional factors associated with vaginal prolapse in ewes*. The Veterinary Record, 1991. **128**: p. 204-208.
35. Kelly, R.W., *Nutrition and placental development*. Proceedings of the Nutrition Society of Australia, 1992. **17**: p. 203-211.
36. Fogarty, N.M., D.G. Hall, and P.J. Holst, *The effect of nutrition in mid pregnancy and ewe liveweight change on birth weight and management for lamb survival in highly fecund ewes*. Australian Journal of Experimental Agriculture, 1992. **32**(1).
37. Holst, P.J., I.D. Killeen, and B.R. Cullis, *Nutrition of the pregnant ewe and its effect on gestation length, lamb birth weight and lamb survival*. Australian Journal of Agricultural Research, 1986. **37**(6).
38. Holst, P.J. and C.J. Allan, *The timing of a moderate nutritional restriction in mid pregnancy and its effect on lamb birth weight and ewe gestation length*. Australian Journal of Experimental Agriculture, 1992. **32**(1).
39. Holst, P.J., C.J. Allan, and A.R. Gilmour, *Effects of a restricted diet during mid pregnancy of ewes on uterine and fetal growth and lamb birth weight*. Australian Journal of Agricultural Research, 1992. **43**(2).
40. Smeaton, D.C., R.W. Webby, and I.S. Tarbotton, *Nutritional effects, in early pregnancy, on lamb production of Finnish Landrace x Romney ewes*. Proceedings of the New Zealand Society of Animal Production, 1999. **59**.
41. Litherland, A.J., et al., *Calcium balance in mid and late pregnancy and vaginal prolapse*. Proceedings of the New Zealand Society of Animal Production, 2007. **67**: p. 61-67.
42. Casey, M., P.G.G. Wrightson, and D. Stevens, *Reducing Bearings on High Performance Sheep Farms*, in *FITT Final Report 07FT190*. 2008.
43. Ayen, E. and D.E. Noakes, *Distribution of collagen in the vaginal wall of ewes*. Veterinary Journal, 1998. **155**(2).
44. Ayen, E., D.E. Noakes, and S.J. Baker, *Changes in the capacity of the vagina and the compliance of the vaginal wall in ovariectomized, normal cyclical and pregnant ewes, before and after treatment with exogenous oestradiol and progesterone*. Veterinary Journal, 1998. **156**(2): p. 133-143.
45. Ennen, S., et al., *Histological, hormonal and biomolecular analysis of the pathogenesis of ovine Prolapsus vaginae ante partum*. Theriogenology, 2011. **75**(2): p. 212-219.
46. Butcher, G. and S. McIntyre, *Uterine prolapse in Southland ewes*. New Zealand Veterinary Journal, 1998. **46**(1): p. 40-40.

47. Nygaard, I., et al., *Prevalence of symptomatic pelvic floor disorders in US women*. *Jama-Journal of the American Medical Association*, 2008. **300**(11): p. 1311-1316.
48. Haylen, B.T., et al., *An International Urogynecological Association (IUGA)/International Continence Society (ICS) Joint Report on the Terminology for Female Pelvic Floor Dysfunction*. *Neurourology and Urodynamics*, 2010. **29**(1): p. 4-20.
49. Lukacz, E.S., et al., *Parity, mode of delivery, and pelvic floor disorders*. *Obstetrics and Gynecology*, 2006. **107**(6): p. 1253-1260.
50. Gyhagen, M., S. Akervall, and I. Milsom, *Clustering of pelvic floor disorders 20 years after one vaginal or one cesarean birth*. *International Urogynecology Journal*, 2015. **26**(8): p. 1115-1121.
51. Knight, K.M., et al., *Impact of parity on ewe vaginal mechanical properties relative to the nonhuman primate and rodent*. *International Urogynecology Journal*, 2016. **27**(8): p. 1255-1263.
52. Ulrich, D., et al., *Regional Variation in Tissue Composition and Biomechanical Properties of Postmenopausal Ovine and Human Vagina*. *Plos One*, 2014. **9**(8).
53. Beausoleil, N.J., K.J. Stafford, and D.J. Mellor, *Sheep show more aversion to a dog than to a human in an arena test*. *Applied Animal Behaviour Science*, 2005. **91**(3-4): p. 219-232.
54. Javaux, E.J., *The early eukaryotic fossa record*, in *Eukaryotic Membranes and Cytoskeleton: Origins and Evolution*. 2007, Springer-Verlag Berlin: Berlin. p. 1-19.
55. Boraas, M.E., D.B. Seale, and J.E. Boxhorn, *Phagotrophy by a flagellate selects for colonial prey: A possible origin of multicellularity*. *Evolutionary Ecology*, 1998. **12**(2): p. 153-164.
56. Kats, L.B. and L.M. Dill, *The scent of death: Chemosensory assessment of predation risk by prey animals*. *Ecoscience*, 1998. **5**(3): p. 361-394.
57. Kusch, R.C., S.M. Reehan, and D.P. Chivers, *Making sense of predator scents: investigating the sophistication of predator assessment abilities of fathead minnows*. *Behavioral Ecology and Sociobiology*, 2004. **55**: p. 551-555.
58. Pfister, J.A., D. Muller-Schwarze, and D.F. Balph, *Effects of predator fecal odors on feed selection by sheep and cattle*. *Journal of Chemical Ecology*, 1990. **16**(2): p. 573-583.
59. Arnould, C. and J. Signoret, *Sheep food repellents: Efficacy of various products, habituation, and social facilitation*. *Journal of Chemical Ecology*, 1993. **19**(2): p. 225-236.
60. Arnould, C., *Which chemical constituents from dog feces are involved in its food repellent effect in sheep?* *Journal of Chemical Ecology*, 1998. **24**(3): p. 559-576.
61. Apfelbach, R., et al., *Are single odorous components of a predator sufficient to elicit defensive behaviors in prey species?* *Frontiers in Neuroscience*, 2015. **9**.
62. Cox, T.E., et al., *Pest Responses to Odors From Predators Fed a Diet of Target Species Conspecifics and Heterospecifics*. *Journal of Wildlife Management*, 2010. **74**(8): p. 1737-1744.
63. Geist, V., *Mountain Sheep: A study in evolution and behavior*. 1971, London: University of Chicago Press.
64. Wilson, E.O., *Sociobiology : the new synthesis*. 25th anniversary ed. 2000, Cambridge, Mass.: Belknap Press of Harvard University Press. xiii, 697 25 cm.
65. Zeder, M.A., *Documenting domestication : new genetic and archaeological paradigms*. 2006, Berkeley, Calif.: University of California Press. xiv, 361 29 cm.
66. Hansen, I., et al., *Variation in behavioural responses of ewes towards predator-related stimuli*. *Applied Animal Behaviour Science*, 2001. **70**(3): p. 227-237.
67. Dwyer, C.M., *How has the risk of predation shaped the behavioural responses of sheep to fear and distress?* *Animal Welfare*, 2004. **13**(3): p. 269-281.
68. Price, E.O., *Animal domestication and behavior*. 2002, New York: CABI Pub. x, 297 25 cm.
69. Baldock, N.M. and R.M. Sibly, *Effects of handling and transportation on the heart rate and behaviour of sheep*. *Applied Animal Behaviour Science*, 1990. **28**(1-2): p. 15-39.
70. Goddard, P.J., et al., *The behavioural, physiological and immunological responses of lambs from two rearing systems and two genotypes to exposure to humans*. *Applied Animal Behaviour Science*, 2000. **66**(4): p. 305-321.
71. Hargreaves, A.L. and G.D. Hutson, *Some effects of repeated handling on stress responses in sheep*. *Applied Animal Behaviour Science*, 1990. **26**(3).
72. Rasmussen, D.D. and P.V. Malven, *Effects of confinement stress on episodic secretion of LH in ovariectomized sheep*. *Neuroendocrinology*, 1983. **36**(5).
73. Degabriele, R. and L.R. Fell, *Changes in behaviour, cortisol and lymphocyte types during isolation and group confinement of sheep*. *Immunology and Cell Biology*, 2001. **79**(6): p. 583-589.

74. Adrichem, P.W.M.v. and J.E. Vogt, *The effect of isolation and separation on the metabolism of sheep*. Livestock Production Science, 1993. **33**(1/2).
75. Lankin, V.S., *Domestic behavior in sheep: the role of behavioral polymorphism in the regulation of stress reactions*. Genetika (Moskva), 1999. **35**(8).
76. Hall, S.J.G., S.M. Kirkpatrick, and D.M. Broom, *Behavioural and physiological responses of sheep of different breeds to supplementary feeding, social mixing and taming, in the context of transport*. Animal Science, 1998. **67**(3).
77. Nicholson, A.J., *The balance of animal populations*. Journal of Animal Ecology, 1933. **2**: p. 132-178.
78. Murray, B.G., *Can the population regulation controversy be buried and forgotten?* Oikos, 1999. **84**(1): p. 148-152.
79. White, T.C.R., *Opposing paradigms: regulation or limitation of populations?* Oikos, 2001. **93**(1): p. 148-152.
80. White, T.C.R., *The role of food, weather and climate in limiting the abundance of animals*. Biological Reviews, 2008. **83**(3): p. 227-248.
81. Lochmiller, R.L., *Immunocompetence and animal population regulation*. Oikos, 1996. **76**(3): p. 594-602.
82. Sheriff, M.J., C.J. Krebs, and R. Boonstra, *The ghosts of predators past: population cycles and the role of maternal programming under fluctuating predation risk*. Ecology, 2010. **91**(10): p. 2983-2994.
83. Boe, K.E., et al., *Space allowance in confinement housing for sheep: The effect on behaviour*. Livestock Environment VII, Proceedings. 2005, St Joseph: Amer Soc Agr Engineers. 644-650.
84. Denton, D.A., *Gregarious Factor in the Natural Conditioned Salivary Reflexes of Sheep*. Nature, 1957. **179**(4555): p. 341-344.
85. Elton, C. and M. Nicholson, *The ten-year cycle in numbers of the lynx in Canada*. Journal of Animal Ecology, 1942. **11**: p. 215-244.
86. Hik, D.S., *Does risk of predation influence population dynamics - evidence from the cyclic decline of snowshoe hares*. Wildlife Research, 1995. **22**(1): p. 115-129.
87. Sheriff, M.J., C.J. Krebs, and R. Boonstra, *The sensitive hare: sublethal effects of predator stress on reproduction in snowshoe hares*. Journal of Animal Ecology, 2009. **78**(6): p. 1249-1258.
88. Preisser, E.L., *The physiology of predator stress in free-ranging prey*. Journal of Animal Ecology, 2009. **78**(6): p. 1103-1105.
89. Malenka, R.C. and E.F. Nestler, *Neural and neuroendocrine control of the internal milieu*, in *Molecular Neuropharmacology: A Foundation for Clinical Neuroscience*, A. Sydor and R.Y. Brown, Editors. 2009, McGraw-Hill Medical, New York. p. 248-259.
90. Juster, R.P., B.S. McEwen, and S.J. Lupien, *Allostatic load biomarkers of chronic stress and impact on health and cognition*. Neuroscience and Biobehavioral Reviews, 2010. **35**(1): p. 2-16.
91. de Kloet, E.R., M. Joels, and F. Holsboer, *Stress and the brain: From adaptation to disease*. Nature Reviews Neuroscience, 2005. **6**(6): p. 463-475.
92. Selye, H., *The effect of adaptation to various damaging agents on the female sex organs in the rat*. Endocrinology, 1939. **25**(4): p. 615-624.
93. Chand, D. and D.A. Lovejoy, *Stress and reproduction: Controversies and challenges*. General and Comparative Endocrinology, 2011. **171**(3): p. 253-257.
94. Nakamura, K., S. Sheps, and P.C. Arck, *Stress and reproductive failure: past notions, present insights and future directions*. Journal of Assisted Reproduction and Genetics, 2008. **25**(2-3): p. 47-62.
95. Fish, E.W., et al., *Epigenetic programming of stress responses through variations in maternal care*, in *Youth Violence: Scientific Approaches to Prevention*, J. Devine, et al., Editors. 2004, New York Acad Sciences: New York. p. 167-180.
96. Hadany, L., et al., *Why is stress so deadly? An evolutionary perspective*. Proceedings of the Royal Society B-Biological Sciences, 2006. **273**(1588): p. 881-885.
97. Pipia, A., et al., *Effect of predation risk on grouping pattern and whistling behaviour in a wild mouflon Ovis aries population*. Acta Theriologica, 2009. **54**(1): p. 77-86.
98. Frid, A., *Vigilance by female Dall's sheep: Interactions between predation risk factors*. Animal Behaviour, 1997. **53**: p. 799-808.

99. Bush, I.E. and K.A. Ferguson, *The secretion of the adrenal cortex in the sheep*. Journal of Endocrinology, 1953. **10**(1): p. 1-8.
100. Trevisi, E., Lombardelli, R., Bionaz, M., A., Bertoni, G., *Plasma cortisol level in relation to welfare conditions in dairy farms*. Proceedings of the 56th Annual Meeting of the European Association for Animal Production, 2005. **Session 10**(Ph2.7).
101. Lee, D.Y., E. Kim, and M.H. Choi, *Technical and clinical aspects of cortisol as a biochemical marker of chronic stress*. Bmb Reports, 2015. **48**(4): p. 209-216.
102. Miller, G.E., E. Chen, and E.S. Zhou, *If it goes up, must it come down? Chronic stress and the hypothalamic-pituitary-adrenocortical axis in humans*. Psychological Bulletin, 2007. **133**(1): p. 25-45.
103. Weiss, D., et al., *Coping capacity of dairy cows during the change from conventional to automatic milking*. Journal of Animal Science, 2004. **82**(2): p. 563-570.
104. Heim, C., U. Ehlert, and D.H. Hellhammer, *The potential role of hypocortisolism in the pathophysiology of stress-related bodily disorders*. Psychoneuroendocrinology, 2000. **25**(1): p. 1-35.
105. Fanson, K.V. and M.L. Parrott, *The value of eutherian-marsupial comparisons for understanding the function of glucocorticoids in female mammal reproduction*. Hormones and Behavior, 2015. **76**: p. 41-47.
106. Kiecoltglaser, J.K., et al., *Chronic stress and immunity in family caregivers of alzheimers disease victims*. Psychosomatic Medicine, 1987. **49**(5): p. 523-535.
107. Trevisi, E. and G. Bertoni, *Some physiological and biochemical methods for acute and chronic stress evaluation in dairy cows*. Italian Journal of Animal Science, 2009. **8**: p. 265-286.
108. Cronin, G.M., et al., *Identifying animal welfare issues for sheep in Australia*. Wool Technology and Sheep Breeding, 2002. **50**(4): p. 534-540.
109. Eckersall, P.D. and R. Bell, *Acute phase proteins: Biomarkers of infection and inflammation in veterinary medicine*. Veterinary Journal, 2010. **185**(1): p. 23-27.
110. Tothova, C., O. Nagy, and G. Kovac, *Acute phase proteins and their use in the diagnosis of diseases in ruminants: a review*. Veterinarni Medicina, 2014. **59**(4): p. 163-180.
111. Moshage, H.J., et al., *Fibrinogen and albumin synthesis are regulated at the transcriptional level during the acute phase response*. Biochimica Et Biophysica Acta, 1988. **950**(3): p. 450-454.
112. Pang, W.W., et al., *Can the acute-phase reactant proteins be used as cancer biomarkers?* International Journal of Biological Markers, 2010. **25**(1): p. 1-11.
113. Watterson, C., et al., *A Comparative Analysis of Acute-phase Proteins as Inflammatory Biomarkers in Preclinical Toxicology Studies: Implications for Preclinical to Clinical Translation*. Toxicologic Pathology, 2009. **37**(1): p. 28-33.
114. Ridker, P.M., *Inflammatory biomarkers and risks of myocardial infarction, stroke, diabetes, and total mortality: Implications for longevity*. Nutrition Reviews, 2007. **65**(12): p. S253-S259.
115. Hilliquin, P., *Biological markers in inflammatory rheumatic diseases*. Cellular and Molecular Biology, 1995. **41**(8): p. 993-1006.
116. Cray, C., J. Zaias, and N.H. Altman, *Acute Phase Response in Animals: A Review*. Comparative Medicine, 2009. **59**(6): p. 517-526.
117. Mine, K., et al., *Proteome analysis of human placentae: Pre-eclampsia versus normal pregnancy*. Placenta, 2007. **28**(7): p. 676-687.
118. Pineiro, M., et al., *Characterisation of the pig acute phase protein response to road transport*. Veterinary Journal, 2007. **173**(3): p. 669-674.
119. Lephherd, M.L., et al., *Assessment of the short-term systemic effect of and acute phase response to mulesing and other options for controlling breech flystrike in Merino lambs*. Australian Veterinary Journal, 2011. **89**(1-2): p. 19-26.
120. World Health Organisation. *Biomarkers In Risk Assessment: Validity And Validation*. 2001; Available from: <http://www.inchem.org/documents/ehc/ehc/ehc222.htm#9.0>.
121. Strimbu, K. and J.A. Tavel, *What are biomarkers?* Current Opinion in Hiv and Aids, 2010. **5**(6): p. 463-466.
122. Atkinson, A.J., et al., *Biomarkers and surrogate endpoints: Preferred definitions and conceptual framework*. Clinical Pharmacology & Therapeutics, 2001. **69**(3): p. 89-95.
123. National Cancer Institute. *Biomarker definition*. Available from: <https://www.cancer.gov/publications/dictionaries/cancer-terms?cdrid=45618>.

124. Desai, M., N. Stockbridge, and R. Temple, *Blood pressure as an example of a biomarker that functions as a surrogate*. *Aaps Journal*, 2006. **8**(1): p. E146-E152.
125. Graf, A. and R. Oehler, *Study design in DIGE-based biomarker discovery*, in *Differential Gel Electrophoresis (DIGE)*, R. Cramer and W. R., Editors. 2012, Springer. p. 195-206.
126. Meng, Z. and T.D. Veenstra, *Proteomic analysis of serum, plasma, and lymph for the identification of biomarkers*. *Proteomics Clinical Applications*, 2007. **1**(8): p. 747-757.
127. Rezaie, A., R.D. Parker, and M. Abdollahi, *Oxidative stress and pathogenesis of inflammatory bowel disease: An epiphenomenon or the cause?* *Digestive Diseases and Sciences*, 2007. **52**(9): p. 2015-2021.
128. Kasperska-Zajac, A., *Acute-phase response in chronic urticaria*. *Journal of the European Academy of Dermatology and Venereology*, 2012. **26**(6): p. 665-672.
129. Burillo, E., et al., *Paraoxonase-1 overexpression prevents experimental abdominal aortic aneurysm progression*. *Clinical Science*, 2016. **130**(12): p. 1027-1038.
130. Liu, Z.T., et al., *Alanine Aminotransferase-Old Biomarker and New Concept: A Review*. *International Journal of Medical Sciences*, 2014. **11**(9): p. 925-935.
131. Jacobs, J.M., et al., *Utilizing human blood plasma for proteomic biomarker discovery*. *Journal of Proteome Research*, 2005. **4**(4): p. 1073-1085.
132. Anderson, N.L. and N.G. Anderson, *The human plasma proteome - History, character, and diagnostic prospects*. *Molecular & Cellular Proteomics*, 2002. **1**(11): p. 845-867.
133. Aslam, B., et al., *Proteomics: Technologies and Their Applications*. *Journal of Chromatographic Science*, 2017. **55**(2): p. 182-196.
134. Ceciliani, F., L. Restelli, and C. Lecchi, *Proteomics in farm animals models of human diseases*. *Proteomics Clinical Applications*, 2014. **8**(9-10): p. 677-688.
135. Bousette, N., A.O. Gramolini, and T. Kislinger, *Proteomics-based investigations of animal models of disease*. *Proteomics Clinical Applications*, 2008. **2**(5): p. 638-653.
136. Ahmed, N., et al., *An approach to remove albumin for the proteomic analysis of low abundance biomarkers in human serum*. *Proteomics*, 2003. **3**(10): p. 1980-1987.
137. Sidki, A. and D.H. Hirst, *Establishing albumin levels in sheep serum by a specific fluoroimmunoassay*. *Veterinary Journal*, 1998. **156**(1): p. 67-72.
138. Aalund, O., J.W. Osebold, and F.A. Murphy, *Isolation and characterization of ovine gamma globulins*. *Archives of Biochemistry and Biophysics*, 1965. **109**(1): p. 142-+.
139. Lathrop, J.T., et al., *Rarity gives a charm: evaluation of trace proteins in plasma and serum*. *Expert Review of Proteomics*, 2005. **2**(3): p. 393-406.
140. Gianazza, E. and P. Arnaud, *A general method for fractionation of plasma proteins - dye ligand affinity chromatography on immobilized cibacron blue F3GA*. *Biochemical Journal*, 1982. **201**(1): p. 129-136.
141. Fountoulakis, M., et al., *Depletion of the high-abundance plasma proteins*. *Amino Acids*, 2004. **27**(3-4): p. 249-259.
142. Steel, L.F., et al., *Efficient and specific removal of albumin from human serum samples*. *Molecular & Cellular Proteomics*, 2003. **2**(4): p. 262-270.
143. Tam, S.W., J. Pirro, and D. Hinerfeld, *Depletion and fractionation technologies in plasma proteomic analysis*. *Expert Review of Proteomics*, 2004. **1**(4): p. 411-420.
144. Hinerfeld, D., et al., *Serum/Plasma Depletion with Chicken Immunoglobulin Y Antibodies for Proteomic Analysis from Multiple Mammalian Species*. *Journal of Biomolecular Techniques*, 2004. **15**(3): p. 184-190.
145. Johnson, J.I., et al. *The Navigable Atlas of the Sheep Brain*. 2003 2003, August 1]; Available from: <http://msu.edu/user/brains/sheepatlas>.
146. Pieper, R., et al., *Multi-component immunoaffinity subtraction chromatography: An innovative step towards a comprehensive survey of the human plasma proteome*. *Proteomics*, 2003. **3**(4): p. 422-432.
147. Huang, L., et al., *Immunoaffinity separation of plasma proteins by IgY microbeads: Meeting the needs of proteomic sample preparation and analysis*. *Proteomics*, 2005. **5**(13): p. 3314-3328.
148. Polaskova, V., et al., *High-abundance protein depletion: Comparison of methods for human plasma biomarker discovery*. *Electrophoresis*, 2010. **31**(3): p. 471-482.
149. Grubbs, J.K., et al., *Investigation of the efficacy of albumin removal procedures on porcine serum proteome profile*. *Journal of Animal Science*, 2015. **93**(4): p. 1592-1598.

150. Gundry, R.L., et al., *Assessment of albumin removal from an immunoaffinity spin column: Critical implications for proteomic examination of the albuminome and albumin-depleted samples.* Proteomics, 2009. **9**(7): p. 2021-2028.
151. Bhonsle, H.S., et al., *Low Plasma Albumin Levels Are Associated with Increased Plasma Protein Glycation and HbA1c in Diabetes.* Journal of Proteome Research, 2012. **11**(2): p. 1391-1396.
152. Gundry, R.L., et al., *Investigation of an albumin-enriched fraction of human serum and its albuminome.* Proteomics Clinical Applications, 2007. **1**(1): p. 73-88.
153. O'Farrell, P.H., *High resolution two-dimensional electrophoresis of proteins.* Journal of Biological Chemistry, 1975. **250**(10): p. 4007-4021.
154. Gorg, A., et al., *The current state of two-dimensional electrophoresis with immobilized pH gradients.* Electrophoresis, 2000. **21**(6): p. 1037-1053.
155. Rabilloud, T., *Two-dimensional gel electrophoresis in proteomics: Old, old fashioned, but it still climbs up the mountains.* Proteomics, 2002. **2**(1): p. 3-10.
156. Gianazza, E. and P.G. Righetti, *Immobilized pH gradients.* Electrophoresis, 2009. **30**: p. S112-S121.
157. Shaw, J., et al., *Evaluation of saturation labelling two-dimensional difference gel electrophoresis fluorescent dyes.* Proteomics, 2003. **3**(7): p. 1181-1195.
158. Adessi, C., et al., *Two-dimensional electrophoresis of membrane proteins: A current challenge for immobilized pH gradients.* Electrophoresis, 1997. **18**(1): p. 127-135.
159. Roncada, P., et al., *Acrylamide-agarose copolymers: Improved resolution of high molecular mass proteins in two-dimensional gel electrophoresis.* Proteomics, 2005. **5**(9): p. 2331-2339.
160. Shaw, M.M. and B.M. Riederer, *Sample preparation for two-dimensional gel electrophoresis.* Proteomics, 2003. **3**(8): p. 1408-1417.
161. Conradsen, K. and J. Pedersen, *Analysis of 2-dimensional electrophoretic gels.* Biometrics, 1992. **48**(4): p. 1273-1287.
162. Rye, M. and E.M. Fargestad, *Preprocessing of electrophoretic images in 2-DE analysis.* Chemometrics and Intelligent Laboratory Systems, 2012. **117**: p. 70-79.
163. Carrette, O., et al., *State-of-the-art two-dimensional gel electrophoresis: a key tool of proteomics research.* Nature Protocols, 2006. **1**(2): p. 812-823.
164. Million, R., et al., *Improved instrumentation for large-size two-dimensional protein maps.* Electrophoresis, 2010. **31**(23-24): p. 3863-3866.
165. Marouga, R., S. David, and E. Hawkins, *The development of the DIGE system: 2D fluorescence difference gel analysis technology.* Analytical and Bioanalytical Chemistry, 2005. **382**(3): p. 669-678.
166. Karp, N.A., et al., *Experimental and statistical considerations to avoid false conclusions in proteomics studies using differential in-gel electrophoresis.* Molecular & Cellular Proteomics, 2007. **6**(8): p. 1354-1364.
167. Tonge, R., et al., *Validation and development of fluorescence two-dimensional differential gel electrophoresis proteomics technology.* Proteomics, 2001. **1**(3): p. 377-396.
168. Moulder, R., et al., *Analysis of the plasma proteome using iTRAQ and TMT-based Isobaric labeling.* Mass Spectrometry Reviews, 2018. **37**(5): p. 583-606.
169. Oliveira, B.M., J.R. Coorsen, and D. Martins-de-Souza, *2DE: The Phoenix of Proteomics.* Journal of Proteomics, 2014. **104**: p. 140-150.
170. Chiaradia, E., et al., *Proteomic evaluation of sheep serum proteins.* BMC Veterinary Research, 2012. **8**(66): p. 1-13.
171. Fountoulakis, M. and B. Takacs, *Effect of strong detergents and chaotropes on the detection of proteins in two-dimensional gels.* Electrophoresis, 2001. **22**(9): p. 1593-1602.
172. McCarthy, J., et al., *Carbamylation of proteins in 2-D electrophoresis - Myth or reality?* Journal of Proteome Research, 2003. **2**(3): p. 239-242.
173. Bisht, D., et al., *An improved sample preparation method for analyzing mycobacterial proteins in two-dimensional gels.* Biochemistry-Moscow, 2007. **72**(6): p. 672-674.
174. Harder, A., et al., *Comparison of yeast cell protein solubilization procedures for two-dimensional electrophoresis.* Electrophoresis, 1999. **20**(4-5): p. 826-829.
175. Perdew, G.H., H.W. Schaup, and D.P. Selivonchick, *The use of a zwitterionic detergent in two-dimensional gel electrophoresis of trout liver microsomes.* Analytical Biochemistry, 1983. **135**(2): p. 453-455.

176. Altland, K., et al., *Isoelectric focusing of basic proteins - the problem of oxidation of cysteines*. Electrophoresis, 1988. **9**(9): p. 474-485.
177. Righetti, P.G., G. Tudor, and E. Gianazza, *Effect of 2-mercaptoethanol on pH gradients in isoelectric focusing*. Journal of Biochemical and Biophysical Methods, 1982. **6**(3): p. 219-227.
178. Hoving, S., et al., *Preparative two-dimensional gel electrophoresis at alkaline pH using narrow range immobilized pH gradients*. Proteomics, 2002. **2**(2): p. 127-134.
179. Gorg, A., et al., *2-dimensional polyacrylamide gel electrophoresis with immobilized pH gradients in the first dimension (IPG-Dalt) - the state of the art and the controversy of vertical versus horizontal systems*. Electrophoresis, 1995. **16**(7): p. 1079-1086.
180. Olsson, I., et al., *Organic disulfides as a means to generate streak-free two-dimensional maps with narrow range basic immobilized pH gradient strips as first Product dimension*. Proteomics, 2002. **2**(11): p. 1630-1632.
181. Herbert, B., et al., *Reduction and alkylation of proteins in preparation of two-dimensional map analysis: Why, when, and how?* Electrophoresis, 2001. **22**(10): p. 2046-2057.
182. Sebastiano, R., et al., *A new deuterated alkylating agent for quantitative proteomics*. Rapid Communications in Mass Spectrometry, 2003. **17**(21): p. 2380-2386.
183. Bai, F.J., S. Liu, and F.A. Witzmann, *A "de-streaking" method for two-dimensional electrophoresis using the reducing agent tris(2-carboxyethyl)-phosphine hydrochloride and alkylating agent vinylpyridine*. Proteomics, 2005. **5**(8): p. 2043-2047.
184. Righetti, P.G., *Real and imaginary artefacts in proteome analysis via two-dimensional maps*. Journal of Chromatography B-Analytical Technologies in the Biomedical and Life Sciences, 2006. **841**(1-2): p. 14-22.
185. Strahler, J.R., et al., *Effect of salt on the performance of immobilized pH gradient isoelectric focusing gels*. Electrophoresis, 1988. **9**(2): p. 74-80.
186. Cham, B.E. and B.R. Knowles, *Solvent system for delipidation of plasma or serum without protein precipitation*. Journal of Lipid Research, 1976. **17**(2): p. 176-181.
187. Zuobi-Hasona, K., et al., *Solubilization of cellular membrane proteins from Streptococcus mutans for two-dimensional gel electrophoresis*. Electrophoresis, 2005. **26**(6): p. 1200-1205.
188. Fu, Q., et al., *A robust, streamlined, and reproducible method for proteomic analysis of serum by delipidation, albumin and IgG depletion, and two-dimensional gel electrophoresis*. Proteomics, 2005. **5**(10): p. 2656-2664.
189. Khan, A. and N.H. Packer, *Simple urinary sample preparation for proteomic analysis*. Journal of Proteome Research, 2006. **5**(10): p. 2824-2838.
190. Centlow, M., S.R. Hansson, and C. Welinder, *Differential Proteome Analysis of the Preeclamptic Placenta Using Optimized Protein Extraction*. Journal of Biomedicine and Biotechnology, 2010.
191. Jiang, L., L. He, and M. Fountoulakis, *Comparison of protein precipitation methods for sample preparation prior to proteomic analysis*. Journal of Chromatography A, 2004. **1023**(2): p. 317-320.
192. Schmidt, A.C., B. Storr, and N.A. Kummer, *Influence of one- and two-dimensional gel electrophoresis procedure on metal-protein bindings examined by electrospray ionization mass spectrometry, inductively coupled plasma mass spectrometry, and ultrafiltration*. Talanta, 2011. **85**(2): p. 1118-1128.
193. Rabilloud, T., *Solubilization of proteins for electrophoretic analyses*. Electrophoresis, 1996. **17**(5): p. 813-829.
194. Nandakumar, M.P., et al., *Solubilization of trichloroacetic acid (TCA) precipitated microbial proteins via NaOH for two-dimensional electrophoresis*. Journal of Proteome Research, 2003. **2**(1): p. 89-93.
195. Simpson, R.J., *Proteins and Proteomics; A Laboratory Manual 2003*, New York: Cold Spring Harbor Laboratory Press.
196. Herbert, B.R., et al., *Improved 2-DE of microorganisms after acidic extraction*. Electrophoresis, 2006. **27**(8): p. 1630-1640.
197. Oh, J., et al., *Establishment of a near-standard two-dimensional human urine proteomic map*. Proteomics, 2004. **4**(11): p. 3485-3497.
198. Smejkal, G.B., et al., *Simultaneous reduction and alkylation of protein disulfides in a centrifugal ultrafiltration device prior to two-dimensional gel electrophoresis*. Journal of Proteome Research, 2006. **5**(4): p. 983-987.

199. Luque-Garcia, J.L. and T.A. Neubert, *Sample preparation for serum/plasma profiling and biomarker identification by mass spectrometry*. Journal of Chromatography A, 2007. **1153**(1-2): p. 259-276.
200. Righetti, P.G., M. Chiari, and C. Gelfi, *Immobilized pH gradients - effect of salts, added carrier ampholytes and voltage gradients on protein patterns*. Electrophoresis, 1988. **9**(2): p. 65-73.
201. Arakawa, T. and S.N. Timasheff, *Mechanism of protein salting in and salting out by divalent cation salts - balance between hydration and salt binding*. Biochemistry, 1984. **23**(25): p. 5912-5923.
202. Lee, K., *Evaluation of an effective sample prefractionation method for the proteome analysis of breast cancer tissue using narrow range two-dimensional gel electrophoresis*. Bioscience Biotechnology and Biochemistry, 2008. **72**(6): p. 1464-1474.
203. Righetti, P.G., et al., *Carrier ampholytes for IEF, on their fortieth anniversary (1967-2007), brought to trial in court: The verdict*. Electrophoresis, 2007. **28**(21): p. 3799-3810.
204. Cho, J.H., et al., *Improvement of Plant Protein Solubilization and 2-DE Gel Resolution through Optimization of the Concentration of Tris in the Solubilization Buffer*. Molecules and Cells, 2010. **29**(6): p. 611-616.
205. Unlu, M., M.E. Morgan, and J.S. Minden, *Difference gel electrophoresis: A single gel method for detecting changes in protein extracts*. Electrophoresis, 1997. **18**(11): p. 2071-2077.
206. Barry, R.C., et al., *Quantitative evaluation of sample application methods for semipreparative separations of basic proteins by two-dimensional gel electrophoresis*. Electrophoresis, 2003. **24**(19-20): p. 3390-3404.
207. Depagne, J. and F. Chevalier, *Technical updates to basic proteins focalization using IPG strips*. Proteome Science, 2012. **10**.
208. Sabounchi-Schutt, F., et al., *An Immobilized DryStrip application method enabling high-capacity two-dimensional gel electrophoresis*. Electrophoresis, 2000. **21**(17): p. 3649-3656.
209. Koga, K., *G-electrode-loading method for isoelectric focusing, enabling separation of low-abundance and high-molecular-mass proteins*. Analytical Biochemistry, 2008. **382**(1): p. 23-28.
210. Long, X.H., J.F. Lin, and Y.Z. Zhang, *A novel droplet-tap sample-loading method for two-dimensional gel electrophoresis*. Analytical and Bioanalytical Chemistry, 2006. **384**(7-8): p. 1578-1583.
211. Luche, S., V. Santoni, and T. Rabilloud, *Evaluation of nonionic and zwitterionic detergents as membrane protein solubilizers in two-dimensional electrophoresis*. Proteomics, 2003. **3**(3): p. 249-253.
212. Bjellqvist, B., et al., *Moving and stationary boundaries in immobilized pH gradients*. Electrophoresis, 1988. **9**(9): p. 453-463.
213. Stoyanov, A.V. and P.G. Righetti, *Dynamics of protein isoelectric focusing in immobilized pH gradient gels*. Electrophoresis, 1996. **17**(8): p. 1313-1318.
214. Wu, H.C., et al., *Isoelectric Focusing Management: An Investigation for Salt Interference and an Algorithm for Optimization*. Journal of Proteome Research, 2010. **9**(11): p. 5542-5556.
215. Zue, X. and D.W. Speicher, *Quantitative evaluation of protein recoveries in two-dimensional electrophoresis with immobilized pH gradients*. Electrophoresis, 2000. **21**(14): p. 3035-3047.
216. Westermeier, R., T. Naven, and H.-R. Höpker, eds. *Proteomics in practice : a guide to successful experimental design*. 2nd ed. 2008, Wiley-VCH, John Wiley distributor: Weinheim, Chichester.
217. Gorg, A., et al., *Very alkaline immobilized pH gradients for two-dimensional electrophoresis of ribosomal and nuclear proteins*. Electrophoresis, 1997. **18**(3-4): p. 328-337.
218. Kask, L., K. Larsson, and B. Bjellqvist, *Elimination of basic gaps at high pH values in 2-DE*. Proteomics, 2009. **9**(24): p. 5558-5561.
219. Bengtsson, K., S. Nilsson, and N.D. Robinson, *Conducting Polymer Electrodes for Gel Electrophoresis*. Plos One, 2014. **9**(2).
220. Bischoff, R. and T.M. Luider, *Methodological advances in the discovery of protein and peptide disease markers*. Journal of Chromatography B-Analytical Technologies in the Biomedical and Life Sciences, 2004. **803**(1): p. 27-40.
221. Jalili, P.R., T. Gheyi, and C. Dass, *Proteome analysis in bovine adrenal medulla using matrix-assisted laser desorption/ionization mass spectrometry*. Rapid Communications in Mass Spectrometry, 2004. **18**: p. 914-916.
222. Bi, B., et al., *Vimentin and PRG4 as candidate biomarkers of ovarian cancer using serum proteomic analysis of 2D-DIGE*. International Journal of Clinical and Experimental Medicine, 2017. **10**(3): p. 4547-4555.

223. Lilley, K.S. and D.B. Friedman, *All about DIGE: quantification technology for differential-display 2D-gel proteomics*. Expert Review of Proteomics, 2004. **1**(4): p. 401-409.
224. Stevens, S.M., A.D. Zharikova, and L. Prokai, *Proteomic analysis of the synaptic plasma membrane fraction isolated from rat forebrain*. Molecular Brain Research, 2003. **117**(2): p. 116-128.
225. Clerc, F., et al., *Human plasma protein N-glycosylation*. Glycoconjugate Journal, 2016. **33**(3): p. 309-343.
226. Herbert, B.R., et al., *What place for polyacrylamide in proteomics?* Trends in Biotechnology, 2001. **19**(10): p. S3-S9.
227. Cairns, D.A., *Statistical issues in quality control of proteomic analyses: Good experimental design and planning*. Proteomics, 2011. **11**(6): p. 1037-1048.
228. Maurer, M.H., *Software analysis of two-dimensional electrophoretic gels in proteomic experiments*. Current Bioinformatics, 2006. **1**(2): p. 255-262.
229. Benjamini, Y. and Y. Hochberg, *Controlling the false discovery rate - a practical and powerful approach to multiple testing*. Journal of the Royal Statistical Society Series B-Methodological, 1995. **57**(1): p. 289-300.
230. Benjamini, Y. and Y. Hochberg, *On the adaptive control of the false discovery rate in multiple testing with independent statistics*. Journal of Educational and Behavioral Statistics, 2000. **25**(1): p. 60-83.
231. Karp, N.A., D.P. Kreil, and K.S. Lilley, *Determining a significant change in protein expression with DeCyder (TM) during a pair-wise comparison using two-dimensional difference gel electrophoresis*. Proteomics, 2004. **4**(5): p. 1421-1432.
232. Blakesley, R.E., et al., *Comparisons of Methods for Multiple Hypothesis Testing in Neuropsychological Research*. Neuropsychology, 2009. **23**(2): p. 255-264.
233. Storey, J.D. and R. Tibshirani, *Statistical significance for genomewide studies*. Proceedings of the National Academy of Sciences of the United States of America, 2003. **100**(16): p. 9440-9445.
234. Friedman, D.B., *Assessing signal-to-noise in quantitative proteomics: Multivariate statistical analysis in DIGE experiments*, in *Differential Gel Electrophoresis (DIGE)*, R. Cramer and W. R., Editors. 2012, Springer. p. 31-45.
235. Addis, M.F., et al., *2D DIGE/MS to investigate the impact of slaughtering techniques on postmortem integrity of fish filet proteins*. Journal of Proteomics, 2012. **75**(12): p. 3654-3664.
236. Williams, G.J., *Rattle: A Data Mining GUI for R*. R Journal, 2009. **1**(2): p. 45-55.
237. Shevchenko, A., et al., *Mass spectrometric sequencing of proteins from silver stained polyacrylamide gels*. Analytical Chemistry, 1996. **68**(5): p. 850-858.
238. Granvogl, B., M. Ploscher, and L.A. Eichacker, *Sample preparation by in-gel digestion for mass spectrometry-based proteomics*. Analytical and Bioanalytical Chemistry, 2007. **389**(4): p. 991-1002.
239. Stuhler, K. and H.E. Meyer, *MALDI: More than peptide mass fingerprints*. Current Opinion in Molecular Therapeutics, 2004. **6**(3): p. 239-248.
240. Bruins, A.P., *Mechanistic aspects of electrospray ionization*. Journal of Chromatography A, 1998. **794**(1-2): p. 345-357.
241. Biemann, K., *Sequencing of peptides by tandem mass-spectrometry and high energy collision induced dissociation*. Methods in Enzymology, 1990. **193**: p. 455-479.
242. Henzel, W.J., et al., *Identifying proteins from 2-dimensional gels by molecular mass searching of peptide fragments in protein sequence databases*. Proceedings of the National Academy of Sciences of the United States of America, 1993. **90**(11): p. 5011-5015.
243. Deutsch, E.W., H. Lam, and R. Aebersold, *Data analysis and bioinformatics tools for tandem mass spectrometry in proteomics*. Physiological Genomics, 2008. **33**(1): p. 18-25.
244. Deutsch, E.W., et al., *A guided tour of the Trans-Proteomic Pipeline*. Proteomics, 2010. **10**(6): p. 1150-1159.
245. Kong, A.T., et al., *MSFragger: ultrafast and comprehensive peptide identification in mass spectrometry-based proteomics*. Nature Methods, 2017. **14**(5): p. 513-+.
246. GE_Healthcare, *2-D Electrophoresis, principles and methods*. 3rd ed. 2004: GE Healthcare.
247. Wessel, D. and U.I. Fugge, *A method for the quantitative recovery of protein in dilute solution in the presence of detergents and lipids*. Analytical Biochemistry, 1984. **138**(1): p. 141-143.
248. Goldfinch, G.M., et al., *The proteome of gastric lymph in normal and nematode infected sheep*. Proteomics, 2008. **8**(9): p. 1909-1918.

249. Penno, M., M. Ernst, and P. Hoffmann, *Comparative 2D DIGE analysis of the depleted serum proteome*, in *Methods in molecular biology 854; Difference gel electrophoresis (DIGE), methods and protocols*, R. Cramer and R. Westermeier, Editors. 2012, Springer: London. p. 207-220.
250. Pereira, R.A., de Araujo, P. A., Castañeda-Espinosa, J. C., & Mondelli, R. F. L., *Comparative analysis of the shrinkage stress of composite resins*. Journal of Applied Oral Science., 2008. **16**(1): p. 30-34.
251. GE_Healthcare, *Ettan DALTsix Electrophoresis System User Manual*. 2006: GE Lifesciences: Sweden.
252. GE_Healthcare, *DeCyder 2D 7.0 User Manual*. 2008.
253. Brown, S. and G. Norris, *Improved consistency in 2D gel electrophoresis: Sheep plasma as a test case*. Electrophoresis, 2017. **38**(6): p. 906-913.
254. Bolstad, B.M., et al., *A comparison of normalization methods for high density oligonucleotide array data based on variance and bias*. Bioinformatics, 2003. **19**(2): p. 185-193.
255. Artigaud, S., O. Gauthier, and V. Pichereau, *Identifying differentially expressed proteins in two-dimensional electrophoresis experiments: inputs from transcriptomics statistical tools*. Bioinformatics, 2013. **29**(21): p. 2729-2734.
256. Meunier, B., et al., *Data analysis methods for detection of differential protein expression in two-dimensional gel electrophoresis*. Analytical Biochemistry, 2005. **340**(2): p. 226-230.
257. Rocke, D.M. and B. Durbin, *A model for measurement error for gene expression arrays*. Journal of Computational Biology, 2001. **8**(6): p. 557-569.
258. Huber, W., et al., *Variance stabilization applied to microarray data calibration and to the quantification of differential expression*. Bioinformatics (Oxford, England), 2002. **18 Suppl 1**: p. S96-104.
259. Hicks, S.C. and R.A. Irizarry, *quantro: a data-driven approach to guide the choice of an appropriate normalization method*. Genome Biology, 2015. **16**.
260. Albrecht, D., et al., *Missing values in gel-based proteomics*. Proteomics, 2010. **10**(6): p. 1202-1211.
261. Wang, W., et al., *Impact of Quenching Failure of Cy Dyes in Differential Gel Electrophoresis*. Plos One, 2011. **6**(3).
262. Rocke, D.M. and B. Durbin, *Approximate variance-stabilizing transformations for gene-expression microarray data*. Bioinformatics, 2003. **19**(8): p. 966-972.
263. Henry, L.W., Hadley, *rlang: Functions for Base Types and Core R and 'Tidyverse' Features*. R package version 0.1.2. 2017: <https://CRAN.R-project.org/package=rlang>.
264. Fox, J. and S. Weisberg, *An R companion to applied regression*. 2nd ed ed. 2011, Thousand Oaks, Calif.: SAGE Publications. xxii, 449 p.
265. R Core Team, *R: A language and environment for statistical computing*. 2017, R Foundation for Statistical Computing (Vienna, Austria). <https://www.R-project.org/>.
266. Meleth, S., J. Deshane, and H. Kim, *The case for well-conducted experiments to validate statistical protocols for 2D gels: different pre-processing = different lists of significant proteins*. BMC Biotechnology, 2005. **5**: p. 15.
267. Storey, J.D., *The positive false discovery rate: A Bayesian interpretation and the q-value*. Annals of Statistics, 2003. **31**(6): p. 2013-2035.
268. Arentz, G., et al., *State of the art of 2D DIGE*. Proteomics Clinical Applications, 2015. **9**(3-4): p. 277-288.
269. Beckett, P., *The basics of 2D DIGE*, in *Methods in molecular biology 854; Difference gel electrophoresis (DIGE), methods and protocols*, R. Cramer and R. Westermeier, Editors. 2012, Springer: London. p. 9-19.
270. Yu, L.B., et al., *Fully Moderated T-statistic for Small Sample Size Gene Expression Arrays*. Statistical Applications in Genetics and Molecular Biology, 2011. **10**(1).
271. Smyth Gordon, K., *Linear Models and Empirical Bayes Methods for Assessing Differential Expression in Microarray Experiments*, in *Statistical Applications in Genetics and Molecular Biology*. 2004. p. 1.
272. Schwammle, V., I.R. Leon, and O.N. Jensen, *Assessment and Improvement of Statistical Tools for Comparative Proteomics Analysis of Sparse Data Sets with Few Experimental Replicates*. Journal of Proteome Research, 2013. **12**(9): p. 3874-3883.

273. Wiśniewski, J. and M. Mann, *A Proteomics Approach to the Protein Normalization Problem: Selection of Unvarying Proteins for MS-Based Proteomics and Western Blotting*. Journal of Proteome Research, 2016. **15**(7): p. 2321-6.
274. Harrell, F., *Hmisc: Harrell miscellaneous. R package version 4.1-1*. 2018.
275. Nelson, E.K., et al., *LabKey Server: An open source platform for scientific data integration, analysis and collaboration*. BMC Bioinformatics, 2011. **12**.
276. Penno, M.A.S., et al., *2D-DIGE analysis of sera from transgenic mouse models reveals novel candidate protein biomarkers for human gastric cancer*. Journal of Proteomics, 2012. **77**: p. 40-58.
277. Iliev, P.T. and T.M. Georgieva, *Acute phase proteins in sheep and goats - Function, reference ranges and assessment methods: An overview*. Bulgarian Journal of Veterinary Medicine, 2018. **21**(1): p. 1-16.
278. Eckersall, P.D., et al., *An automated biochemical assay for haptoglobin: Prevention of interference from albumin*. Comparative Haematology International, 1999. **9**(3): p. 117-124.
279. Bazydlo, L.A.L., M. Needham, and N.S. Harris, *Calcium, Magnesium, and Phosphate*. Labmedicine, 2014. **45**(1): p. E44-E50.
280. Halaby, D.M. and J.P.E. Mornon, *The immunoglobulin superfamily: An insight on its tissular, species, and functional diversity*. Journal of Molecular Evolution, 1998. **46**(4): p. 389-400.
281. Udby, L., A.H. Johnsen, and N. Borregaard, *Human CRISP-3 binds serum alpha B-1-glycoprotein across species*. Biochimica Et Biophysica Acta-General Subjects, 2010. **1800**(4): p. 481-485.
282. Udby, L., et al., *Cysteine-rich secretory protein 3 is a ligand of alpha-1B-glycoprotein in human plasma*. Biochemistry, 2004. **43**(40): p. 12877-12886.
283. Liu, Y.S., et al., *Integrative Proteomics and Tissue Microarray Profiling Indicate the Association between Overexpressed Serum Proteins and Non-Small Cell Lung Cancer*. Plos One, 2012. **7**(12).
284. Canales, N.A.G., et al., *A1BG and C3 are overexpressed in patients with cervical intraepithelial neoplasia III*. Oncology Letters, 2014. **8**(2): p. 939-947.
285. Dutta, M., et al., *Investigation of serum proteome alterations in human endometriosis*. Journal of Proteomics, 2015. **114**: p. 182-196.
286. Qiu, Y.H., et al., *Plasma glycoprotein profiling for colorectal cancer biomarker identification by lectin glycoarray and lectin blot*. Journal of Proteome Research, 2008. **7**(4): p. 1693-1703.
287. Zeng, Z., et al., *A Proteomics Platform Combining Depletion, Multi-lectin Affinity Chromatography (M-LAC), and Isoelectric Focusing to Study the Breast Cancer Proteome*. Analytical Chemistry, 2011. **83**(12): p. 4845-4854.
288. Sun, S.S., et al., *Site-Specific Profiling of Serum Glycoproteins Using N-Linked Glycan and Glycosite Analysis Revealing Atypical N-Glycosylation Sites on Albumin and alpha-1B-Glycoprotein*. Analytical Chemistry, 2018. **90**(10): p. 6292-6299.
289. Ghafouri, B., et al., *Biomarkers of systemic inflammation in farmers with musculoskeletal disorders; a plasma proteomic study*. BMC Musculoskeletal Disorders, 2016. **17**(206).
290. Doherty, N.S., et al., *Analysis of changes in acute-phase plasma proteins in an acute inflammatory response and in rheumatoid arthritis using two-dimensional gel electrophoresis*. Electrophoresis, 1998. **19**(2): p. 355-363.
291. Biswas, S., et al., *Identification of Novel Autoantigen in the Synovial Fluid of Rheumatoid Arthritis Patients Using an Immunoproteomics Approach*. Plos One, 2013. **8**(2).
292. Huang, W., et al., *Quantitative proteomic analysis of synovial tissue from rats with collagen-induced arthritis*. Rsc Advances, 2015. **5**(105): p. 86088-86101.
293. McDonough, C.W., et al., *Pharmacogenomic Association of Nonsynonymous SNPs in SIGLEC12, A1BG, and the Selectin Region and Cardiovascular Outcomes*. Hypertension, 2013. **62**(1): p. 48-54.
294. Morimatsu, M., et al., *Isolation and characterization of bovine haptoglobin from acute phase sera*. Journal of Biological Chemistry, 1991. **266**(18): p. 11833-11837.
295. Mikkat, S., et al., *Mass spectrometric protein structure characterization reveals cause of migration differences of haptoglobin a chains in two-dimensional gel electrophoresis*. Proteomics, 2004. **4**(12): p. 3921-3932.
296. Eckersall, P.D. and J.G. Conner, *Plasma haptoglobin in cattle (bos-taurus) exists as polymers in association with albumin*. Comparative Biochemistry and Physiology B-Biochemistry & Molecular Biology, 1990. **96**(2): p. 309-314.

297. Polonovski, M. and M. Jayle, *Existence in the blood plasma of a substance hastening the peroxydasic activity of the hemoglobin*. Comptes Rendus Des Seances De La Societe De Biologie Et De Ses Filiales, 1938. **129**: p. 457-460.
298. Lim, S.K., et al., *Increased susceptibility in Hp knockout mice during acute hemolysis*. Blood, 1998. **92**(6): p. 1870-1877.
299. Yang, H., et al., *Identification of CD163 as an antiinflammatory receptor for HMGB1-haptoglobin complexes*. Jci Insight, 2016. **1**(7).
300. Cecilian, F., et al., *Acute phase proteins in ruminants*. Journal of Proteomics, 2012. **75**(14): p. 4207-4231.
301. Conner, J.G., et al., *Bovine acute phase response following turpentine injection*. Research in Veterinary Science, 1988. **44**(1): p. 82-88.
302. Eckersall, P.D., *Acute phase proteins as markers of inflammatory lesions*. Comparative Haematology International, 1995. **5**(2): p. 93-97.
303. Conner, J.G., et al., *Acute phase response and mastitis in the cow*. Research in Veterinary Science, 1986. **41**(1): p. 126-128.
304. Dudek, K., D. Bednarek, and M. Szymanska-Czerwinska, *Acute phase response in calves as a result of experimental challenge with Mycoplasma bovis*. Bulletin of the Veterinary Institute in Pulawy, 2010. **54**(4): p. 517-520.
305. Chan, J.P.W., et al., *Association of increased serum acute-phase protein concentrations with reproductive performance in dairy cows with postpartum metritis*. Veterinary Clinical Pathology, 2010. **39**(1): p. 72-78.
306. Kaya, S., et al., *Determination of ceruloplasmin, some other acute phase proteins, and biochemical parameters in cows with endometritis*. Veterinary World, 2016. **9**(10): p. 1056-1062.
307. Georgieva, T.M., E. Dishlyanova, and S. Jotov, *Plasma Haptoglobin concentrations after normal parturition and caesarean operation in ewes with dystocia (preliminary study)*. Revue De Medecine Veterinaire, 2011. **162**(12): p. 607-612.
308. Aziz, D.M. and M.B. Taha, *Effect of dystocia on serum haptoglobin in Awassi ewes*. Theriogenology, 1997. **48**(4): p. 559-562.
309. Shin, D.H., et al., *Associations between serum haptoglobin concentration and peri- and postpartum disorders, milk yield, and reproductive performance in dairy cows*. Livestock Science, 2018. **213**: p. 14-18.
310. Hirvonen, J. and S. Pyorala, *Acute-phase response in dairy cows with surgically-treated abdominal disorders*. Veterinary Journal, 1998. **155**(1): p. 53-61.
311. Nazifi, S., et al., *Study on diagnostic values of haptoglobin and serum amyloid A concentration in bovine heart diseases*. Comparative Clinical Pathology, 2009. **18**(1): p. 47-51.
312. Smith, B.I., J. Kauffold, and L. Sherman, *Serum haptoglobin concentrations in dairy cattle with lameness due to claw disorders*. Veterinary Journal, 2010. **186**(2): p. 162-165.
313. Gurdogan, F., E. Balikci, and A. Yildiz, *Some acute phase proteins, oxidative stress biomarkers and antioxidant enzyme activities in ewes with pregnancy toxemia*. Iranian Journal of Veterinary Research, 2014. **15**(3): p. 297-299.
314. Gonzalez, F.H.D., et al., *Acute phase proteins in experimentally induced pregnancy toxemia in goats*. Journal of Veterinary Diagnostic Investigation, 2011. **23**(1): p. 57-62.
315. El-Deeb, W.M. and S.M. El-Bahr, *Biomarkers of ketosis in dairy cows at postparturient period: acute phase proteins and pro-inflammatory cytokines*. Veterinarski Arhiv, 2017. **87**(4): p. 431-440.
316. Piccione, G., et al., *Utility of acute phase proteins as biomarkers of transport stress in ewes*. Small Ruminant Research, 2012. **107**(2-3): p. 167-171.
317. Al-Dawood, A., *Acute phase proteins as indicators of stress in Baladi goats from Jordan*. Acta Agriculturae Scandinavica Section a-Animal Science, 2017. **67**(1-2): p. 58-65.
318. Bastos, B.L., et al., *Association between haptoglobin and IgM levels and the clinical progression of caseous lymphadenitis in sheep*. BMC Veterinary Research, 2013. **9**.
319. Bond, J.J., et al., *Efferent intestinal lymph protein responses in nematode-resistant, -resilient and -susceptible lambs under challenge with Trichostrongylus colubriformis*. Journal of Proteomics, 2014. **109**: p. 356-367.
320. Ulutas, P.A., et al., *Haptoglobin, Serum Amyloid-A and Ceruloplasmin Concentrations in Goats with Mixed Helminth Infection*. Turkiye Parazitoloji Dergisi, 2008. **32**(3): p. 229-233.

321. Hashemnia, M., et al., *Changing Patterns of Acute Phase Proteins and Inflammatory Mediators in Experimental Caprine Coccidiosis*. Korean Journal of Parasitology, 2011. **49**(3): p. 213-219.
322. González, F.H.D., et al., *Haptoglobin and serum amyloid A in subacute ruminal acidosis in goats*. Revista de la Facultad de Medicina Veterinaria y de Zootecnia, 2010. **57**(3): p. 159-167.
323. Nedelkov, D., *Human proteoforms as new targets for clinical mass spectrometry protein tests*. Expert Review of Proteomics, 2017. **14**(8): p. 691-699.
324. Durand, G. and N. Seta, *Protein glycosylation and diseases: Blood and urinary oligosaccharides as markers for diagnosis and therapeutic monitoring*. Clinical Chemistry, 2000. **46**(6): p. 795-805.
325. Andersson, M. and E. Sevelius, *Abnormal microheterogeneity of haptoglobin in serum from dogs with various diseases*. Veterinary Record, 2001. **148**(1): p. 14-17.
326. Zhang, S., et al., *Insights on N-glycosylation of human haptoglobin and its association with cancers*. Glycobiology, 2016. **26**(7): p. 684-692.
327. Takeda, Y., et al., *Fucosylated haptoglobin is a novel type of cancer biomarker linked to the prognosis after an operation in colorectal cancer*. Cancer, 2012. **118**(12): p. 3036-3043.
328. Mondal, G., et al., *Altered glycosylation, expression of serum haptoglobin and alpha-1-antitrypsin in chronic hepatitis C, hepatitis C induced liver cirrhosis and hepatocellular carcinoma patients*. Glycoconjugate Journal, 2016. **33**(2): p. 209-218.
329. Hao, P.L., et al., *Recent advances in mass spectrometric analysis of protein deamidation*. Mass Spectrometry Reviews, 2017. **36**(6): p. 677-692.
330. Shah, A., et al., *Differential Serum Level of Specific Haptoglobin Isoforms in Small Cell Lung Cancer*. Current Proteomics, 2010. **7**(1): p. 49-56.
331. Gupta, N., N.P. Shankernarayan, and K. Dharmalingam, *Serum proteome of leprosy patients undergoing erythema nodosum leprosum reaction: Regulation of expression of the Isoforms of haptoglobin*. Journal of Proteome Research, 2007. **6**(9): p. 3669-3679.
332. Yang, F.M., et al., *Identification and characterization of human haptoglobin cDNA*. Proceedings of the National Academy of Sciences of the United States of America-Biological Sciences, 1983. **80**(19): p. 5875-5879.
333. Osawa, M., et al., *Association of alpha 2-HS glycoprotein (AHSG, fetuin-A) polymorphism with AHSG and phosphate serum levels*. Human Genetics, 2005. **116**(3): p. 146-151.
334. Barton, R.H., et al., *The influence of EDTA and citrate anticoagulant addition to human plasma on information recovery from NMR-based metabolic profiling studies*. Molecular Biosystems, 2010. **6**(1): p. 215-224.
335. Silverman, G.A., et al., *Serpins Flex Their Muscle I. Putting the clamps on proteolysis in diverse biological systems*. Journal of Biological Chemistry, 2010. **285**(32): p. 24299-24305.
336. Silverman, G.A., et al., *The serpins are an expanding superfamily of structurally similar but functionally diverse proteins - Evolution, mechanism of inhibition, novel functions, and a revised nomenclature*. Journal of Biological Chemistry, 2001. **276**(36): p. 33293-33296.
337. Ferreira, A.M., et al., *The sheep (Ovis aries) muscle proteome: Decoding the mechanisms of tolerance to Seasonal Weight Loss using label-free proteomics*. Journal of Proteomics, 2017. **161**: p. 57-67.
338. Marchitelli, C., et al., *Splicing Variants of SERPINA1 Gene in Ovine Milk: Characterization of cDNA and Identification of Polymorphisms*. Plos One, 2013. **8**(8).
339. Balli, U., et al., *The levels of visceral adipose tissue-derived serpin, omentin-1 and tumor necrosis factor-alpha in the gingival crevicular fluid of obese patients following periodontal therapy*. Journal of Oral Science, 2016. **58**(4): p. 465-473.
340. Jesse, S., et al., *Differential Sialylation of Serpin A1 in the Early Diagnosis of Parkinson's Disease Dementia*. Plos One, 2012. **7**(11).
341. Renucci, J.F., et al., *Endothelial cell markers, TFPI, PAI-1 and cardio-vascular risk factors*. Thrombosis and Haemostasis, 1999: p. 567-567.
342. Tanigawa, C., et al., *Species-Specific Serological Detection for Schistosomiasis by Serine Protease Inhibitor (SERPIN) in Multiplex Assay*. Plos Neglected Tropical Diseases, 2015. **9**(8).
343. Parry, S., et al., *Maternal serum serpin B7 is associated with early spontaneous preterm birth*. American Journal of Obstetrics and Gynecology, 2014. **211**(6).
344. Pascarella, S., et al., *SerpinA1 C-Terminal Peptides as Collagen Turnover Modulators*. Chemmedchem, 2016. **11**(16): p. 1850-1855.

345. Declerck, P.J. and A. Gils, *Three Decades of Research on Plasminogen Activator Inhibitor-1: A Multifaceted Serpin*. Seminars in Thrombosis and Hemostasis, 2013. **39**(4): p. 356-364.
346. McMillen, I.C., G.D. Thorburn, and D.W. Walker, *Diurnal variations in plasma concentrations of cortisol, prolactin, growth hormone and glucose in the fetal sheep and pregnant ewe during late gestation*. Journal of Endocrinology, 1987. **114**(1): p. 65-72.
347. Gonzalez-Cabrera, J., et al., *Acute and chronic stress increase salivary cortisol: a study in the real-life setting of a national examination undertaken by medical graduates*. Stress-the International Journal on the Biology of Stress, 2014. **17**(2): p. 149-156.
348. Fazio, E., et al., *Cortisol changes in pregnant and post-partum ewes: Effects of single or twin births*, in *Trends in Veterinary Science*, C. Boiti, et al., Editors. 2013, Springer-Verlag: Berlin. p. 51-54.
349. Kaneko, J.J., J.W. Harvey, and M. Bruss, *Clinical biochemistry of domestic animals*. 6th ed. 2008: Amsterdam ; Boston : Academic Press/Elsevier.
350. Saba, N., *Plasma cortisol levels in pregnant ewes*. Journal of Agricultural Science, 1965. **64**: p. 11-14.
351. Lindner, H.R., *Blood cortisol in the sheep - normal concentration and changes in ketosis of pregnancy*. Nature, 1959. **184**(4699): p. 1645-1646.
352. Moghaddam, G. and A. Hassanpour, *Comparison of Blood Serum Glucose, Beta Hydroxybutyric Acid, Blood Urea Nitrogen and Calcium Concentrations in Pregnant and Lamed Ewes*. Journal of Animal and Veterinary Advances, 2008. **7**(3): p. 308-311.
353. Fleming, M.W., *Cortisol as an indicator of severity of parasitic infections of Haemonchus contortus in lambs (Ovis aries)*. Comparative Biochemistry and Physiology B-Biochemistry & Molecular Biology, 1997. **116**(1): p. 41-44.
354. Ley, S.J., et al., *Effect of chronic pain associated with lameness on plasma-cortisol concentrations in sheep - a field study*. Research in Veterinary Science, 1994. **57**(3): p. 332-335.
355. Colditz, I.G., et al., *Some physiological responses associated with reduced wool growth during blowfly strike in Merino sheep*. Australian Veterinary Journal, 2005. **83**(11): p. 695-699.
356. You, Q.M., et al., *Variation in the ovine cortisol response to systemic bacterial endotoxin challenge is predominantly determined by signalling within the hypothalamic-pituitary-adrenal axis*. Toxicology and Applied Pharmacology, 2008. **230**(1): p. 1-8.
357. Llonch, P., et al., *Association of Temperament and Acute Stress Responsiveness with Productivity, Feed Efficiency, and Methane Emissions in Beef Cattle: An Observational Study*. Frontiers in veterinary science, 2016. **3**(43).
358. Llonch, P., et al., *Changes in feed intake during isolation stress in respiration chambers may impact methane emissions assessment*. Animal Production Science, 2018. **58**(6): p. 1011-1016.
359. Liu, Q., et al., *Forestomach fermentation characteristics and diet digestibility in alpacas (Lama pacos) and sheep (Ovis aries) fed two forage diets*. Animal Feed Science and Technology, 2009. **154**(3-4): p. 151-159.
360. Sanford, M.T. and L.V. Rodriguez, *The role of environmental stress on lower urinary tract symptoms*. Current Opinion in Urology, 2017. **27**(3): p. 268-273.
361. Grossman, D. and B.K. Siddle, *Psychological Effects of Combat*, in *Stress of War, Conflict and Disaster*, G. Fink, Editor. 2008, Academic Press.
362. Krebs, C.J., *Of lemmings and snowshoe hares: the ecology of northern Canada*. Proceedings of the Royal Society B-Biological Sciences, 2011. **278**(1705): p. 481-489.
363. Boonstra, R., et al., *Equipped for Life in the Boreal Forest: The Role of the Stress Axis in Mammals*. Arctic, 2014. **67**: p. 82-97.
364. Larzul, C., et al. *Genetic determinism of cortisol levels in pig*. in *Proceedings of the World Congress on Genetics Applied to Livestock Production*. 2018. Auckland, New Zealand.
365. Galluzzi, L., O. Kepp, and G. Kroemer, *Mitochondria: master regulators of danger signalling*. Nature Reviews Molecular Cell Biology, 2012. **13**(12): p. 780-788.
366. Puscheck, E.E., et al., *Molecular Biology of the Stress Response in the Early Embryo and its Stem Cells*, in *Cell Signaling during Mammalian Early Embryo Development*, H.J. Leese and D.R. Brison, Editors. 2015. p. 77-128.
367. Liang, S.F., et al., *Quantitative Proteomics for Cancer Biomarker Discovery*. Combinatorial Chemistry & High Throughput Screening, 2012. **15**(3): p. 221-231.
368. Li, X.H., et al., *Comparison of alternative analytical techniques for the characterisation of the human serum proteome in HUPO Plasma Proteome Project*. Proteomics, 2005. **5**(13): p. 3423-3441.

369. van Roekel, E.H., et al., *Metabolomics in epidemiologic research: challenges and opportunities for early-career epidemiologists*. *Metabolomics*, 2019. **15**(1).
370. Wang, M.K., G.Q. Yu, and H.W. Ransom, *Integrative Analysis of Proteomic, Glycomic, and Metabolomic Data for Biomarker Discovery*. *Ieee Journal of Biomedical and Health Informatics*, 2016. **20**(5).
371. Nejad, J.G., et al., *Wool cortisol is a better indicator of stress than blood cortisol in ewes exposed to heat stress and water restriction*. *Animal*, 2014. **8**(1): p. 128-132.
372. Marshall, S., *Dannevirke Seasonal Update*. *VetNews* (HawkesBay/Wairarapa), 2018. **September/October**.

Statement of contribution to publication

DRC 16



MASSEY UNIVERSITY
GRADUATE RESEARCH SCHOOL

STATEMENT OF CONTRIBUTION DOCTORATE WITH PUBLICATIONS/MANUSCRIPTS

We, the candidate and the candidate's Primary Supervisor, certify that all co-authors have consented to their work being included in the thesis and they have accepted the candidate's contribution as indicated below in the *Statement of Originality*.

Name of candidate:	Stuart Brown	
Name/title of Primary Supervisor:	Associate Professor Gillian Norris	
Name of Research Output and full reference:		
Improved consistency in 2D gel electrophoresis: Sheep plasma as a test case. Electrophoresis 2017, 00,1-8.		
In which Chapter is the Manuscript /Published work:	Appendix	
Please indicate:		
<ul style="list-style-type: none"> The percentage of the manuscript/Published Work that was contributed by the candidate: 	90%	
and		
<ul style="list-style-type: none"> Describe the contribution that the candidate has made to the Manuscript/Published Work: 		
Stuart came up with the ideas, did all the lab work and wrote the paper. Gill helped with editing.		
For manuscripts intended for publication please indicate target journal:		
Electrophoresis		
Candidate's Signature:		
Date:	28/2/2019	
Primary Supervisor's Signature:		
Date:	28/2/2019	

(This form should appear at the end of each thesis chapter/section/appendix submitted as a manuscript/ publication or collected as an appendix at the end of the thesis)

GRS Version 4– January 2019